

# Identifying Dysregulated Protein Activities Using Activity-Based Proteomics

Author: Julianne Martell

Persistent link: <http://hdl.handle.net/2345/bc-ir:106812>

This work is posted on [eScholarship@BC](#),  
Boston College University Libraries.

---

Boston College Electronic Thesis or Dissertation, 2016

Copyright is held by the author, with all rights reserved, unless otherwise noted.

# Identifying Dysregulated Protein Activities Using Activity-Based Proteomics

Julianne Martell

A dissertation  
submitted to the Faculty of  
the department of Chemistry  
in partial fulfillment  
of the requirements for the degree of  
Doctor of Philosophy

Boston College  
Morrissey College of Arts and Sciences  
Graduate School

April 2016





# Identifying Dysregulated Protein Activities Using Activity-Based Proteomics

by

Julianne Martell

Thesis Advisor: Eranthie Weerapana

## Abstract

Activity-based protein profiling (ABPP) is a chemical proteomic technique that allows for selective labeling, visualization, and enrichment of the subset of active enzymes in a complex proteome. Given the dominant role of posttranslational modifications in regulating protein function *in vivo*, ABPP provides a direct readout of activity that is not attained through traditional proteomic methods. The first application of chemical proteomics in *C. elegans* was used to identify dysregulated serine hydrolase and cysteine-mediated protein activities in the long-lived *daf-2* mutant, revealing LBP-3, K02D7.1, and C23H4.2 as novel regulators of lifespan and dauer formation. The tools of ABPP were also utilized in studying protein interactions at the host-pathogen interface of *V. cholerae* infection, discovering four pathogen-secreted proteases that alter the biochemical composition of the host, decrease the activity of host serine hydrolases, and inhibit bacterial binding by a host-secreted lectin. Lastly, ABPP was used to study the targets of protein arginine deiminases (PADs) using a citrulline-specific activity-based probe (ABP), highlighting its utility in detecting biologically relevant PAD substrates as well as identifying mRNA processing factors as previously unknown targets of PAD. Taken together, these studies demonstrate the ability of ABPP to discover novel protein regulators of physiological and pathological processes.

## Acknowledgements

The first and most important thank you goes to my advisor, Professor Eranthie Weerapana. My transition into a lab took some detours but I am so thankful that I had the opportunity to join yours. I appreciate your patience and willingness to answer the countless questions I had in the beginning of my research. I'm grateful for the experiences I had being a member of your lab, from traveling to New York to learn about *C. elegans* to meeting and becoming good friends with some really great people through collaborations. I genuinely enjoyed working for you! Thank you so much to my thesis committee Jianmin Gao and Abhishek Chatterjee for reading my thesis. While unfortunately unable to be on my thesis committee, I'd also like to say thanks to Mary Roberts for letting me do research in your lab before joining Eranthie, as well as for all your advice and enthusiastic interest in my worms.

Thank you to all the collaborators I worked with. A special thanks goes to Dr. Stavroula Hatzios, over the several years of collaborating I always enjoyed our conversations, you were an absolute pleasure to work with. I also want to thank Dr. Heidi Tissenbaum and the members of her lab, especially Dr. YongHak Seo, for teaching me so much and allowing me to work and be a part of your lab over the summer.

I need to thank all the Weerapana lab members for everything you've done to help me, to teach me, and for making coming to lab each day so fun and enjoyable: Katie, Tyler, Kyle, Lisa (Stanks), Shalise, Alex, Nick, Yani, Ranjan, Haley, Dan B, and Masahiro. You are strange people and absolutely wonderful friends. The thing I will miss most about grad school is getting to hang out with you all everyday. To the OG Weerapana lab (Yani, Nick, and Alex): Your positivity, ambition, and camaraderie was

remarkable and so much appreciated while we all were pretty much making it up as we went along. I am so thankful that you were the people I had the opportunity to experience grad school with. Thank you to all the other friends I've made at BC who are on to bigger and better things: Hilan, Dan S, Kevin, Carolyn, and Hekla. You are fabulously incredible people and helped me create so many memorable experiences that I'll remember forever.

Thank you to all the Boston College Chemistry Department staff that I got the chance to interact with throughout my years at BC: Steve, Lori, Ginny, Dale, Lynne P, Lynne O, Howard, Ian, Jen, and Bill. Your constant enthusiasm and encouragement were really appreciated.

Finally, I'd like to give special thanks to my family. Mom and Dad, you both are exceptionally supportive and have been my entire life. While explaining my research may have left you even more confused, I truly appreciate your interest and excitement in everything that I do. I want you to know that a significant driving force behind completing my degree was to make you proud. Also, thank you so much to my twin sister Katie. I'm so grateful for the friendship we have and everything you have done for me. I am constantly impressed by the amazing things you're able to accomplish, hopefully getting a PhD will help raise me toward your totally unreachable level of awesomeness.

Lastly, I was to acknowledge my cousin Marc (sup cuz). Our entire lives we have been fascinated in how the universe works, and I loved all the conversations we had trying to figure it out. Your eagerness in seeking knowledge was infectious and you helped me understand how cool being a complete and utter geek could be. I wish you were here to celebrate science and life with me. "Shine on you crazy diamond".

## Table of Contents

Acknowledgements.....	i
Table of Contents.....	iii
List of Figures.....	vii
List of Tables.....	xi
List of Abbreviations.....	xiii
<b>Chapter 1. Activity-Based Protein Profiling.....</b>	<b>1</b>
Introduction.....	2
Electrophilic enzyme family-directed ABPs.....	4
Directed ABPs to target functional amino acids.....	9
Non-electrophilic ABPs for enzyme family active sites.....	12
Non-directed ABP libraries.....	13
Directed ABPs for modified amino acids.....	14
CuAAC-mediated ABPP.....	16
Applications of CuAAC in Mass Spectrometry-Based ABPP.....	19
Conclusion.....	20
References.....	21
<b>Chapter 2. An Isotopically Tagged Azobenzene-Based Cleavable Linker for Quantitative ABPP.....</b>	<b>31</b>
Introduction.....	32
Isotopically Tagged Azobenzene-Based Cleavable Linker.....	37
Evaluation of the efficiency of cleavage of the Azo-L and Azo-H tags.....	39
Evaluation of the quantitative accuracy of the isotopic Azo-tag platform.....	40

Application of the isotopic Azo-tag platform to compare two biologically independent samples .....	42
Release of intact proteins from streptavidin beads.....	43
Conclusion.....	46
Experimental Procedures.....	47
References .....	56
<b>Chapter 3. Identifying Dysregulated Cysteine-Mediated Protein Activities During Impaired Insulin/IGF-1 Signaling in <i>C. elegans</i></b> .....	61
Introduction .....	62
Insulin signaling and its role in lifespan regulation .....	64
Global profiling of DAF-16 transcriptional targets.....	68
Reactive-cysteine profiling reveals functional cysteines in <i>C. elegans</i> .....	71
Chemical-proteomic analysis identifies changes in cysteine reactivity between <i>daf-2</i> and <i>daf-16;daf-2</i> mutants .....	76
RNAi-mediated knockdown of <i>lbp-3</i> and <i>K02D7.1</i> results in modulation of lifespan and dauer formation.....	81
<i>C. elegans</i> lipid binding protein-3 .....	85
<i>C. elegans</i> protein K02D7.1 .....	87
Conclusion.....	88
Experimental procedures .....	90
References .....	98
<b>Chapter 4. Fluorophosphonate ABPs to Investigate the Roles of Serine Hydrolases in Impaired Insulin Signaling/Lifespan Regulation in <i>C. elegans</i></b> .....	110

Introduction .....	111
Investigating serine hydrolase activity changes in impaired insulin/IGF-1 signaling in <i>C. elegans</i> .....	112
Chemical-proteomic analysis reveals previously unidentified changes in SH activity between <i>daf-2</i> and <i>daf-16;daf-2</i> mutants.....	113
RNAi-mediated knockdown of ZK370.4 and C23H4.2 affects lifespan and dauer formation .....	115
Conclusion.....	118
Experimental Procedures.....	118
References .....	121
<b>Chapter 5. Chemoproteomic Profiling of Host and Pathogen Enzymes Active in Cholera</b> .....	125
Introduction .....	126
ABPP identifies serine hydrolases active in cholera .....	127
IvaP influences the activity of other serine hydrolases .....	130
<i>V. cholerae</i> proteases alter host protein abundance .....	131
Intelectin binds <i>V. cholerae</i> and other enteric bacteria .....	133
<i>V. cholerae</i> proteases decrease intelectin binding in vivo.....	134
Conclusion.....	135
Experimental Procedures.....	136
References .....	139
<b>Chapter 6. Chemical Proteomic Platform To Identify Citrullinated Proteins</b> .....	142
Introduction .....	143

Characterization of the PAD2 citrullinome.....	145
The use of biotin-PG to identify dysregulated citrullination in RA.....	148
Conclusion.....	153
Experimental Procedures.....	153
Experimental Procedures.....	154
<b>Appendix I.</b> <i>C. elegans</i> lifespan data.....	163
<b>Appendix II.</b> Mass spectrometry tables.....	167

## List of Figures

### Chapter 1.

**Figure 1-1.** (a) Activity-based probes containing a reactive group for covalent modification and a reporter group for protein visualization, enrichment, and identification. (b) Rhodamine reporter groups can be used to visualize proteins in SDS-PAGE. (c) Biotin reporter groups can be used to visualize proteins in western blots using anti-biotin antibodies, or enriched with avidin for identification using mass spectrometry.

**Figure 1-2.** (a) Mechanism of serine modification via the fluorophosphonate ABP. (b) Other serine-specific electrophiles used in ABP.

**Figure 1-3.** (a) Mechanism of inactivation of cysteine proteases by AOMKs. (b) Structure of the ABP DCG-04 and the papain inhibitor E-64 which it is based on.

**Figure 1-4.** Modes of mechanism-based inactivation of cytochrome P450 enzymes by (a) Aryl alkynes (b) Propynyl groups (c) Furanocoumarins.

**Figure 1-5.** (a) Functional roles performed by cysteine residues. (b) Oxidative post-translational modifications of cysteine residues.

**Figure 1-6.** (a) Cysteine-reactive iodoacetamide. (b) Other electrophiles reactive toward cysteine. (c) Electrophiles to target lysine (dichlorotriazine and acyl phosphate) and tyrosine/serine (sulfonyl fluoride) residues.

**Figure 1-7.** (a) MMP inhibitor GM6001 shown chelating to an active site zinc. (b) MMP ABP HxBP-Rh with the zinc-chelating hydroxamate group highlighted in red and the photo-crosslinking benzophenone group highlighted in blue.

**Figure 1-8.** Design of the  $\alpha$ -chloroacetamide dipeptide probe library, with the R1-R2 binding groups specified (pTyr = phosphotyrosine).

**Figure 1-9.** (a) Dimedone selectively labels cysteine sulfenic acids. (b) Citrullination of arginine via PAD. The PG-probe labels citrulline over arginine at acidic pH.

**Figure 1-10.** ABP with bulky reporter groups are replaced with an alkyne handle to allow conjugation to an azide-containing reporter group via copper catalyzed click chemistry.

### Chapter 2.

**Figure 2-1.** (a) Structure of the TEV-tag. (b) Structures of WRR-086 and its ABP version, Alkyne-086.

**Figure 2-2.** Structure of SV1 ABP containing an azobenzene cleavable linker.

**Figure 2-3.** (a) Structure of the photo-affinity glycoprobe. (b) Structure of the photo-cleavable biotin affinity tag.

**Figure 2-4.** Structure of the TEV-cleavable linker.

**Figure 2-5.** Structure of the Azo-H cleavable linker.

**Figure 2-6.** Workflow of the Azo-tag quantitative proteomics platform.

**Figure 2-7.** (a) Structure of the iodoacetamide-alkyne (IA-alkyne) probe. (b) Number of peptides identified from IA-alkyne-labeled proteomes using the valine-free Azo, Azo-L, Azo-H, and Azo-L + Azo-H (a 1:1 ratio of Azo-L and Azo-H tagged proteomes) tags.

**Figure 2-8.** (a) The light/heavy ratios of 2:1, 1:1, 1:2, and 1:5 Azo-L/Azo-H tagged proteomes. (b) Chromatography traces for two labeled peptides from UBE1Y1 and SHMT2 from samples mixed in light/heavy ratios of 1:5, 1:2, 1:1, 2:1, and 5:1.

**Figure 2-9.** (a) mock and GSTO1 transfected HEK293T cells labeled with IA-alkyne are tagged with Azo-H (mock) or Azo-L (GSTO1). GSTO1 overexpression confirmed by immunoblotting with anti-GSTO antibody. (b) Light/heavy ratios for all IA-alkyne-labeled peptides from the two transfected HEK293T cells.

**Figure 2-10.** (a) Cleavage of whole GAPDH protein from streptavidin beads. (b) Elution of GAPDH from streptavidin beads in the background of a complex mouse proteome.

**Figure 2-11.** (a) Sequence coverage for GAPDH after sodium dithionite cleavage of intact proteins followed by in-solution tryptic digestion. Peptide regions shaded in gray signify peptides that were identified in the analysis. The two cysteine-containing peptides that were tagged by Azo-L/Azo-H are underlined. (b) Two IA-alkyne labeled cysteine-containing peptides identified with light/heavy ratios of 1. The extracted ion chromatograms and isotopic envelopes for the light species are shown in red, and the heavy species in blue.

### Chapter 3.

**Figure 3-1.** The *C. elegans* lifecycle at 25°C.

**Figure 3-2.** The *C. elegans* DAF-2/insulin-like pathway.

**Figure 3-3.** (a) Percent dauer formation in WT and *daf-2* mutant *C. elegans*, grown at 22.5 °C. (b) Lifespan of WT (N2), *daf-2* and *daf-16;daf-2* *C. elegans*

**Figure 3-4.** (a) Workflow to identify hyperreactive cysteines in the *daf-2* mutant proteome. (b) Cysteine-containing peptides in order from high to low reactivity. (c) Cysteines with annotated biological functions in either *C. elegans* or the corresponding human homolog are highlighted in white along the ratio plot. (d) Cysteine-containing peptides sorted into 3 groups:  $R < 3$  (hyperreactive),  $R = 3-6$  (medium reactivity),  $R > 6$  (low reactivity).

**Figure 3-5.** (a) Workflow to quantify cysteine reactivity changes between *daf-2* and *daf-16;daf-2* mutants. (b) Identified cysteine-containing peptides plotted against the log<sub>10</sub> value of each light:heavy ratio.

**Figure 3-6.** Survival plots of *daf-2* mutants treated with (a) *lbp-3* siRNA or (b) *K02D7.1* siRNA and compared to a vector-treated control. (c) Dauer-arrest assay comparing the percent dauer formation of *daf-2* mutants with RNAi-mediated knockdown of *lbp-3* and *K02D7.1* compared to a vector-treated control. (d) RT-PCR of *daf-2* mutants treated with *lbp-3* or *K02D7.1* siRNA using primers for *lbp-3*, *K02D7.1*, or *pmp-3* as a control.

**Figure 3-7.** (a) Lifespan assays of RNAi-mediated knockdown of *lbp-3* and *K02D7.1* in the background of *daf-16* mutants, *daf-16;daf-2* double mutants, and wild type (N2) worms. (b) RT-PCR of the three strains treated with *lbp-3* or *K02D7.1* siRNA using primers for *lbp-3*, *K02D7.1*, or *pmp-3* as a control.

**Figure 3-8.** Alignment of *C. elegans* LBP-3 with the human FABP family.

**Figure 3-9.** Alignment of *C. elegans* K02D7.1 with purine nucleoside phosphorylases from other species.

## Chapter 4

**Figure 4-1.** Structure of the FP-biotin probe.

**Figure 4-2.** Lifespan of *daf-2* mutants upon RNAi-mediated knockdown of ZK370.4

**Figure 4-3.** RNAi-mediated knockdown of C23H4.2 in *daf-2* mutants shows a decrease in (a) lifespan and (b) dauer formation.

## Chapter 5

**Figure 5-1.** Workflow of FP-biotin labeling human choleric stool and rabbit cecal fluid with the structure of FP-biotin also shown.

## Chapter 6

**Figure 6-1.** (a) Structure of Biotin-PG. (b) Biotin-PG labeling of citrulline residues.

**Figure 6-2.** HEK294T·PAD2 cells treated with or without ionomycin and calcium, labeled with biotin-PG, and enriched on streptavidin beads.

## Appendix.

**Figure 3A-1.** Lifespan assays on RNAi-mediated knockdown of cysteine-containing proteins with the greatest reactivity change between *daf-2* and *daf-16;daf-2* mutants.

**Figure 4A-1.** Lifespan assays on RNAi-mediated knockdown of serine hydrolases labeled by FP-biotin with the greatest activity changes between *daf-2* and *daf-16;daf-2* mutants.

## List of Tables

### Chapter 3.

**Table 3-1.** Hyperreactive cysteines identified in the *daf-2* mutant proteome with annotated biological function in either *C. elegans* or human UniProt databases.

**Table 3-2.** Cysteine residues with a  $\geq 2$ -fold change between *daf-2* and *daf-16;daf-2* mutants.

**Table 3-3.** Lifespan changes upon RNAi-mediated knockdown of the 12 selected genes against a vector-treated control. Dauer formation changes with RNAi-mediated knockdown of the 3 genes decreased in the *daf-2* mutant with the greatest increases in lifespan.

### Chapter 4.

**Table 4-1.** Top 10 decreased and top 10 increased FP-biotin-labeled proteins in the *daf-2* proteome. Those available in the Ahringer RNAi library are highlighted in green.

### Chapter 5.

**Table 5-1.** Human and *V. cholerae* proteins enriched with FP-biotin from choleric stool.

**Table 5-2.** Rabbit proteins enriched with FP-biotin from *V. cholerae* infected rabbit cecal fluid.

**Table 5-3.** *V. cholerae* proteins enriched with FP-biotin from *V. cholerae* infected rabbit cecal fluid.

**Table 5-4.** Comparison of *V. cholerae* and rabbit proteins enriched from cecal fluid infected with WT and IvaP<sup>S361A</sup> mutant *V. cholerae*.

**Table 5-5.** *V. cholerae* virulence factors identified from unfractionated rabbit cecal fluid.

**Table 5-6.** *V. cholerae* proteins identified from unfractionated human choleric stool. All proteins but the two highlighted in gray were also detected in rabbit cecal fluid.

**Table 5-7.** The nine rabbit proteins identified from unfractionated cecal that were more abundant in the  $\Delta$ quad mutant *V. cholerae*.

## Chapter 6.

**Table 6-1.** Proteins identified with a greater than 2-fold change in PAD2 overexpressing cells versus parental cells.

**Table 6-2.** Citrullinated proteins showing the most significant changes in RA versus healthy sera.

## Appendix.

**Table 3A-1.** MS results showing the 578 cysteine-containing peptides identified in the *daf-2* lysates, ranked by reactivity based on their average light:heavy ratios (R) from  $R \sim 1$  (high reactivity) to  $R \gg 1$  (low reactivity). The closest human homologue for each *C. elegans* protein and conservation of its cysteine across various species are also shown.

**Table 3A-2.** MS results showing the 338 cysteine-containing peptides identified in *daf-2* and *daf-16;daf-2* lysates, in order from average light:heavy ratios of  $< 1$  (decreased cysteine labeling in *daf-2*) to  $> 1$  (increased cysteine labeling in *daf-2*)

**Table 4A-1.** MS results showing the 87 *C. elegans* serine hydrolase proteins labeled by FP-biotin in 4 day old *daf-2* and *daf-16;daf-2* mutants.

**Table 6A-1.** MS results showing the 363 biotin-PG-labeled proteins in human healthy and RA sera.

## List of Abbreviations

Standard 3-letter and 1-letter codes are used for the 20 natural amino acids

ABP	activity-based probe
ABPP	activity-based protein profiling
ACPA	anti-citrullinated protein antibody
AGE-1	phosphoinositide 3-kinase ( <i>C. elegans</i> )
AKT/PKB	protein kinase AKT/protein kinases B
AMPK	adenosine monophosphate-activated protein kinase
AOMK	acyloxymethyl ketone
Azo	azobenzene
C18	octadecyl carbon chain (C18)-bonded silica
CA	chloroacetamide
CES	carboxylesterase
CID	collision-induced dissociation
CP	cysteine protease
CuAAC	copper (I)-catalyzed azide-alkyne cycloaddition
DAF-16	FOXO family transcription factor ( <i>C. elegans</i> )
DAF-2	insulin-like growth factor receptor ( <i>C. elegans</i> )
DDAH	dimethylarginine dimethylaminohydrolase
DMEM	dulbecco's modified eagle's medium
DMSO	dimethyl sulfoxide
DTT	dithiothreitol

EDTA	ethylenediaminetetraacetic acid
EEF-2	eukaryotic translation elongation factor
FABP	fatty-acid-binding protein
FASN	fatty acid synthase
FP	fluorophosphate
FTMS	fourier transform ion cyclotron resonance mass spectrometry
FUDR	<i>5-fluorodeoxyuridine</i>
Gal	$\beta$ -D-galactose
GAPDH	glyceraldehyde 3-phosphate dehydrogenase
GES-1	gut esterase 1
GSPD-1	glucose-6-phosphate dehydrogenase 1
GSTO1	glutathione-S-transferase omega 1
HCV	hepatitis C virus
HRP	horseradish peroxidase
HSP	heat-shock protein
IA	iodoacetamide
ICAT	isotope-coded affinity tag
IgG	Immunoglobulin G
IIS	insulin/insulin-like growth factor signaling
INF-1	initiation factor 1
isoTOP-ABPP	isotopic tandem orthogonal proteolysis-ABPP
ITMS	ion trap mobility spectrometry
iTRAQ	isobaric tags for relative and absolute quantification

KRT	keratin protein
LBP-3	lipid binding protein 3
LC	liquid chromatography
LTQ	linear trap quadropole
MeOH	methanol
MMP	matrix metalloproteinase
MS	mass spectrometry
MTL	metallothionein
MudPIT	multidimensional Protein Identification Technology
N2	wild type <i>C. elegans</i>
PAD	protein arginine deiminase
PBS	phosphate buffered saline
PCK-1	phosphoenolpyruvate carboxykinase 1
PDK-1	3-phosphoinositide dependent protein kinase-1
PG	phenylglyoxal
PIP <sub>3</sub>	phosphatidylinositol (3,4,5)-triphosphate
PMP-3	peroxisomal membrane protein 3
PNP	purine nucleoside phosphorylase
PS	phenyl sulfonate
PTM	posttranslational modification
RA	rheumatoid arthritis
Rh	rhodamine
RNAi	RNA interference

ROS	reactive oxygen species
RT	room temperature
RT-PCR	real time polymerase chain reaction
SCX	strong cation exchange
SDS	sodium dodecyl sulfate
SDS-PAGE	sodium dodecyl sulfate polyacrylamide gel
SH	Serine hydrolases
SILAC	stable-isotope labeling with amino acids in cell culture
siRNA	small interfering RNA
SNP	Single-nucleotide polymorphism
SOD	superoxide dismutase
SODH-1	sorbitol dehydrogenase 1
SOH	sulfenic acid
TAG	triacylglycerol
TBS-T	tris-buffered saline with 1% Tween 20
TCA	trichloroacetic acid
TCEP	<i>tris</i> (2-carboxyethyl)phosphine
TEV	tobacco-etch virus
UBL	ubiquitin-like protein
UC	ulcerative colitis
VIT	vitellogenins
WT	wild type
XDH	xanthine dehydrogenase

## Chapter 1

### Activity-Based Protein Profiling

A significant portion of the work described in this chapter has been published in:

Martell, J., Weerapana, E. Applications of copper-catalyzed click chemistry in activity-based protein profiling. *Molecules*. **2014**, *19*(2), 1378-1393.

## Introduction

The advancements in genome sequencing have allowed a better understanding of the molecular fundamentals of life. The first complete genome sequencing of a living organism was achieved in 1995 on the bacterium *Haemophilus influenza*<sup>1</sup>. In 1996 *Saccharomyces cerevisiae* became the first fully sequenced eukaryotic genome, and 1998 delivered the first sequenced multicellular eukaryotic genome, *Caenorhabditis elegans*<sup>2</sup>. Information gained from the genome itself is limited as it does not reveal the details of physiological or pathological processes, which are mostly controlled by the expression of these genes as RNA molecules and proteins. Preventing specific gene expression by gene knockout/knockdown experiments can provide insight into the roles its protein plays. Since gene expression is so dynamic in varying cellular conditions, global profiling of gene expression products at a given time, cell type, or organism paints a much clearer picture of the processes these molecules control. Global transcriptomic analysis, such as microarrays, can reveal the amounts of different mRNA expressed in a certain cell. However, mRNA levels are not directly correlated to the amount of the protein they code for, which are the key players in physiological pathways<sup>3</sup>. Global proteomic analysis confirms the presence of these proteins and provides information on protein abundance and changes in their abundance at a given time or cell type. Gel electrophoresis and western blotting are common techniques used to visualize and quantify the amount of protein while mass spectrometry can not only quantify but identify proteins within a specific proteome.

Similar to the problems associated with measuring mRNA levels to evaluate protein abundance, simply looking at protein abundance does not reflect on the activity

state of those proteins, which are regulated by a number of post-translational events<sup>4</sup>. Examples of post-translational modifications (PTMs) that can regulate the function of proteins include: the addition of functional groups such as oxidation and phosphorylation; chemical modification of amino acids like arginine citrullination and glutamine/asparagine deamidation; and structural changes involving the proteolysis of an inactive precursor or disulfide linkages between cysteine residues. The activity of proteins can also be governed by interactions with other proteins as well as endogenous inhibitors or activators<sup>5</sup>. To complement abundance-based global profiling methods such as transcriptomics and proteomics, the field of activity-based protein profiling (ABPP) has evolved to directly measure protein activity in complex proteomes<sup>6</sup>.

ABPP relies on the use of chemical probes that selectively react with the active subset of a particular protein population<sup>7</sup>. These activity-based probes (ABPs) are typically composed of a reactive group to bind and covalently modify a specific protein residue, and a reporter group, such as a fluorophore for visualization by in-gel fluorescence, or a biotin for both western blot analysis and avidin enrichment prior to mass-spectrometry (MS)-based identification (Figure 1-1)<sup>8</sup>. ABPs are generally designed to profile protein activity using either a directed or non-directed approach<sup>9</sup>. ABPs designed using the directed approach utilize reactive groups that covalently bind to functional proteins based on their specificity to an enzyme or enzyme family active site, a particular protein residue, or residue modification. A non-directed approach involves the use of probes or screening libraries of probes containing non-covalent small molecules that direct the probe to target proteins, and a photo-crosslinking or non-specific electrophilic group to irreversibly bind the ABP to the protein of interest<sup>10</sup>.

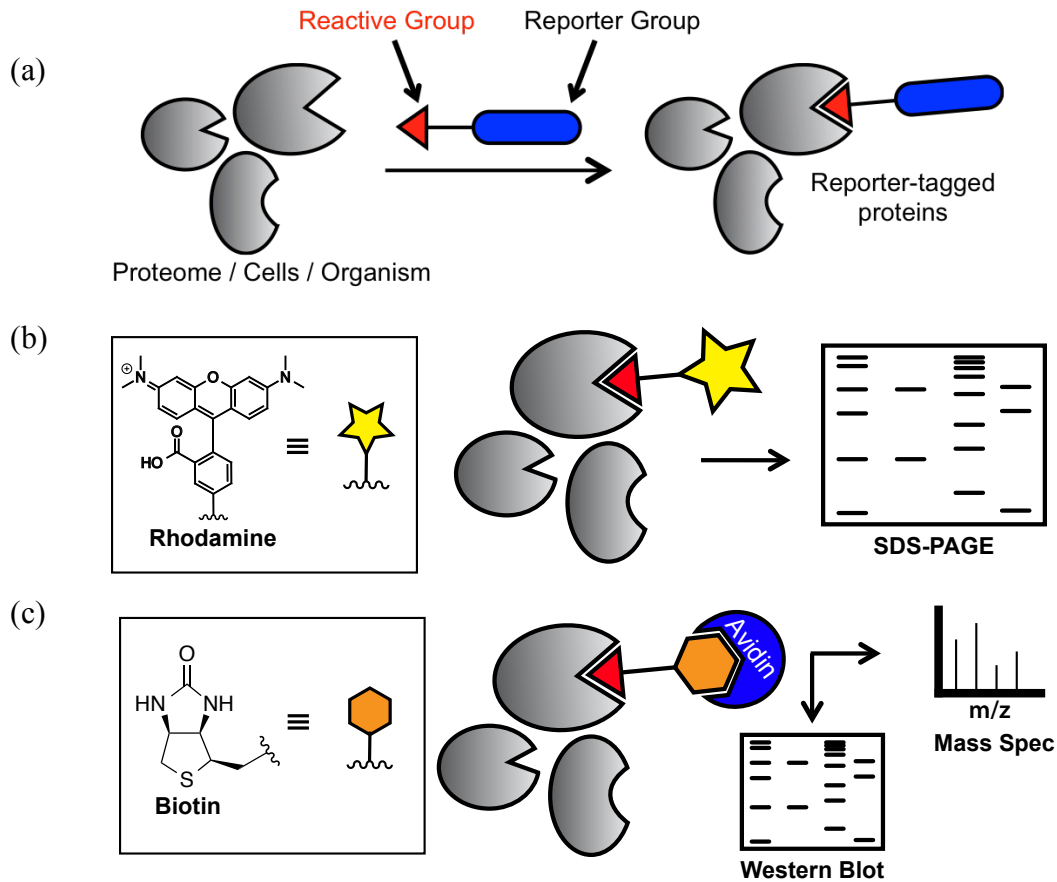


**Figure 1-1.** (a) Active enzymes are labeled within a complex proteome by activity-based probes containing a reactive group for covalent modification and a reporter group for protein visualization, enrichment, and identification. (b) Rhodamine reporter groups can be used to visualize proteins in SDS-PAGE. (c) Biotin reporter groups can be used to visualize proteins in western blots using anti-biotin antibodies, or enriched with avidin for identification using mass spectrometry.

### Electrophilic enzyme family-directed ABPs

The most extensively utilized ABPs are those designed to bind to a specific enzyme or enzyme family active site. The advantage of using ABPP over traditional proteomic methods is the ability to study which forms of a transiently active enzyme are

functional. Covalent modification of the ABP depends on the catalytic capability of the enzyme and not solely its substrate-binding ability<sup>11</sup>. The first class of enzymes targeted for ABPP studies were the serine hydrolases (SH). SHs are one of the largest families of enzymes, making up about 1% of the human proteome. SHs include proteases, peptidases, lipases, esterases, and amidases that perform numerous roles in physiological processes including blood coagulation, inflammation, and angiogenesis, as well as pathological processes such as inflammation, angiogenesis, cancer, and diabetes<sup>12</sup>. This family of enzymes is characterized by an active site serine residue that is rendered nucleophilic by the presence of a catalytic dyad or triad involving proximal lysine, aspartate, and histidine residues. The activated serine attacks a substrate ester/thioester/amide bond to form an acyl-enzyme intermediate, followed by a water-catalyzed hydrolysis of this intermediate to release the product<sup>13</sup>.

ABPs for this family of enzymes were derived from electrophilic fluorophosphonates (FP), which were known to be mechanism-based inhibitors that mimic the enzyme-substrate tetrahedral intermediate and covalently trap the active site serine<sup>14, 15</sup> (Figure 1-2a). FP-based probes react only with the active SH, and not the inactive serine mutant, zymogen, or inhibitor-bound forms, allowing modification of only functioning SH within the proteome. Electrophilic groups other than the fluorophosphonate have also been used to study the activity of SHs within a complex proteome, including diphenyl phosphonates<sup>16</sup>, 4-chloroisocoumarin<sup>17</sup>, and carbamates<sup>7</sup> (Figure 1-2b).

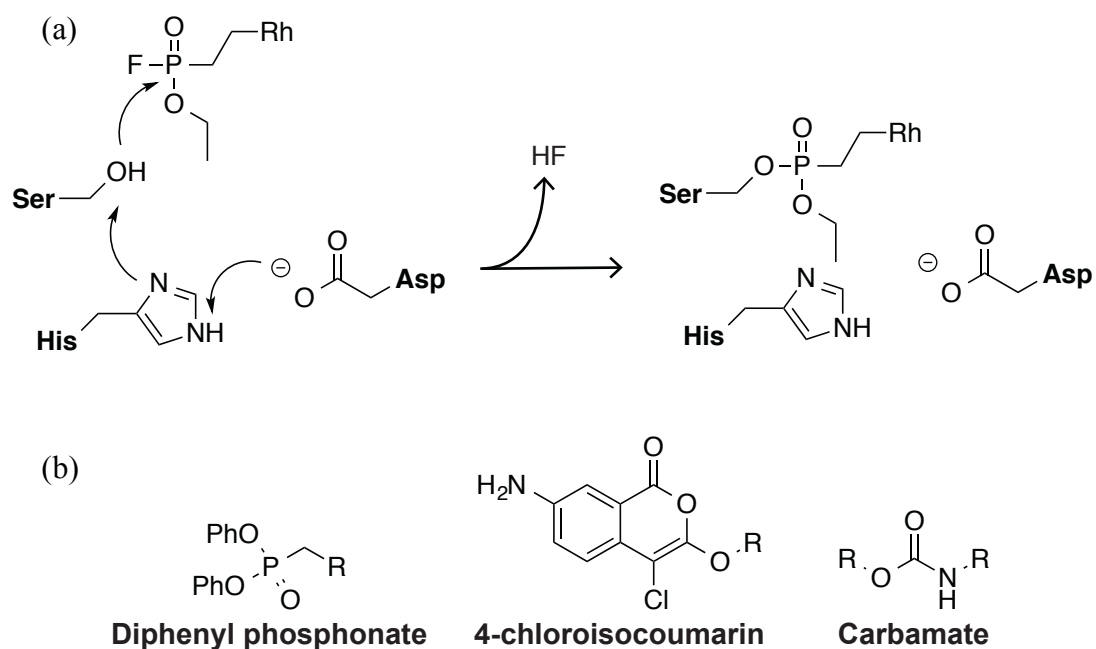
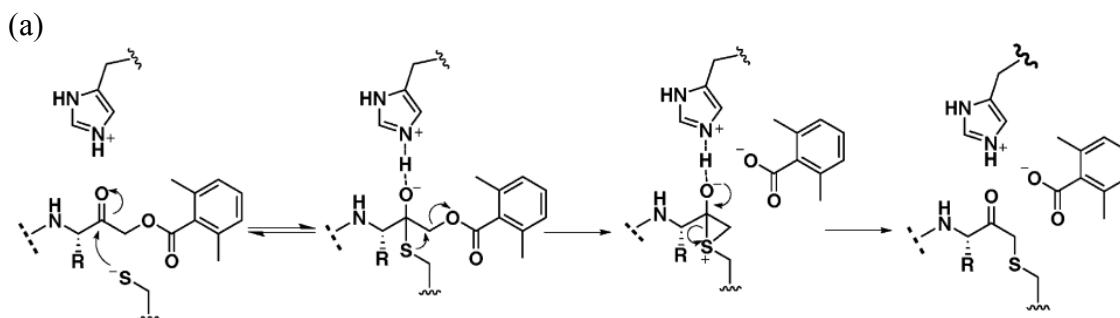


**Figure 1-2.** (a) Mechanism of serine modification via the fluorophosphonate ABP. (b) Other serine-specific electrophiles used in ABP.

Similar to serine hydrolases, cysteine proteases (CP) are another large enzyme with physiological and pathological roles in apoptosis, bone remodeling, cancer invasion, and bacterial virulence factors, among many others<sup>11, 18</sup>. This enzyme class shares a common catalytic mechanism which starts with deprotonation of the active site cysteine, usually by an adjacent histidine. This activated thiolate performs a nucleophilic attack on the substrate carbonyl carbon to form a tetrahedral intermediate. The histidine residue is deprotonated, forming a thioester intermediate and releasing a fragment of the substrate with an amine terminus. The thioester bond is hydrolyzed to generate a carboxylic acid on the remaining substrate and restoring the active enzyme<sup>7</sup>. Since the catalytic

mechanisms of CPs are distinct from SHs, the use of different electrophiles to target their active site are required.

Many cysteine-reactive electrophiles have been used in ABPs for CPs including diazo- and fluoromethyl ketones, vinyl sulfones, epoxides, and acyloxymethyl ketones (AOMKs)<sup>7</sup>. ABPs with an AOMK reactive group have been shown to be especially selective for cysteine proteases over enzymes with weaker active site nucleophiles. A library of ABPs containing this reactive group was shown to target several members CPs including caspase-3, legumain, Arg-gingipain, Lys-gingipain, cathepsin B cathepsin L<sup>19</sup> (Figure 1-3a). E-64 is an epoxide-containing natural product inhibitor with potent specificity for the active site cysteine in the papain family and limited cross-reactivity with other CPs. These characteristics have caused it to be the central structural element of several papain-specific ABPs, including DCG-04 that includes a biotin for avidin enrichment and an ionizable tyrosine for mass spectrometry analysis. DCG-04 has been used to determine functional roles of papain-like proteases in tumor progression, cataract formation, prohormone processing, parasitic invasion, and cell cycle regulation<sup>9</sup> (Figure 1-3b).



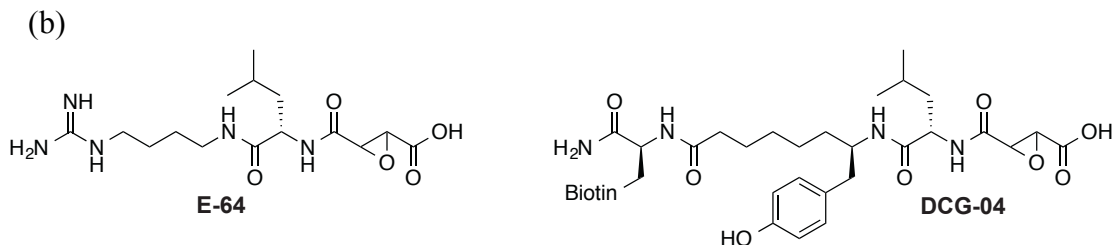


**Figure 1-3.** (a) Mechanism of inactivation of cysteine proteases by AOMKs. (b) Structure of the ABP DCG-04 and the papain inhibitor E-64 which it is based on.

Cytochrome P450 enzymes are central to the metabolism of numerous drugs, xenobiotics, and endogenous metabolites<sup>20</sup>. The activity of P450 enzymes is regulated by multiple factors including protein-binding, post-translational modifications, and regulatory enzymes<sup>4</sup>. The ability to identify the subset of active P450 enzymes is essential to the drug development process. A set of ABPs based on three different mechanism-based inhibitors, containing aryl alkynes, propynyl groups, or furanocoumarin, was synthesized and demonstrated complementarity in profiling the entire family of human P450s. Enzyme-catalyzed oxidation of the aryl alkyne generates a highly reactive ketene intermediate that can then acylate nucleophilic residues within the P450 active site (Figure 1-4a). ABPs bearing a propynyl group are oxidized to a Michael acceptor and subsequently reacts with an active site nucleophile (Figure 1-4b). Furanocoumarin-containing ABPs are oxidized to electrophilic furan epoxides and covalently modify nucleophilic residues in the active site<sup>21</sup>(Figure 1-4c).

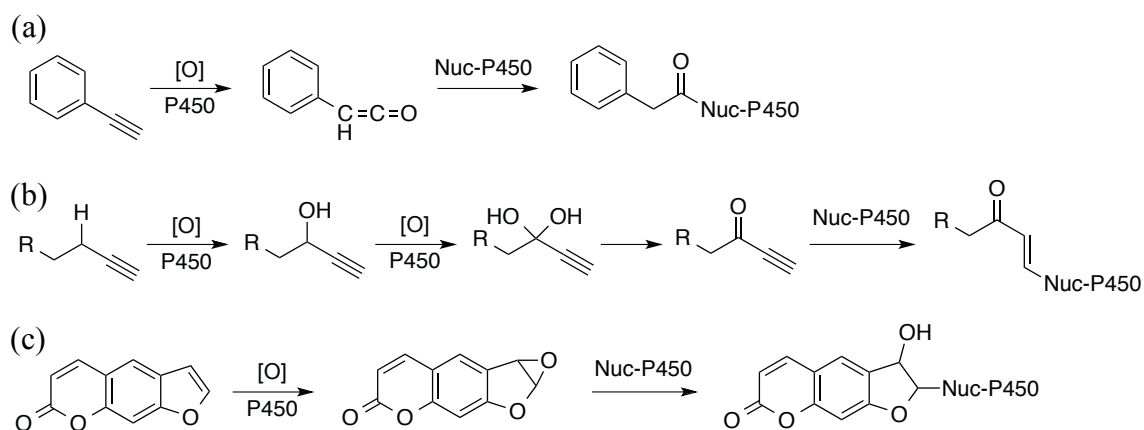


**Figure 1-4.** Modes of mechanism-based inactivation of cytochrome P450 enzymes by (a) Aryl alkynes (b) Propynyl groups (c) Furanocoumarins. Figure adapted from Wright *et al*<sup>21</sup>.

### Directed ABPs to target functional amino acids

The reactivity of an amino acid side-chain can change markedly depending on its local microenvironment<sup>22</sup>. This change in reactivity can lead to the gain or loss of covalent modifiers that have dramatic effects on its protein's function, whether by affecting an active site or the overall structure of the protein<sup>23</sup>. Using ABPP to globally identify specific amino acids with increased susceptibility to function-affecting modifications allows a more comprehensive biochemical characterization of proteomes. An excellent example of an amino acid with significant functional impact is cysteine. Depending on the microenvironment, cysteine thiols are readily deprotonated at physiological pH, making them one of the most reactive nucleophilic functional groups found in proteins<sup>24</sup>. This reactivity is utilized in proteins for catalysis, protein structure, regulation, and metal binding (Figure 1-5a); it also makes cysteines subject to oxidative

modifications such as sulfonation, sulfinitation, nitrosation, disulfide formation, and glutathionylation (Figure 1-5b)<sup>25-27</sup>.

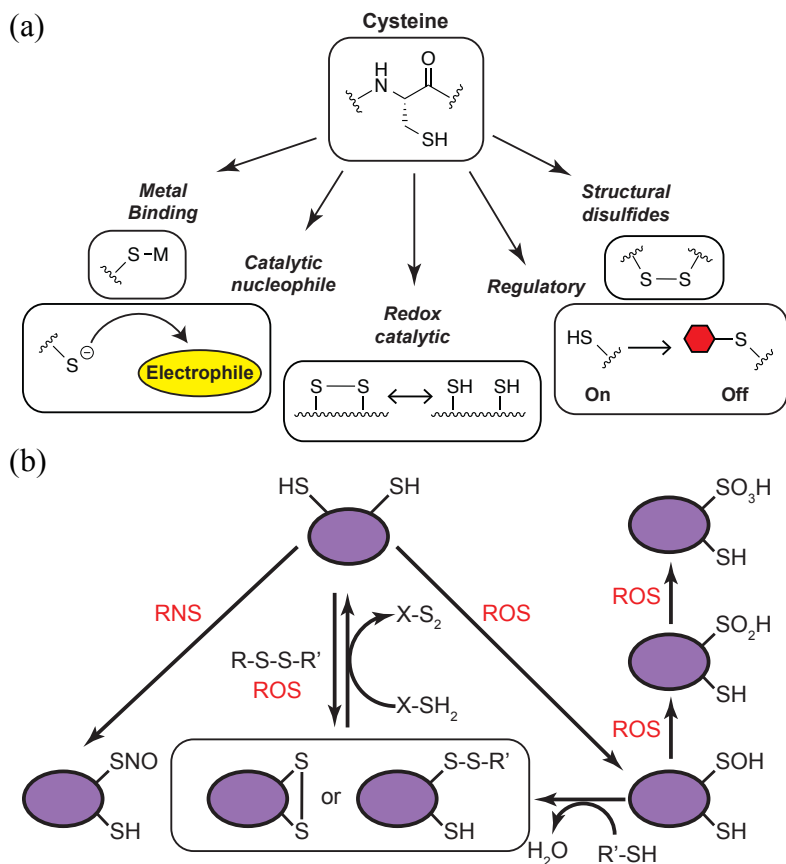


**Figure 1-5.** (a) Functional roles performed by cysteine residues. (b) Oxidative post-translational modifications of cysteine residues. Figures adapted from Pace *et al*<sup>27</sup> and Green *et al*<sup>26</sup>.

The global characterization of cysteine functionality is limited by the fact that there is no common sequence motif to identify functional cysteines. To address this issue, a cysteine-directed ABP was designed to exploit the intrinsically high nucleophilicity of cysteines. The thiol is a much softer nucleophile compared to the hydroxyl group of

serine or threonine, so the ABP utilized a softer electrophile, iodoacetamide, as the reactive group (Figure 1-6a). This ABP was used to profile cysteine reactivity in the MCF7 breast cancer cell line. The use of this residue-specific ABP allowed for the first proteome-wide survey of cysteine reactivity and demonstrated a correlation between elevated cysteine reactivity and functionality<sup>22</sup>. Electrophilic reactive groups such as other haloacetamides (chloro-fluoro-),  $\alpha,\beta$ -unsaturated ketones, and epoxides have also been shown to be highly selective for the thiol group of reactive cysteine residues<sup>22, 28, 29</sup> (Figure 1-6b). In addition to cysteine, directed ABPs using electrophilic reactive groups that target other amino acids have been developed including dichlorotriazines and acyl phosphates to target lysine residues and sulfonyl fluorides to modify active tyrosine and serine residues<sup>30-32</sup> (Figure 1-6c).

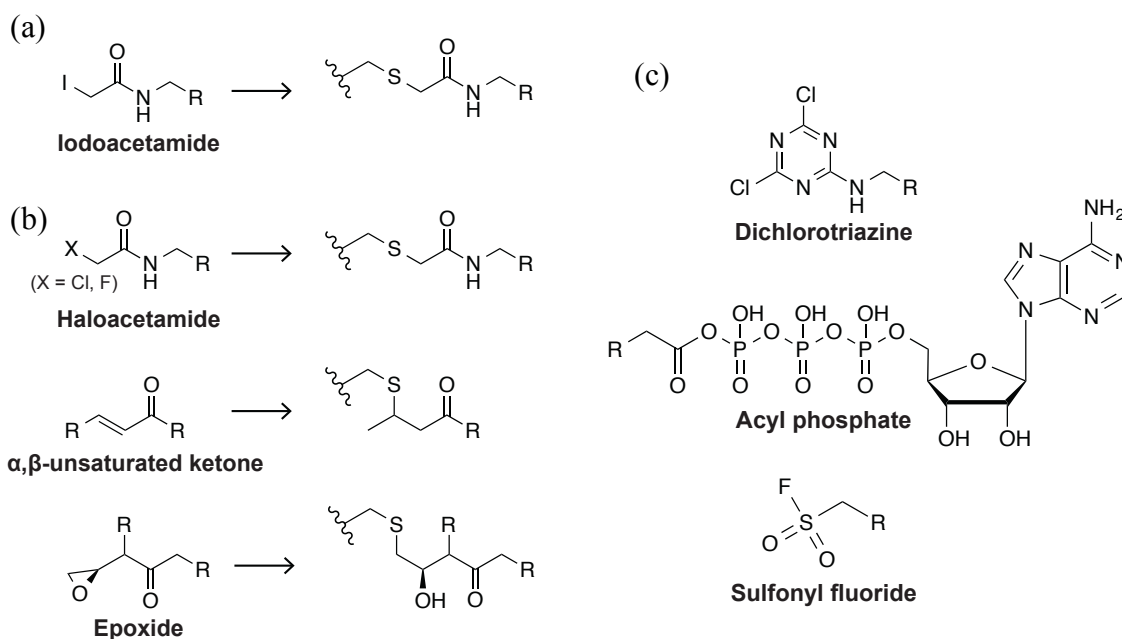


**Figure 1-6.** (a) Cysteine-reactive iodoacetamide. (b) Other electrophiles reactive toward cysteine. (c) Electrophiles to target lysine (dichlorotriazine and acyl phosphate) and tyrosine/serine (sulfonyl fluoride) residues.

## Non-electrophilic ABPs for enzyme family active sites.

Matrix metalloproteinases (MMPs) are a class of metallohydrolases which, unlike serine or cysteine hydrolases, use a zinc-activated water molecule (rather than a protein-bound nucleophile) for catalysis<sup>33</sup>. These enzymes mediate the breakdown of connective tissue and are targets for therapeutic inhibitors of inflammatory, malignant, and degenerative diseases. MMPs are also subject to a variety of posttranslational regulation including production as inactive zymogens and endogenous protein inhibition<sup>34</sup>. The development of selective and tight-binding, yet reversible, MMP inhibitors were based on known substrates and included a hydroxamate group to coordinate the conserved active site zinc atom (Figure 1-7a). To convert these reversible inhibitors into active site-directed ABPs, such as HxBP-Rh, the hydrophobic moiety within the molecule was replaced with a photo-crosslinking benzophenone group and a biotin or rhodamine reporter group was added (Figure 1-7b). Upon UV radiation, MMP-bound probes become irreversibly conjugated to the active site. These ABPs were found to selectively label active MMPs, but not the zymogen or inhibitor-bound forms<sup>33</sup>.

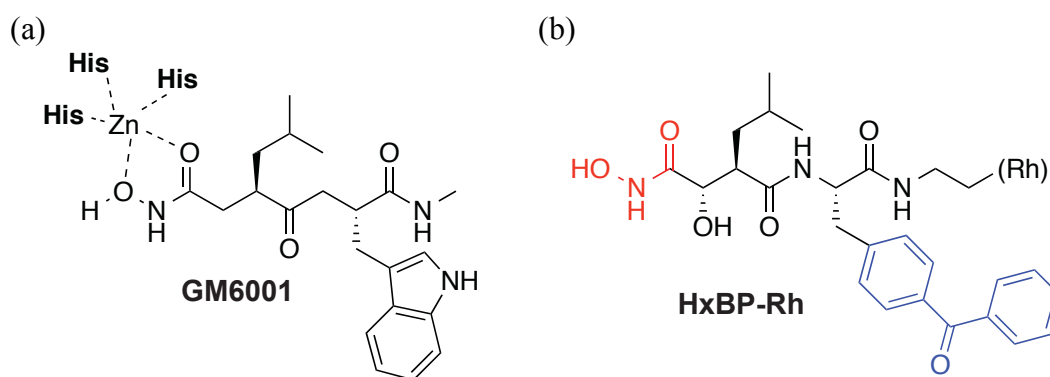


**Figure 1-7.** (a) MMP inhibitor GM6001 shown chelating to an active site zinc. (b) MMP ABP HxBP-Rh with the zinc-chelating hydroxamate group highlighted in red and the photo-crosslinking benzophenone group highlighted in blue.

## Non-directed ABP libraries

Designing ABPs for enzymes classes without known covalent inhibitors or well understood catalytic mechanism are much more challenging. To expand the breadth of ABPP, a non-directed approach has been developed in which libraries of probes are screened against a complex proteome to identify specific protein labeling events<sup>10</sup>. In addition to a reactive group for covalent modification and a reporter group for visualization, probes designed using a non-directed strategy also contain a non-covalent binding group to direct the molecule to an enzyme's active site. Unlike enzyme-directed approaches, these libraries typically use promiscuous electrophiles that react with diverse amino acids as to not be strongly biased toward a specific residue or enzyme class<sup>35</sup>. In one example of the development and screening of a library of candidate ABPs, probes bearing an  $\alpha$ -chloroacetamide ( $\alpha$ -CA) reactive group, a rhodamine reporter group, and a variable dipeptide binding group were synthesized and screened against mouse tissue proteomes (Figure 1-8). The library's reactive group was chosen to be an  $\alpha$ -CA because it is sterically small with no enzyme class specificity, making it unlikely to influence non-covalent protein labeling. It was found that each member of this library reacted with a very different set of proteins, highlighting the ability of the variable binding group to dictate specific protein interactions. Enzymes from a variety of classes were labeled by this  $\alpha$ -CA library, some previously identified to react with only  $\alpha$ -CA ABPs, others that have been labeled using a different electrophile. The Asp-Asp- $\alpha$ -CA was a very strong enzyme-directed ABP candidate as it labeled only creatine kinase with little background reactivity with other proteins. Additionally, this specific interaction was shown to be

heat-sensitive and outcompeted by ATP, suggesting the probe-protein interaction was structure- and activity-based<sup>35</sup>.

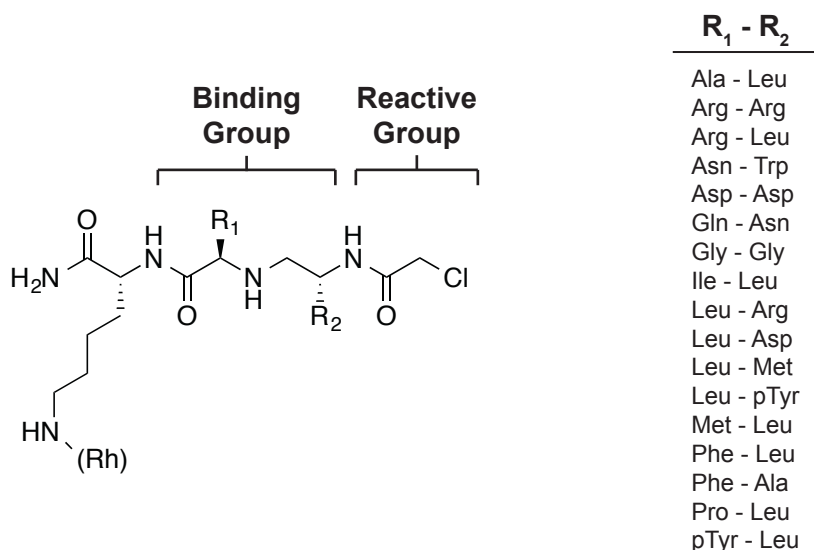


**Figure 1-8.** Design of the  $\alpha$ -chloroacetamide dipeptide probe library, with the R1-R2 binding groups specified (pTyr = phosphotyrosine).

### Directed ABPs for modified amino acids

Instead of globally profiling enzyme activity based on whether their active site residue is functional or inactivated by PTMs, the methods of ABPP can be adapted to globally profile specific PTMs within complex proteomes. The reactive group in this case is specific for a certain amino acid modification instead of an active site residue. Two examples of PTMs that have been profiled using chemical probes are cysteine hydroxylation (sulfenic acid) and arginine citrullination. The formation of reversible cysteine sulfenic acids (SOH) is a major component in regulating cell-signaling pathways by reactive oxygen species. Due to the transient nature of cysteine SOH, it has been challenging to monitor and identify proteins with redox-regulated cysteines. SOH

formation gives the typically nucleophilic sulfur atom electrophilic characteristics, allowing unique reactivity toward nucleophiles such as 5,5-dimethyl-1,3-cyclohexadione (dimedone)<sup>36</sup> (Figure 1-9a). Dimedone is able to trap SOH, forming a covalent thioether linkage that is not reversible by reductants like DTT or TCEP<sup>37</sup>. It is also unreactive toward S-nitrosothiol, methionine sulfoxide, aldehydes, and amines<sup>38</sup>. Incorporating either a rhodamine or biotin reporter group attached through a linker to dimedone enabled the identification of sets of previously unknown oxidation-sensitive proteins<sup>39-41</sup>.

Protein arginine deiminases (PADs) catalyze the conversion of arginine to citrulline in the presence of calcium, commonly called deimination or citrullination (Figure 1-9b)<sup>42</sup>. Increased PAD activity has been observed in a variety of diseases including rheumatoid arthritis (RA)<sup>43</sup>, Alzheimer's disease<sup>44</sup>, and ulcerative colitis (UC)<sup>45</sup>, however the roles and targets of these enzymes are still poorly understood. A citrulline-specific probe was designed based on the selective reaction between phenylglyoxal (PG) and citrulline under acidic conditions (Figure 1-9a). While also able to form a thiohemiacetal with cysteine residues in acidic conditions, the PG-citrulline condensation product is stable at neutral pH while the thiohemiacetal is not. A rhodamine was attached to the PG group (Rh-PG) and used to visualize citrullinated proteins within the proteome of a disease mouse model of UC. A correlation between disease severity and citrulline level was observed, demonstrating the utility of this probe in identifying citrullination in the context of a disease<sup>46</sup>.

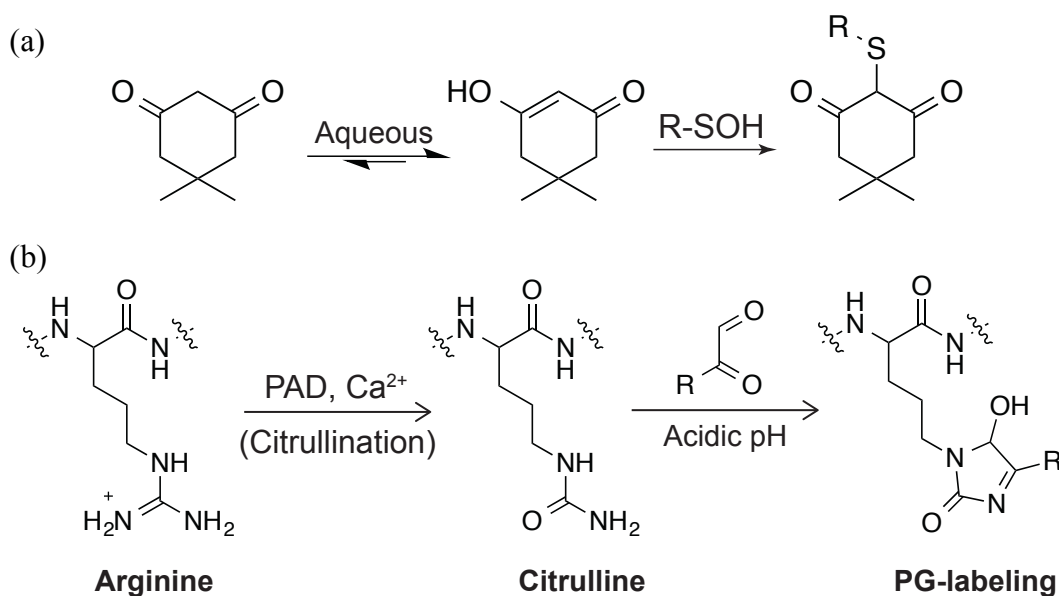


**Figure 1-9.** (a) Dimedone selectively labels cysteine sulfenic acids. (b) Citrullination of arginine via PAD. The PG-probe labels citrulline over arginine at acidic pH.

### CuAAC-mediated ABPP

The advent of click chemistry, in particular, the copper (I)-catalyzed azide-alkyne cycloaddition (CuAAC), has benefitted the field of ABPP by replacing bulky reporter groups with smaller alkyne or azide groups to promote cell permeability and better access to active sites as well as adding modularity to the system; now a single probe can be diversified with a variety of reporter groups without the need to develop new synthetic routes<sup>47</sup> (Figure 1-10). CuAAC is the most widely used click chemistry reaction involving an azide and a terminal alkyne to generate a 1,4-disubstituted 1,2,3-triazole<sup>48</sup> (Figure 1-10). The CuAAC reaction was first utilized in the field of ABPP to couple an azide-derivatized phenyl sulfonate ester ABP (PS-N3) to an alkyne-bearing rhodamine moiety (Rh-alkyne)<sup>47</sup>. The PS-N3 probe labeled GSTO 1-1 proteins in cell lysates more efficiently than the standard rhodamine-tagged phenyl sulfonate probe (PS-Rh).

Furthermore, PS-N3 was shown to facilitate *in vivo* ABPP, as cells and animals treated with PS-N3 showed robust protein labeling upon administration of the CuAAC reagents *ex vivo*<sup>47</sup>. Further optimization of this platform revealed that the use of rhodamine-azide (Rh-N3) greatly reduced the high background labeling of proteins that was observed with Rh-alkyne, although with lower kinetics of labeling<sup>49</sup>.

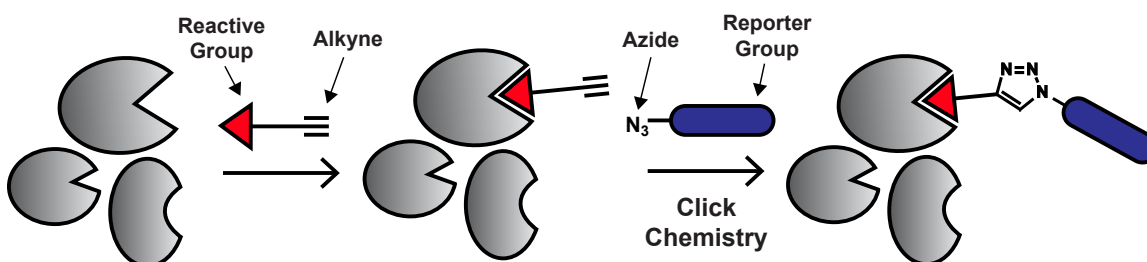


**Figure 1-10.** ABP with bulky reporter groups are replaced with an alkyne handle to allow conjugation to an azide-containing reporter group via copper catalyzed click chemistry.

Most ABPP studies for SHs are performed using biotin or rhodamine tagged FP, but CuAAC has shown utility in the profiling of these enzymes with the generation of the FP-alkyne<sup>50-52</sup>. This probe was shown to label serine proteases with greater affinity than the reporter-tag functionalized FP probes. More importantly, the vastly improved cell permeability of FP-alkyne facilitates profiling of SH activity directly in living cells. This improved cell permeability enabled the development of a competitive ABPP platform to screen inhibitor selectivity in native cellular environments instead of in lysates where information pertaining to subcellular localization is disrupted<sup>51</sup>. FP-based probes for specific SHs have also been developed with inclusion of an alkyne handle for CuAAC. For example, the hepatitis C virus (HCV) induces alterations of host cells to

facilitate its life cycle. Fatty acid synthase (FASN) is a multidomain enzyme that plays a key role in the biosynthesis of fatty acids and is upregulated during HCV infection. Orlistat, a  $\beta$ -lactone-based covalent inhibitor of FASN was converted to an ABP by functionalizing its alkyl chain with a terminal alkyne. This did not alter the enzyme selectivity of Orlistat and allowed the post-labeling conjugation of Rh-N<sub>3</sub> by CuAAC to image the localization of FASN during HCV infection<sup>53</sup>.

Another family of enzymes whose studies were facilitated by the use of CuAAC-mediated ABPP were those in the ubiquitin and ubiquitin-like protein (UBL) signaling pathways<sup>54</sup>. A series of ubiquitin-conjugating enzymes tag proteins with ubiquitin for targeted degradation by the proteasome, including UBL activating enzymes (UBE1), UBL conjugating enzymes (UBE2), and UBL ligases (UBE3)<sup>55</sup>. Since UBE1 enzymes dictate the activity of the entire ubiquitin-signaling pathway, they have been recognized as emerging drug targets to treat human diseases. The lack of methods to discover UBL proteins and monitor the intracellular activity of UBE1 enzymes inspired the development of a CuAAC-compatible ABP for UBE1 enzymes was developed to measure UBE1 activity inside cells. The UBE1 ABP was designed to mimic and bind the AMP binding site of the UBE1-UBL thioester complex, positioning a nucleophilic sulfamate group for attack of the UBE1-UBL thioester to form a covalent adduct. This cell permeable ABP1 efficiently labels active UBE1 enzymes in numerous cancer cell lines, allowing for profiling the selectivity of UBE1 inhibitors within cells, and facilitating the discovery of previously unknown UBL proteins<sup>54</sup>.

Lastly, CuAAC-mediated ABPP has been extended to directly profile the activity of the PAD protein family. PAD probes were constructed around mechanism-based

inactivators that contain a haloacetamide (Cl or F) to covalently modify the active site cysteine<sup>56</sup>. Alkyne-functionalized PAD ABPs were shown to be more selective and efficient at labeling PAD4 in cells compared to the biotin and fluorescein-tagged counterparts<sup>57</sup>. This increased efficiency of labeling is attributed to the rapid degradation of PAD4 in cell lysates, which is circumvented by in-cell labeling with CuAAC-compatible probes. A similar alkyne-functionalized chloroacetamide probe was shown to label the related enzyme dimethylarginine dimethylaminohydrolase (DDAH). Similar to the PADs, DDAH activity is diminished in lysates due to inactivation by a variety of effector molecules, therefore in vivo labeling using CuAAC-compatible probes serves to preserve enzyme activity<sup>58</sup>.

### **Applications of CuAAC in Mass Spectrometry-Based ABPP**

SDS-PAGE and in-gel fluorescence only reveal a fraction of proteins targeted by APBs, and therefore, many mass spectrometry (MS)-based methods have emerged as gel-free alternatives that provide higher resolution and greater sensitivity<sup>59</sup>. One of the advantages of CuAAC-based ABPP methods is the ability to conjugate probe-labeled proteins to a variety of linkers that enable a diverse array of mass-spectrometry analyses. Typical MS-ABPP strategies utilize CuAAC to couple a biotin-azide for subsequent enrichment and identification of labeled proteins by mass spectrometry<sup>60</sup>. Discussed in Chapter 2, more advanced MS experiments involve the installment of a chemically or proteolytically cleavable linker that further allows for identification of the site of probe labeling, as well as the relative quantification of labeled proteins from two or more biological samples<sup>61, 62</sup>. These platforms have expanded the scope and utility of ABPP

through applications evaluating the amino-acid specificity of electrophiles used for ABPP<sup>28</sup>, ranking cysteine residues in the proteome by their nucleophilicity so as to globally identify functional cysteines<sup>22</sup>, and identifying residues subject to post-translational modification through reactive lipid species<sup>63</sup> and metal binding<sup>64</sup>.

Another application of CuAAC in ABPP involves using imaging mass spectrometry to study the distribution of active serine hydrolases in tissue. In this study, tissue sections were treated with FP-alkyne, followed by incorporation of a mass-tagged dendrimer using CuAAC. The mass tags are connected to the dendrimer via laser-cleavable linkers, thereby releasing the mass tags upon laser irradiation for direct analysis by MALDI-MS<sup>65</sup>. CuAAC has also been used in the absolute quantification of serine protease activity using ICP/MS<sup>66</sup>. Alkyne functionalized AEBSF (serine protease inhibitor) analogs were modified with a europium-loaded azido-monoamide-DOTA using CuAAC. Serine proteases that reacted with this probe were analyzed by ICP/MS allowing for the absolute quantification of active serine proteases in a mixture<sup>66</sup>.

## **Conclusion**

Activity-based protein profiling is a chemical proteomic technique that allows for selective labeling, visualization, and enrichment of active enzymes in a complex proteome. Given the dominant role of posttranslational modifications in regulating protein function in vivo, ABPP provides a direct readout of activity that is not attained through traditional proteomic methods. Directed and non-directed ABP designs bearing various reactive and reporter groups have been used to profile the functional activity of specific protein residues such as cysteines and lysines as well as diverse enzymes and

enzyme classes including serine hydrolases, cysteine proteases, cytochrome P450 enzymes, and matrix metalloproteinases. ABP-like compounds have also been developed to profile distinct post-translational modifications like cysteine oxidation and arginine citrullination. The application of CuAAC has significantly modularized ABPP approaches, whereby a single ABP can now be conjugated to a variety of reporter elements depending on the application of interest. Furthermore, CuAAC compatible probes are much smaller than reporter-tagged probes, causing minimal steric interaction with enzyme active sites, thereby improving binding affinity and enhancing probe labeling in lysates as well as within the unperturbed environment of a live cell or animal. Finally, the advent of CuAAC has facilitated the expansion of ABPP by coupling to advanced analytical platforms such as MALDI-imaging of active enzyme in tissue slices, absolute quantitation of active enzyme by ICP-MS, and direct identification and quantitation of the exact sites of probe labeling.

## References

1. Fleischmann, R. D.; Adams, M. D.; White, O.; Clayton, R. A.; Kirkness, E. F.; Kerlavage, A. R.; Bult, C. J.; Tomb, J. F.; Dougherty, B. A.; Merrick, J. M.; et al., Whole-genome random sequencing and assembly of *Haemophilus influenzae* Rd. *Science* **1995**, *269* (5223), 496-512.
2. Consortium, C. e. S., Genome sequence of the nematode *C. elegans*: a platform for investigating biology. *Science* **1998**, *282* (5396), 2012-8.

3. Tian, Q.; Stepaniants, S. B.; Mao, M.; Weng, L.; Feetham, M. C.; Doyle, M. J.; Yi, E. C.; Dai, H.; Thorsson, V.; Eng, J.; Goodlett, D.; Berger, J. P.; Gunter, B.; Linseley, P. S.; Stoughton, R. B.; Aebersold, R.; Collins, S. J.; Hanlon, W. A.; Hood, L. E., Integrated genomic and proteomic analyses of gene expression in Mammalian cells. *Molecular & cellular proteomics : MCP* **2004**, *3* (10), 960-9.
4. Cravatt, B. F.; Wright, A. T.; Kozarich, J. W., Activity-based protein profiling: from enzyme chemistry to proteomic chemistry. *Annual review of biochemistry* **2008**, *77*, 383-414.
5. Kobe, B.; Kemp, B. E., Active site-directed protein regulation. *Nature* **1999**, *402* (6760), 373-6.
6. Adam, G. C.; Sorensen, E. J.; Cravatt, B. F., Chemical strategies for functional proteomics. *Molecular & cellular proteomics : MCP* **2002**, *1* (10), 781-90.
7. Evans, M. J.; Cravatt, B. F., Mechanism-based profiling of enzyme families. *Chemical reviews* **2006**, *106* (8), 3279-301.
8. Speers, A. E.; Cravatt, B. F., Chemical strategies for activity-based proteomics. *Chembiochem : a European journal of chemical biology* **2004**, *5* (1), 41-7.
9. Fonovic, M.; Bogyo, M., Activity based probes for proteases: applications to biomarker discovery, molecular imaging and drug screening. *Current pharmaceutical design* **2007**, *13* (3), 253-61.
10. Adam, G. C.; Burbaum, J.; Kozarich, J. W.; Patricelli, M. P.; Cravatt, B. F., Mapping enzyme active sites in complex proteomes. *Journal of the American Chemical Society* **2004**, *126* (5), 1363-8.

11. Sanman, L. E.; Bogyo, M., Activity-based profiling of proteases. *Annual review of biochemistry* **2014**, *83*, 249-73.
12. Long, J. Z.; Cravatt, B. F., The metabolic serine hydrolases and their functions in mammalian physiology and disease. *Chemical reviews* **2011**, *111* (10), 6022-63.
13. Dodson, G.; Wlodawer, A., Catalytic triads and their relatives. *Trends in biochemical sciences* **1998**, *23* (9), 347-52.
14. Kidd, D.; Liu, Y.; Cravatt, B. F., Profiling serine hydrolase activities in complex proteomes. *Biochemistry* **2001**, *40* (13), 4005-15.
15. Liu, Y.; Patricelli, M. P.; Cravatt, B. F., Activity-based protein profiling: the serine hydrolases. *Proceedings of the National Academy of Sciences of the United States of America* **1999**, *96* (26), 14694-9.
16. Joossens, J.; Van der Veken, P.; Surpateanu, G.; Lambeir, A. M.; El-Sayed, I.; Ali, O. M.; Augustyns, K.; Haemers, A., Diphenyl phosphonate inhibitors for the urokinase-type plasminogen activator: optimization of the P4 position. *Journal of medicinal chemistry* **2006**, *49* (19), 5785-93.
17. Haedke, U.; Gotz, M.; Baer, P.; Verhelst, S. H., Alkyne derivatives of isocoumarins as clickable activity-based probes for serine proteases. *Bioorganic & medicinal chemistry* **2012**, *20* (2), 633-40.
18. Gocheva, V.; Joyce, J. A., Cysteine cathepsins and the cutting edge of cancer invasion. *Cell cycle* **2007**, *6* (1), 60-4.
19. Kato, D.; Boatright, K. M.; Berger, A. B.; Nazif, T.; Blum, G.; Ryan, C.; Chehade, K. A.; Salvesen, G. S.; Bogyo, M., Activity-based probes that target diverse cysteine protease families. *Nature chemical biology* **2005**, *1* (1), 33-8.

20. Denisov, I. G.; Makris, T. M.; Sligar, S. G.; Schlichting, I., Structure and chemistry of cytochrome P450. *Chemical reviews* **2005**, *105* (6), 2253-77.
21. Wright, A. T.; Song, J. D.; Cravatt, B. F., A suite of activity-based probes for human cytochrome P450 enzymes. *Journal of the American Chemical Society* **2009**, *131* (30), 10692-700.
22. Weerapana, E.; Wang, C.; Simon, G. M.; Richter, F.; Khare, S.; Dillon, M. B.; Bachovchin, D. A.; Mowen, K.; Baker, D.; Cravatt, B. F., Quantitative reactivity profiling predicts functional cysteines in proteomes. *Nature* **2010**, *468* (7325), 790-5.
23. Zhao, Y.; Jensen, O. N., Modification-specific proteomics: strategies for characterization of post-translational modifications using enrichment techniques. *Proteomics* **2009**, *9* (20), 4632-41.
24. Bulaj, G.; Kortemme, T.; Goldenberg, D. P., Ionization-reactivity relationships for cysteine thiols in polypeptides. *Biochemistry* **1998**, *37* (25), 8965-72.
25. Reddie, K. G.; Carroll, K. S., Expanding the functional diversity of proteins through cysteine oxidation. *Current opinion in chemical biology* **2008**, *12* (6), 746-54.
26. Green, J.; Paget, M. S., Bacterial redox sensors. *Nature reviews. Microbiology* **2004**, *2* (12), 954-66.
27. Pace, N. J.; Weerapana, E., Diverse functional roles of reactive cysteines. *ACS chemical biology* **2013**, *8* (2), 283-96.
28. Weerapana, E.; Simon, G. M.; Cravatt, B. F., Disparate proteome reactivity profiles of carbon electrophiles. *Nature chemical biology* **2008**, *4* (7), 405-7.

29. Yang, Z.; Fonovic, M.; Verhelst, S. H.; Blum, G.; Bogoy, M., Evaluation of alpha,beta-unsaturated ketone-based probes for papain-family cysteine proteases. *Bioorganic & medicinal chemistry* **2009**, *17* (3), 1071-8.
30. Shannon, D. A.; Banerjee, R.; Webster, E. R.; Bak, D. W.; Wang, C.; Weerapana, E., Investigating the proteome reactivity and selectivity of aryl halides. *Journal of the American Chemical Society* **2014**, *136* (9), 3330-3.
31. Patricelli, M. P.; Szardenings, A. K.; Liyanage, M.; Nomanbhoy, T. K.; Wu, M.; Weissig, H.; Aban, A.; Chun, D.; Tanner, S.; Kozarich, J. W., Functional interrogation of the kinome using nucleotide acyl phosphates. *Biochemistry* **2007**, *46* (2), 350-8.
32. Gu, C.; Shannon, D. A.; Colby, T.; Wang, Z.; Shabab, M.; Kumari, S.; Villamor, J. G.; McLaughlin, C. J.; Weerapana, E.; Kaiser, M.; Cravatt, B. F.; van der Hoorn, R. A., Chemical proteomics with sulfonyl fluoride probes reveals selective labeling of functional tyrosines in glutathione transferases. *Chemistry & biology* **2013**, *20* (4), 541-8.
33. Saghatelian, A.; Jessani, N.; Joseph, A.; Humphrey, M.; Cravatt, B. F., Activity-based probes for the proteomic profiling of metalloproteases. *Proceedings of the National Academy of Sciences of the United States of America* **2004**, *101* (27), 10000-5.
34. Whittaker, M.; Floyd, C. D.; Brown, P.; Gearing, A. J., Design and therapeutic application of matrix metalloproteinase inhibitors. *Chemical reviews* **1999**, *99* (9), 2735-76.
35. Barglow, K. T.; Cravatt, B. F., Discovering disease-associated enzymes by proteome reactivity profiling. *Chemistry & biology* **2004**, *11* (11), 1523-31.

36. Leonard, S. E.; Reddie, K. G.; Carroll, K. S., Mining the thiol proteome for sulfenic acid modifications reveals new targets for oxidation in cells. *ACS chemical biology* **2009**, *4* (9), 783-99.
37. Furdui, C. M.; Poole, L. B., Chemical approaches to detect and analyze protein sulfenic acids. *Mass spectrometry reviews* **2014**, *33* (2), 126-46.
38. Poole, L. B.; Zeng, B. B.; Knaggs, S. A.; Yakubu, M.; King, S. B., Synthesis of chemical probes to map sulfenic acid modifications on proteins. *Bioconjugate chemistry* **2005**, *16* (6), 1624-8.
39. Charles, R. L.; Schroder, E.; May, G.; Free, P.; Gaffney, P. R.; Wait, R.; Begum, S.; Heads, R. J.; Eaton, P., Protein sulfenation as a redox sensor: proteomics studies using a novel biotinylated dimedone analogue. *Molecular & cellular proteomics : MCP* **2007**, *6* (9), 1473-84.
40. Reddie, K. G.; Seo, Y. H.; Muse Iii, W. B.; Leonard, S. E.; Carroll, K. S., A chemical approach for detecting sulfenic acid-modified proteins in living cells. *Molecular bioSystems* **2008**, *4* (6), 521-31.
41. Wani, R.; Qian, J.; Yin, L.; Bechtold, E.; King, S. B.; Poole, L. B.; Paek, E.; Tsang, A. W.; Furdui, C. M., Isoform-specific regulation of Akt by PDGF-induced reactive oxygen species. *Proceedings of the National Academy of Sciences of the United States of America* **2011**, *108* (26), 10550-5.
42. Jones, J. E.; Causey, C. P.; Knuckley, B.; Slack-Noyes, J. L.; Thompson, P. R., Protein arginine deiminase 4 (PAD4): Current understanding and future therapeutic potential. *Current opinion in drug discovery & development* **2009**, *12* (5), 616-27.

43. Suzuki, A.; Yamada, R.; Chang, X.; Tokuhira, S.; Sawada, T.; Suzuki, M.; Nagasaki, M.; Nakayama-Hamada, M.; Kawaida, R.; Ono, M.; Ohtsuki, M.; Furukawa, H.; Yoshino, S.; Yukioka, M.; Tohma, S.; Matsubara, T.; Wakitani, S.; Teshima, R.; Nishioka, Y.; Sekine, A.; Iida, A.; Takahashi, A.; Tsunoda, T.; Nakamura, Y.; Yamamoto, K., Functional haplotypes of PADI4, encoding citrullinating enzyme peptidylarginine deiminase 4, are associated with rheumatoid arthritis. *Nature genetics* **2003**, *34* (4), 395-402.
44. Ishigami, A.; Ohsawa, T.; Hiratsuka, M.; Taguchi, H.; Kobayashi, S.; Saito, Y.; Murayama, S.; Asaga, H.; Toda, T.; Kimura, N.; Maruyama, N., Abnormal accumulation of citrullinated proteins catalyzed by peptidylarginine deiminase in hippocampal extracts from patients with Alzheimer's disease. *Journal of neuroscience research* **2005**, *80* (1), 120-8.
45. Chen, C. C.; Isomoto, H.; Narumi, Y.; Sato, K.; Oishi, Y.; Kobayashi, T.; Yanagihara, K.; Mizuta, Y.; Kohno, S.; Tsukamoto, K., Haplotypes of PADI4 susceptible to rheumatoid arthritis are also associated with ulcerative colitis in the Japanese population. *Clinical immunology* **2008**, *126* (2), 165-71.
46. Bicker, K. L.; Subramanian, V.; Chumanevich, A. A.; Hofseth, L. J.; Thompson, P. R., Seeing citrulline: development of a phenylglyoxal-based probe to visualize protein citrullination. *Journal of the American Chemical Society* **2012**, *134* (41), 17015-8.
47. Speers, A. E.; Adam, G. C.; Cravatt, B. F., Activity-based protein profiling in vivo using a copper(i)-catalyzed azide-alkyne [3 + 2] cycloaddition. *Journal of the American Chemical Society* **2003**, *125* (16), 4686-7.

48. Wang, Q.; Chan, T. R.; Hilgraf, R.; Fokin, V. V.; Sharpless, K. B.; Finn, M. G., Bioconjugation by copper(I)-catalyzed azide-alkyne [3 + 2] cycloaddition. *Journal of the American Chemical Society* **2003**, *125* (11), 3192-3.
49. Speers, A. E.; Cravatt, B. F., Profiling enzyme activities in vivo using click chemistry methods. *Chemistry & biology* **2004**, *11* (4), 535-46.
50. Simon, G. M.; Cravatt, B. F., Activity-based proteomics of enzyme superfamilies: serine hydrolases as a case study. *The Journal of biological chemistry* **2010**, *285* (15), 11051-5.
51. Gillet, L. C.; Namoto, K.; Ruchti, A.; Hoving, S.; Boesch, D.; Inverardi, B.; Mueller, D.; Coulot, M.; Schindler, P.; Schweigler, P.; Bernardi, A.; Gil-Parrado, S., In-cell selectivity profiling of serine protease inhibitors by activity-based proteomics. *Molecular & cellular proteomics : MCP* **2008**, *7* (7), 1241-53.
52. Tully, S. E.; Cravatt, B. F., Activity-based probes that target functional subclasses of phospholipases in proteomes. *Journal of the American Chemical Society* **2010**, *132* (10), 3264-5.
53. Nasheri, N.; Joyce, M.; Rouleau, Y.; Yang, P.; Yao, S.; Tyrrell, D. L.; Pezacki, J. P., Modulation of fatty acid synthase enzyme activity and expression during hepatitis C virus replication. *Chemistry & biology* **2013**, *20* (4), 570-82.
54. An, H.; Statsyuk, A. V., Development of activity-based probes for ubiquitin and ubiquitin-like protein signaling pathways. *Journal of the American Chemical Society* **2013**, *135* (45), 16948-62.

55. Ciechanover, A., Intracellular protein degradation: from a vague idea through the lysosome and the ubiquitin-proteasome system and onto human diseases and drug targeting. *Neuro-degenerative diseases* **2012**, *10* (1-4), 7-22.
56. Luo, Y.; Knuckley, B.; Bhatia, M.; Pellechia, P. J.; Thompson, P. R., Activity-based protein profiling reagents for protein arginine deiminase 4 (PAD4): synthesis and in vitro evaluation of a fluorescently labeled probe. *Journal of the American Chemical Society* **2006**, *128* (45), 14468-9.
57. Slack, J. L.; Causey, C. P.; Luo, Y.; Thompson, P. R., Development and use of clickable activity based protein profiling agents for protein arginine deiminase 4. *ACS chemical biology* **2011**, *6* (5), 466-76.
58. Wang, Y.; Hu, S.; Fast, W., A click chemistry mediated in vivo activity probe for dimethylarginine dimethylaminohydrolase. *Journal of the American Chemical Society* **2009**, *131* (42), 15096-7.
59. Cravatt, B. F.; Simon, G. M.; Yates, J. R., 3rd, The biological impact of mass-spectrometry-based proteomics. *Nature* **2007**, *450* (7172), 991-1000.
60. Speers, A. E.; Cravatt, B. F., Activity-Based Protein Profiling (ABPP) and Click Chemistry (CC)-ABPP by MudPIT Mass Spectrometry. *Current protocols in chemical biology* **2009**, *1*, 29-41.
61. Weerapana, E.; Speers, A. E.; Cravatt, B. F., Tandem orthogonal proteolysis-activity-based protein profiling (TOP-ABPP)--a general method for mapping sites of probe modification in proteomes. *Nature protocols* **2007**, *2* (6), 1414-25.

62. Speers, A. E.; Cravatt, B. F., A tandem orthogonal proteolysis strategy for high-content chemical proteomics. *Journal of the American Chemical Society* **2005**, *127* (28), 10018-9.
63. Wang, C.; Weerapana, E.; Blewett, M. M.; Cravatt, B. F., A chemoproteomic platform to quantitatively map targets of lipid-derived electrophiles. *Nature methods* **2014**, *11* (1), 79-85.
64. Pace, N. J.; Weerapana, E., A competitive chemical-proteomic platform to identify zinc-binding cysteines. *ACS chemical biology* **2014**, *9* (1), 258-65.
65. Yang, J.; Chaurand, P.; Norris, J. L.; Porter, N. A.; Caprioli, R. M., Activity-based probes linked with laser-cleavable mass tags for signal amplification in imaging mass spectrometry: analysis of serine hydrolase enzymes in mammalian tissue. *Analytical chemistry* **2012**, *84* (8), 3689-95.
66. Yan, X.; Luo, Y.; Zhang, Z.; Li, Z.; Luo, Q.; Yang, L.; Zhang, B.; Chen, H.; Bai, P.; Wang, Q., Europium-labeled activity-based probe through click chemistry: absolute serine protease quantification using  $(^{153}\text{Eu})$  isotope dilution ICP/MS. *Angewandte Chemie* **2012**, *51* (14), 3358-63.

## Chapter 2

### An Isotopically Tagged Azobenzene-Based Cleavable Linker for Quantitative ABPP

A significant portion of the work described in this chapter has been published in:

Qian, Y., Martell, J., Pace, N.J., Ballard, T.E., Johnson, D.S., Weerapana E. An isotopically tagged azobenzene-based cleavable linker for quantitative proteomics. *ChemBioChem*. **2013**, *14* (12), 1410-1414.

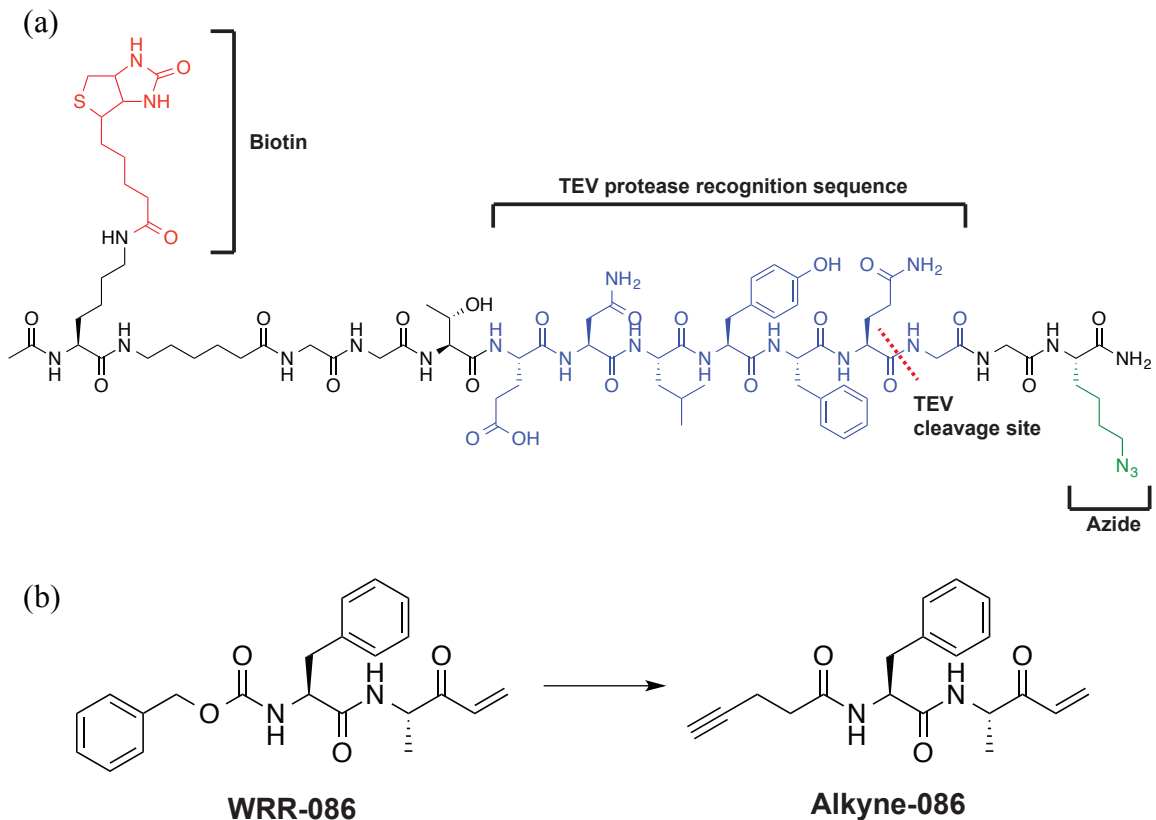
Azo tags were synthesized by Nick Pace in collaboration with Pfizer. Nick Pace created the GSTO1 overexpressing HEK293T cells and I confirmed overexpression by western blot. Comparison of IA labeling between mock-transfected and GSTO1 overexpressed HEK293T cells as well as the cleavage of whole GAPDH protein from streptavidin beads were done by me. Dr. Yu Qian performed all other experiments.

## Introduction

The utility of mass spectrometry (MS) in ABPP studies is hindered by the low abundance of probe-modified peptides, especially within the background of a whole proteome<sup>1</sup>. The biotin–avidin interaction is commonly exploited to selectively enrich biotin-tagged proteins from a complex proteomic mixture prior to analysis by MS. Direct elution of these biotinylated proteins from avidin beads requires harsh denaturing conditions and does not differentiate between biotin-tagged, endogenously biotinylated, and non-specifically bound proteins<sup>2</sup>. Additionally, fragmentation of the bulky biotin tag during collision-induced dissociation (CID) complicates interpretation of the ion mass spectra for peptide identification<sup>3</sup>. One strategy to circumvent these obstacles is to use a cleavable linker, which will elute only probe-modified proteins or peptides under mild conditions that are amenable to MS analysis. Furthermore, the unique mass of the residue appended to the cleaved linker can be exploited to identify exact sites of probe labeling<sup>1</sup>. Numerous linkers incorporating a protease-recognition site<sup>1, 4, 5</sup>, a photo-cleavable group<sup>6-8</sup>, or a chemically-cleavable group<sup>9, 10</sup> have been generated for this purpose.

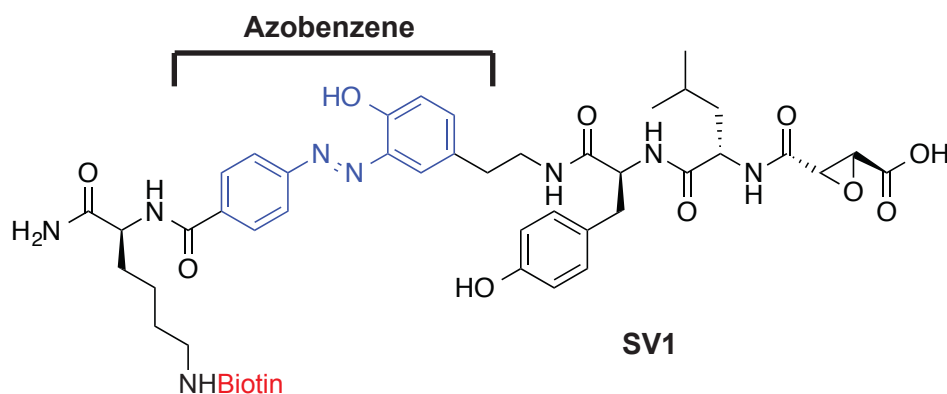
The tandem orthogonal proteolysis-ABPP (TOP-ABPP) strategy utilizes a tobacco-etch virus protease (TEV) cleavage site, which is placed between an azide group for click chemistry conjugation to alkynyl ABPs and a biotin group for avidin enrichment (TEV-tag) (Figure 2-1a)<sup>1</sup>. Following enrichment, the probe-labeled proteins are digested with trypsin and the resulting peptides are released by TEV proteolysis. This generates peptides bearing an additional mass on the modified residue corresponding to the ABP and cleaved TEV-tag<sup>1</sup>. In one application, TOP-ABPP was used in investigating the mechanisms that drive *Toxoplasma gondii* infection. Screening a library of covalent

inhibitors revealed a cysteine-reactive enone-containing compound, WRR-086, capable of blocking *T. gondii* attachment and invasion of host cells. This small molecule was converted to an ABP by incorporating an alkyne handle to use in TOP-ABPP (Alkyne-086, Figure 2-1b). MS analysis identified a single probe-labeled cysteine residue (C127) on the *T. gondii* DJ-1 protein (TgDJ-1). C127S mutants of TgDJ-1 prevented WRR-086 inhibition of host cell attachment and invasion as well as obstruct microneme secretion and parasite motility, identifying TgDJ-1 as a previously unknown regulator of *T. gondii* infection.



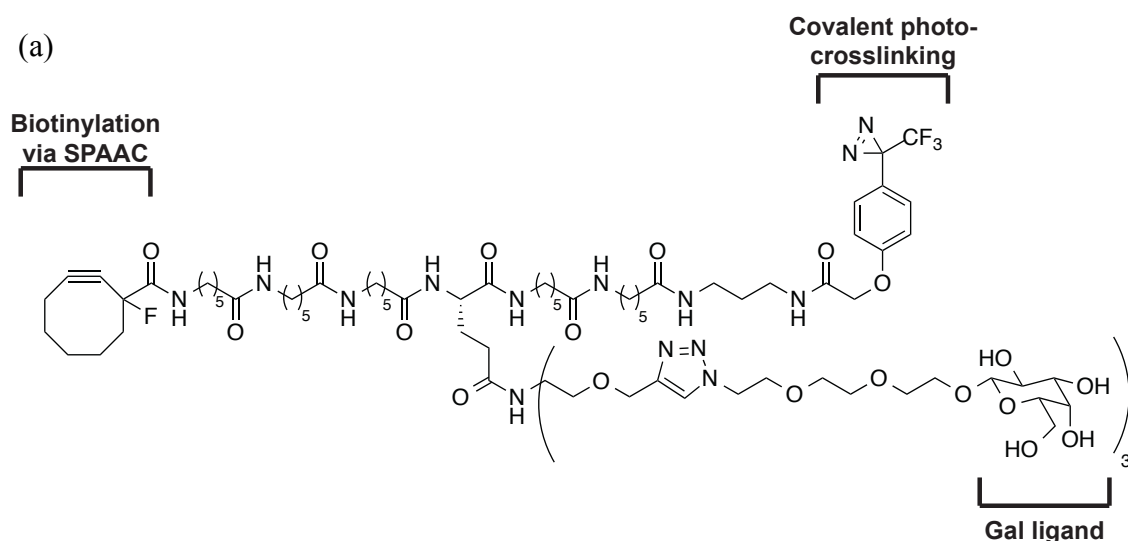
**Figure 2-1.** (a) Structure of the TEV-tag. (b) Structures of WRR-086 and its ABP version, Alkyne-086.

To reduce cleavage time and avoid variability in protease activity, a large number of chemically cleavable linkers have also been developed. These include functional groups that cleave under acidic conditions (dialkoxydiphenylsilane<sup>11</sup>, acylhydrazone<sup>12</sup>, and “Wang”-type<sup>9</sup>), nucleophilic conditions (levulinoyl ester<sup>13</sup>, nitrobenzenesulfonamide<sup>8</sup>) and dithionite treatment (azobenzene<sup>10, 11, 14</sup>). Azobenzene-containing linkers have the advantage of mild cleavage conditions by using sodium dithionite as the reducing agent<sup>10</sup>. Additionally, the azobenzene moiety is unaffected by other reducing agents commonly used in click chemistry and MS preparation protocols (e.g. TCEP, DTT)<sup>15</sup>. The first azobenzene-based linker was developed by insertion of an azobenzene group between the biotin tag and reactive group of the previously mentioned papain-specific ABP, DCG-04 (Figure 2-2). This new ABP, termed SV1, was used to label active cathepsin proteases in rat liver lysates. After enrichment with streptavidin beads, the probe-labeled proteins were cleaved using sodium dithionite. The eluted proteins were digested with trypsin and analyzed by LC-MS/MS, identifying multiple peptides from each of the expected cathepsin proteases, without any contamination by background proteins<sup>10</sup>.



**Figure 2-2.** Structure of SV1 ABP containing an azobenzene cleavable linker.

The use of a photo-cleavable linker is beneficial as it circumvents the use of additional reagents to release enriched proteins<sup>6</sup>. O-Nitrobenzyl derivatives are useful as photo-cleavable groups because of their rapid photolysis, which yields a nitroso from the nitro group and an aldehyde or ketone from the oxidation of the benzyl alcohol group<sup>16</sup>. The O-nitrobenzyl group was recently incorporated into a glycoprobe for affinity labeling of carbohydrate-binding lectin proteins. Since lectins specifically but noncovalently bind cell-surface carbohydrates, this ligand-based probe contains three  $\beta$ -D-galactose (Gal) units for affinity binding to the target lectin as well as a (trifluoromethyl)-phenyldiazirine photo-crosslinking group to covalently bind the probe upon UV radiation (Figure 2-3a). This probe also contains a cyclooctyne group for attachment of an azide-containing, photo-cleavable biotin tag via click chemistry (Figure 2-3b). This two-step strategy allows for the covalent modification and enrichment of carbohydrate-binding lectins and subsequent UV light-dependent release of the target proteins<sup>6</sup>.



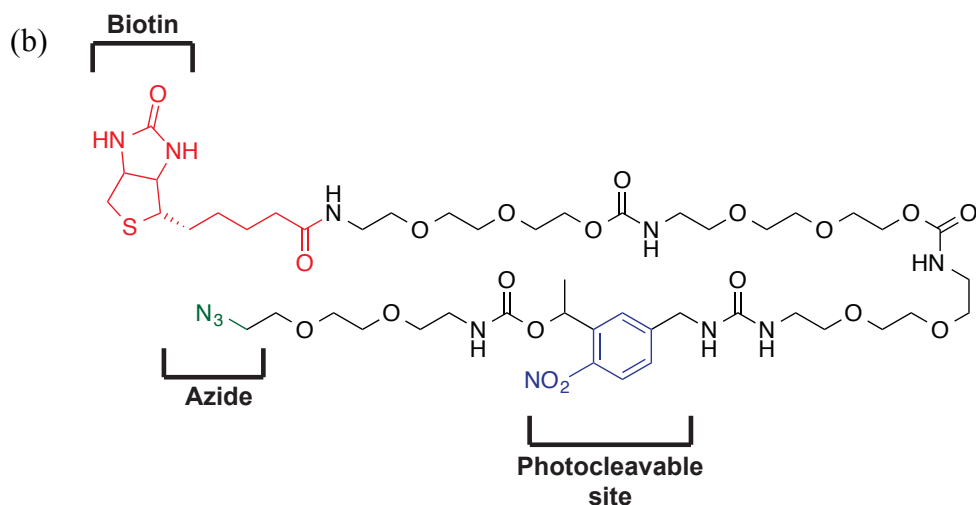


**Figure 2-3.** (a) Structure of the photo-affinity glycoprobe. (b) Structure of the photo-cleavable biotin affinity tag.

Many current proteomics applications, however, necessitate the quantitative comparison of protein(s) of interest across two or more different proteomes. The relative quantitation of protein abundance from complex proteomes has been facilitated by the development of numerous stable-isotope incorporation strategies<sup>17</sup>. These include platforms such as stable-isotope labeling with amino acids in cell culture (SILAC)<sup>18</sup>, isotope-coded affinity tag (ICAT)<sup>19</sup>, isobaric tags for relative and absolute quantification (iTRAQ)<sup>20</sup> and tandem mass tags (TMT)<sup>21</sup>. To enable quantitative analysis in applications such as ABPP, a click-chemistry-compatible, isotope-tagged, cleavable linker is necessary. A TEV-cleavable linker was recently optimized for quantitative proteomics of probe-labeled peptides in a platform termed isotopic tandem orthogonal proteolysis-ABPP (isoTOP-ABPP)<sup>22</sup>. This TEV-cleavable linker contains an azide for CuAAC-mediated conjugation to proteins modified with an alkyne-bearing ABP, a biotin for avidin enrichment, and a TEV protease recognition domain containing an unlabeled

(light) or isotopically labeled (heavy) valine (Figure 2-4). Despite the versatility and efficiency of cleavage of the TEV-cleavable linker, we envisioned that a chemically cleavable analogue could have several advantages, including lower cost of reagents, reduced time of cleavage and increased robustness to variations in cleavage conditions. Here, we explored the use of the sodium dithionite ( $\text{Na}_2\text{S}_2\text{O}_4$ )-cleavable azobenzene in place of the TEV-protease recognition domain, as a chemically cleavable linker for quantitative chemical proteomics.

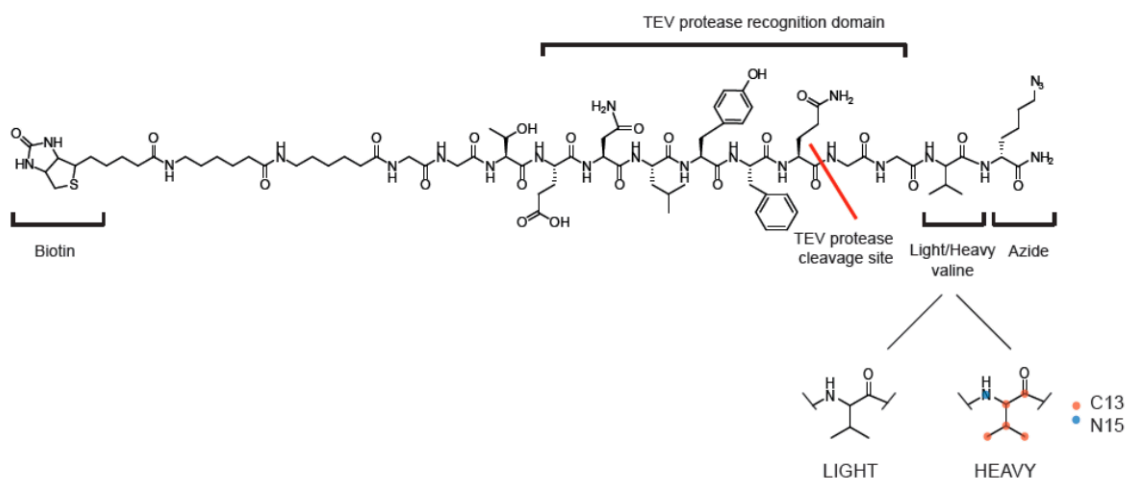


**Figure 2-4.** Structure of the TEV-cleavable linker.

### Isotopically Tagged Azobenzene-Based Cleavable Linker

The azobenzene was first developed as a mildly cleaved linker for protease-directed activity-based probes<sup>10, 23</sup>. Since then, click-chemistry-compatible azobenzene tags have been utilized to identify acetylated<sup>24</sup> and S-palmitoylated<sup>25</sup> proteins, lipoproteins<sup>26</sup> and newly synthesized proteins<sup>27</sup> that have been tagged with alkyne reporter elements. This linker has been shown to be efficiently cleaved by sodium dithionite at room temperature within a few hours<sup>14</sup>, and was deemed a good candidate

for replacing the TEV-protease recognition domain of our biotin tags for quantitative proteomics. We adapted the previously described azobenzene linker (Azo)<sup>14</sup>, by incorporating a “light” (12C and 14N) or “heavy” (13C and 15N) valine between the azide and the azobenzene to generate Azo-Light tag (Azo-L) and Azo-Heavy tag (Azo-H) with a mass difference of 6 Da. The resulting Azo-L/Azo-H linkers contain an azide for click chemistry conjugation to alkyne-functionalized proteins, an isotopically tagged valine for quantitation, a cleavable azobenzene unit, and a biotin group for avidin enrichment of proteins of interest (Figure 2-5).

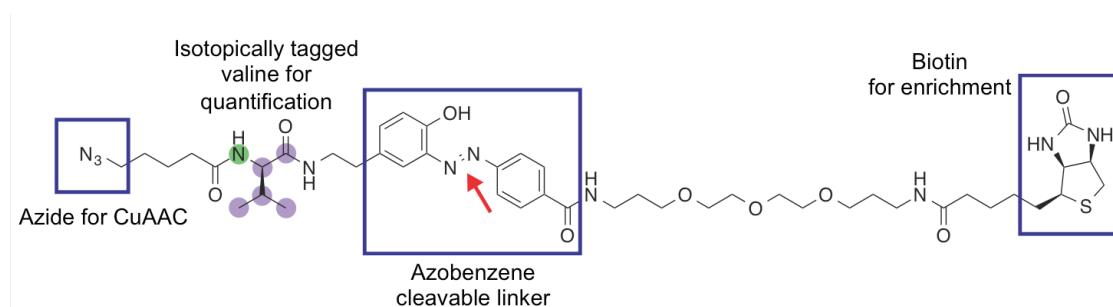


**Figure 2-5.** Structure of the Azo-H cleavable linker.

We envisioned a workflow similar to that utilized in the isoTOP-ABPP platform<sup>22</sup>, whereby two probe-labeled proteomes (Samples 1 and 2, Figure 2-6) are subjected to click chemistry with either the Azo-L or Azo-H tags. The samples are combined and tagged proteins are enriched on streptavidin beads and subjected to on-bead trypsin digestion to remove all unlabeled peptides. The remaining isotopically tagged, probe-labeled peptides are selectively eluted with sodium dithionite treatment and analyzed using LC/LC-MS/MS. Peptides are identified from the generated MS2 data and quantified using the corresponding high-resolution MS1 spectra. A light/heavy ratio (R)

is generated for each peptide that reflects the relative abundance of that peptide in each of the two samples.

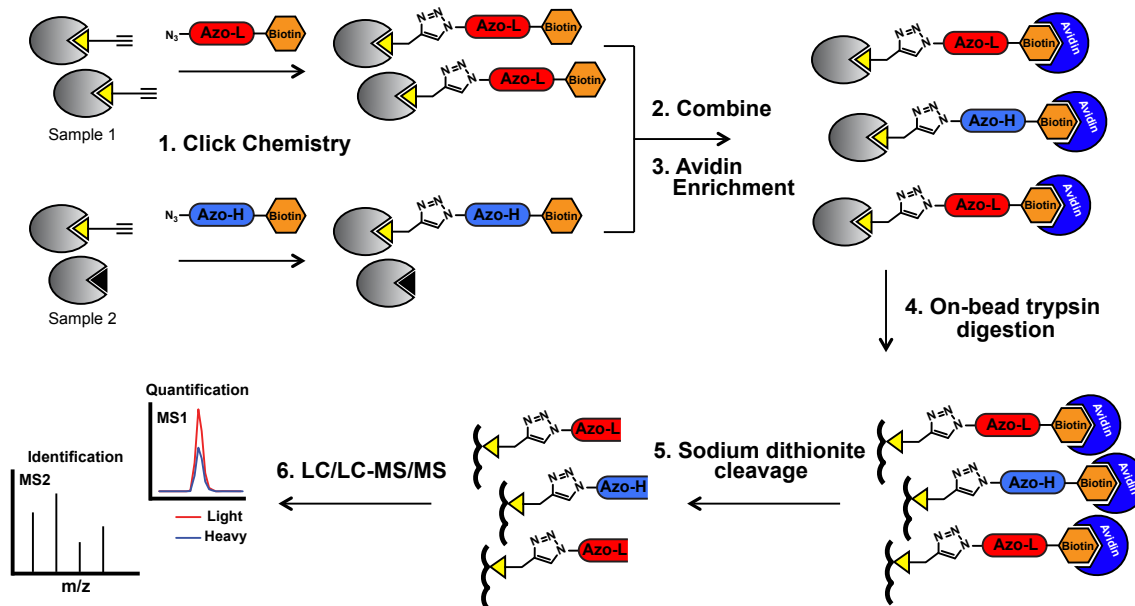


**Figure 2-6.** Workflow of the Azo-tag quantitative proteomics platform.

### Evaluation of the efficiency of cleavage of the Azo-L and Azo-H tags

To evaluate cleavage efficiency of the isotopic tags, we labeled mouse-liver proteomes with the cysteine-reactive iodoacetamide-alkyne (IA-alkyne) probe (Figure 2-7a). To ensure that the addition of the valine did not disrupt the cleavage of the azobenzene, we compared our Azo-L and Azo-H tags, including a combined 1:1 ratio of Azo-L and Azo-H tagged proteomes, to the previously reported Azo tag. The isotopically tagged linkers allowed identification of a similar number of peptides as the Azo tag (Figure 2-7a), and furthermore, these numbers are comparable to the peptide identifications obtained using the TEV-cleavable linker<sup>22</sup>. The optimized cleavage conditions are 2 hours at room temperature, compared to the overnight cleavage at 30 °C

required for TEV cleavage. The decreased number of peptides in the combined Azo-L/Azo-H sample is typical of isotopic dilution experiments, and is a result of reduced fragmentation of independent peptide species due to the presence of two isotopic species for each peptide

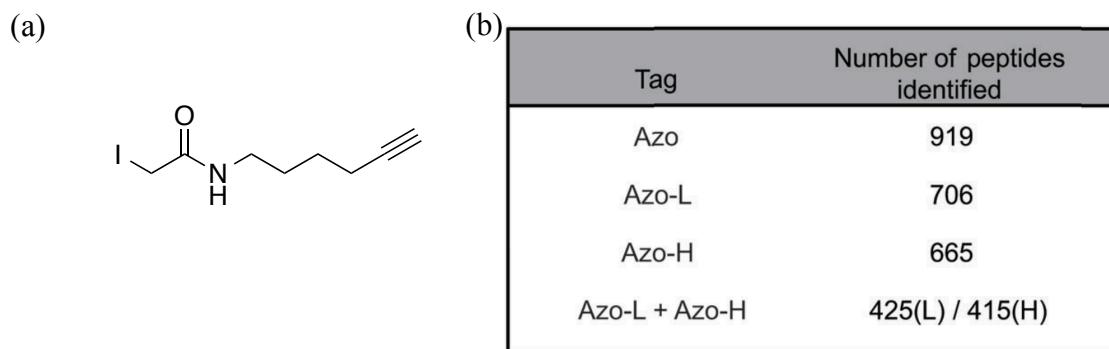


**Figure 2-7.** (a) Structure of the iodoacetamide-alkyne (IA-alkyne) probe. (b) Number of peptides identified from IA-alkyne-labeled proteomes using the valine-free Azo, Azo-L, Azo-H, and Azo-L + Azo-H (a 1:1 ratio of Azo-L and Azo-H tagged proteomes) tags.

### Evaluation of the quantitative accuracy of the isotopic Azo-tag platform

To evaluate the quantitative accuracy of our Azo-L/Azo-H system, we mixed Azo-L and Azo-H-tagged proteomes in predetermined light/heavy ratios of 2:1, 1:1, 1:2 and 1:5. These samples were analyzed using mass spectrometry and a value of R was obtained for each peptide in each of the four runs (Figure 2-8A). As demonstrated, across the >300 peptides identified, the experimental ratios were closely scattered around the expected ratios. For two of the peptides identified (parent proteins: UBE1Y1 and SHMT2), a representative mass spectra and isotope envelopes are shown to demonstrate

the coelution of the light and heavy species, the high signal-to-noise, and the characteristic isotopic peak pattern generated by the labeled peptides (Figure 2-8B).

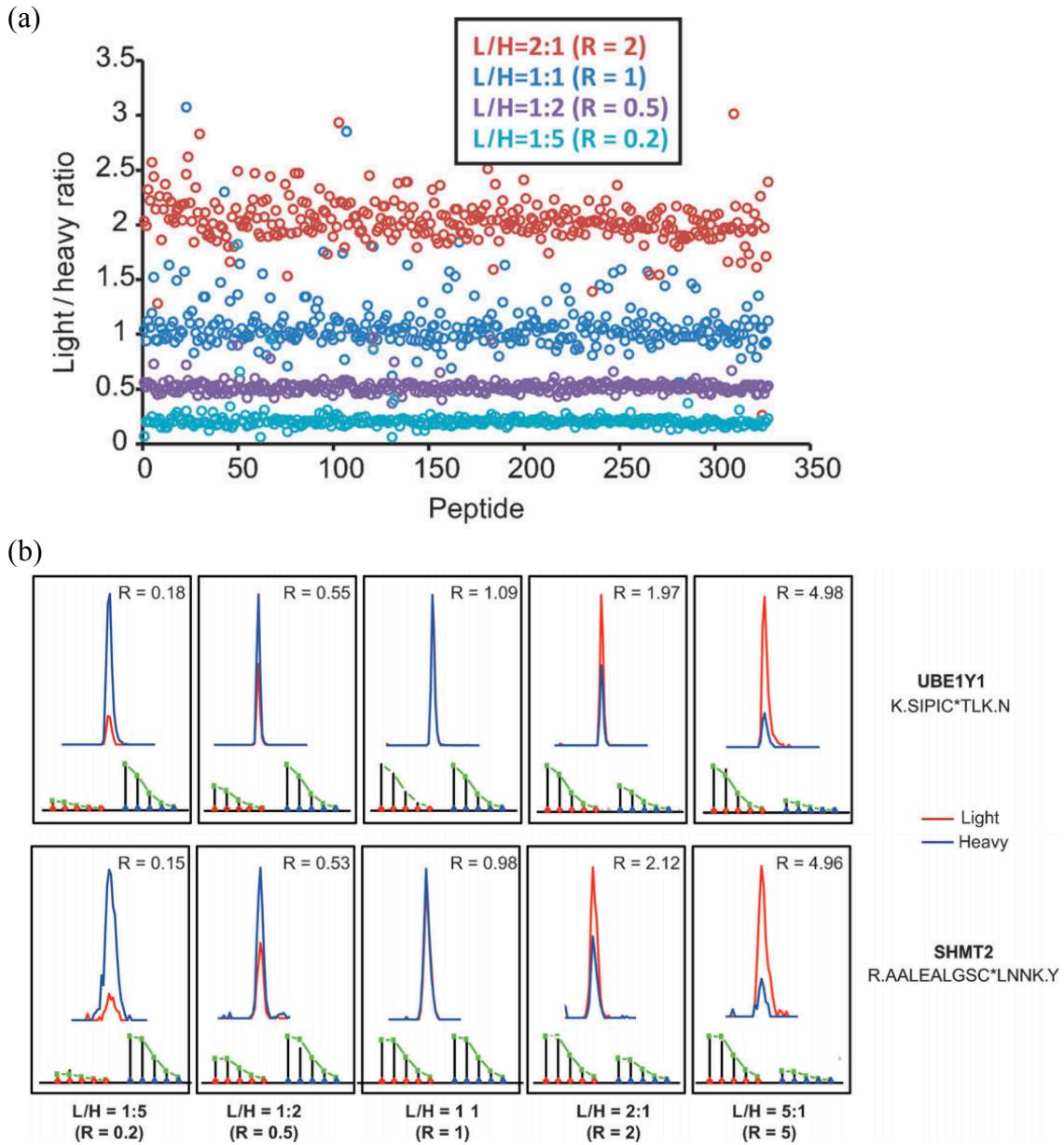


**Figure 2-8.** (a) The light/heavy ratios of 2:1, 1:1, 1:2, and 1:5 Azo-L/Azo-H tagged proteomes. (b) Chromatography traces for two labeled peptides from UBE1Y1 and SHMT2 from samples mixed in light/heavy ratios of 1:5, 1:2, 1:1, 2:1, and 5:1.

## **Application of the isotopic Azo-tag platform to compare two biologically independent samples**

To further illustrate the quantitative accuracy of this new isotopically tagged cleavable linker, we wanted to compare the relative quantitation of labeled peptides from two biologically independent samples. To achieve this, we compared mock-transfected HEK293T cells to cells overexpressing glutathione-S-transferase omega (GSTO1; Figure 2-9a). GSTO1 was chosen due to the presence of a highly reactive cysteine that is known to react with the IA-alkyne probe<sup>22</sup>. Overexpression of GSTO1 was confirmed using immunoblotting with a GSTO1 antibody (Figure 2-9a). Lysates from both samples were labeled with IA-alkyne and click chemistry was performed to incorporate Azo-L into the GSTO1 sample and Azo-H into the mock sample. The samples were analyzed according to the workflow in Figure 2-6.

We identified approximately 250 IA-alkyne-labeled peptides from these samples, and all but two of the peptides were identified to have light/heavy ratios of  $R \sim 1$  (Figure 2-9b). These two peptides are both cysteine-containing peptides derived from GSTO1 and were identified with  $R$  values of 31 for the known active-site cysteine of GSTO1, and 9 for a second reactive cysteine on this protein (Figure 2-9b). This illustrates the highly quantitative nature of this new cleavable-linker system, and illustrates the proficiency of this platform to accurately compare the relative abundance of labeled peptides from two biologically distinct samples.

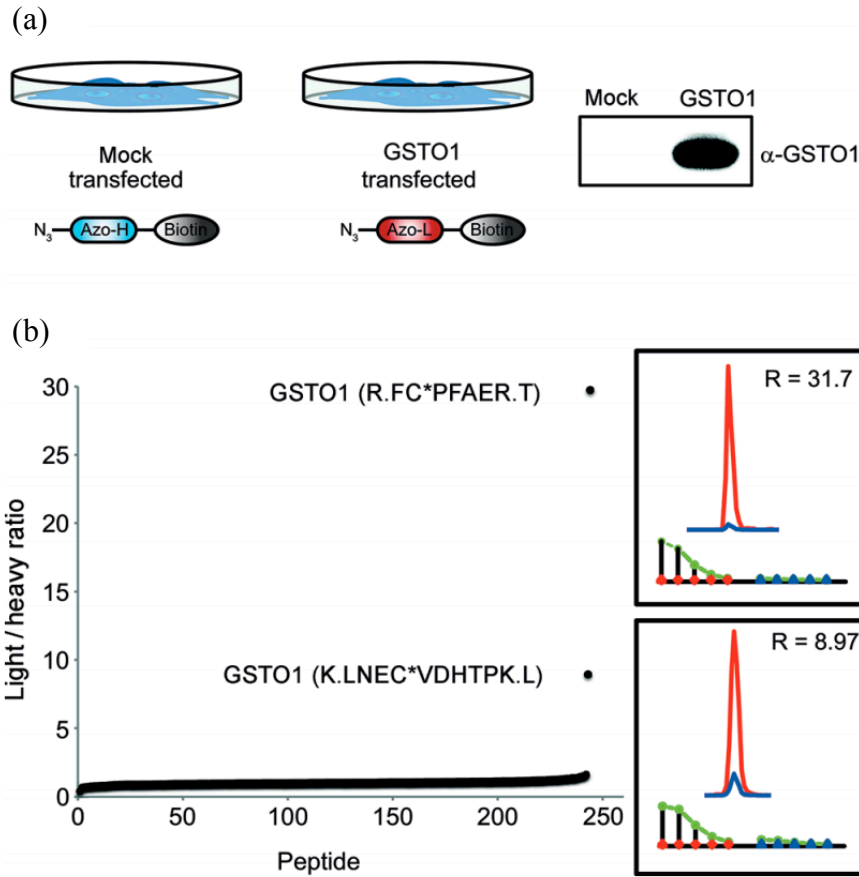


**Figure 2-9.** (a) mock and GSTO1 transfected HEK293T cells labeled with IA-alkyne are tagged with Azo-H (mock) or Azo-L (GSTO1). GSTO1 overexpression confirmed by immunoblotting with anti-GSTO antibody. (b) Light/heavy ratios for all IA-alkyne-labeled peptides from the two transfected HEK293T cells.

### Release of intact proteins from streptavidin beads

One final application we were interested in exploring was the use of this cleavable linker to release intact proteins from the streptavidin beads. The ability to release intact proteins would reduce the contamination of mass spectrometry samples by proteins that nonspecifically interact with the bead matrix. The workflow we envisioned was to mix proteomes from two samples as outlined in Figure 2-6, but after streptavidin enrichment,

and prior to trypsin digestion, intact proteins are cleaved from the beads using sodium dithionite. These eluted proteins could either be subjected to an in-solution tryptic digest, or a further round of fractionation by SDS-PAGE to select for a protein of interest for in-gel tryptic digestion. To optimize conditions for intact protein release, we utilized commercially available rabbit glyceraldehyde 3-phosphate dehydrogenase (GAPDH), which contains a reactive cysteine that is known to be labeled by our IA-alkyne probe<sup>22</sup>. A 1:1 mixture of the Azo-L/H tags were appended to IA-alkyne-labeled GAPDH using click chemistry, and the tagged proteins were enriched on streptavidin beads, and subjected to sodium dithionite cleavage. Comparing the protein in the eluent (lane 2) to the protein left on the bead after cleavage (lane 3), we achieve greater than 60% recovery of the bound GAPDH (Figure 2-10a).

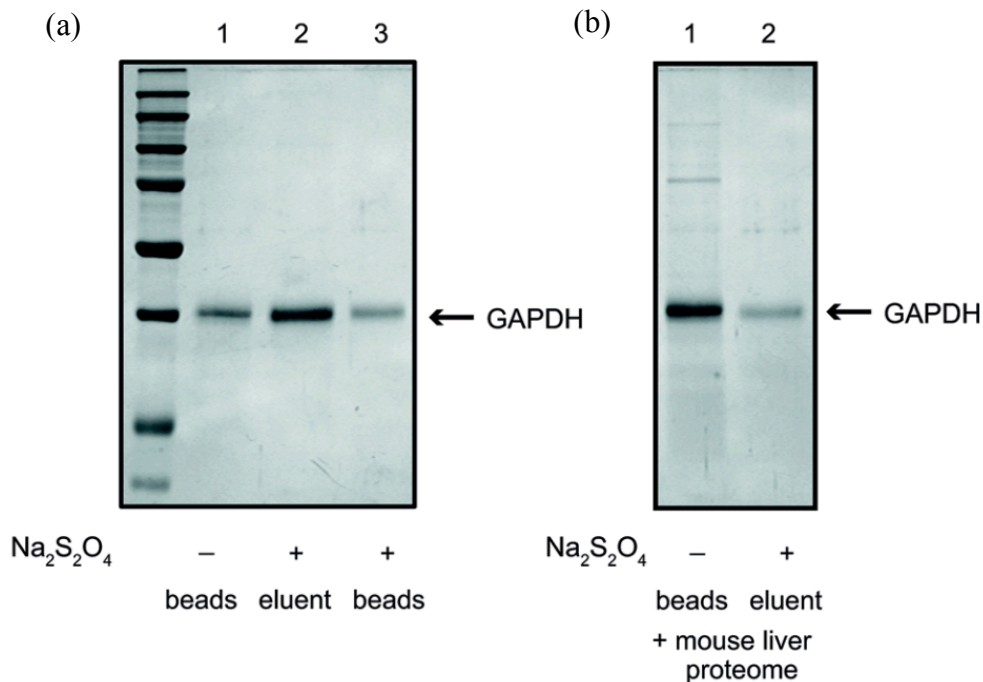


**Figure 2-10.** (a) Cleavage of whole GAPDH protein from streptavidin beads. (b) Elution of GAPDH from streptavidin beads in the background of a complex mouse proteome.

We further evaluated release of intact proteins in the context of an entire proteome. To achieve this, pre-labeled and Azo-L/H-tagged GAPDH was added to an unlabeled mouse liver proteome and enriched on streptavidin beads. After boiling of the beads and subsequent SDS-PAGE analysis, we visualized the presence of higher molecular weight protein bands that are indicative of nonspecific interactions with the bead matrix (Figure 2-10b, lane 1). When treated with sodium dithionite, a significant amount of GAPDH is released, albeit with lower efficiency than was observed for the pure protein (Figure 2-10b, lane 2). More importantly, none of the higher molecular weight, non-specifically bound proteins were eluted, demonstrating that this approach can serve to decrease background noise associated with selective protein enrichment.

To demonstrate that these intact proteins can still be quantitatively analyzed using mass spectrometry, we used a premixed Azo-L/Azo-H ratio of 1:1 to tag GAPDH. After streptavidin enrichment, the Azo-tagged intact protein was eluted with sodium dithionite. Eluted proteins were subjected to trypsin digestion and mass spectrometry analysis. We achieved >75% sequence coverage of GAPDH with two Azo-tagged peptide identifications (Figure 2-11a). Both these peptides contain known reactive cysteines, and an R value of 1 was calculated for both peptides, reflecting the initial ratio of tags used in this experiment (Figure 2-11b). This application highlights the versatility of the Azo-L and Azo-H system, which can be applied to cleave either peptides or intact proteins from streptavidin beads for quantitative mass spectrometry analysis.

(a)

MVKVGVNGFGRIGRLVTRAAFNSGKVDVVAINDPFIDLHYMVYM  
FQYDSTHGKFGHTVKAENGLVINGKAITIFQERDPANIKWGDAG  
AEYVVESTGVFTTMEKAGAHLKGGAKRVIISAPSADAPMFVMGVN  
HEKYDNSLKIVSNASCTTNCLAPLAKVIHDHFGIVEGLMTTVHAIT  
ATQKTVDGPSGKLWRDGRGAAQNIIPASTGAAKAVGKVIPELNGK  
LTGMAFRVVPTPNVSVVDLTCRLEKAAKYDDIKKVVKQASEGPLK  
GILGYTEDQVVSCDFNSATHSSTFDAGAGIALNDHFVKLISWYDNE  
FGYSNRVVDLMVHMASKE

(b)

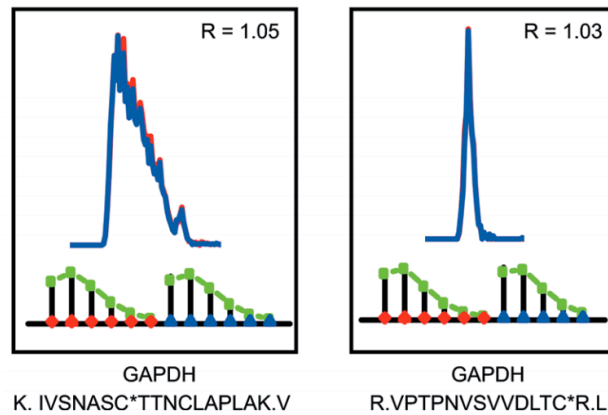


**Figure 2-11.** (a) Sequence coverage for GAPDH after sodium dithionite cleavage of intact proteins followed by in-solution tryptic digestion. Peptide regions shaded in gray signify peptides that were identified in the analysis. The two cysteine-containing peptides that were tagged by Azo-L/Azo-H are underlined. (b) Two IA-alkyne labeled cysteine-containing peptides identified with light/heavy ratios of 1. The extracted ion chromatograms and isotopic envelopes for the light species are shown in red, and the heavy species in blue.

## Conclusion

We have evaluated an isotopic, chemically cleavable linker for quantitative proteomics applications. This tag contains an azide for click chemistry conjugation to

alkyne-functionalized proteins, an isotopically light or heavy valine for quantitation by mass spectrometry, a dithionite-cleavable azobenzene linker and a biotin for enrichment on streptavidin beads. We demonstrate the efficiency of cleavage, the highly accurate quantitation of labeled peptides from two biologically distinct proteomes, and the release of intact proteins from streptavidin beads to reduce nonspecific protein contamination. This chemically cleavable linker demonstrates several advantages over the previously reported TEV-cleavable linker, including lower cost, shorter cleavage time, increased robustness to variations in buffer and temperature, and the ability to cleave intact proteins from streptavidin beads.

## **Experimental Procedures**

All chemicals were purchased from Sigma Aldrich unless otherwise noted. PBS buffer, DMEM high glucose media and penicillin streptomycin (pen/strep) were purchased from Thermal-Scientific (Armarillo, TX). Trypsin-EDTA was purchased from Invitrogen (Carlsbad, CA). The GSTO1 HRP-linked antibody was purchased from Cell Signaling (Danvers, MA). X-tremeGENE 9 DNA transfection reagent was purchased from Roche (Indianapolis, IN).

### **Preparation of mouse liver proteome**

Frozen mouse liver tissues were thawed, homogenized in PBS, pH 7.4 and sonicated for 30 sec at 80 % amplitude. Tissue mixture was centrifuged at  $200,000 \times g$  for 45 min. The supernatant was obtained and used as soluble mouse liver proteome.

Protein concentration of the proteome was determined using the Bio-Rad DC protein assay kit and the proteomes were stored at -80 °C until use.

### **Probe labeling and click chemistry**

Mouse liver samples were diluted to a 2 mg protein/mL solution in PBS and aliquoted into 0.5 mL volumes. Each sample (2 x 0.5 mL aliquots) was treated with 100  $\mu$ M of IA-alkyne using 5  $\mu$ L of a 10 mM stock in DMSO. The labeling reactions were incubated at room temperature for 1 hour. Click chemistry was performed by the addition of 100  $\mu$ M of either the Azo, Azo-L or Azo-H (10  $\mu$ L of a 5 mM stock), 1 mM TCEP (fresh 50X stock in water), 100  $\mu$ M ligand (17X stock in DMSO:t-Butanol 1:4) and 1 mM CuSO<sub>4</sub> (50X stock in water). Samples were allowed to react at room temperature for 1 hour. For the combined Azo-L/Azo-H sample, the Azo-L and Azo-H samples were mixed together immediately following click chemistry. The samples were centrifuged (5900 x g, 4 min, 4 °C) to pellet the precipitated proteins. The pellets were washed twice in cold MeOH, after which the pellet was solubilized in PBS containing 1.2% SDS via sonication and heating (5 min, 80 °C).

For the quantitative analysis, mouse proteomes were labeled with IA-alkyne as before. Click chemistry was performed in 0.5 mL aliquots with either the Azo-L or the Azo-H tag. After the one hour of incubation, the Azo-L and AzoH labeled samples were mixed together in different ratios (5:1, 2:1, 1:1, 1:2 and 1:5), centrifuged and processed as described above.

### **Streptavidin enrichment of Azo-tagged proteins**

The SDS-solubilized, AzoL/Azo-H tagged proteome samples were diluted with 5 mL of PBS for a final SDS concentration of 0.2%. The solutions were then incubated with 100  $\mu$ L of streptavidin-agarose beads (Pierce) overnight at 4 °C. The beads were washed with 5 mL 0.2% SDS/PBS, 3 x 5 mL PBS and 3 x 5 mL H<sub>2</sub>O and the beads were pelleted by centrifugation (1300 x g, 2 min) between washes.

### **On-bead trypsin and sodium dithionite treatment**

The washed beads from above were suspended in 500  $\mu$ L of 6 M urea/PBS and 10 mM DTT (from 20X stock in H<sub>2</sub>O) and placed in a 65 °C heat block for 15 minutes. 20 mM iodoacetamide (from 50X stock in H<sub>2</sub>O) was then added and allowed to react at 37 °C for 30 minutes. Following reduction and alkylation, the beads were pelleted by centrifugation (1300 x g, 2 min) and resuspended in 200  $\mu$ L of 2 M urea/PBS, 1 mM CaCl<sub>2</sub> (100X stock in H<sub>2</sub>O), and trypsin (2  $\mu$ g). The digestion was allowed to proceed overnight at 37 °C. The digest was separated from the beads using a Micro Bio-Spin column and the beads were then washed with 3 x 500  $\mu$ L PBS, 3 x 500  $\mu$ L H<sub>2</sub>O. The azobenzene cleavage was carried out by incubating the beads with 50  $\mu$ L of fresh 25 mM sodium dithionite for 30 min at room temperature on a rotator. After centrifugation, the supernatant was then transferred to a new eppendorf tube. The peptide cleavage process was then repeated twice to reach maximal cleavage and all the supernatants were combined (150  $\mu$ L total). In addition, the beads were then washed twice with 75  $\mu$ L water and the wash was combined with the supernatant collected from the cleavage step to

reach 300  $\mu\text{L}$  final. Formic acid (15  $\mu\text{L}$ ) was added to the sample, which was stored at -20  $^{\circ}\text{C}$  until mass spectrometry analysis.

### **Liquid chromatography-mass spectrometry (LC/LC-MS/MS) analysis**

LC/LC-MS/MS analysis was performed on an LTQ-Orbitrap mass spectrometer (ThermoFisher) coupled to an Agilent 1200 series HPLC. Peptide digests were pressure loaded onto a 250  $\mu\text{m}$  fused silica desalting column packed with 4 cm of Aqua C18 reverse phase resin (Phenomenex). The peptides were then eluted onto a biphasic column (100  $\mu\text{m}$  fused silica with a 5  $\mu\text{m}$  tip, packed with 10 cm C18 and 3 cm Partisphere strong cation exchange resin (SCX, Whatman) using a gradient 5-100% Buffer B in Buffer A (Buffer A: 95% water, 5% acetonitrile, 0.1% formic acid; Buffer B: 20% water, 80% acetonitrile, 0.1% formic acid). The peptides were then eluted from the SCX onto the C18 resin and into the mass spectrometer using four salt steps as previously described<sup>1,28</sup>. The flow rate through the column was set to  $\sim 0.25$   $\mu\text{L}/\text{min}$  and the spray voltage was set to 2.75 kV. One full MS scan (FTMS) (400-1800 MW) was followed by 18 data dependent scans (ITMS) of the *n*th most intense ions with dynamic exclusion disabled.

### **MS data analysis – peptide identification**

The tandem MS data were searched using the SEQUEST algorithm<sup>29</sup> using a concatenated target/decoy variant of the human and mouse IPI databases. A static modification of +57.02146 on cysteine was specified to account for iodoacetamide alkylation and differential modifications of + 258.1480 (Azo modification), + 456.2849 (Azo-L modification) and + 462.2987 (Azo-H modification) were specified on cysteine to

account for probe modifications. SEQUEST output files were filtered using DTASelect 2.0<sup>30, 31</sup>. Reported peptides were required to be fully tryptic and contain the desired probe modification and discriminant analyses were performed to achieve a peptide false-positive rate below 5%. The actual false positive rate was assessed at this stage according to established guidelines<sup>32</sup> and found to be ~3.5%. Additional assessments of the false-positive rate were performed following the application of additional filters (described below) resulting in a final false-positive rate below 0.05%.

### **MS data analysis – quantification**

Quantification of light/heavy ratios (R) was performed using the CIMAGE quantification package as previously described<sup>22</sup>.

### **Overexpression of GSTO1-wt in HEK293T cells**

HEK293T cells were grown at 37 °C under 5% CO<sub>2</sub> in DMEM media supplemented with 1% penicillin/streptomycin and 10% fetal bovine serum. Transfections were performed on 10 cm cell plates of ~60% confluency. Serum free DMEM media (600 µL) and X-tremeGENE DNA transfection reagent (20 µL) were combined in an eppendorf tube and vortexed. Either empty plasmid (pcDNA-3.1-myc/his (Invitrogen)) or WT-GSTO1-pcDNA-3.1-myc/his<sup>33</sup> (6 µg) were added and the sample was shaken and remained at room temperature for 15 mins. This plasmid solution was added dropwise to the HEK 293T cells. The cells were incubated for 48 hours. After transfection, cells were washed (3 times) with PBS, harvested by scraping and resuspended in an appropriate amount of PBS. Cells were then sonicated (using a COLE-

PARMER 130W ultrasonic processor) to lyse. These lysates were separated by centrifugation (using a MX-120 Thermo micro-ultra centrifuge) at 45,000 rpm at 4°C for 45 min. to yield soluble and membrane protein lysates. The supernatant was collected and the soluble protein concentration was determined using a Bio-RAD DC Protein Assay

### **Western blot analysis**

SDS-PAGE loading buffer 2x (reducing, 50  $\mu$ L) was added to the soluble protein samples and 25  $\mu$ L of this solution was separated by SDS-PAGE for 217 volt hours on a 10% polyacrylamide gel. The SDS-PAGE gels were transferred by electroblotting onto nitrocellulose membranes at 150 volt hours. The membranes were blocked in tris-buffered saline with 1% Tween 20 (TBS-T) and 5% (w/v) non-fat dry milk at room temperature for 2 hrs. Each blot was washed with TBS-T three times (5 min/wash), then treated with antiGSTO1 tag rabbit antibody (Cell Signaling, 1:1000) overnight at 4°C. The blots were washed with TBS-T three times (5 min/wash). The blots were treated with the anti-rabbit-HRP conjugated secondary antibody (Cell Signaling, 1:10,000) for 2 hrs at room temperature. The blots were washed three times with TBS-T (5 min/wash), treated with HRP super signal chemiluminescence reagents and exposed to film for 1 min before development. Development took place using a Kodak X-OMAT 2000A processor.

### **Mass spectrometry sample preparation**

Mock and GSTO1-overexpressing soluble cell lysates were diluted to a 2 mg/mL solution in PBS. Each sample (2 x 0.5 mL aliquots) was treated with 100  $\mu$ M of IA-alkyne using 5  $\mu$ L of a 10 mM stock in DMSO. The labeling reactions were incubated at

room temperature for 1 hour. Click chemistry was performed by the addition of 100  $\mu\text{M}$  of Azo-L (GSTO1) or Azo-H (mock). The samples were combined after the one-hour incubation and analyzed as described above.

### **Elution of purified GAPDH from streptavidin beads and gel analysis**

10  $\mu\text{g}$  of purified GAPDH were dissolved in 150  $\mu\text{L}$  of PBS and each sample was treated with 100  $\mu\text{M}$  of IA-alkyne (1.5  $\mu\text{L}$  of 10 mM). The labeling reactions were incubated at room temperature for 1 hour. Click chemistry was performed by the addition of 100  $\mu\text{M}$  of the Azo-L (3  $\mu\text{L}$  of a 5 mM stock), 1 mM TCEP (3  $\mu\text{L}$  of a fresh 50X stock in water), 100  $\mu\text{M}$  ligand (9  $\mu\text{L}$  of a 17X stock in DMSO:t-Butanol 1:4) and 1 mM  $\text{CuSO}_4$  (3  $\mu\text{L}$  of a 50X stock in water). Samples were allowed to react at room temperature for 1 hr. Following click chemistry, precipitated GAPDH was pelleted by centrifugation at 10,000 rpm for 5 min at room temperature. The supernatant was removed and the pellet was washed twice with 200  $\mu\text{L}$  of cold methanol and then solubilized in 300  $\mu\text{L}$  of 1.2% SDS in PBS by sonication and heating. The solubilized GAPDH was diluted with 1.5mL of PBS to a 0.2% SDS concentration and this solution was incubated with 30  $\mu\text{L}$  of streptavidin-agarose beads at room temperature for 3 hrs on a rotator. The beads were transferred to a Micro Bio-Spin column and washed 1 x 500  $\mu\text{L}$  0.2% SDS in PBS, 3 x 500  $\mu\text{L}$  PBS, and 3 x 500  $\mu\text{L}$  water. The release of intact proteins from the beads was achieved by incubating the beads in 50  $\mu\text{L}$  of fresh 50 mM sodium dithionite for 60 min at room temperature on a rotator. After centrifugation, the supernatant was transferred to a new eppendorf tube and the cleavage process was repeated twice. All three supernatants were combined giving a final volume of 150  $\mu\text{L}$ .

After cleavage, the remaining beads were washed 3 x 500  $\mu$ L of water and suspended in 150  $\mu$ L of PBS. 50  $\mu$ L of 4x SDSPAGE sample loading buffer was added to both the cleavage product and suspended beads. Proteins that remained bound to the beads were removed by boiling in sample loading buffer for 10 mins. All samples were loaded onto a 10% SDS-PAGE gel and run for 200 volt hours. Proteins were visualized using silver staining.

### **Elution of GAPDH from streptavidin beads in the background of a complex proteome**

Mouse liver was diluted to 5 mg/mL and click chemistry was performed on a 500  $\mu$ L sample. The precipitated proteins were washed twice with cold methanol, solubilized in 1.2% SDS in PBS, and combined with Azo-L labeled GAPDH from above. The solution was diluted to 0.2% SDS in PBS and incubated with 100  $\mu$ L of streptavidin-agarose beads at room temperature for 3 hrs on a rotator. The beads were processed for gel analysis as described above.

### **GAPDH mass spectrometry analysis**

IA labeling, click chemistry, and cleavage were performed on 220  $\mu$ g of GAPDH as described above except the Azo-linker used was a 1:1 combination of Azo-L and Azo-H. Following cleavage of GAPDH, the beads were washed twice with 75  $\mu$ L of water and combined with the previous eluent giving a final volume of 300  $\mu$ L. The eluted protein was precipitated using 30  $\mu$ L of a 100% trichloroacetic acid solution (100mg in 100  $\mu$ L PBS) and frozen at -80  $^{\circ}$ C overnight. The samples were thawed and centrifuged at 10,000

rpm for 10 minutes. The GAPDH pellet was washed once in 500  $\mu$ L of cold acetone. After centrifugation, acetone was removed and the pellet allowed to air dry. The GAPDH pellet was resuspended in 30  $\mu$ L of 8M urea in PBS followed by 70  $\mu$ L of 100 mM ammonium bicarbonate. This was heated at 65  $^{\circ}$ C for 15 minutes with 15 mM dithiothreitol (1.5  $\mu$ L of 1 M). 2.5  $\mu$ L of 500 mM Iodoacetamide was then added and allowed to incubate at room temperature for 30 minutes. The reaction was quenched with 120  $\mu$ L of PBS and trypsin digestion was performed by adding 4  $\mu$ L of trypsin (0.5  $\mu$ g/ $\mu$ L) and 2.5  $\mu$ L of 100 mM calcium chloride. The sample was agitated overnight at 37  $^{\circ}$ C. After digestion, trypsin was quenched with 10  $\mu$ L of formic acid and centrifuged at 10,000 rpm for 10 minutes to pellet undigested and precipitated protein. 10  $\mu$ L of the supernatant was removed and pressure loaded onto a 100  $\mu$ m fused silica column packed with 10 cm of Aqua C18 reverse phase resin. LC-MS analysis was performed on an LTQ-Orbitrap mass spectrometer (ThermoFisher) coupled to an Agilent 1200 series HPLC. The peptides were eluted from the C18 resin using a two-hour gradient of 5-100% Buffer B in Buffer A (Buffer A: 95% water, 5% acetonitrile, 0.1% formic acid; Buffer B: 20% water, 80% acetonitrile, 0.1% formic acid). The flow rate through the column was set to  $\sim$ 0.25  $\mu$ L/min and the spray voltage was set to 2.75 kV. One full MS scan (FTMS) (400-1800 MW) was followed by 8 data dependent scans (ITMS) of the nth most intense ions with dynamic exclusion enabled.

## References

1. Speers, A. E.; Cravatt, B. F., A tandem orthogonal proteolysis strategy for high-content chemical proteomics. *Journal of the American Chemical Society* **2005**, *127* (28), 10018-9.
2. Rudolf, G. C.; Heydenreuter, W.; Sieber, S. A., Chemical proteomics: ligation and cleavage of protein modifications. *Current opinion in chemical biology* **2013**, *17* (1), 110-7.
3. Guo, J.; Prokai, L., To tag or not to tag: a comparative evaluation of immunoaffinity-labeling and tandem mass spectrometry for the identification and localization of posttranslational protein carbonylation by 4-hydroxy-2-nonenal, an end-product of lipid peroxidation. *Journal of proteomics* **2011**, *74* (11), 2360-9.
4. Hall, C. I.; Reese, M. L.; Weerapana, E.; Child, M. A.; Bowyer, P. W.; Albrow, V. E.; Haraldsen, J. D.; Phillips, M. R.; Sandoval, E. D.; Ward, G. E.; Cravatt, B. F.; Boothroyd, J. C.; Bogyo, M., Chemical genetic screen identifies Toxoplasma DJ-1 as a regulator of parasite secretion, attachment, and invasion. *Proceedings of the National Academy of Sciences of the United States of America* **2011**, *108* (26), 10568-73.
5. Sato, S.; Murata, A.; Orihara, T.; Shirakawa, T.; Suenaga, K.; Kigoshi, H.; Uesugi, M., Marine natural product aurilide activates the OPA1-mediated apoptosis by binding to prohibitin. *Chemistry & biology* **2011**, *18* (1), 131-9.
6. Chang, T. C.; Adak, A. K.; Lin, T. W.; Li, P. J.; Chen, Y. J.; Lai, C. H.; Liang, C. F.; Chen, Y. J.; Lin, C. C., A photo-cleavable biotin affinity tag for the facile release of a photo-crosslinked carbohydrate-binding protein. *Bioorganic & medicinal chemistry* **2016**.

7. Olejnik, J.; Sonar, S.; Krzymanska-Olejnik, E.; Rothschild, K. J., Photocleavable biotin derivatives: a versatile approach for the isolation of biomolecules. *Proceedings of the National Academy of Sciences of the United States of America* **1995**, *92* (16), 7590-4.
8. Yokoshima, S.; Abe, Y.; Watanabe, N.; Kita, Y.; Kan, T.; Iwatsubo, T.; Tomita, T.; Fukuyama, T., Development of photoaffinity probes for gamma-secretase equipped with a nitrobenzenesulfonamide-type cleavable linker. *Bioorganic & medicinal chemistry letters* **2009**, *19* (24), 6869-71.
9. van der Veken, P.; Dirksen, E. H.; Ruijter, E.; Elgersma, R. C.; Heck, A. J.; Rijkers, D. T.; Slijper, M.; Liskamp, R. M., Development of a novel chemical probe for the selective enrichment of phosphorylated serine- and threonine-containing peptides. *Chembiochem : a European journal of chemical biology* **2005**, *6* (12), 2271-80.
10. Verhelst, S. H.; Fonovic, M.; Bogyo, M., A mild chemically cleavable linker system for functional proteomic applications. *Angewandte Chemie* **2007**, *46* (8), 1284-6.
11. Szychowski, J.; Mahdavi, A.; Hodas, J. J.; Bagert, J. D.; Ngo, J. T.; Landgraf, P.; Dieterich, D. C.; Schuman, E. M.; Tirrell, D. A., Cleavable biotin probes for labeling of biomolecules via azide-alkyne cycloaddition. *Journal of the American Chemical Society* **2010**, *132* (51), 18351-60.
12. Park, K. D.; Liu, R.; Kohn, H., Useful tools for biomolecule isolation, detection, and identification: acylhydrazone-based cleavable linkers. *Chemistry & biology* **2009**, *16* (7), 763-72.
13. Geurink, P. P.; Florea, B. I.; Li, N.; Witte, M. D.; Verasdonck, J.; Kuo, C. L.; van der Marel, G. A.; Overkleeft, H. S., A cleavable linker based on the levulinoyl ester for activity-based protein profiling. *Angewandte Chemie* **2010**, *49* (38), 6802-5.

14. Yang, Y. Y.; Grammel, M.; Raghavan, A. S.; Charron, G.; Hang, H. C., Comparative analysis of cleavable azobenzene-based affinity tags for bioorthogonal chemical proteomics. *Chemistry & biology* **2010**, *17* (11), 1212-22.
15. Choo, J. A.; Thong, S. Y.; Yap, J.; van Esch, W. J.; Raida, M.; Meijers, R.; Lescar, J.; Verhelst, S. H.; Grotenbreg, G. M., Bioorthogonal cleavage and exchange of major histocompatibility complex ligands by employing azobenzene-containing peptides. *Angewandte Chemie* **2014**, *53* (49), 13390-4.
16. Aujard, I.; Benbrahim, C.; Gouget, M.; Ruel, O.; Baudin, J. B.; Neveu, P.; Jullien, L., o-nitrobenzyl photolabile protecting groups with red-shifted absorption: syntheses and uncaging cross-sections for one- and two-photon excitation. *Chemistry* **2006**, *12* (26), 6865-79.
17. Xie, F.; Liu, T.; Qian, W. J.; Petyuk, V. A.; Smith, R. D., Liquid chromatography-mass spectrometry-based quantitative proteomics. *The Journal of biological chemistry* **2011**, *286* (29), 25443-9.
18. Ong, S. E.; Blagoev, B.; Kratchmarova, I.; Kristensen, D. B.; Steen, H.; Pandey, A.; Mann, M., Stable isotope labeling by amino acids in cell culture, SILAC, as a simple and accurate approach to expression proteomics. *Molecular & cellular proteomics : MCP* **2002**, *1* (5), 376-86.
19. Gygi, S. P.; Rist, B.; Gerber, S. A.; Turecek, F.; Gelb, M. H.; Aebersold, R., Quantitative analysis of complex protein mixtures using isotope-coded affinity tags. *Nature biotechnology* **1999**, *17* (10), 994-9.
20. Ross, P. L.; Huang, Y. N.; Marchese, J. N.; Williamson, B.; Parker, K.; Hattan, S.; Khainovski, N.; Pillai, S.; Dey, S.; Daniels, S.; Purkayastha, S.; Juhasz, P.; Martin, S.;

Bartlett-Jones, M.; He, F.; Jacobson, A.; Pappin, D. J., Multiplexed protein quantitation in *Saccharomyces cerevisiae* using amine-reactive isobaric tagging reagents. *Molecular & cellular proteomics : MCP* **2004**, *3* (12), 1154-69.

21. Kuhn, K.; Prinz, T.; Schafer, J.; Baumann, C.; Scharfke, M.; Kienle, S.; Schwarz, J.; Steiner, S.; Hamon, C., Protein sequence tags: a novel solution for comparative proteomics. *Proteomics* **2005**, *5* (9), 2364-8.

22. Weerapana, E.; Wang, C.; Simon, G. M.; Richter, F.; Khare, S.; Dillon, M. B.; Bachovchin, D. A.; Mowen, K.; Baker, D.; Cravatt, B. F., Quantitative reactivity profiling predicts functional cysteines in proteomes. *Nature* **2010**, *468* (7325), 790-5.

23. Fonovic, M.; Verhelst, S. H.; Sorum, M. T.; Bogoy, M., Proteomics evaluation of chemically cleavable activity-based probes. *Molecular & cellular proteomics : MCP* **2007**, *6* (10), 1761-70.

24. Yang, Y. Y.; Ascano, J. M.; Hang, H. C., Bioorthogonal chemical reporters for monitoring protein acetylation. *Journal of the American Chemical Society* **2010**, *132* (11), 3640-1.

25. Yount, J. S.; Moltedo, B.; Yang, Y. Y.; Charron, G.; Moran, T. M.; Lopez, C. B.; Hang, H. C., Palmitoylome profiling reveals S-palmitoylation-dependent antiviral activity of IFITM3. *Nature chemical biology* **2010**, *6* (8), 610-4.

26. Rangan, K. J.; Yang, Y. Y.; Charron, G.; Hang, H. C., Rapid visualization and large-scale profiling of bacterial lipoproteins with chemical reporters. *Journal of the American Chemical Society* **2010**, *132* (31), 10628-9.

27. Grammel, M.; Zhang, M. M.; Hang, H. C., Orthogonal alkynyl amino acid reporter for selective labeling of bacterial proteomes during infection. *Angewandte Chemie* **2010**, *49* (34), 5970-4.
28. Weerapana, E.; Speers, A. E.; Cravatt, B. F., Tandem orthogonal proteolysis-activity-based protein profiling (TOP-ABPP)--a general method for mapping sites of probe modification in proteomes. *Nature protocols* **2007**, *2* (6), 1414-25.
29. Eng, J. K.; McCormack, A. L.; Yates, J. R., An approach to correlate tandem mass spectral data of peptides with amino acid sequences in a protein database. *Journal of the American Society for Mass Spectrometry* **1994**, *5* (11), 976-89.
30. Cociorva, D.; Yates, J. R. In *DTASelect 2.0: Improving the Confidence of Peptide and Protein Identifications*, 54th ASMS Annual Meeting Proceedings, 2006.
31. Tabb, D. L.; McDonald, W. H.; Yates, J. R., 3rd, DTASelect and Contrast: tools for assembling and comparing protein identifications from shotgun proteomics. *Journal of proteome research* **2002**, *1* (1), 21-6.
32. Elias, J. E.; Gygi, S. P., Target-decoy search strategy for increased confidence in large-scale protein identifications by mass spectrometry. *Nature methods* **2007**, *4* (3), 207-14.
33. Pace, N. J.; Pimental, D. R.; Weerapana, E., An inhibitor of glutathione S-transferase omega 1 that selectively targets apoptotic cells. *Angewandte Chemie* **2012**, *51* (33), 8365-8.

### Chapter 3

#### Identifying Dysregulated Cysteine-Mediated Protein Activities During Impaired Insulin/IGF-1 Signaling in *C. elegans*

A significant portion of the work described in this chapter comes from:

Martell, J., Seo, Y.H., Bak, D.W., Tissenbaum, H.A., Weerapana, E. Identifying dysregulated cysteine-mediated protein activities during impaired insulin/IGF-1 signaling in *C. elegans*.” *Cell Chem. Biol.* **2015**, *Manuscript in review*

BLAST searches, functional annotation, homology determination, and cysteine conservation were performed using a program created by Dr. Daniel Bak. *C. elegans* RNAi knockdown, lifespan assays, and dauer assays were done with the help of Dr. YongHak Seo at UMass Medical School in Worcester, MA.

## Introduction

The elucidation of protein activities dysregulated during the aging process is a vital step toward the discovery of signaling networks and metabolic pathways directly implicated in aging. *Caenorhabditis elegans* provides an ideal model organism for investigating the mechanistic basis of aging and physiological decline: *C. elegans* are transparent and can be observed under the microscope; they are able to grow in large populations on solid or in liquid media; mutant strains can be frozen, stored, and recovered; they are hermaphroditic and mostly reproduce *via* self-fertilization, although males can be created and used for crossbreeding; they eat easily sustainable *E. coli*; they can also be age-synchronized by treating young adults with floxuridine (FUDR), an inhibitor of thymidylate synthase and DNA replication. Compared to other commonly studied organisms, *C. elegans* have a short and relatively invariant lifespan of 14-21 days, a brief reproductive cycle of 2.5-4 days, and distinct developmental stages. Their development and lifespan are temperature dependent (more rapid development, shorter lifespan with increased temperature) and are typically grown between 15-25 °C. All of these features enable the use of *C. elegans* in simple screens to examine genetic and environmental effects on aging<sup>1</sup>.

The *C. elegans* life cycle is comprised of the embryonic stage, four larval stages (L1-L4) and the adult stage (Figure 3-1). After hatching, larval development is suspended at the L1 stage and can survive up to 6-10 days until food becomes available<sup>2</sup>. If food and environmental conditions are favorable, the *C. elegans* larva will mature through each larval stage in about 10 hours. The end of each stage is marked with a molt in which a new cuticle is created and the old one is shed<sup>3</sup>. Under conditions of stress such as

increased temperature, high population density, and lack of food, *C. elegans* may enter an alternative third larval stage called dauer larva (Figure 3-1). During this dauer state, development is suppressed, feeding stops, and movement is significantly reduced. Dauer larva are very thin, have a thick cuticle, and exhibit increased stress resistance, altered metabolism, and the ability to survive for months without food. When conditions improve, dauer larva molt to the L4 stage and enter adulthood with no affect on the adult's lifespan, regardless of the time spent in the dauer state<sup>4</sup>.

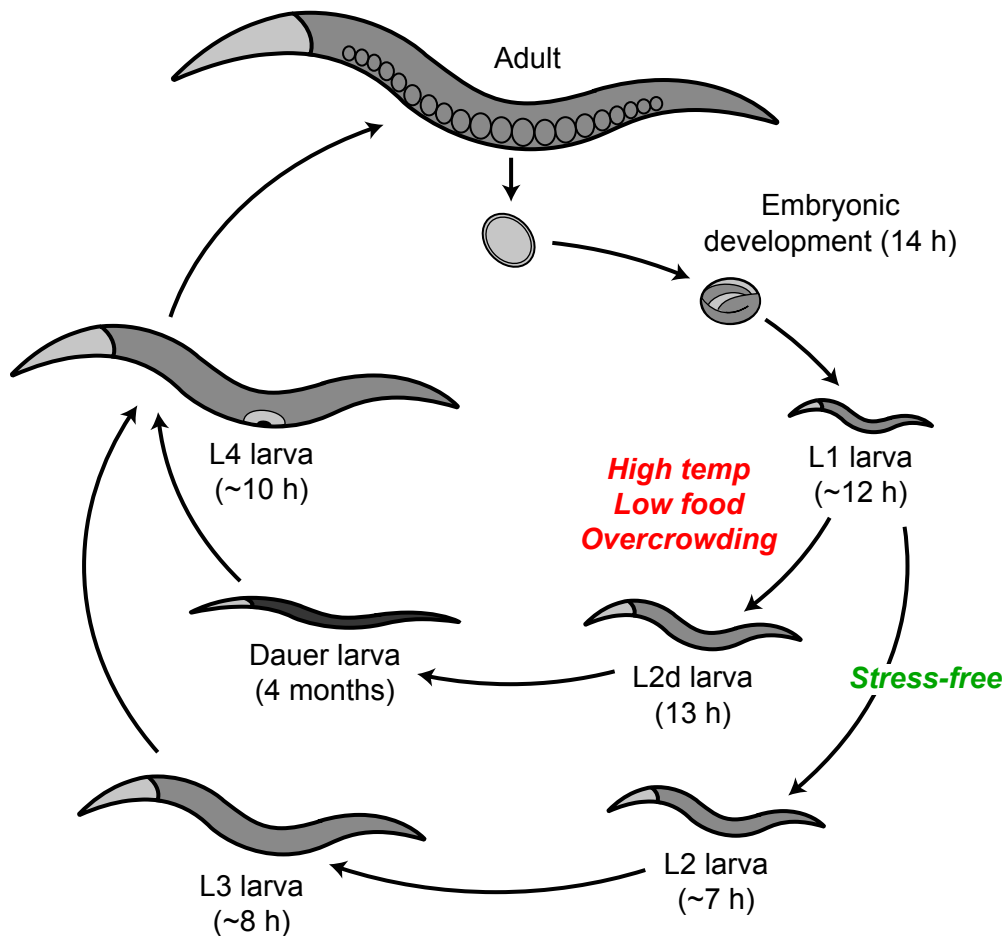


**Figure 3-1.** The *C. elegans* lifecycle at 25°C. Figure adapted from Jorgensen and Mango<sup>5</sup>.

### **Insulin signaling and its role in lifespan regulation**

Dauer development is control by 4 distinct signaling pathways: the guanylyl cyclase, TGF $\beta$ -like, steroid hormone, and insulin-like pathway<sup>6, 7</sup>. The insulin-like pathway is homologous to mammalian insulin/insulin-like growth factor (IGF) signaling (IIS) and regulates numerous cellular processes including growth, differentiation, and metabolism<sup>8</sup>. In *C. elegans*, and other invertebrates, insulin-like peptides are secreted in response to food and bind to a single insulin/IGF-1-like tyrosine kinase receptor (DAF-2). This binding leads to DAF-2 self-phosphorylation and dimerization, and the activated receptor then phosphorylates phosphoinositide 3-kinase (AGE-1), stimulating the production of phosphatidylinositol (3,4,5)-triphosphate (PIP<sub>3</sub>) products. Elevated levels of PIP<sub>3</sub> turn on 3-phosphoinositide dependent protein kinase-1 (PDK-1) and its activation of the protein kinase AKT/protein kinases B (AKT/PKB). AKT/PKB phosphorylates the FOXO transcription factor DAF-16 causing its inactivation and translocation out of the nucleus and into the cytosol<sup>9</sup> (Figure 3-2).

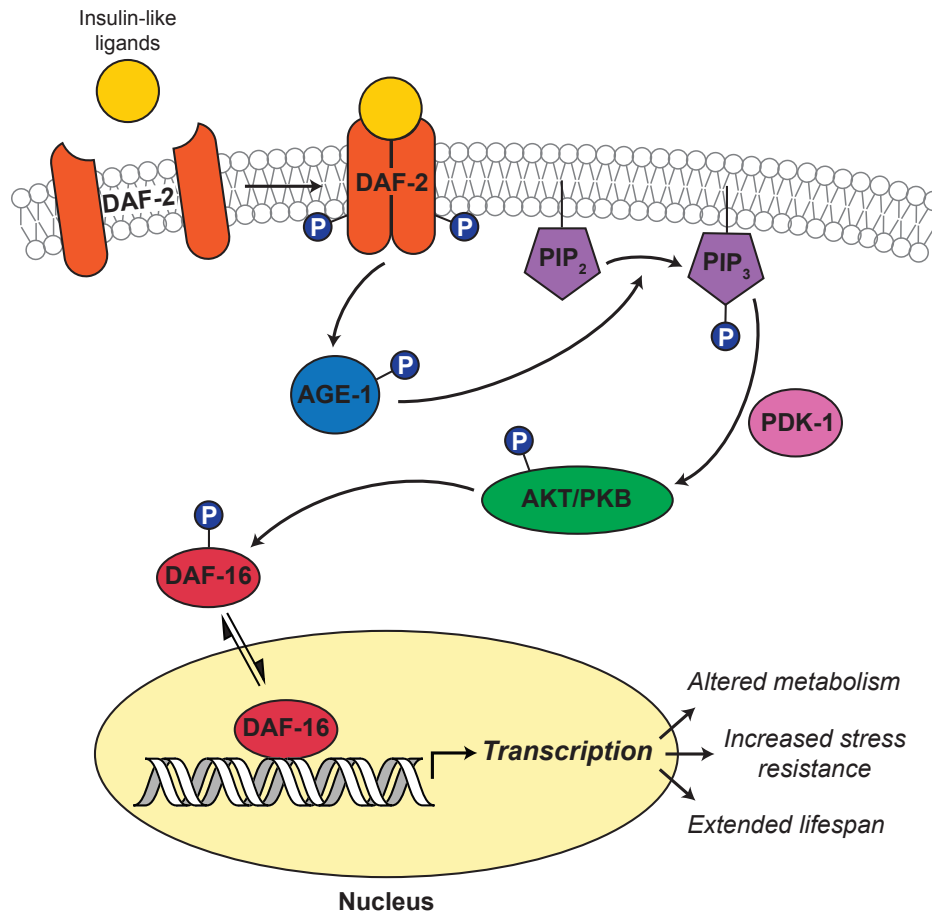


**Figure 3-2.** The *C. elegans* DAF-2/insulin-like pathway. Figure adapted from Nemoto and Finkel<sup>9</sup>

The core of this signaling pathway is evolutionarily conserved and has been demonstrated to play a significant role in stress resistance and controlling lifespan<sup>8</sup>. Inactivation of DAF-2, or several other kinases in this pathway, allows DAF-16 to enter the nucleus and regulate the transcription of genes that enhance longevity<sup>10-13</sup>. The activity of DAF-16 is required for longevity as double mutants of DAF-16 and DAF-2 lack this long-lived phenotype<sup>14-16</sup>. The life-extending properties of altering this pathway have been seen in a variety of organisms: In *Drosophila melanogaster* it was observed

that mutations in the insulin receptor substrate CHICO could increase lifespan by 48% and mutations in InR, the insulin-like receptor equivalent to DAF-2, could increase lifespan up to 85%<sup>17, 18</sup>. *Saccharomyces cerevisiae* lacks the insulin receptor but does have similar kinases to those downstream of this receptor, such as the AKT homologue Sch9, which enhanced yeast longevity upon deletion<sup>19</sup>.

While the core of this pathway is highly conserved, mammalian IIS is far more complex than its invertebrate equivalent. Three different ligands are present in mammals (insulin, IGF-1 and IGF-2) as well as three distinct receptors (insulin receptor, IGF-1 receptor, and IR related receptor), and ligand binding activates two major signaling pathways, the PI-3K-PKB/AKT pathway and the Ras-MAPK pathway. Mammalian IIS is also linked to growth hormone (GH) that regulates the release of IGF-1<sup>20</sup>. While difficult to decipher their specific roles in longevity, mouse mutants with reduced GH, IGF-1, or insulin have been shown to live longer than wild type mice. For example, the mean lifespan of fat-specific insulin receptor knockout (FIRKO) mice were increased by 18% and mice with mutated GH and reduced IGF-1 production also displayed extended lifespans<sup>21</sup>.

With the relationship between IIS and longevity seen in a variety of organisms, and many age-related developmental processes in humans are also controlled hormonally, it's likely that IIS contributes to human lifespan regulation as well. Studies on groups of long-lived humans reveal common polymorphisms in several of the IIS genes already implicated in invertebrate longevity. A SNP in AKT1 was significantly associated with lifespan in an analysis across three Caucasian study groups<sup>22</sup>. In the Leiden 85-plus Study, a correlation was seen between longevity and SNPs in *GHI*, *IGF1*, and *IRS1* that

reduces IIS activation<sup>23</sup>. Mutations in insulin receptor of a Japanese population were observed more frequently in semi-supercentenarians (older than 105) than the younger control group<sup>24</sup>. Additionally, variants of FOXO3A have been most consistently related to long-lived human populations<sup>22, 25-28</sup>.

Much of the evidence that supports aging as a hormonally regulated process originates from studies on *C. elegans*. Mutations in genes that induce the formation of long-lived dauer larva were studied for their effect on adult *C. elegans* lifespan. Three different mutations in the *daf-2* gene were found to dramatically increase dauer formation in a temperature-dependent manner<sup>29</sup>. *Daf-2* mutants grown at a permissive temperature (15 °C) develop normally like wild type, while 100% of mutants grown at the non-permissive temperature (25 °C) become constitutive dauers. The percentage of dauer formation can be manipulated by culturing the mutants at slightly lower temperatures, for example 93% of *daf-2* mutants grown at 22.5 °C develop into dauers (Figure 3-3a)<sup>30</sup>. When *daf-2* mutants were allowed to develop through the larva stages at the permissive temperature and then moved to a non-permissive temperature once they reach early adulthood, these mutants were found to live 2.3 times longer than wild type. Additionally, this lifespan expansion requires the activity of the DAF-16 transcription factor, as mutations in both *daf-2* and *daf-16* returned the lifespan to that of wild type<sup>29</sup> (Figure 3-3b).

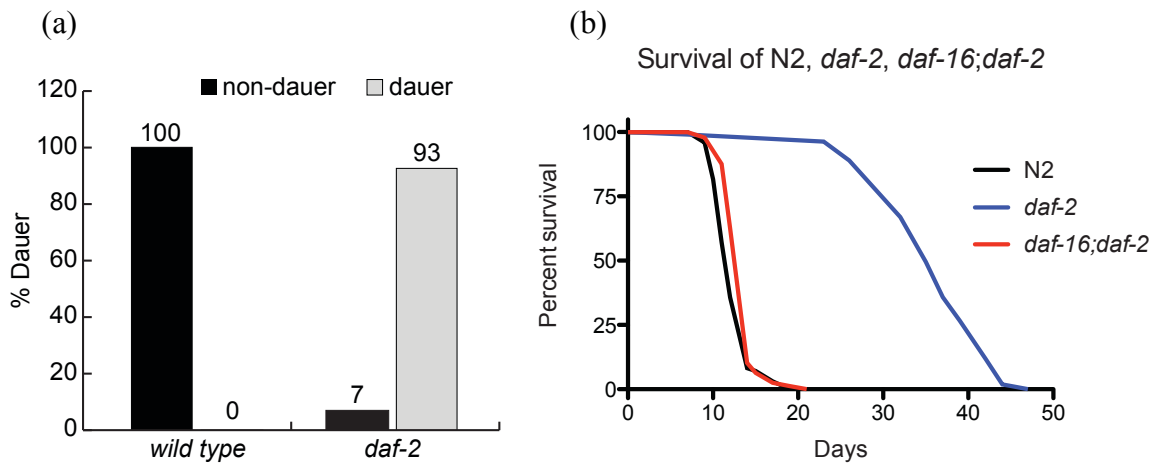


**Figure 3-3.** (a) Percent dauer formation in WT and *daf-2* mutant *C. elegans*, grown at 22.5 °C. Figure adapted from Hanover *et al.*<sup>30</sup>. (b) Lifespan of WT (N2), *daf-2* and *daf-16;daf-2* *C. elegans* (data from this study).

### Global profiling of DAF-16 transcriptional targets

The identification of *C. elegans* genes that act downstream of *daf-16* could contribute to a better understanding of how lifespan can be extended. Gene targets of the DAF-16 transcription factor have been investigated in several genomic and proteomic studies by comparing the changes in mRNA levels and protein abundance between *daf-2* and *daf-2;daf-16* mutants. *Daf-2* mutants are not only long-lived but also resistant to oxidative stress, heat, and heavy metals<sup>31</sup>. Studies specifically looking for changes in expression of genes involved in such resistance showed that proteins such as superoxide dismutase (SOD-3), metallothionein (MTL-1), and heat-shock proteins (HSP-16) were in fact upregulated in *daf-2* mutants<sup>31-33</sup>. Global transcriptomic analyses using microarrays identified additional upregulated genes that function in bacterial resistance, metabolism, steroid and lipid synthesis, and dauer formation. Downregulated genes were involved in

translation elongation, protein degradation, apolipoproteins, and peptide and lipid transport<sup>34-39</sup>. Global proteomic analyses profiling the *daf-2* proteome using quantitative <sup>15</sup>N stable isotope labeling and quantitative mass spectrometry identified similar genes differentially expressed in *daf-2* mutants as well as many changes in protein abundance that were not detected in the microarray analysis<sup>40, 41</sup>.

We wanted to complement these studies by using the tools of ABPP to profile protein-activity changes associated with impaired IIS in *C. elegans*. In particular, we are interested in the activity changes of cysteine residues because of the critical roles they play in catalysis and regulation<sup>42</sup>. Diverse proteins families, including proteases, kinases, and oxidoreductases, contain cysteine residues that are essential for protein function. These functional cysteines demonstrate elevated reactivity<sup>43</sup> and are often susceptible to a variety of oxidative modifications that serve to modulate protein activity<sup>44</sup>. In *C. elegans*, proteins involved in stress resistance, such as heat-shock proteins<sup>45</sup>, oxidoreductases (e.g. peroxiredoxins)<sup>46</sup>, and detoxifying enzymes (e.g. glutathione S-transferase)<sup>47</sup>, are regulated by the IIS and rely on critical cysteine residues for function. Additionally, dysregulated reactive oxygen species (ROS) is a characteristic feature of impaired IIS, resulting in changes to the oxidation state and subsequent function of cysteine-mediated proteins<sup>32, 46</sup>.

The relationship between ROS and lifespan extension through IIS is complex and multifaceted. Acute inhibition of DAF-2 results in a transient increase in ROS levels due to an increase in metabolic rate to compensate for decreased glucose uptake; this spike in ROS then triggers the activation of a variety of antioxidant systems and the subsequent lowering of ROS levels<sup>46</sup>. Therefore, chronic inactivation of DAF-2 results in creased

expression of antioxidant enzymes such as SOD-3 and catalase that render lower ROS levels in *daf-2* mutants<sup>32</sup>. Due to the sensitivity of cysteine-mediated protein activities to changes in ROS, the abundance of these proteins is not a true representation of activity state. The use of ABPP can therefore serve to identify posttranslational regulatory mechanisms active during IIS, while also enriching for low-abundant members of this protein class that are undetected by traditional abundance-based proteomic measurements. Previous studies have applied redox proteomic methods to identify *C. elegans* proteins that are oxidized upon exposure to peroxide<sup>48</sup>, but similar studies have not been utilized to explore endogenous oxidative events associated with impaired IIS.

Comparing changes in cysteine reactivity across *daf-2* and *daf-16;daf-2* mutants allows identification of changes in protein abundance and/or oxidation driven by impaired IIS. We applied a promiscuous cysteine-reactive chemical probe, coupled with quantitative MS, to globally quantify cysteine-reactivity changes between *daf-2* and *daf-16;daf-2* mutants<sup>43, 49</sup>. Our studies identified 40 cysteine-containing proteins that show a greater than two-fold change in cysteine reactivity upon impaired IIS. Subsequent RNAi-mediated knockdown of 17 genes identified *lbp-3* and *K02D7.1* as novel modulators of *C. elegans* lifespan and dauer formation. Importantly, our studies represent the first application of the tools of ABPP in *C. elegans* and highlight the ability of chemical proteomics to complement traditional transcriptomic and proteomic methods used to study IIS.

## Reactive-cysteine profiling reveals functional cysteines in *C. elegans*

Cysteine is one of the most intrinsically nucleophilic amino acid, and this nucleophilicity can be modulated by the protein microenvironment to enable diverse biochemical functions<sup>42, 50</sup>. A global proteomic evaluation of cysteine reactivity demonstrated that functional cysteines involved in catalysis and regulation display elevated reactivity relative to non-functional cysteines in the proteome<sup>43</sup>. In this previous study, the intrinsic reactivity of hundreds of cysteines in human proteomes was monitored using a promiscuous cysteine-reactive iodoacetamide-alkyne (IA) probe. Comparison of the extent of cysteine labeling as a function of time or IA concentration, revealed a subset of hyperreactive cysteines that saturated labeling at low time points, or low IA concentrations. This subset of hyperreactive cysteines was enriched in functional cysteines. To determine if a similar strategy would allow identification of functional cysteines in *C. elegans* lysates, we performed a concentration-dependent analysis of cysteine labeling by the IA probe.

Lysates from *daf-2* mutants were used for these studies. These lysates were treated with either 10  $\mu$ M or 100  $\mu$ M IA probe prior to conjugation to isotopically labeled, chemically cleavable biotin tags (Azo-tags)<sup>49</sup> using copper(I)-catalyzed azide-alkyne cycloaddition (CuAAC)<sup>51</sup>. The Azo-tags are comprised of an azide, a biotin, a chemically cleavable azobenzene linker, and an isotopically light or heavy valine, as described in chapter 2. *C. elegans* lysates, treated with 10  $\mu$ M or 100  $\mu$ M IA, were conjugated to heavy and light Azo-tags, respectively. These samples were then combined and subjected to streptavidin enrichment, on-bead trypsin digestion and treatment with sodium dithionite to release the probe-labeled peptides for analysis by high-resolution

LC/LC-MS/MS (Figure 3-4a). MS analysis identified 578 unique cysteine-containing peptides in the *daf-2* lysates, and for each of these peptides, a light:heavy ratio (R) was calculated that reflects the degree of cysteine labeling between the 10  $\mu$ M or 100  $\mu$ M IA-treated samples (Table 3-1, Table 3A-1). A cysteine that is hyperreactive and saturates labeling at the low IA concentration will display R values of  $\sim 1$ , whereas less reactive cysteines will display R values  $\gg 1$ . The 578 cysteine-containing peptides identified displayed a wide range of R values (Figure 3-4b), with 21 cysteine demonstrating R values  $< 3$  (Figure 3-4b; inset).

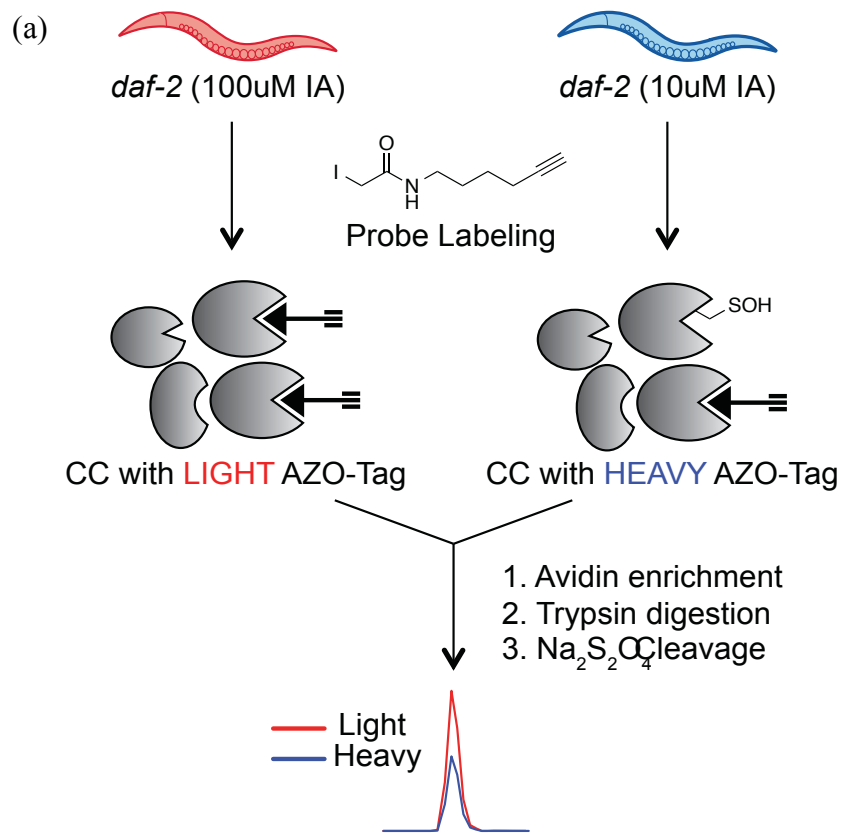
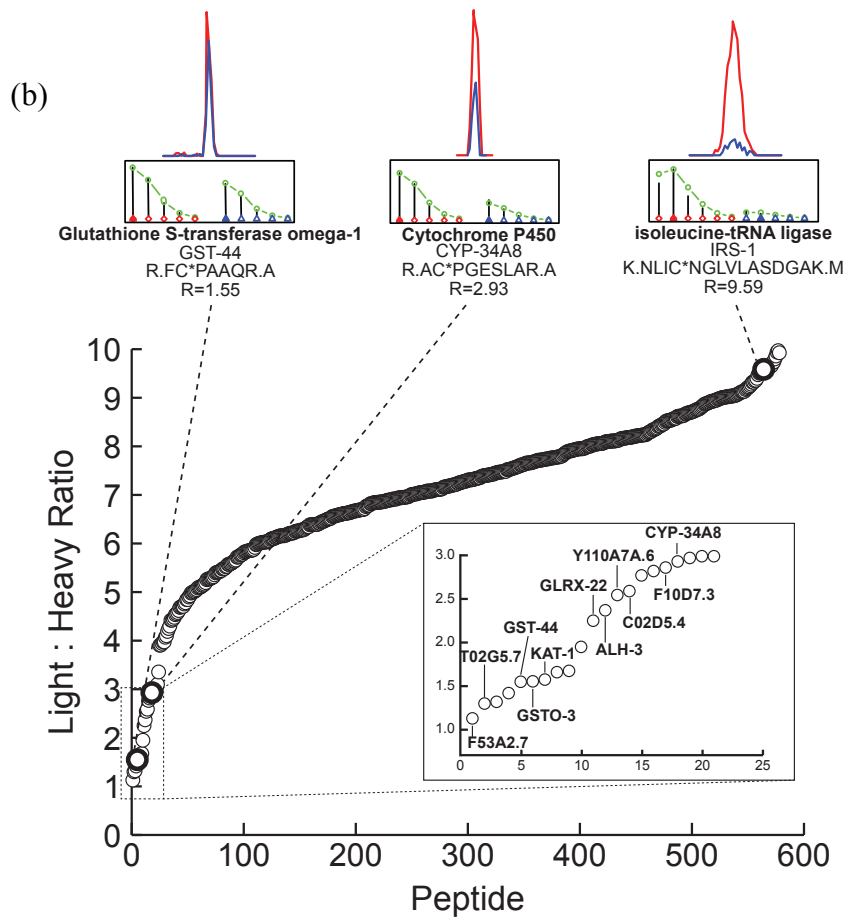
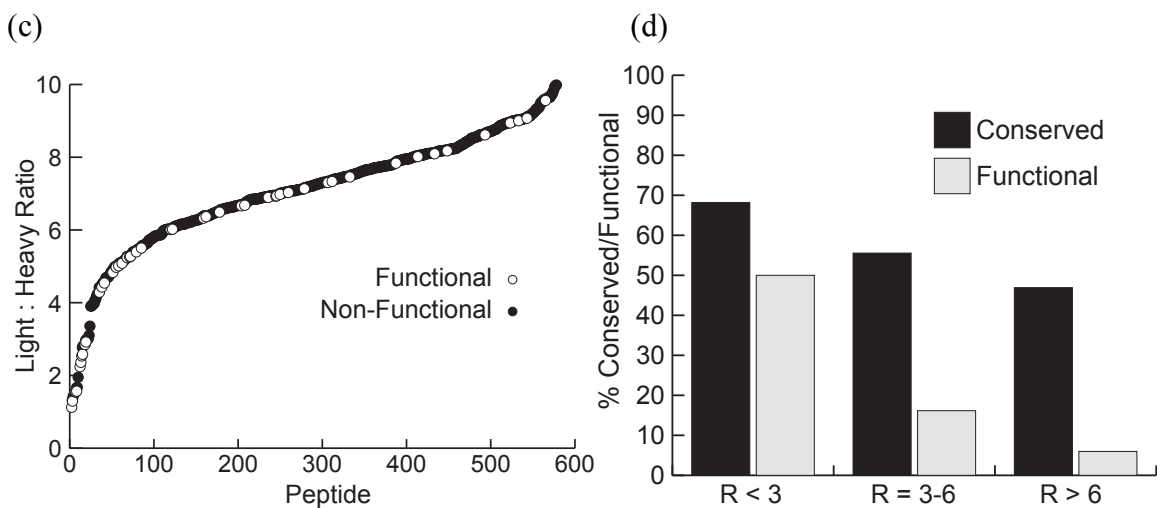


**Figure 3-4.** (a) Workflow to identify hyperreactive cysteines in the *daf-2* mutant proteome.



(b) Cysteine-containing peptides in order from high to low reactivity. Inset displays 21 most reactive cysteines in the *daf-2* mutant proteome.



(c) Cysteines with annotated biological functions in either *C. elegans* or the corresponding human homolog are highlighted in white along the ratio plot. (d) Cysteine-containing peptides sorted into 3 groups:  $R < 3$  (hyperreactive),  $R = 3-6$  (medium reactivity),  $R > 6$  (low reactivity). The percentage of cysteines in each grouping that are conserved in humans (black) or have annotated biological function (gray) are shown.

To determine if those cysteines with low ratio values ( $R < 3$ ) were enriched in known functional residues, we mined the *C. elegans* UniProt database for functional annotation of the identified cysteines as catalytic or regulatory residues. However, the *C. elegans* UniProt entries have poor annotation of residue and protein functions. Therefore, we also performed a BLAST search of each identified *C. elegans* protein against the human UniProt database and identified those cysteine residues that were conserved in the corresponding human homolog and were functionally annotated to be involved in catalysis and regulation (Table 3A-1). Comparing functional annotation with the observed R values for each cysteine demonstrated that cysteine with low R values (i.e. hyperreactive cysteines) were enriched in known functional residues (Figure 3-4c), similar to what was observed in human proteomes<sup>43</sup>. Approximately 50% of all cysteines identified with ratios  $< 3$  are known to be functional in either *C. elegans* or the corresponding human homolog (Figure 3-4d), whereas only 6% of cysteines with  $R > 6$  were annotated to be functional. A similar trend in cysteine conservation was also observed (Figure 3-4d), albeit with less of a dramatic enrichment amongst the hyperreactive subset of cysteines, suggesting that cysteine reactivity rather than conservation, predicts cysteine functionality more effectively. Functionally annotated

hyperreactive cysteines in *C. elegans* include active-site cysteines in glutathione S-transferases, aldehyde dehydrogenase and glutaredoxins (Table 3-1). These studies constitute the first evaluation of cysteine reactivity in *C. elegans* and provide a list of hyperreactive cysteines, including unannotated cysteines for future functional characterization. These data also demonstrate that the IA probe labels functional cysteines within *C. elegans* proteomes, and comparing IA labeling between *daf-2* and *daf-16;daf-2* mutants will reveal reactivity changes across functionally relevant cysteine residues implicated in IIS.

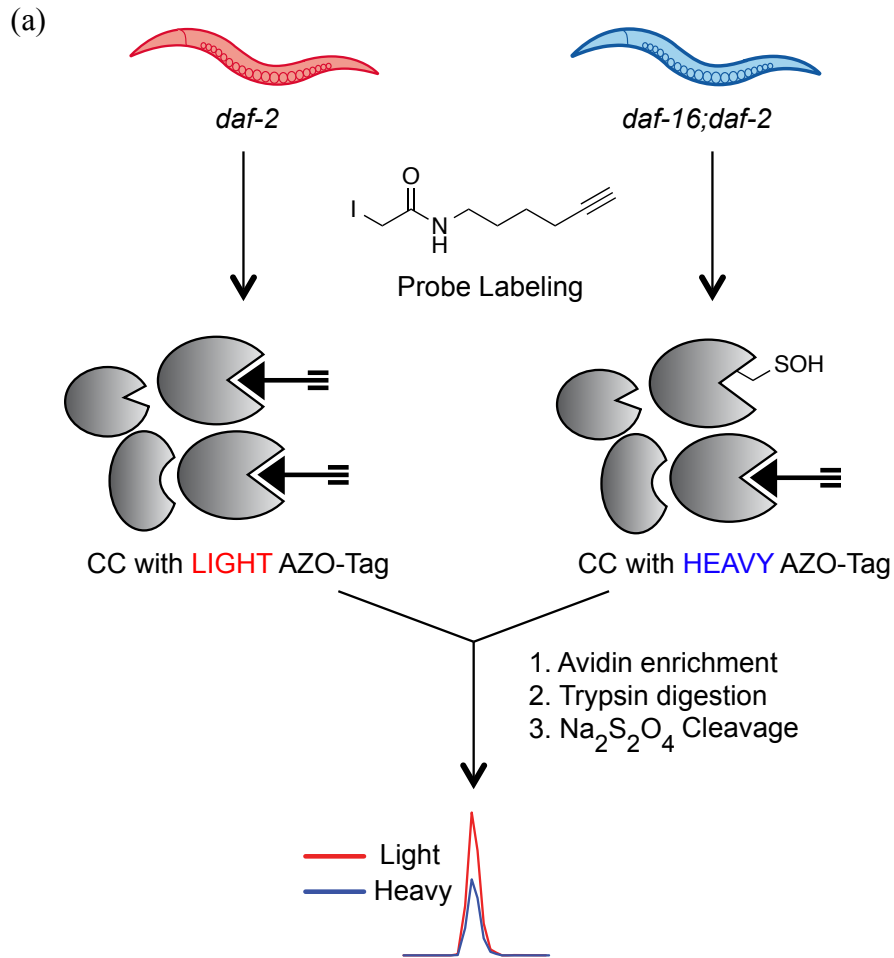
Gene Symbol	Protein Name	Sequence	Ratio	Function
F53A2.7	3-ketoacyl-CoA thiolase #	R.LC*GSGFQAVVNAQAQIK.L	1.13	Acyl-thioester intermediate
T02G5.7	Acetyl-CoA acetyltransferase#	K.VC*SSSMK.A	1.3	Acyl-thioester intermediate
gst-44	Glutathione S-transferase	R.FC*PAAQR.A	1.55	Active Site Nucleophile
gsto-3	Glutathione S-transferase omega	R.FC*PYAQR.V	1.555	Active Site Nucleophile
kat-1	Acetyl-CoA acetyltransferase#	K.VC*SSGLK.A	1.575	Acyl-thioester intermediate
glrx-22	Glutaredoxin-2	K.DGC*GYCVK.A	2.25	Redox-Active Disulfide
alh-3	Aldehyde Dehydrogenase	K.GENC*IAAGR.V	2.37	Active Site Nucleophile
Y110A7A.6	6-phosphofructo-2-kinase/fructose-2, 6-bisphosphatase#	R.VFFVESVC*DDPDIINSNITEVK.I	2.545	Active Site
C02D5.4	Glutathione S-transferase omega#	R.FC*PWAQR.A	2.59	Active Site Nucleophile
F10D7.3	Glutaredoxin-1#	K.TYC*PWSK.R	2.86	Iron-Sulfur/Redox-Active Disulfide
cyp-34a8	Cytochrome P450#	R.AC*PGESLAR.A	2.93	Iron Binding

**Table 3-1.** Hyperreactive cysteines identified in the *daf-2* mutant proteome with annotated biological function in either *C. elegans* or human UniProt databases. (#Human homologue of unannotated *C. elegans* proteins.)

## **Chemical-proteomic analysis identifies changes in cysteine reactivity between *daf-2* and *daf-16;daf-2* mutants**

Given that the IA probe labels a large number of functionally relevant cysteine residues in *C. elegans*, we set out to compare cysteine labeling across *daf-2* and *daf-16;daf-2* mutants. These studies will reveal variations in protein abundance and cysteine posttranslational-modification state in the long-lived *daf-2* mutants relative to the *daf-16;daf-2* mutants. Initially, to confirm the longevity phenotype of the *daf-2* mutants, a lifespan assay was performed on WT (N2), *daf-2* and *daf-16;daf-2* mutants cultured under identical conditions. As expected, *daf-2* mutants demonstrated an almost 100% lifespan extension (Figure 3-3)<sup>29</sup>. To quantify cysteine-reactivity changes between *daf-2* and *daf-16;daf-2* mutants, lysates from *daf-2* and *daf-16;daf-2* animals were treated with 100  $\mu$ M IA, appended to Azo-L and Azo-H, respectively, and subjected to the MS workflow utilized previously (Figure 3-5a). MS analysis provided R-values for 338 cysteine-containing peptides (Figure 3-5b) from two biological replicates, whereby a high R-value is indicative of a cysteine with increased reactivity in *daf-2* mutants, whereas low R-values represent cysteines with decreased reactivity in *daf-2* mutants. The majority of identified cysteines (84.9%) demonstrated R-values in the range  $0.5 < R < 2$ , demonstrating less than 2-fold change across the *daf-2* and *daf-16;daf-2* proteomes (Table 3A-2). In total, 48 cysteine residues on 40 proteins displayed a  $\geq 2$ -fold change (Table 3-2), with 36 showing increases in *daf-2* and 14 showing decreases in *daf-2* mutants. Our proteomic data was compared to transcriptomic data available for *daf-2* and *daf-16;daf-2* mutants<sup>52, 53</sup>, to determine if the changes we observed were also present at the transcript level. Of the 40 proteins that showed significant changes in *daf-2* mutants,

transcriptomic data was available for 25. In terms of the general trend (increase vs. decrease in *daf-2* animals) all but one hit (protein Y39E4A.3) agreed with the previously reported transcriptomic data (Table 3-2).



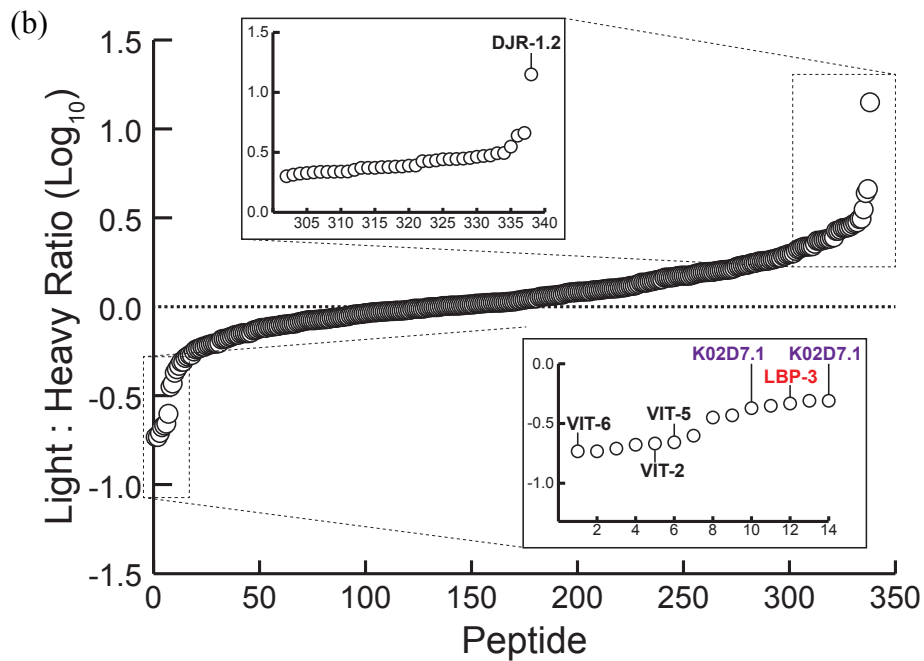


**Figure 3-5.** (a) Workflow to quantify cysteine reactivity changes between *daf-2* and *daf-16;daf-2* mutants. (b) Identified cysteine-containing peptides plotted against the log<sub>10</sub> value of each light:heavy ratio. Log<sub>10</sub> values < 0 indicate cysteines with decreased reactivity in *daf-2* mutants, log<sub>10</sub> values > 0 indicate cysteines with increased reactivity in *daf-2* mutants. Proteins with a previously observed role in lifespan regulation (DJR-1.2, Vit-2,5,6) and those that we demonstrate to affect lifespan and dauer formation upon RNAi-mediated knockdown (LBP-3, K02D7.1) are indicated.

Decrease in *daf-2*

Gene ID	Symbol	Description	Sequence	Average	LogFC	Reference
K07H8.6	vit-6	Vitellogenin-6	VIC*PIAEVGTK	0.185 ± 0.005	-3.912782	McElwee et al. 2003
			TEEGLIC*R	0.185 ± 0.025		
			EC*NEEQLEQIYR	0.195 ± 0.005		
			SYANNESPC*EQTFSSR	0.21 ± 0.01		
			NQFTPC*YSLVAK	0.25 ± 0.02		
C42D8.2	vit-2	Protein VIT-2, isoform b	VAIVC*SK	0.215 ± 0.005	-3.0831914	McElwee et al. 2003
C04F6.1	vit-5	Vitellogenin-5	APLTTC*YSLVAK	0.22 ± 0.01	-4.7545872	McElwee et al. 2003
ZK228.3	ZK228.3	Protein ZK228.3	DGVVYSVAC*STHQFV	0.355 ± 0.015	-2.7870228	McElwee et al. 2003
C17H12.13	C17H12.13	Protein C17H12.13, isoform b	DLVQDSLQC*SSTCVIR	0.37 ± 0.01	-1.6453787	McElwee et al. 2004
K02D7.1	K02D7.1	Protein K02D7.1	ADLGIIC*GSLGPIGDTVQDATILPYSK	0.425 ± 0.025		
			TVGADALGMSTC*HEVTVAR	0.49 ± 0.05		
R11H6.1	pes-9	Protein PES-9	EGC*SIPITLTFQELTGK	0.445 ± 0.035	-1.1148371	McElwee et al. 2003
F40F4.4	lbp-3	Fatty acid-binding protein homolog 3	MVNNGITC*R	0.465 ± 0.015	-2.3463961	McElwee et al. 2003
					-0.7969711	McElwee et al. 2004
F32D1.5	F32D1.5	Probable GMP reductase	SAC*TYTGAK	0.49 ± 0.02		

Increase in *daf-2*

Gene ID	Symbol	Description	Sequence	Average	LogFC	Reference
F54E7.2	rps-12	40S ribosomal protein S12	GLHETC*K	2 ± 0.12		
Y39E4A.3	Y39E4A.3	Protein Y39E4A.3, isoform a	GYTMENFMNQC*YGNADDLGGK	2.06 ± 0.2	-0.88701738	McElwee et al. 2003
					-0.79790038	McElwee et al. 2004
C08B11.7	ubh-4	Probable ubiquitin carboxyl-terminal hydrolase ubh	GHC*LSNSEIIR	2.105 ± 0.135		
R03D7.6	gst-5	Probable glutathione S-transferase 5	ETC*AAPFGQLPFLEVDGK	2.125 ± 0.025		
F36H1.6	alh-3	Protein ALH-3	GENC*IAAGR	2.155 ± 0.115		
Y54E10BR.6	rpb-7	Protein RPB-7	LFNEVEGTC*TGK	2.175 ± 0.335		
T20G5.1	chc-1	Probable clathrin heavy chain 1	AAIGQLC*EK	2.175 ± 0.825		
K08E3.5	K08E3.5	Protein K08E3.5, isoform f	LNGGLGTSMGC*K	2.18 ± 0.04		
T08B2.10	rps-17	40S ribosomal protein S17	VC*DEVAIIGSK	2.185 ± 0.105		
F09E10.3	dhs-25	Protein DHS-25	TPMTEAMPPTVLAEIC*K	2.19 ± 0.02		
K11H3.1	gpdh-2	Protein GPDH-2, isoform c	NVVAC*AAAGTFDGLGYGDNTK	2.26 ± 0.06		
K12G11.3	sodh-1	Alcohol dehydrogenase 1	LMNFNC*LNCFCK	2.35 ± 0.21	2.77488663	McElwee et al. 2003
			LMNFNCLNC*EFCK	2.35 ± 0.21		
			LMNFNCLNCFCK	2.35 ± 0.21		
			DTNLAAAPILC*AGVTVYK	4.355 ± 0.135		
C26D10.2	hel-1	Spliceosome RNA helicase DDX39B homolog	YFVDEC*DK	2.38 ± 0.05		
W05G11.6	W05G11.6	Protein W05G11.6, isoform a	AELMNPAGIYIC*DGSQK	2.385 ± 0.065	1.225460275	McElwee et al. 2003
			TNAMAMESC*R	2.405 ± 0.155		
			FIAAAFSPAC*GK	3.53 ± 0.13		
C36A4.9	acs-19	Protein ACS-19, isoform a	TNISYNC*LER	2.41 ± 0.14	1.04628319	McElwee et al. 2003
					1.25650399	McElwee et al. 2004
F55H12.4	F55H12.4	Protein F55H12.4	GSTGHC*YK	2.45 ± 0.18	0.86801231	McElwee et al. 2004
Y113G7B.23	swsn-1	Protein SWSN-1	GVQAAAASC*LAAAARK	2.455 ± 0.245		
ZK829.4	gdh-1	Glutamate dehydrogenase	CDIFVPAAC*EK	2.67 ± 0.37		
C05C10.6	ufd-3	Protein UFD-3, isoform b	ALAVTQGGC*LISGGR	2.71 ± 0.04		
K08F4.9	dhs-12	Protein DHS-12	AAIVNIGSDC*ASQALNLR	2.77 ± 0.17	0.95337266	McElwee et al. 2004
F01G10.1	tk1-1	Protein TKT-1	ISSIEMTC*ASK	2.775 ± 0.225	1.09186927	McElwee et al. 2003
					1.95300157	McElwee et al. 2003
B0286.3	B0286.3	Probable multifunctional protein ADE2	MPNGIGC*TTVLDPSEAAALAAK	2.785 ± 0.095	1.2433513	McElwee et al. 2004
F32A7.5	F32A7.5	Protein F32A7.5, isoform d	DISGEQLQAILC*GK	2.805 ± 0.015		
F20D6.11	F20D6.11	Protein F20D6.11	FSGC*NQGSTK	2.84 ± 0.48	1.13544319	McElwee et al. 2004
F57B9.6	inf-1	Eukaryotic initiation factor 4A	AIVPC*TTGK	2.905 ± 0.155		
B0035.5	gsdp-1	Glucose-6-phosphate 1-dehydrogenase	SSC*ELSTHLAK	2.95 ± 0.36		
ZK829.7	ZK829.7	Protein ZK829.7	AILEVC*DPSSALDADQSGGVPIPAATSE	2.98 ± 0.31	0.98562873	McElwee et al. 2004
K09A9.2	rab-14	Protein RAB-14	AFAEENGLTFLEC*SAK	3.11 ± 1.7		
W01A11.6	moc-2	Protein MOC-2	VCVITVSDTC*SAGTR	3.125 ± 0.125		
F20G2.2	F20G2.2	Protein F20G2.2	SC*SIDLAK	4.59 ± 0.55		
C49G7.11	djr-1.2	Protein DJR-1.2	LAEC*PVIGELLK	14.115 ± 1.505	3.26971892	McElwee et al. 2003
					3.42744981	McElwee et al. 2004

**Table 3-2.** Cysteine residues with a  $\geq 2$ -fold change between *daf-2* and *daf-16;daf-2* mutants. Transcriptomic changes (LogFC) of the corresponding genes previously identified in microarray analysis of *daf-2* and *daf-16;daf-2* are shown. Highlighted in yellow are the two identified proteins (K02D7.1 and LBP-3) that when knocked down in *daf-2* mutants show the most dramatic effect on lifespan and dauer formation.

Several of the protein targets we identified have been characterized using RNAi knockdown and phenotypic analysis, including the vitellogenins (VIT-2/5/6) and the DJR-1.2 glyoxalase<sup>36, 54-56</sup>. Vitellogenesis is the process of egg yolk, or vitellogenin, production that provides the major nutrient source for developing embryos. Vitellogenesis is suppressed in the *daf-2* mutant, possibly extending lifespan by using those resources to maintain somatic cells<sup>57</sup>. Vitellogenins are among the most downregulated proteins in *daf-2* mutants and RNAi-mediated knockdown lengthened the lifespan of *daf-2* (+) animals<sup>36</sup>. DJR-1.2 has been similarly functionally characterized. DJR-1.2 is homologous to the human DJ-1 protein and defects in the *dj-1* gene are a cause of autosomal recessive early-onset Parkinson's disease<sup>58</sup>. DJ-1 is a multifunctional redox-sensitive protein that plays roles in dampening mitochondrial oxidative stress and regulation of anti-apoptotic and anti-oxidant gene expression. DJ-1 also regulates toll-like receptor signaling, suggesting a role in innate immunity<sup>59</sup>. DJR-1.2 showed the most marked increase in cysteine labeling in *daf-2*, and has been found to be upregulated in both *daf-2* and dauer larva, showing a DAF-16-dependent decrease in stress resistance and viability upon knockdown<sup>55</sup>. These previous RNAi-mediated knockdown and subsequent evaluation of lifespan and stress-resistance for vitellogenins and DJR-1.2 glyoxalase serves to validate the proteins identified in our chemical-proteomic studies as IIS-regulated mediators of lifespan.

## **RNAi-mediated knockdown of *lbp-3* and *K02D7.1* results in modulation of lifespan and dauer formation**

To determine if other proteins identified in our cysteine-reactivity profiling studies were implicated in IIS-mediated lifespan regulation, we performed RNAi-mediated knockdown studies followed by subsequent lifespan analysis. For these RNAi studies, we focused on a set of 20 genes, corresponding to the 10 proteins that showed the largest decrease (*vit-6*, *vit-2*, *vit-5*, *ZK228.3*, *C17H12.13*, *K02D7.1*, *pes-9*, *lbp-3*, *F32D1.5*, *eef-2*) and the 10 proteins with the largest increase (*djr-1.2*, *F20G2.2*, *sodh-1*, *pck-1*, *moc-2*, *rab-14*, *ZK829.7*, *gspd-1*, *inf-1*, *F20D6.11*) in *daf-2* mutants consistent across the two biological replicates from our proteomic data (Table 3-2). Of these, in addition to the vitellogenin genes (*vit-6/2/5*) and *djr-1.2* discussed previously, four other genes had already been subjected to RNAi and phenotypic analysis (*sodh-1*<sup>36</sup>, *eef-2*<sup>60</sup>, *inf-1*<sup>61</sup>, and *pck-1*<sup>56</sup>). The remaining 12 genes with no previous RNAi and phenotypic data related to lifespan could be targeted using bacterial strains available in the Ahringer RNAi library<sup>62</sup> (Table 3-3). We performed RNAi on these 12 genes and subsequently monitored lifespan with respect to vector-treated controls (Figure 3A-1). We observed a greater than 15% increase in lifespan for four of the genes tested (*K02D7.1*, *pes-9*, *lbp-3* and *gspd-1*) (Figure 3-6a and b, Figure 3A-1 and Table 3-3). Of these four genes, *K02D7.1*, *pes-9* and *lbp-3*, corresponded to proteins that decreased in *daf-2* mutants according to our proteomic data, supporting the idea that further decreases in the levels of these proteins using RNAi would result in augmentation of the longevity phenotype.

	Gene	Median Lifespan			Dauer Formation		
		RNAi	Vector	Change	RNAi	Vector	Change
Decrease in <i>daf-2</i>	<i>ZK228.3</i>	37.4	35.2	6.34%	-	-	-
	<i>C17H12.13</i>	30.3	26.5	14.2%	-	-	-
	<i>K02D7.1</i>	45.7	30.0	52.6%	48.0%	16.4%	31.6%
	<i>pes-9</i>	45.0	38.1	18.3%	24.8%	31.6%	-6.80%
	<i>lbp-3</i>	41.4	35.6	16.3%	29.7%	16.4%	13.3%
	<i>F32D1.5</i>	33.2	35.2	-5.67%	-	-	-
Increase in <i>daf-2</i>	<i>F20D6.11</i>	40.4	38.1	6.2%	-	-	-
	<i>gspd-1</i>	41.2	26.5	55.4%	-	-	-
	<i>ZK829.7</i>	35.1	35.2	-0.40%	-	-	-
	<i>Rab-14</i>	32.9	35.2	-6.43%	-	-	-
	<i>Moc-2</i>	32.1	35.2	-8.77%	-	-	-
	<i>F20G2.2</i>	31.6	35.2	-10.3%	-	-	-

**Table 3-3.** Lifespan changes upon RNAi-mediated knockdown of the 12 selected genes against a vector-treated control. Dauer formation changes with RNAi-mediated knockdown of the 3 genes decreased in the *daf-2* mutant with the greatest increases in lifespan.

To determine if inactivation of *K02D7.1*, *pes-9* and *lbp-3*, would further augment dauer formation in *daf-2* mutants, dauer-arrest assays were performed upon RNAi-mediated knockdown. At 22.5 °C, 16.4% of *daf-2* mutants developed into dauer larva. Reduction of levels of both LBP-3 and K02D7.1 increased dauer formation to 29.7% and 48.0%, respectively (Figure 3-6c and (Table 3-3). In contrast, inactivation of *pes-9*, showed no significant change in dauer formation (Table 3-3). Therefore *C. elegans* LBP-3 and K02D7.1 proteins are implicated in both lifespan regulation and entry into the dauer state. RT-PCR was used to confirm knockdown of *lbp-3* and *K02D7.1*, and compared against the control gene *pmp-3*, which demonstrates unusually stable

expression levels with little variation between adults, dauers, and L3 larvae, or between wild-type and *daf-2* or *daf-16* mutant adults (Figure 3-6d)<sup>63</sup>.

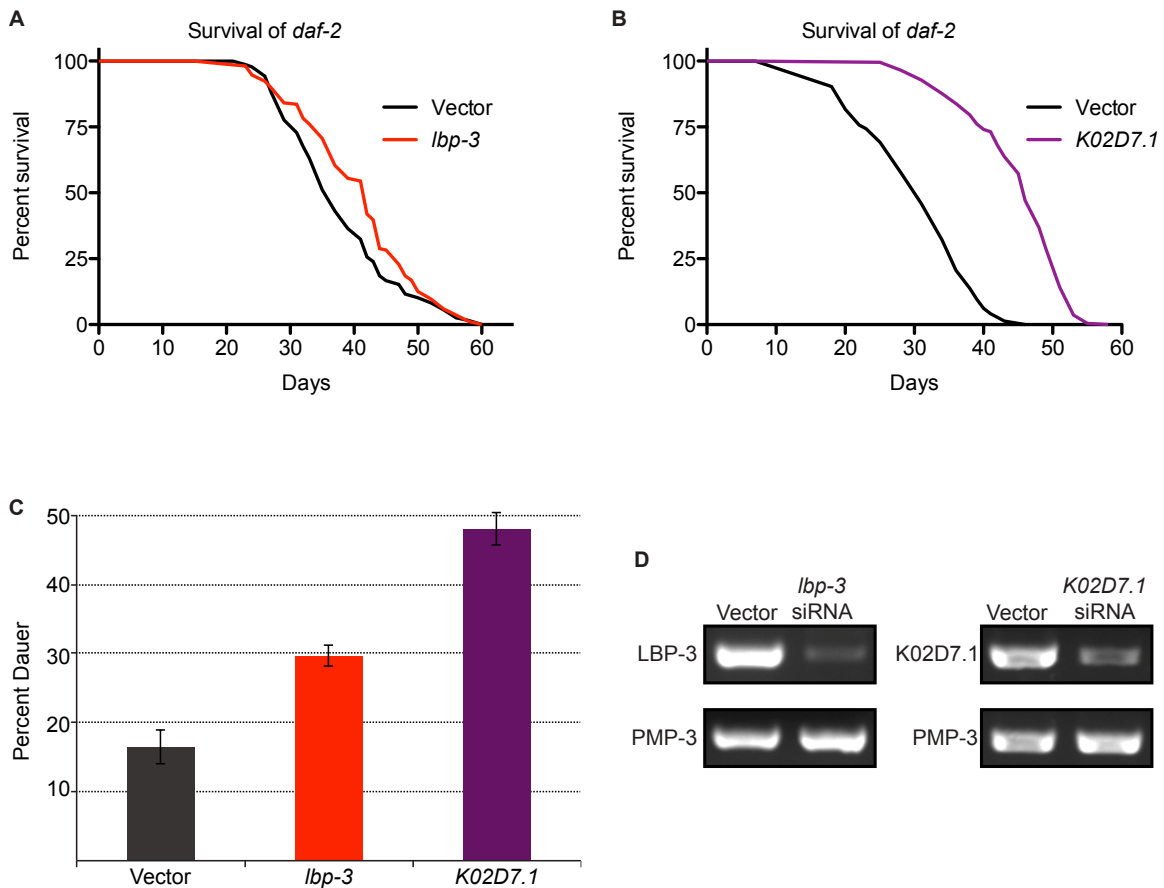


**Figure 3-6.** Survival plots of *daf-2* mutants treated with (a) *lbp-3* siRNA or (b) *K02D7.1* siRNA and compared to a vector- treated control. (c) Dauer-arrest assay comparing the percent dauer formation of *daf-2* mutants with RNAi-mediated knockdown of *lbp-3* and *K02D7.1* compared to a vector-treated control. (d) RT-PCR of *daf-2* mutants treated with *lbp-3* or *K02D7.1* siRNA using primers for *lbp-3*, *K02D7.1*, or *pmp-3* as a control.

From our RNAi knockdown and phenotypic analyses, we conclude that the most dramatic effects on extending lifespan and dauer formation were observed for

knockdown of *lbp-3* and *K02D7.1* (Figure 3-6). To determine if the observed effects on lifespan were dependent on the presence of functional DAF-2 and DAF-16, lifespan assays were repeated in the background of *daf-16* mutants, *daf-16;daf-2* double mutants, and WT (N2) animals (Figure 3-7a), and gene knockdown was confirmed with RT-PCR (Figure 3-7b). Knockdown of *lbp-3* only affected the lifespan of *daf-2* mutants, whereas *K02D7.1* knockdown extended lifespan in all 4 mutant backgrounds.

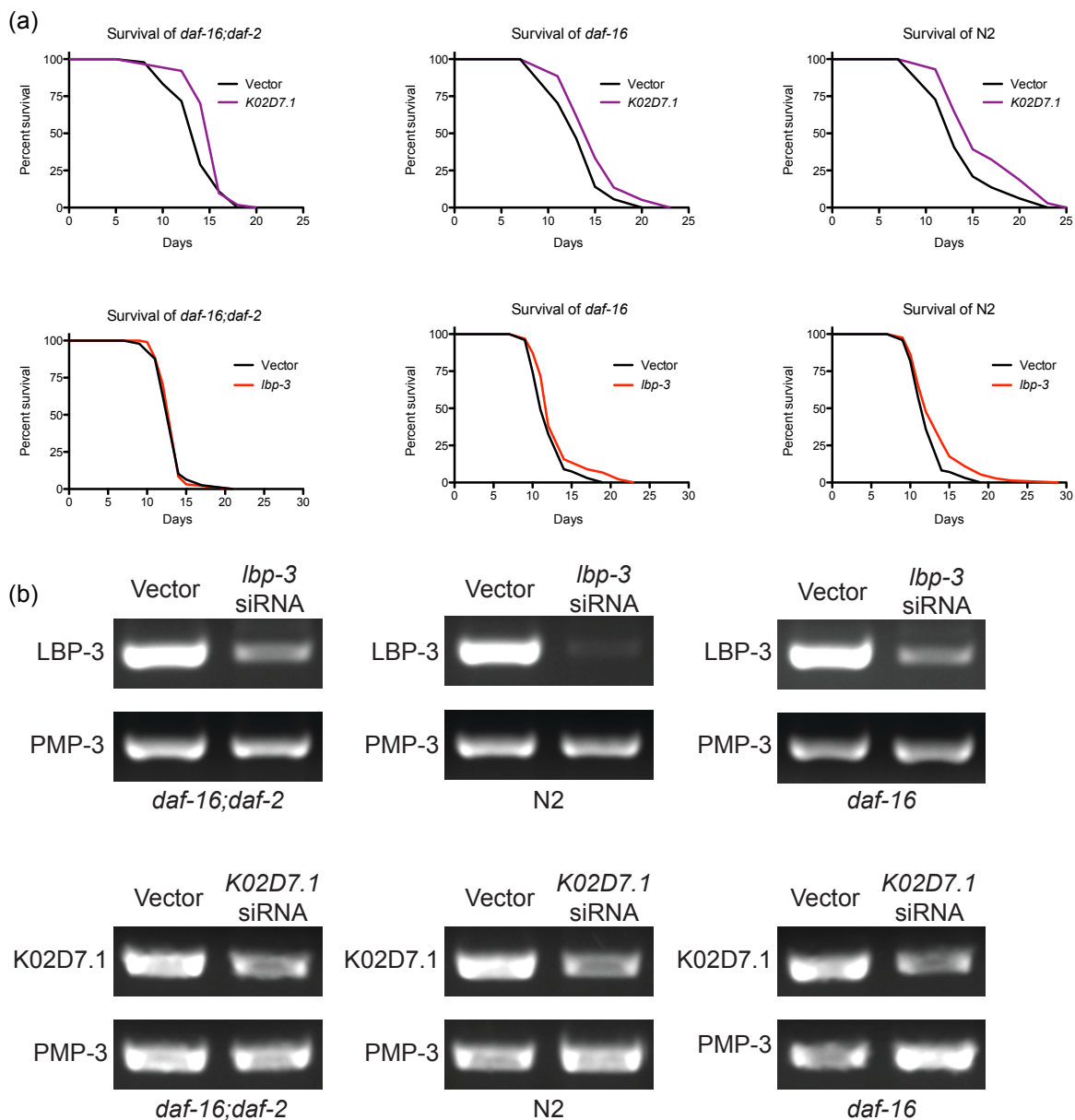


**Figure 3-7.** (a) Lifespan assays of RNAi-mediated knockdown of *lbp-3* and *K02D7.1* in the background of *daf-16* mutants, *daf-16;daf-2* double mutants, and wild type (N2) worms. (b) RT-PCR of the three strains treated with *lbp-3* or *K02D7.1* siRNA using primers for *lbp-3*, *K02D7.1*, or *pmp-3* as a control.

### ***C. elegans* lipid binding protein-3**

LBP-3 is an intracellular lipid chaperone in the fatty-acid-binding protein (FABP) family. FABPs are conserved from *C. elegans* to humans and are involved in fatty-acid uptake, transport and oxidation<sup>64</sup>. The *C. elegans* genome contains nine LBP genes and the exact functions of these individual LBPs remains unclear<sup>65</sup>. Of the *C. elegans* LBPs, LBP-5 appears to be the most extensively studied, whereby RNAi-mediated knockdown of *lbp-5* results in fat accumulation in the intestine<sup>66</sup>. The putative role of the *C. elegans* LBPs in fat accumulation and transport is notable because a characteristic feature of the *daf-2* mutants and long-lived dauers is increased fat content<sup>67</sup>. Previous studies have also shown that mutational inactivation of other lipid transport proteins, such as the intramembrane transporters, NDG-4 and NRF-5/6, increase stress resistance and lifespan through the IIS pathway<sup>68</sup>. These previous studies into the lipid-binding protein family and related proteins supports a potential role for LBP-3 in *C. elegans* lipid metabolism and IIS.

Given the lack of functional characterization of the *C. elegans* LBPs, we probed the mammalian FABPs for insight into the function and regulation of this class of proteins. There are at least nine human FABPs and these have distinct tissue localization patterns. All FABPs are small intracellular proteins that can localize to the nucleus<sup>69, 70</sup>,

and bind long-chain fatty acids, albeit with different binding affinities. In our cysteine-profiling studies, we identified Cys154 as labeled by the IA probe; this cysteine is not annotated as functional in the *C. elegans* UniProt database, but is conserved in several of the human FABPs (Figure 3-8). *C. elegans* LBP-3 shares the most homology with human FABP-5 (27% sequence identity), which contains a disulfide bond between Cys120 and Cys127 that regulates protein structure and function under reducing/oxidizing conditions<sup>71</sup>. In fact, several FABPs have been shown to be oxidized, glutathionylated and/or modified by oxidized lipid species such as 4-hydroxynonenal (HNE) at cysteine with effects on the lipid-binding ability and proteolytic stability<sup>72-74</sup>. It is therefore likely that Cys154 in *C. elegans* LBP-3 is similarly regulated through redox modifications. Interestingly, the 2.2-fold decrease in IA-labeled LBP-3 that we observed in the *daf-2* animals is significantly less than the change reported for *lbp-3* using transcriptomic analyses (~5-fold decrease). This suggests that either there is poor correlation between *lbp-3* mRNA and protein levels, or there is reduced enrichment due to partial oxidation of Cys154 in *daf-16;daf-2* mutants. The higher levels of ROS observed in *daf-16;daf-2* double mutants supports the possibility of increased protein oxidation in this strain compared to the single *daf-2* mutants<sup>32, 46</sup>.

```

LBP-3 1 MNLYLTLF SFCFLA IMAEAA SEIPEK FFGKYD LDRSENFDEFLAAKGVSWFVRQMIKLA K VSKVLAKNETPGKY NMENLTSKK 83
FABP1 1 -----MSFSGKYQLQSQENFEAFMKAIGLPEELIQKGDIKGVSEI VQNGKH--FKFTIT-AGS 56
FABP2 1 -----MAFDSTWVKVDRSENYDKFMEKMGVNI VKRKLA AHDNLKLTITQENK--FTVK-ESSAF 56
FABP3 1 -----MVDALFGTWKLVDSKNFDDYMKSLGVGFATRQVASMTKPTTIIEKNGDI--LTLK-THSTF 58
FABP4 1 -----MCDALVGTWKLVSSENFDDYMKLEVGVGFATRQVASMTKPTTIIEKNGDI--LTLK-SESTF 58
FABP5 1 -----MATVQQL EGRWRLVDSKGFDEYMKELGVGIALRKMGA M K PDCIITCDGKN--LTIK-TESTL 60
FABP6 1 -----MAFTGKFEMESEKNYDEFMKLLG I SSDVIEKARNFKIVTEVQQDGD--FTWSQHYSGG 57
FABP7 1 -----MVEAFCATWKL TN SQNFDEYMKALGVGFATRQVGNVTKPTVIISQEGDK--VVIR-TLSTF 58
FABP8 1 -----MSNKF LGTWKLVSSSENFDDYMKALGVGLATRKLGNLAKPTVIISKKGDI--ITIR-TESTF 58
FABP9 1 -----MVEPELGTWKLVSSENFEDYMKELGVNF AARNMAGLVKPTVTIISVDGKM--MTIR-TESSF 58

LBP-3 84 NTLYHG WELGKTFEAEGLDGV AHK I TFSFKDG-VLSEHHIRLNDPEHSAETYYYYIENDQLVMKMVNNGI TCR R WFKRSTGKK 165
FABP1 57 KVIQNEFTVGECELETMTGEKVKTVVQLLEGDNKLVTTFFK-----NIKSVTELNGDIINTMTLGDIVFKRISKRI---- 127
FABP2 57 RNIIEVVFELGVTFNYNLADGTEL RGTWSLEGN-KLIGKFKRTDNGN--ELNTVREIIGDELVQTYVYEGVEAKRIFKKD---- 132
FABP3 59 KNTEISFKLGVEFDETTADDRKVKSI VTL DGG-KLVHLQK--WDGK--ETTLVRELIDGKLLTLTHGTAVCTRITYEKEA--- 133
FABP4 59 KNTEISFILGQEFDETTADDRKVKSTITLDGG-VLVHVQK--WDGK--STTIKRKREDDKLVVECV M KGVSTSTRVYERA--- 132
FABP5 61 KTTQFSCTLGKFEFETTADGRKTQTVCNFTDG-ALVQHQE--WDGK--ESTITRKLKDGKLVVECV M NNVCTRIYEKVE--- 135
FABP6 58 HTMTNKFTVQKESNIQT MGGKTFKATVQMEGG-KLVVNF-----NYHQTSEIVGDKLVEVSTIGGVTYERVSKRLA--- 128
FABP7 59 KNTEISFQLGEEFDETTADDRNCKSVVSLDGD-KLVHIQK--WDGK--ETNFVREIKDGKMMVMTLTFGDVVAVRHYEKA--- 132
FABP8 59 KNTEISFKLQGEFEETTADNRKTKSIVTLQRG-SLNQVQR--WDGK--ETTIKRKL VNGK MVAECKMGGV VCTR IYEK V--- 132
FABP9 59 QDTKISFKLGEFEDETTADNRKVKSTITL ENG-SM I HVQK--WLGK--ETTIKRKIVDEK M VVECKMNNIVSTR IYEK V--- 132

```

**Figure 3-8.** Alignment of *C. elegans* LBP-3 with the human FABP family. Cys154 is the reactive cysteine identified in our proteomic studies (red) C and is conserved in several FABP family members (bold).

### ***C. elegans* protein K02D7.1**

K02D7.1 is an uncharacterized protein in *C. elegans* but homologous to human purine nucleoside phosphorylase (PNP) with 47% sequence identity. The IA-modified cysteines have no known functional annotation, but one of these cysteines are located in a highly conserved region (IIC\*GSGLG), with conservation seen throughout humans, mice, flies, and yeast (Figure 3-9). PNP catalyzes cleavage of the glycosidic bond of (deoxy)ribonucleosides, forming the corresponding free purine base and pentose-1-phosphate in the purine salvage pathway<sup>75</sup>. Although PNP has not been directly implicated in IIS and lifespan regulation, the purine nucleotide synthesis pathway has been shown to be regulated by PI3K/AKT signaling, suggesting that enzymes within this pathway are under IIS control<sup>76</sup>. Furthermore, a downstream enzyme involved in purine metabolism, xanthine dehydrogenase (XDH), was identified in a systematic screen for longevity genes in *C. elegans*. RNAi knockdown of XDH in *C. elegans* caused a ~12% increase in median lifespan<sup>77</sup>, suggesting that purine metabolism can modulate longevity. These previous studies indicate that *K02D7.1*, similar to XDH, is a regulator of *C. elegans* lifespan and is a promising target for further characterization to determine the exact biochemical function and role of this protein in IIS.



the subset of hyperreactive cysteines were several unannotated cysteines for future functional characterization in *C. elegans* and other organisms in which these cysteines are conserved. Given the wide utility of *C. elegans* as a model organism for aging, and the well-characterized role of impaired IIS in regulating longevity in this organism, we applied chemical proteomics to identify dysregulated protein activities with potential implications in IIS-mediated longevity regulation. Importantly, chemical-proteomic approaches such as ABPP have the advantage of identifying posttranslational modifications as well as low-abundance proteins, that are intractable to abundance based transcriptomic and proteomic approaches. Comparison of cysteine reactivity across *daf-2* and *daf-16;daf-2* mutants, identified 40 proteins with >2-fold change across these proteomes. The majority of these changes were previously identified in transcriptomic studies and validated to regulate lifespan, serving to substantiate our chemical-proteomic data. Previously uncharacterized proteins were also identified, underscoring the complementarity of chemical-proteomic techniques to existing global transcriptomic and proteomic studies. Coupling chemical-proteomic tools with RNAi-mediated knockdown and phenotypic assays resulted in the identification of two proteins, LBP-3 and K02D7.1, as novel mediators of *C. elegans* lifespan and dauer formation.

## Experimental procedures

### C. elegans culture for MS and RNAi experiments

#### Strain maintenance

Worm strains were grown at 15 °C on OP50 *E. coli*-seeded nematode growth medium (NGM) stock plates using standard *C. elegans* techniques<sup>78</sup>. The following strains were used:

***daf16;daf-2***: DR1309 *daf-16(m26) I; daf-2(e1370) III*

***daf-2***: CB1370 *daf-2(e1370) III*

***daf-16***: GR1307 *daf-16(mgDf50) I*

**Wild-type**: N2

Strains were provided by the CGC, which is funded by NIH Office of Research Infrastructure Programs (P40 OD010440)

#### Preparation of 4 day old *daf-2* and *daf-16;daf-2* worms for MS analysis

Age-synchronization of worms was done by shaking ~3000 gravid adult worms in a solution of sterile water (5.0 mL), KOH (1.0 mL, 5 M), and bleach (4.0 mL) for 5 minutes until only the eggs remained. The eggs were centrifuged for 30 seconds (4 °C, 2500 rpm), the supernatant was removed and the eggs were washed with S Medium (5 x 10 mL). The eggs were resuspended in S Medium (8 mL) and allowed to hatch overnight in a 15 °C incubator. The next day, the hatched L1 worms (~100,000) were aliquoted onto 10 NGM plates and synchronized growth began with the addition of OP50 *E. coli*

(100  $\mu$ L, 100 mg/mL). The worms were grown at 15  $^{\circ}$ C until the L4 larval stage where they were transferred to 25 floxuridine-containing plates (FUDR, 0.05 mg/mL) to prevent reproduction. The worms were fed OP50 (150  $\mu$ L), and moved to a 25  $^{\circ}$ C incubator. The following day was counted as day 1 of adulthood and the worms were grown until they were 4 days old. Additional OP50 was added daily as needed to prevent starvation. After 4 days, the worms were washed off the plates with PBS and any remaining bacteria, eggs, larva, deceased worms, or debris was removed via sucrose gradient separation: worms were washed with 3 x 5 mL cold 0.1 M NaCl and then suspended in 2.5 mL cold 0.1 M NaCl and 2.5 mL cold 60% sucrose in water. This was spun in a 4  $^{\circ}$ C centrifuge at 3500 rpm for 5 minutes, allowing the age-synchronized worms to float on the sucrose and pelleting the unwanted debris. The worms were carefully removed, washed with 5 x 5 mL PBS, and stored at -80  $^{\circ}$ C until lysis. The worms were resuspended in 4 mL PBS, sonicated to lyse, and spun at 5000 rpm for 10 minutes to isolate the protein extracts

### **Quantitative mass spectrometry analysis using isotopic azobenzene tags: reactive cysteines in *daf-2***

#### **Click chemistry and streptavidin enrichment of probe-labeled proteins**

For each MS sample, *daf-2* worms lysates (4 x 500  $\mu$ L, 2 mg/mL) in PBS were aliquoted into 1.5 mL eppendorf tubes. Two tubes were treated with the high concentration of IA-alkyne (100  $\mu$ M from 100x stock) and the other two tubes treated with the low concentration of IA-alkyne (10  $\mu$ M from 100x stock) for 1 hour at room temperature. The heavy azobenzene tag (Azo-H; 100  $\mu$ M) and light azobenzene tag (Azo-L; 100  $\mu$ M) were

added to the samples treated with 10  $\mu\text{M}$  IA-alkyne and 100  $\mu\text{M}$  IA-alkyne, respectively, and conjugated through click chemistry by the addition TCEP (1.0 mM from fresh 50X stock in water), ligand (100  $\mu\text{M}$  from 17X stock in DMSO:t-Butanol 1:4) and  $\text{CuSO}_4$  (1.0 mM from 50X stock in water). Samples were allowed to react at room temperature for 1 hour. The tubes were combined pairwise, centrifuged for 10 minutes (5,900 g at 4  $^\circ\text{C}$ ) to pellet the precipitated proteins, and resuspended in cold MeOH (500  $\mu\text{L}$ ) by sonication. The tubes were again combined pairwise, centrifuged, and washed in MeOH, after which the pellet was solubilized in PBS containing 1.2% SDS via sonication and heating (5 min, 80 $^\circ\text{C}$ ). The SDS-solubilized, probe-labeled proteome samples were diluted with PBS (5 mL) for a final SDS concentration of 0.2%. The solutions were incubated with 100  $\mu\text{L}$  streptavidin-agarose beads (Thermo Scientific) at 4  $^\circ\text{C}$  for 16 hrs. The solutions were then incubated at room temperature for 3 hrs. The beads were washed with 0.2% SDS/PBS (5 mL) for 10 mins, PBS (3 x 5 mL), and water (3 x 5 mL). The beads were pelleted by centrifugation (1400 g, 3 mins) between washes.

### **On-bead trypsin digestion and azobenzene cleavage**

The washed beads were suspended in 6 M urea/PBS (500  $\mu\text{L}$ ) and 10 mM dithiothreitol (DTT) (from 20X stock in water) and placed in a 65  $^\circ\text{C}$  heat block for 15 mins. Iodoacetamide (20 mM, from 50X stock in water) was then added and the samples were placed in a 37  $^\circ\text{C}$  incubator and agitated for 30 mins. Following reduction and alkylation, the beads were pelleted by centrifugation (1400 g, 3 min) and resuspended in 200  $\mu\text{L}$  of 2 M urea/PBS, 1 mM  $\text{CaCl}_2$  (from 100X stock in water), and trypsin (2  $\mu\text{g}$ ). The digestion was allowed to proceed overnight at 37  $^\circ\text{C}$ . The digested peptides were separated from the beads using a Micro Bio-Spin column (BioRad). The beads were washed with PBS (3

x 500  $\mu$ L) and water (3 x 500  $\mu$ L) and subsequently transferred to screw-cap eppendorf tubes. The azobenzene cleavage was carried out by incubating the beads with 50  $\mu$ L of fresh sodium dithionite in PBS (25 mM) for 1 hour at room temperature on a rotator. After centrifugation, the supernatant was transferred to a new eppendorf tube. The cleavage process was repeated twice more with 75  $\mu$ L of 25 mM dithionite solution and 75  $\mu$ L of 50 mM dithionite solution to ensure completion, each time combining the supernatants in the eppendorf. The beads were additionally washed twice with water (75  $\mu$ L). Formic acid (17.5  $\mu$ L) was added to the samples and stored at -20  $^{\circ}$ C until mass spectrometry analysis.

#### **Liquid chromatography-mass spectrometry (LC-MS/MS)**

LC-MS/MS analysis was performed on an LTQ-Orbitrap Discovery mass spectrometer (ThermoFisher) coupled to an Agilent 1200 series HPLC. Peptide digests were pressure loaded onto a 250  $\mu$ m fused silica desalting column packed with 4 cm of Aqua C18 reverse phase resin (Phenomenex). The peptides were then eluted onto a biphasic column (100  $\mu$ m fused silica with a 5  $\mu$ m tip, packed with 10 cm C18 and 3 cm Partisphere strong cation exchange resin (SCX, Whatman)) using a gradient 5-100% Buffer B in Buffer A (Buffer A: 95% water, 5% acetonitrile, 0.1% formic acid; Buffer B: 20% water, 80% acetonitrile, 0.1% formic acid). The peptides were then eluted from the SCX onto the C18 resin and into the mass spectrometer using four salt steps as previously described<sup>79</sup>. The flow rate through the column was set to  $\sim$ 0.25  $\mu$ L/min and the spray voltage was set to 2.75 kV. One full MS scan (FTMS) (400-1800 MW) was followed by 18 data dependent scans (ITMS) of the nth most intense ions with dynamic exclusion disabled

### **MS data analysis - peptide identification**

The generated tandem MS data were searched using the SEQUEST algorithm<sup>80</sup> against the Uniprot *C. elegans* database (UP000001940). A static modification of +57.02146 on cysteine was specified to account for alkylation by iodoacetamide and differential modifications of +443.2897 (AZO-L tag) and +449.3035 (AZO-H tag) were specified on cysteine to account for probe modifications. SEQUEST output files were filtered using DTASelect2.0.5 and quantification of light:heavy ratios was performed using the CIMAGE quantification package as previously described<sup>43</sup>.

### **Quantitative mass spectrometry analysis using isotopic azobenzene tags: *daf-2* vs. *daf-16;daf-2***

For each MS sample, *daf-2* and *daf-16;daf-2* worms lysates (2 x 500  $\mu$ L, 2 mg/mL each) were aliquoted into 1.5 mL eppendorf tubes. The tubes were treated with IA-alkyne (100  $\mu$ M from 100x stock) for 1 hour at room temperature. The Azo-H (100  $\mu$ M) was added to the *daf-16;daf-2* lysates, and the Azo-L (100  $\mu$ M) was added to the *daf-2* lysates and conjugated through click chemistry for 1 hour at room temperature. The rest of the procedure is the same as described above.

### **RNAi-mediated knockdown experiments**

#### **RNAi bacterial culture and RNAi feeding plate preparation**

RNAi bacterial clones came from the Ahringer Lab RNAi feeding library (provided by the Tissenbaum Lab), which uses the L4440 vector containing T7 promoters and the TetR

gene transformed into HT115 (DE3), an RNase III-deficient *E. coli* strain with IPTG-inducible T7 polymerase activity and ampicillin resistance<sup>81, 82</sup>. Frozen stocks from the library were streaked on LB agar plates containing ampicillin (100 µg/mL) and tetracycline (12.5 µg/mL) and grown overnight at 37 °C. Single colonies were inoculated and used to make frozen glycerol stocks from which all RNAi plates were made. Frozen stocks were grown overnight at 37 °C in LB media (3.0 mL) with ampicillin and tetracycline. The overnight cultures (200 µL) were added to LB media (20 mL) with ampicillin only and grown for 6 hours at 37 °C. RNAi plates containing ampicillin and IPTG (1.0 mM) were seeded with this RNAi bacterial culture (~800 µL) and allowed to dry overnight in the dark. RNAi plates used for lifespan assays also contained floxuridine (FUDR, 0.1 mg/mL

### **Lifespan assays**

Worms were cultured for two generations on RNAi plates at 15 °C. For each lifespan assay, 120 second generation L4 worms were transferred to 4 new RNAi plates (with FUDR) and moved to 20 °C. After 7 days, the worms were censored for “sick” phenotypes (e.g. vulva bursting) and then scored by gently tapping with a platinum wire every 2-3 days. Worms that crawled off the plate or into mold that was excised out of the agar were censored from the analysis.

### **Dauer formation assays**

*daf-2* worms were cultured for two generations on RNAi plates at 15 °C. For each dauer formation assay, 9 second generation L4 worms from each RNAi plate were transferred to 3 new RNAi plates and allowed to lay eggs overnight. The next day, adult worms were removed from the plates and the remaining eggs were moved to a 22.5 °C incubator.

After 4 days, the worms were scored for dauer larva and the percentage of dauer larva was compared to L4440 vector-treated *daf-2* control worms. Several temperatures between 20-25 °C were tested to determine which was most appropriate to cause 10-20% dauer arrest in the control worms (not shown).

### **Evaluation of mRNA levels in L4440 vector- and RNAi-treated *C. elegans***

#### **RNA Extraction**

Worms grown on RNAi plates were removed via washing with DEPC-water into an RNase-free 1.5 mL eppendorf tube. After the worms were allowed to settle, the supernatant was removed and the worms were washed with 1 mL of DEPC-water and rotated at room temperature for 20 minutes to remove excess RNAi bacteria. This washing step was repeated 4 more times. Excess DEPC-water was removed and TRIzol reagent (1.0 mL) was added, briefly agitated, and allowed to incubate at room temperature for 5 minutes. Chloroform (200 µL) was added to the tube, inverted to mix, let sit at room temperature for 3 minutes, and centrifuged for 15 minutes at 4 °C. The top layer was carefully transferred to another eppendorf tube and isopropanol (400 µL) added, vortexed well, and allowed to sit at room temperature for 10 minutes. The tube was centrifuged for 10 minutes at 4 °C and the supernatant was removed, leaving a white pellet which was then washed with a 75% EtOH in DEPC-water solution (200 µL). The tube was centrifuged for 5 minutes at 4 °C, the supernatant was removed, and the RNA pellet was allowed to air dry for ~10 minutes. The pellet was resuspended in DEPC-water (20-30 µL) and RNA concentrations were determined using the Nanodrop.

### **cDNA formation**

RNA stocks were diluted to 500 ng/ $\mu$ L. DEPC-water (9.5  $\mu$ L), RNA (1.0  $\mu$ L, 500 ng/ $\mu$ L = 500 ng), and Oligo-dT's (2.0  $\mu$ L, 100  $\mu$ M) were combined in an RNase-free PCR tube. The tube was incubated at 65 °C for 2 minutes and then chilled on ice for 1 minute. M MuLV Reverse Transcriptase 10x Reaction Buffer (2.0  $\mu$ L), dNTP mix (2.0  $\mu$ L, 10 mM), DTT (2.0  $\mu$ L, 100 mM), RNase Inhibitor (0.5  $\mu$ L), and M MuLV Reverse Transcriptase (1.0  $\mu$ L) were added to the sample giving a total volume of 20.0  $\mu$ L. The tubes were briefly mixed and then incubated at 37 °C for 60 minutes, then 85 °C for 5 minutes to terminate the reaction. The tubes were allowed to sit on ice for 1 minute, and stored at -80 °C.

### **RT-PCR**

The following primers were designed to evaluate LBP-3, K02D7.1, and PMP-3 mRNA levels. PMP-3 was used a control because of its unusually stable expression levels, with little variation between adults, dauer, and L3 larvae, or between wild-type and *daf-2* or *daf-16* mutants. For each gene, the primers were prepared as a mixture of both the forward and reverse primer (10 $\mu$ M each) in DEPC- water.

***lbp-3 forward:*** 5'-GCTGCTAAAGGAGTGAGCT-3'

***lbp-3 reverse:*** 5'-CCATTGTTGACCATTTTCATGAC-3'

***pmp-3 forward:*** 5'-GGCTAACTTATGAAAGTTCCG-3'

***pmp-3 reverse:*** 5'-GATGAGTGACTCCAGCAAGT-3'

***K02D7.1 forward:*** 5'-CAATTCACCAACCAACGCTG-3'

***K02D7.1 reverse:*** 5'-TGAACCGATACAAATCGGGC-3'

For each sample, DEPC-water (16.8  $\mu$ L), 5x HF Buffer (5.0  $\mu$ L), primer mix (1.50  $\mu$ L), cDNA (1.0  $\mu$ L), dNTPs (0.5  $\mu$ L, 10 mM), and Phusion polymerase (0.25  $\mu$ L). The following PCR conditions were used:

30 cycles					
Initial	Denature	Anneal	Elongation	Final	
95 °C	95 °C	55 °C	68 °C	72 °C	4 °C
2 mins	15 sec	15 sec	30 sec	10 mins	End

Xylene cyanol (5.0  $\mu$ L) was added to the samples and each sample (5.0  $\mu$ L) and the Tri-Dye 100 bp DNA ladder were loaded onto a 2% agarose gel. The gel was run at 155 volts for 15 mins and then visualized under UV light.

## References

1. Olsen, A.; Vantipalli, M. C.; Lithgow, G. J., Using *Caenorhabditis elegans* as a model for aging and age-related diseases. *Annals of the New York Academy of Sciences* **2006**, *1067*, 120-8.
2. Johnson, T. E.; Mitchell, D. H.; Kline, S.; Kemal, R.; Foy, J., Arresting development arrests aging in the nematode *Caenorhabditis elegans*. *Mechanisms of ageing and development* **1984**, *28* (1), 23-40.
3. Cassada, R. C.; Russell, R. L., The dauerlarva, a post-embryonic developmental variant of the nematode *Caenorhabditis elegans*. *Developmental biology* **1975**, *46* (2), 326-42.

4. Riddle, D. L.; Blumenthal, T.; Meyer, B. J.; Priess, J. R., Introduction to *C. elegans*. In *C. elegans II*, 2nd ed.; Riddle, D. L.; Blumenthal, T.; Meyer, B. J.; Priess, J. R., Eds. Cold Spring Harbor (NY), 1997.
5. Jorgensen, E. M.; Mango, S. E., The art and design of genetic screens: *Caenorhabditis elegans*. *Nature reviews. Genetics* **2002**, *3* (5), 356-69.
6. Patterson, G. I.; Padgett, R. W., TGF beta-related pathways. Roles in *Caenorhabditis elegans* development. *Trends in genetics : TIG* **2000**, *16* (1), 27-33.
7. Thomas, J. H.; Birnby, D. A.; Vowels, J. J., Evidence for parallel processing of sensory information controlling dauer formation in *Caenorhabditis elegans*. *Genetics* **1993**, *134* (4), 1105-17.
8. Kenyon, C., The first long-lived mutants: discovery of the insulin/IGF-1 pathway for ageing. *Philosophical transactions of the Royal Society of London. Series B, Biological sciences* **2011**, *366* (1561), 9-16.
9. Nemoto, S.; Finkel, T., Ageing and the mystery at Arles. *Nature* **2004**, *429* (6988), 149-52.
10. Chen, A. T.; Guo, C.; Dumas, K. J.; Ashrafi, K.; Hu, P. J., Effects of *Caenorhabditis elegans* *sgk-1* mutations on lifespan, stress resistance, and DAF-16/FoxO regulation. *Aging cell* **2013**, *12* (5), 932-40.
11. Dwyer, D. S.; Aamodt, E. J., Insulin/IGF-1 signaling, including class II/III PI3Ks, beta-arrestin and SGK-1, is required in *C. elegans* to maintain pharyngeal muscle performance during starvation. *PloS one* **2013**, *8* (5), e63851.

12. Hertweck, M.; Gobel, C.; Baumeister, R., C. elegans SGK-1 is the critical component in the Akt/PKB kinase complex to control stress response and life span. *Developmental cell* **2004**, *6* (4), 577-88.
13. Padmanabhan, S.; Mukhopadhyay, A.; Narasimhan, S. D.; Tesz, G.; Czech, M. P.; Tissenbaum, H. A., A PP2A regulatory subunit regulates C. elegans insulin/IGF-1 signaling by modulating AKT-1 phosphorylation. *Cell* **2009**, *136* (5), 939-51.
14. Kwon, E. S.; Narasimhan, S. D.; Yen, K.; Tissenbaum, H. A., A new DAF-16 isoform regulates longevity. *Nature* **2010**, *466* (7305), 498-502.
15. Mukhopadhyay, A.; Oh, S. W.; Tissenbaum, H. A., Worming pathways to and from DAF-16/FOXO. *Experimental gerontology* **2006**, *41* (10), 928-34.
16. Yen, K.; Narasimhan, S. D.; Tissenbaum, H. A., DAF-16/Forkhead box O transcription factor: many paths to a single Fork(head) in the road. *Antioxidants & redox signaling* **2011**, *14* (4), 623-34.
17. Clancy, D. J.; Gems, D.; Harshman, L. G.; Oldham, S.; Stocker, H.; Hafen, E.; Leevers, S. J.; Partridge, L., Extension of life-span by loss of CHICO, a Drosophila insulin receptor substrate protein. *Science* **2001**, *292* (5514), 104-6.
18. Tatar, M.; Kopelman, A.; Epstein, D.; Tu, M. P.; Yin, C. M.; Garofalo, R. S., A mutant Drosophila insulin receptor homolog that extends life-span and impairs neuroendocrine function. *Science* **2001**, *292* (5514), 107-10.
19. Kaeberlein, M.; Powers, R. W., 3rd; Steffen, K. K.; Westman, E. A.; Hu, D.; Dang, N.; Kerr, E. O.; Kirkland, K. T.; Fields, S.; Kennedy, B. K., Regulation of yeast replicative life span by TOR and Sch9 in response to nutrients. *Science* **2005**, *310* (5751), 1193-6.

20. van Heemst, D., Insulin, IGF-1 and longevity. *Aging and disease* **2010**, *1* (2), 147-57.
21. Blucher, M.; Kahn, B. B.; Kahn, C. R., Extended longevity in mice lacking the insulin receptor in adipose tissue. *Science* **2003**, *299* (5606), 572-4.
22. Pawlikowska, L.; Hu, D.; Huntsman, S.; Sung, A.; Chu, C.; Chen, J.; Joyner, A. H.; Schork, N. J.; Hsueh, W. C.; Reiner, A. P.; Psaty, B. M.; Atzmon, G.; Barzilai, N.; Cummings, S. R.; Browner, W. S.; Kwok, P. Y.; Ziv, E.; Study of Osteoporotic, F., Association of common genetic variation in the insulin/IGF1 signaling pathway with human longevity. *Aging cell* **2009**, *8* (4), 460-72.
23. van Heemst, D.; Beekman, M.; Mooijaart, S. P.; Heijmans, B. T.; Brandt, B. W.; Zwaan, B. J.; Slagboom, P. E.; Westendorp, R. G., Reduced insulin/IGF-1 signalling and human longevity. *Aging cell* **2005**, *4* (2), 79-85.
24. Kojima, T.; Kamei, H.; Aizu, T.; Arai, Y.; Takayama, M.; Nakazawa, S.; Ebihara, Y.; Inagaki, H.; Masui, Y.; Gondo, Y.; Sakaki, Y.; Hirose, N., Association analysis between longevity in the Japanese population and polymorphic variants of genes involved in insulin and insulin-like growth factor 1 signaling pathways. *Experimental gerontology* **2004**, *39* (11-12), 1595-8.
25. Anselmi, C. V.; Malovini, A.; Roncarati, R.; Novelli, V.; Villa, F.; Condorelli, G.; Bellazzi, R.; Puca, A. A., Association of the FOXO3A locus with extreme longevity in a southern Italian centenarian study. *Rejuvenation research* **2009**, *12* (2), 95-104.
26. Flachsbart, F.; Caliebe, A.; Kleindorp, R.; Blanche, H.; von Eller-Eberstein, H.; Nikolaus, S.; Schreiber, S.; Nebel, A., Association of FOXO3A variation with human

longevity confirmed in German centenarians. *Proceedings of the National Academy of Sciences of the United States of America* **2009**, *106* (8), 2700-5.

27. Li, Y.; Wang, W. J.; Cao, H.; Lu, J.; Wu, C.; Hu, F. Y.; Guo, J.; Zhao, L.; Yang, F.; Zhang, Y. X.; Li, W.; Zheng, G. Y.; Cui, H.; Chen, X.; Zhu, Z.; He, H.; Dong, B.; Mo, X.; Zeng, Y.; Tian, X. L., Genetic association of FOXO1A and FOXO3A with longevity trait in Han Chinese populations. *Human molecular genetics* **2009**, *18* (24), 4897-904.

28. Willcox, B. J.; Donlon, T. A.; He, Q.; Chen, R.; Grove, J. S.; Yano, K.; Masaki, K. H.; Willcox, D. C.; Rodriguez, B.; Curb, J. D., FOXO3A genotype is strongly associated with human longevity. *Proceedings of the National Academy of Sciences of the United States of America* **2008**, *105* (37), 13987-92.

29. Kenyon, C.; Chang, J.; Gensch, E.; Rudner, A.; Tabtiang, R., A *C. elegans* mutant that lives twice as long as wild type. *Nature* **1993**, *366* (6454), 461-4.

30. Hanover, J. A.; Forsythe, M. E.; Hennessey, P. T.; Brodigan, T. M.; Love, D. C.; Ashwell, G.; Krause, M., A *Caenorhabditis elegans* model of insulin resistance: altered macronutrient storage and dauer formation in an OGT-1 knockout. *Proceedings of the National Academy of Sciences of the United States of America* **2005**, *102* (32), 11266-71.

31. Barsyte, D.; Lovejoy, D. A.; Lithgow, G. J., Longevity and heavy metal resistance in *daf-2* and *age-1* long-lived mutants of *Caenorhabditis elegans*. *Faseb J* **2001**, *15* (3), 627-634.

32. Honda, Y.; Honda, S., The *daf-2* gene network for longevity regulates oxidative stress resistance and Mn-superoxide dismutase gene expression in *Caenorhabditis elegans*. *Faseb J* **1999**, *13* (11), 1385-1393.

33. Walker, G. A.; White, T. M.; McColl, G.; Jenkins, N. L.; Babich, S.; Candido, E. P. M.; Johnson, T. E.; Lithgow, G. J., Heat shock protein accumulation is upregulated in a long-lived mutant of *Caenorhabditis elegans*. *J Gerontol a-Biol* **2001**, *56* (7), B281-B287.
34. Jensen, V. L.; Gallo, M.; Riddle, D. L., Targets of DAF-16 involved in *Caenorhabditis elegans* adult longevity and dauer formation. *Experimental gerontology* **2006**, *41* (10), 922-7.
35. Lamitina, S. T.; Strange, K., Transcriptional targets of DAF-16 insulin signaling pathway protect *C. elegans* from extreme hypertonic stress. *American journal of physiology. Cell physiology* **2005**, *288* (2), C467-74.
36. Murphy, C. T.; McCarroll, S. A.; Bargmann, C. I.; Fraser, A.; Kamath, R. S.; Ahringer, J.; Li, H.; Kenyon, C., Genes that act downstream of DAF-16 to influence the lifespan of *Caenorhabditis elegans*. *Nature* **2003**, *424* (6946), 277-83.
37. Oh, S. W.; Mukhopadhyay, A.; Dixit, B. L.; Raha, T.; Green, M. R.; Tissenbaum, H. A., Identification of direct DAF-16 targets controlling longevity, metabolism and diapause by chromatin immunoprecipitation. *Nature genetics* **2006**, *38* (2), 251-7.
38. Tullet, J. M., DAF-16 target identification in *C. elegans*: past, present and future. *Biogerontology* **2015**, *16* (2), 221-34.
39. Yu, R. X.; Liu, J.; True, N.; Wang, W., Identification of direct target genes using joint sequence and expression likelihood with application to DAF-16. *PloS one* **2008**, *3* (3), e1821.
40. Depuydt, G.; Xie, F.; Petyuk, V. A.; Shanmugam, N.; Smolders, A.; Dhondt, I.; Brewer, H. M.; Camp, D. G.; Smith, R. D.; Braeckman, B. P., Reduced insulin/IGF-1

signaling and dietary restriction inhibit translation but preserve muscle mass in *Caenorhabditis elegans*. *Molecular & cellular proteomics : MCP* **2013**.

41. Dong, M. Q.; Venable, J. D.; Au, N.; Xu, T.; Park, S. K.; Cociorva, D.; Johnson, J. R.; Dillin, A.; Yates, J. R., 3rd, Quantitative mass spectrometry identifies insulin signaling targets in *C. elegans*. *Science* **2007**, *317* (5838), 660-3.

42. Pace, N. J.; Weerapana, E., Diverse functional roles of reactive cysteines. *ACS chemical biology* **2013**, *8* (2), 283-96.

43. Weerapana, E.; Wang, C.; Simon, G. M.; Richter, F.; Khare, S.; Dillon, M. B.; Bachovchin, D. A.; Mowen, K.; Baker, D.; Cravatt, B. F., Quantitative reactivity profiling predicts functional cysteines in proteomes. *Nature* **2010**, *468* (7325), 790-5.

44. Couvertier, S. M.; Zhou, Y.; Weerapana, E., Chemical-proteomic strategies to investigate cysteine posttranslational modifications. *Biochimica et biophysica acta* **2014**, *1844* (12), 2315-2330.

45. Hsu, A. L.; Murphy, C. T.; Kenyon, C., Regulation of aging and age-related disease by DAF-16 and heat-shock factor. *Science* **2003**, *300* (5622), 1142-5.

46. Zarse, K.; Schmeisser, S.; Groth, M.; Priebe, S.; Beuster, G.; Kuhlow, D.; Guthke, R.; Platzer, M.; Kahn, C. R.; Ristow, M., Impaired insulin/IGF1 signaling extends life span by promoting mitochondrial L-proline catabolism to induce a transient ROS signal. *Cell metabolism* **2012**, *15* (4), 451-65.

47. Ayyadevara, S.; Dandapat, A.; Singh, S. P.; Siegel, E. R.; Shmookler Reis, R. J.; Zimniak, L.; Zimniak, P., Life span and stress resistance of *Caenorhabditis elegans* are differentially affected by glutathione transferases metabolizing 4-hydroxynon-2-enal. *Mechanisms of ageing and development* **2007**, *128* (2), 196-205.

48. Kumsta, C.; Thamsen, M.; Jakob, U., Effects of oxidative stress on behavior, physiology, and the redox thiol proteome of *Caenorhabditis elegans*. *Antioxidants & redox signaling* **2011**, *14* (6), 1023-37.
49. Qian, Y.; Martell, J.; Pace, N. J.; Ballard, T. E.; Johnson, D. S.; Weerapana, E., An isotopically tagged azobenzene-based cleavable linker for quantitative proteomics. *Chembiochem : a European journal of chemical biology* **2013**, *14* (12), 1410-4.
50. Giles, N. M.; Giles, G. I.; Jacob, C., Multiple roles of cysteine in biocatalysis. *Biochemical and biophysical research communications* **2003**, *300* (1), 1-4.
51. Rostovtsev, V. V.; Green, L. G.; Fokin, V. V.; Sharpless, K. B., A stepwise Huisgen cycloaddition process: copper(I)-catalyzed regioselective "ligation" of azides and terminal alkynes. *Angewandte Chemie* **2002**, *41* (14), 2596-9.
52. McElwee, J.; Bubb, K.; Thomas, J. H., Transcriptional outputs of the *Caenorhabditis elegans* forkhead protein DAF-16. *Aging cell* **2003**, *2* (2), 111-21.
53. McElwee, J. J.; Schuster, E.; Blanc, E.; Thomas, J. H.; Gems, D., Shared transcriptional signature in *Caenorhabditis elegans* Dauer larvae and long-lived *daf-2* mutants implicates detoxification system in longevity assurance. *The Journal of biological chemistry* **2004**, *279* (43), 44533-43.
54. Fischer, M.; Regitz, C.; Kull, R.; Boll, M.; Wenzel, U., Vitellogenins increase stress resistance of *Caenorhabditis elegans* after *Photorhabdus luminescens* infection depending on the steroid-signaling pathway. *Microbes and infection / Institut Pasteur* **2013**, *15* (8-9), 569-78.
55. Lee, J. Y.; Kim, C.; Kim, J.; Park, C., DJR-1.2 of *Caenorhabditis elegans* is induced by DAF-16 in the dauer state. *Gene* **2013**, *524* (2), 373-6.

56. Yuan, Y.; Kadiyala, C. S.; Ching, T. T.; Hakimi, P.; Saha, S.; Xu, H.; Yuan, C.; Mullangi, V.; Wang, L.; Fivenson, E.; Hanson, R. W.; Ewing, R.; Hsu, A. L.; Miyagi, M.; Feng, Z., Enhanced energy metabolism contributes to the extended life span of calorie-restricted *Caenorhabditis elegans*. *The Journal of biological chemistry* **2012**, *287* (37), 31414-26.
57. DePina, A. S.; Iser, W. B.; Park, S. S.; Maudsley, S.; Wilson, M. A.; Wolkow, C. A., Regulation of *Caenorhabditis elegans* vitellogenesis by DAF-2/IIS through separable transcriptional and posttranscriptional mechanisms. *BMC physiology* **2011**, *11*, 11.
58. Bonifati, V.; Rizzu, P.; van Baren, M. J.; Schaap, O.; Breedveld, G. J.; Krieger, E.; Dekker, M. C.; Squitieri, F.; Ibanez, P.; Joosse, M.; van Dongen, J. W.; Vanacore, N.; van Swieten, J. C.; Brice, A.; Meco, G.; van Duijn, C. M.; Oostra, B. A.; Heutink, P., Mutations in the DJ-1 gene associated with autosomal recessive early-onset parkinsonism. *Science* **2003**, *299* (5604), 256-9.
59. Cornejo Castro, E. M.; Waak, J.; Weber, S. S.; Fiesel, F. C.; Oberhettinger, P.; Schutz, M.; Autenrieth, I. B.; Springer, W.; Kahle, P. J., Parkinson's disease-associated DJ-1 modulates innate immunity signaling in *Caenorhabditis elegans*. *J Neural Transm* **2010**, *117* (5), 599-604.
60. Li, X.; Matilainen, O.; Jin, C.; Glover-Cutter, K. M.; Holmberg, C. I.; Blackwell, T. K., Specific SKN-1/Nrf stress responses to perturbations in translation elongation and proteasome activity. *PLoS genetics* **2011**, *7* (6), e1002119.
61. Curran, S. P.; Ruvkun, G., Lifespan regulation by evolutionarily conserved genes essential for viability. *PLoS genetics* **2007**, *3* (4), e56.

62. Kamath, R. S.; Fraser, A. G.; Dong, Y.; Poulin, G.; Durbin, R.; Gotta, M.; Kanapin, A.; Le Bot, N.; Moreno, S.; Sohrmann, M.; Welchman, D. P.; Zipperlen, P.; Ahringer, J., Systematic functional analysis of the *Caenorhabditis elegans* genome using RNAi. *Nature* **2003**, *421* (6920), 231-7.
63. Hoogewijs, D.; Houthoofd, K.; Matthijssens, F.; Vandesompele, J.; Vanfleteren, J. R., Selection and validation of a set of reliable reference genes for quantitative sod gene expression analysis in *C. elegans*. *BMC molecular biology* **2008**, *9*, 9.
64. Storch, J.; Corsico, B., The emerging functions and mechanisms of mammalian fatty acid-binding proteins. *Annual review of nutrition* **2008**, *28*, 73-95.
65. Plenefisch, J.; Xiao, H.; Mei, B.; Geng, J.; Komuniecki, P. R.; Komuniecki, R., Secretion of a novel class of iFABPs in nematodes: coordinate use of the *Ascaris*/*Caenorhabditis* model systems. *Molecular and biochemical parasitology* **2000**, *105* (2), 223-36.
66. Xu, M.; Joo, H. J.; Paik, Y. K., Novel functions of lipid-binding protein 5 in *Caenorhabditis elegans* fat metabolism. *The Journal of biological chemistry* **2011**, *286* (32), 28111-8.
67. Ogg, S.; Paradis, S.; Gottlieb, S.; Patterson, G. I.; Lee, L.; Tissenbaum, H. A.; Ruvkun, G., The Fork head transcription factor DAF-16 transduces insulin-like metabolic and longevity signals in *C. elegans*. *Nature* **1997**, *389* (6654), 994-9.
68. Brejning, J.; Norgaard, S.; Scholer, L.; Morthorst, T. H.; Jakobsen, H.; Lithgow, G. J.; Jensen, L. T.; Olsen, A., Loss of NDG-4 extends lifespan and stress resistance in *Caenorhabditis elegans*. *Aging cell* **2014**, *13* (1), 156-64.

69. Furuhashi, M.; Hotamisligil, G. S., Fatty acid-binding proteins: role in metabolic diseases and potential as drug targets. *Nature reviews. Drug discovery* **2008**, *7* (6), 489-503.
70. Smathers, R. L.; Petersen, D. R., The human fatty acid-binding protein family: evolutionary divergences and functions. *Human genomics* **2011**, *5* (3), 170-91.
71. Hohoff, C.; Borchers, T.; Rustow, B.; Spener, F.; van Tilbeurgh, H., Expression, purification, and crystal structure determination of recombinant human epidermal-type fatty acid binding protein. *Biochemistry* **1999**, *38* (38), 12229-39.
72. Bennaars-Eiden, A.; Higgins, L.; Hertzfel, A. V.; Kappahn, R. J.; Ferrington, D. A.; Bernlohr, D. A., Covalent modification of epithelial fatty acid-binding protein by 4-hydroxynonenal in vitro and in vivo. Evidence for a role in antioxidant biology. *The Journal of biological chemistry* **2002**, *277* (52), 50693-702.
73. Smathers, R. L.; Fritz, K. S.; Galligan, J. J.; Shearn, C. T.; Reigan, P.; Marks, M. J.; Petersen, D. R., Characterization of 4-HNE modified L-FABP reveals alterations in structural and functional dynamics. *PloS one* **2012**, *7* (6), e38459.
74. Smathers, R. L.; Galligan, J. J.; Shearn, C. T.; Fritz, K. S.; Mercer, K.; Ronis, M.; Orlicky, D. J.; Davidson, N. O.; Petersen, D. R., Susceptibility of L-FABP<sup>-/-</sup> mice to oxidative stress in early-stage alcoholic liver. *Journal of lipid research* **2013**, *54* (5), 1335-45.
75. Bzowska, A.; Kulikowska, E.; Shugar, D., Purine nucleoside phosphorylases: properties, functions, and clinical aspects. *Pharmacology & therapeutics* **2000**, *88* (3), 349-425.

76. Wang, W.; Fridman, A.; Blackledge, W.; Connelly, S.; Wilson, I. A.; Pilz, R. B.; Boss, G. R., The phosphatidylinositol 3-kinase/akt cassette regulates purine nucleotide synthesis. *The Journal of biological chemistry* **2009**, *284* (6), 3521-8.
77. Hamilton, B.; Dong, Y.; Shindo, M.; Liu, W.; Odell, I.; Ruvkun, G.; Lee, S. S., A systematic RNAi screen for longevity genes in *C. elegans*. *Genes & development* **2005**, *19* (13), 1544-55.
78. Stiernagle, T., Maintenance of *C. elegans*. *WormBook : the online review of C. elegans biology* **2006**, 1-11.
79. Weerapana, E.; Speers, A. E.; Cravatt, B. F., Tandem orthogonal proteolysis-activity-based protein profiling (TOP-ABPP)--a general method for mapping sites of probe modification in proteomes. *Nature protocols* **2007**, *2* (6), 1414-25.
80. Eng, J. K.; McCormack, A. L.; Yates, J. R., An approach to correlate tandem mass spectral data of peptides with amino acid sequences in a protein database. *Journal of the American Society for Mass Spectrometry* **1994**, *5* (11), 976-89.
81. Timmons, L.; Court, D. L.; Fire, A., Ingestion of bacterially expressed dsRNAs can produce specific and potent genetic interference in *Caenorhabditis elegans*. *Gene* **2001**, *263* (1-2), 103-12.
82. Timmons, L.; Fire, A., Specific interference by ingested dsRNA. *Nature* **1998**, *395* (6705), 854.

## Chapter 4

### Fluorophosphonate ABPs to Investigate the Roles of Serine Hydrolases in Impaired Insulin Signaling/Lifespan Regulation in *C. elegans*

*C. elegans* RNAi knockdown, lifespan assays, and dauer assays were done with the help of Dr. YongHak Seo at UMass Medical School in Worcester, MA.

## Introduction

As mentioned in chapter 1, serine hydrolases (SHs) make up one of the largest and most diverse enzyme families in nature. SH regulate an assortment of physiological (e.g. blood coagulation, inflammation, angiogenesis) and pathological (emphysema, cancer) processes, however the endogenous functions of many members of this family remain unknown<sup>1</sup>. To identify and characterize their functions, SH activity can be globally profiled with fluorophosphonate (FP) ABPs<sup>2</sup>. Since many SHs are regulated by PTMs such as zymogen cleavage for catalytic activation or inhibitor binding for catalytic inactivation<sup>3</sup>, the use of FP probes are favorable as they specifically and irreversibly react with only catalytically active SHs<sup>2</sup> (the mechanism of serine modification by FP ABPs are detailed in chapter 1, Figure 1-2a).

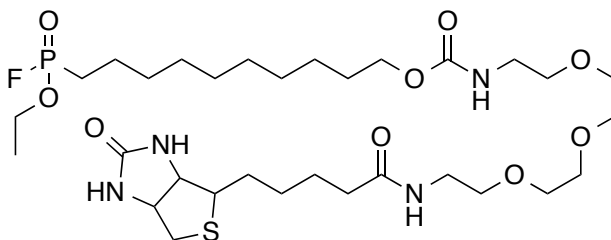


**Figure 4-1.** Structure of the FP-biotin probe.

A biotinylated FP probe (FP-biotin, Figure 4-1) has been used to study novel roles of SH activity in cancer invasiveness<sup>4</sup>, obesity-diabetes<sup>5</sup>, inflammation<sup>6</sup>, and for determining SH inhibitor targets and selectivity<sup>7-9</sup>. In one example, the FP-biotin probe was used to profile the activities of SHs in a panel of human cancer cell lines. These experiments identified a set of enzyme activities, such as KIAA1363, that are consistently up-regulated in more aggressive cancer lines from several different tumor types,

including breast cancer, ovarian cancer, and melanoma<sup>4</sup>. Measuring KIAA1363 mRNA levels across breast tumor samples with varying KIAA1363 activity revealed that its increased activity did not correlate to elevated expression levels<sup>10</sup>, suggesting its activity is regulated by PTM in breast cancer and highlighting the ability of ABPP to distinguish PTM-mediated activity changes that would otherwise go unnoticed by traditional global profiling methods.

### **Investigating serine hydrolase activity changes in impaired insulin/IGF-1 signaling/lifespan regulation in *C. elegans***

Increased fat and altered metabolism are hallmarks of dauer larva as well as the long-lived, dauer-constitutive *daf-2* mutants<sup>11, 12</sup>. The *daf-2* mutant accumulates significantly more triacylglycerol (TAG) in their intestines, the main site of fat storage in *c. elegans*, than the *daf-16;daf-2* in early adulthood<sup>13</sup>. As they age, *daf-2* mutants are able to maintain a high fat content while *daf-16;daf-2* fat levels decrease steadily with age<sup>13</sup>. Decreased fatty acid oxidation is not the cause of increased TAG storage in *daf-2* mutants; multiple studies have demonstrated an increased expression of  $\beta$ -oxidation genes and higher rates of fatty acid oxidation compared to WT worms<sup>14</sup>.  $\beta$ -oxidation is also elevated in non-feeding dauer larva, where their survival depends on the controlled hydrolysis of stored lipids. Dauer larva with reduced AMPK signaling rapidly hydrolyze their lipid stores resulting in a reduction of their lifespan. RNAi-mediated knockdown of the adipose triglyceride lipase (ATGL) homologue blocks the abnormally fast lipid hydrolysis and restores dauer lifespan<sup>15</sup>. Using stable isotope labeling, it was also discovered that adult *daf-2* mutants contain higher levels of *de novo* fatty acids compared

to WT<sup>16</sup>, but do not upregulate fatty acid synthase. Additionally, *daf-2* mutants exhibit a noticeable Eat phenotype (reduced food uptake) that begins in early adulthood<sup>17</sup>.

Taken together, the increased lifespan and fat content in *daf-2* mutants might be a result of the misexpression of genes that ensure dauer larva longevity. It is likely that *daf-2* mutants switch from fat synthesis during development and early adulthood to storage and controlled lipid breakdown for the remainder of life. Metabolic SHs make up nearly half of the SH family, catalyzing the cleavage of ester, amide, or thioester bonds in peptides, proteins, and small molecules (such as lipids)<sup>1</sup>. Lipid synthesis and oxidation are regulated by various nutrient and energy sensing pathways, one of which includes the IIS pathway<sup>14</sup>. While the majority of *C. elegans* SHs are poorly characterized, it is likely that metabolic SHs that play a role in fat storage and metabolism have altered activities when IIS is impaired in *daf-2* mutants. We used the serine hydrolase-targeting FP-biotin ABP to profile changes in SH activity in *daf-2* mutants and investigate the roles of those SHs in lifespan regulation and dauer formation.

### **Chemical-proteomic analysis reveals previously unidentified changes in SH activity between *daf-2* and *daf-16;daf-2* mutants**

Lysates of 4 day old *daf-2* and *daf-16;daf-2* mutants were labeled with 5uM of the FP-biotin probe, excess FP-biotin was removed using a NAP-5 column. Probe-labeled proteins were enriched with streptavidin beads, digested with trypsin, and analyzed by LC/LC-MS/MS. 82 proteins were identified having > 5 spectral counts in at least one sample of either the *daf-2* or *daf-16;daf-2* proteome (Table 4A-1). 12 of those proteins decreased more than 2-fold in the *daf-2* proteome and 36 proteins increased greater than

2-fold. Comparing our data to expression profiles previously observed in the *daf-2* mutant (Dong *et al.*, Murphy *et al.*, and McElee *et al.*), only 6 proteins in our data were identified as having similar changes in *daf-2* mutants: F09C8.1, K12H4.7, Y16B4A.2, and F23B2.12 decreased expression, Y43F8A.3 and R12A1.4 increased expression in *daf-2* mutants, with R12A1.4 (*ges-1*) being identified in all three profiles<sup>18-20</sup>. The remaining 87.5% of the FP-labeled proteins showing a greater than 2-fold change have not been observed previously.

<i>C. elegans</i>			Human Homolog		<i>daff16;daf-2</i>		<i>daf-2</i>		Fold Change	
UniProt ID	Gene ID	Protein Name	UniProt ID	Protein Name	Run 1	Run 2	Run 1	Run 2		
O01300	F09C8.1	Protein F09C8.1	Q6P1J6	Phospholipase B1	159	119	28	22	0.1799	Decreased in <i>daf-2</i>
P34528	K12H4.7	Putative serine protease (K12H4.7)	Q9NQE7	Thymus-specific serine protease	2	8	0	0	0.0000	
Q9NAK4	Y38E10A.7	Protein LIPS-15	G8JLL2	Lysosomal thioesterase PPT2	25	43	17	4	0.3088	
Q17449	B0218.2	Putative fatty acid amide hydrolase (FAAH-1)	O00519	Fatty-acid amide hydrolase 1	131	123	66	23	0.3504	
Q02331	ZK370.4	Uncharacterized NTE family protein ZK370.4	Q6ZV29	Patatin-like phospholipase domain-containing protein 7	33	28	21	6	0.4426	
O45089	F58H7.2	Protein FAAH-3	Q6GMR7	Fatty-acid amide hydrolase	42	55	28	19	0.4845	
Q09991	K10B2.2	Uncharacterized serine carboxypeptidase (ctsa-1)	P10619	Cathepsin A	8	50	21	8	0.5000	
Q17447	B0218.2	Protein FAAH-2	O00519	Fatty-acid amide hydrolase	62	95	44	35	0.5032	
Q21799	R07B7.8	Protein R07B7.8	Q6P1J6-5	Phospholipase B1	34	62	31	25	0.5833	
Q23010	K11G9.1	Protein K11G9.1	P06276	Cholinesterase	82	78	54	55	0.6813	
G5EF86	Y48G10A.1	Protein Y48G10A.1	P10768	S-formylglutathione hydrolase	299	198	396	798	2.4024	Increased in <i>daf-2</i>
Q04457	R12A1.4	Gut esterase 1 ( <i>ges-1</i> )	Q8TDZ9	Brain carboxylesterase	297	710	1227	1511	2.7190	
Q21515	M05B5.4	Protein M05B5.4	Q8NCC3	phospholipase A2	31	38	96	93	2.7391	
Q95QL1	F13H8.11	Protein F13H8.11	Q6P1J6	Phospholipase B1	3	9	34	22	4.6667	
Q21266	K07C11.4	Protein K07C11.4	O00748	Cocaine esterase	12	19	91	59	4.8387	
Q9BIB3	B0464.9	Probable protein phosphatase methyltransferase 1	Q9Y570	Protein phosphatase methyltransferase 1	11	12	39	73	4.8696	
Q09541	F21H12.6	Putative tripeptidyl peptidase II ( <i>tpp-2</i> )	P29144	Tripeptidyl-peptidase 2	8	11	78	34	5.8947	
G5EC56	W07A8.2	Phospholipase A2 ( <i>ipla-3</i> )	O60733	calcium-independent phospholipase A4	0	0	16	9	12.5000	
G4SGU1	M03A1.6	Protein IPLA-1	Q8NEL9	Phospholipase DDHD1	0	0	22	4	13.0000	
Q93251	C23H4.2	Protein C23H4.2	O00748	Cocaine esterase (Carboxylesterase)	0	0	13	13	13.0000	

**Table 4-1.** Top 10 decreased and top 10 increased FP-biotin-labeled proteins in the *daf-2* proteome. Those available in the Ahringer RNAi library are highlighted in green.

Identified in our data but not available in the RNAi library, protein F09C8.1 was among the most decreased in *daf-2* mutants and is paralogous to R07B7.8, also identified to be downregulated in our data (Table 4-1). These proteins are expressed in the intestine and are homologs of human phospholipase B1 (PLB1). PLB1 is also expressed in human

intestines and is involved in hydrolyzing di- and triacylglycerol molecules (Uniprot and Wormbase). LIPS-15 is another protein significantly decreased in *daf-2* mutants. LIPS-15 is largely uncharacterized but predicted to have lipase activity and is a paralog to FIL-1; FIL-1 is involved in lipid catabolism and RNAi knockdown results in persistent high levels of TAG despite extended periods of food depletion. It is very likely that the reduction of these proteins in *daf-2* mutants contributes to their increased TAG levels.

### **RNAi-mediated knockdown of ZK370.4 and C23H4.2 affects lifespan and dauer formation**

We chose 12 proteins to investigate how their RNAi-mediated knock down would affect lifespan and dauer formation in the *daf-2* mutants against a vector-treated control (Figure 4A-1). Proteins were chosen if they had the greatest changes in the *daf-2* proteome, were identified in both replicate runs, had conserved active site serines in their human homologues, and were available in the Ahringer RNAi library (Table 4-1).

Protein ZK370.4 is decreased in *daf-2* and homologous to patatin-like phospholipase domain containing (PNPLA) proteins in humans. The previously mentioned ATGL-1 is another *c. elegans* protein related to the PNPLA family and is involved in TAG hydrolysis as well as regulating the activity of other lipases<sup>21</sup>. RNAi knockdown of ZK370.4 in *daf-2* mutants appears to further extend the median lifespan of 26.5 days in the vector control to 29.0 days, possibly via additional reduction of lipid hydrolysis (Figure 4-2). No dauer assay experiments were performed on ZK370.4 knockdowns, but would be interesting to see if this additional reduction of lipid hydrolysis would also enhance dauer formation.

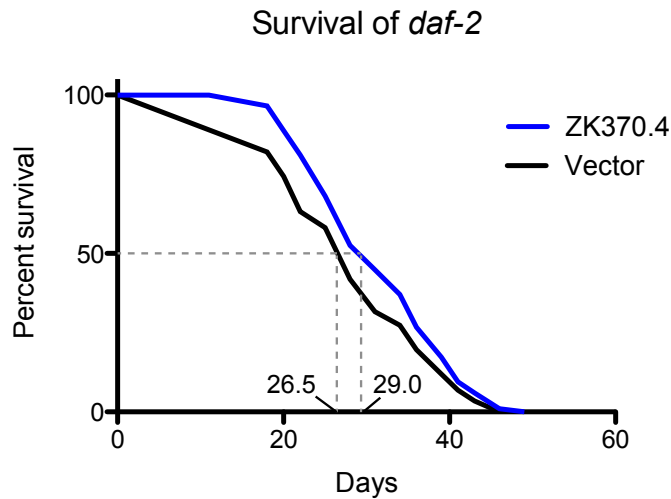


**Figure 4-2.** Lifespan of *daf-2* mutants upon RNAi-mediated knockdown of ZK370.4

Protein M05B5.4, an ortholog of the human gene lecithin-cholesterol acyltransferase (LCAT), tripeptidyl peptidase II (*tpp-2*), and protein C23H4.2, an ortholog of human carboxylesterase 4A (CES4A) have been previously subjected to RNAi and revealed a noticeable decrease in fat content upon knockdown<sup>22</sup>. Our results show that all 3 proteins are upregulated in *daf-2* mutants and appear to play a role in maintaining their elevated fat stores. In humans, CES enzymes play a role in the hydrolysis of various xenobiotics, such as cocaine and heroine, as well as fatty acyl and cholesterol ester metabolism. Compared to the other two proteins involved in TAG storage, RNAi-mediated knockdown of C23H4.2 in *daf-2* mutants moderately reduced lifespan in addition to significantly decreasing dauer formation from 31.6% in the vector control to 6.0% (Figure 4-3). As genes involved in IIS affect both lifespan and dauer formation, C23H4.2 is possibly upregulated by DAF-16 to promote lifespan extension and dauer formation by maintaining TAG storage.

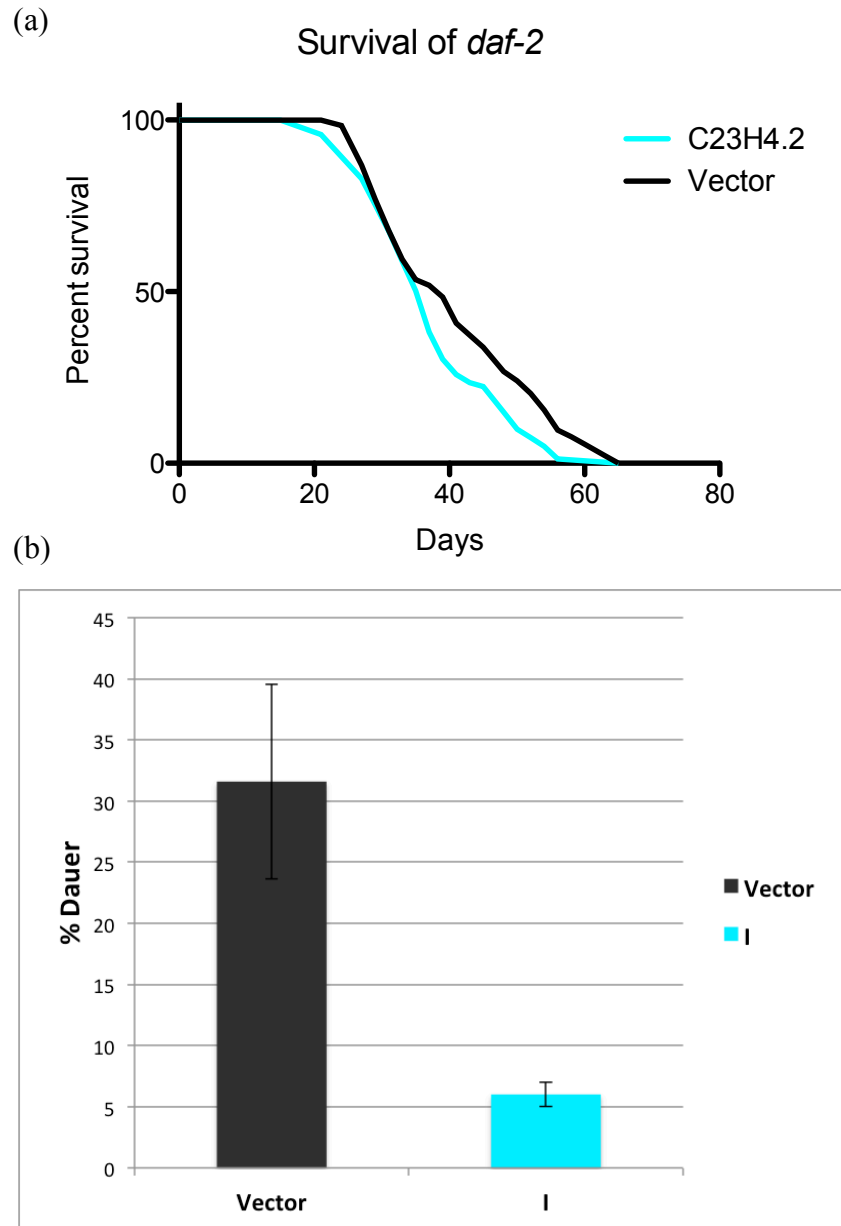


**Figure 4-3.** RNAi-mediated knockdown of C23H4.2 in *daf-2* mutants shows a decrease in (a) lifespan and (b) dauer formation.

## Conclusion

These experiments demonstrate the ability of activity-based protein profiling to study enzyme changes in the context of dysregulated IIS. Over 85% of SHs showing a greater than 2-fold change between *daf-2* and *daf-16-daf-2* mutants had not been identified in previous expression change profiles. We identified 4 lipases (or lipase-related proteins) that were decreased in the *daf-2* mutant, and 3 three proteins with a known role in maintaining TAG stores increased in *daf-2* mutants. Further decreasing the putative lipase ZK370.4 caused an extension in *daf-2* lifespan and knockdown of the upregulated, TAG storage-related protein C23H4.2 shortened lifespan and reduced dauer formation. Overall, our data support previous studies implicating increased fat storage and decreased lipid hydrolysis in *daf-2* longevity, while also potentially identifying novel regulators of these processes.

## Experimental Procedures

### Probe labeling and affinity purification of labeled proteins for ABPP-MudPIT.

*daf-2* and *daf-16;daf-2* proteomes were prepared as described in chapter 3 and lysates were normalized to 3.5 mg/mL. Samples were labeled with FP-biotin (5  $\mu$ M) for 1 h at RT and a NAP-5 column (GE Healthcare) was used to remove the unreacted probe from each sample. The resulting probe-labeled protein was added to a solution of SDS/PBS (1.2% (w/v) final SDS concentration), heated for 5 min at 90 °C, and diluted to a final SDS concentration of 0.2% with PBS. The solutions were incubated with 100  $\mu$ L

streptavidin-agarose beads (Thermo Scientific) at 4 °C for 16 h and at RT for 3 h. The beads were washed with 0.2% SDS in PBS (5 ml), PBS (3 × 5 ml), and water (3 × 5 ml). The beads were pelleted by centrifugation (1,400 × g, 4 °C, 3 min) between washes.

### **On-bead trypsin digestion.**

The washed beads were suspended in 6 M urea in PBS (500 μL) and DTT (10 mM final concentration, diluted from a 20× stock in water) and incubated at 65 °C for 15 min. Iodoacetamide (20 mM final concentration, diluted from a 20× stock in water) was then reacted with the samples at 37 °C for 30 min. After reduction and alkylation, the beads were pelleted by centrifugation (1,400 × g, 4 °C, 3 min) and suspended in 200 μL of 2 M urea, 1 mM CaCl<sub>2</sub> (diluted from a 100× stock in water), and sequencing-grade modified trypsin (2 μg; Promega) in PBS. The digestion was allowed to proceed overnight at 37 °C. The digested peptides were separated from the beads using a Micro Bio-Spin column (BioRad). The beads were washed twice with 50 μL ultrapure water, and formic acid (15 μL) was added to the eluted peptides, which were stored at -20 °C until MS analysis.

### **Liquid chromatography-MS (LC-MS) analysis.**

LC-MS analysis was performed on an LTQ Orbitrap Discovery mass spectrometer (ThermoFisher) coupled to an Agilent 1200 series HPLC. Digests were pressure-loaded onto a 250-μm fused silica desalting column packed with 4 cm of Aqua C18 reverse phase resin (Phenomenex). Digests of affinity-purified samples were loaded in their entirety, whereas unfractionated sample digests were centrifuged (16,873 × g, 4 °C, 2 min) before loading half of each sample onto the column. The peptides were eluted

onto a biphasic column (100- $\mu$ m fused silica with a 5- $\mu$ m tip, packed with 10-cm C18 and 3-cm Partisphere strong cation exchange resin (SCX, Whatman)). The peptides were eluted from the SCX onto the C18 resin and into the mass spectrometer as previously described<sup>20</sup>.

### **MS data analysis.**

The *daf-2* and *daf-16;daf-2* data was searched against the *C. elegans* Uniprot database (UP000001940). A static modification of +57.0215m/z on cysteine was specified to account for iodoacetamide alkylation. The SEQUEST output files generated from the digests were filtered using DTASelect (v2.0.39). MS data files have been deposited to the ProteomeXchange Consortium via the PRIDE partner repository with the data set identifier PXD003000. MS data are presented in the form of spectral counts, which is standard for ABPP-MudPIT analyses with FP-biotin.

RNAi-mediated knockdown experiments were performed as described in chapter 3.

## References

1. Long, J. Z.; Cravatt, B. F., The metabolic serine hydrolases and their functions in mammalian physiology and disease. *Chemical reviews* **2011**, *111* (10), 6022-63.
2. Liu, Y.; Patricelli, M. P.; Cravatt, B. F., Activity-based protein profiling: the serine hydrolases. *Proceedings of the National Academy of Sciences of the United States of America* **1999**, *96* (26), 14694-9.
3. Kidd, D.; Liu, Y.; Cravatt, B. F., Profiling serine hydrolase activities in complex proteomes. *Biochemistry* **2001**, *40* (13), 4005-15.
4. Jessani, N.; Liu, Y.; Humphrey, M.; Cravatt, B. F., Enzyme activity profiles of the secreted and membrane proteome that depict cancer cell invasiveness. *Proceedings of the National Academy of Sciences of the United States of America* **2002**, *99* (16), 10335-40.
5. Dominguez, E.; Galmozzi, A.; Chang, J. W.; Hsu, K. L.; Pawlak, J.; Li, W.; Godio, C.; Thomas, J.; Partida, D.; Niessen, S.; O'Brien, P. E.; Russell, A. P.; Watt, M. J.; Nomura, D. K.; Cravatt, B. F.; Saez, E., Integrated phenotypic and activity-based profiling links Ces3 to obesity and diabetes. *Nature chemical biology* **2014**, *10* (2), 113-21.
6. Szafran, B.; Borazjani, A.; Lee, J. H.; Ross, M. K.; Kaplan, B. L., Lipopolysaccharide suppresses carboxylesterase 2g activity and 2-arachidonoylglycerol hydrolysis: A possible mechanism to regulate inflammation. *Prostaglandins & other lipid mediators* **2015**, *121* (Pt B), 199-206.
7. Bachovchin, D. A.; Ji, T.; Li, W.; Simon, G. M.; Blankman, J. L.; Adibekian, A.; Hoover, H.; Niessen, S.; Cravatt, B. F., Superfamily-wide portrait of serine hydrolase

inhibition achieved by library-versus-library screening. *Proceedings of the National Academy of Sciences of the United States of America* **2010**, *107* (49), 20941-6.

8. Li, W.; Blankman, J. L.; Cravatt, B. F., A functional proteomic strategy to discover inhibitors for uncharacterized hydrolases. *Journal of the American Chemical Society* **2007**, *129* (31), 9594-5.

9. Muelbaier, M.; Drewes, G., Drug selectivity: Running in the family. *Nature chemical biology* **2014**, *10* (8), 608-9.

10. Jessani, N.; Niessen, S.; Wei, B. Q.; Nicolau, M.; Humphrey, M.; Ji, Y.; Han, W.; Noh, D. Y.; Yates, J. R., 3rd; Jeffrey, S. S.; Cravatt, B. F., A streamlined platform for high-content functional proteomics of primary human specimens. *Nature methods* **2005**, *2* (9), 691-7.

11. McElwee, J. J.; Schuster, E.; Blanc, E.; Thornton, J.; Gems, D., Diapause-associated metabolic traits reiterated in long-lived *daf-2* mutants in the nematode *Caenorhabditis elegans*. *Mechanisms of ageing and development* **2006**, *127* (5), 458-72.

12. McKay, R. M.; McKay, J. P.; Avery, L.; Graff, J. M., *C. elegans*: a model for exploring the genetics of fat storage. *Developmental cell* **2003**, *4* (1), 131-42.

13. Depuydt, G.; Xie, F.; Petyuk, V. A.; Smolders, A.; Brewer, H. M.; Camp, D. G., 2nd; Smith, R. D.; Braeckman, B. P., LC-MS proteomics analysis of the insulin/IGF-1-deficient *Caenorhabditis elegans* *daf-2(e1370)* mutant reveals extensive restructuring of intermediary metabolism. *Journal of proteome research* **2014**, *13* (4), 1938-56.

14. Shi, X.; Li, J.; Zou, X.; Greggain, J.; Rodkaer, S. V.; Faergeman, N. J.; Liang, B.; Watts, J. L., Regulation of lipid droplet size and phospholipid composition by stearoyl-CoA desaturase. *Journal of lipid research* **2013**, *54* (9), 2504-14.

15. Branicky, R.; Desjardins, D.; Liu, J. L.; Hekimi, S., Lipid transport and signaling in *Caenorhabditis elegans*. *Developmental dynamics : an official publication of the American Association of Anatomists* **2010**, *239* (5), 1365-77.
16. Perez, C. L.; Van Gilst, M. R., A <sup>13</sup>C isotope labeling strategy reveals the influence of insulin signaling on lipogenesis in *C. elegans*. *Cell metabolism* **2008**, *8* (3), 266-74.
17. Lakowski, B.; Hekimi, S., The genetics of caloric restriction in *Caenorhabditis elegans*. *Proceedings of the National Academy of Sciences of the United States of America* **1998**, *95* (22), 13091-6.
18. Dong, M. Q.; Venable, J. D.; Au, N.; Xu, T.; Park, S. K.; Cociorva, D.; Johnson, J. R.; Dillin, A.; Yates, J. R., 3rd, Quantitative mass spectrometry identifies insulin signaling targets in *C. elegans*. *Science* **2007**, *317* (5838), 660-3.
19. Murphy, C. T.; McCarroll, S. A.; Bargmann, C. I.; Fraser, A.; Kamath, R. S.; Ahringer, J.; Li, H.; Kenyon, C., Genes that act downstream of DAF-16 to influence the lifespan of *Caenorhabditis elegans*. *Nature* **2003**, *424* (6946), 277-83.
20. McElwee, J. J.; Schuster, E.; Blanc, E.; Thomas, J. H.; Gems, D., Shared transcriptional signature in *Caenorhabditis elegans* Dauer larvae and long-lived *daf-2* mutants implicates detoxification system in longevity assurance. *The Journal of biological chemistry* **2004**, *279* (43), 44533-43.
21. Xie, M.; Roy, R., Increased levels of hydrogen peroxide induce a HIF-1-dependent modification of lipid metabolism in AMPK compromised *C. elegans* dauer larvae. *Cell metabolism* **2012**, *16* (3), 322-35.

22. Ashrafi, K.; Chang, F. Y.; Watts, J. L.; Fraser, A. G.; Kamath, R. S.; Ahringer, J.; Ruvkun, G., Genome-wide RNAi analysis of *Caenorhabditis elegans* fat regulatory genes. *Nature* **2003**, *421* (6920), 268-72.

## Chapter 5

### Chemoproteomic Profiling of Host and Pathogen Enzymes Active in Cholera

A significant portion of the work described in this chapter has been published in:

Hatzios, S. K., Abel, S., Martell, J., Hubbard, T., Sasabe, J., Munera, D., Clark, L., Bachovchin, D. A., Qadri, F., Ryan, E. T., Davis, B. M., Weerapana, E. Waldor, M. K. Chemoproteomic profiling of host and pathogen enzymes active in cholera. *Nature chemical biology* **2016**, *12*, 268-274.

I instructed Dr. Stavroula Hatzios on how to perform the FP-biotin labeling, affinity purification, and on-bead tryptic digestion for MS as well as performed the MS experiments and assisted with MS data analysis

## Introduction

During the course of infection, both pathogen and host express, and often secrete, enzymes that actively shape the biochemical landscape of a disease. Enzymes that are active at the host-pathogen interface can be critical for bacterial virulence or the host's response to infection and constitute potential therapeutic targets<sup>1-3</sup>. *V. cholerae*, the Gram-negative bacterium that causes the severe and potentially fatal diarrheal disease cholera, is an extracellular pathogen that proliferates in the small intestine of infected hosts<sup>4</sup>. To identify host and pathogen enzymes active during *V. cholerae* infection, FP-ABPs were used to globally profile secreted serine hydrolase activity in the cecal fluid of *V. cholerae*-infected infant rabbits and human choleric stool.

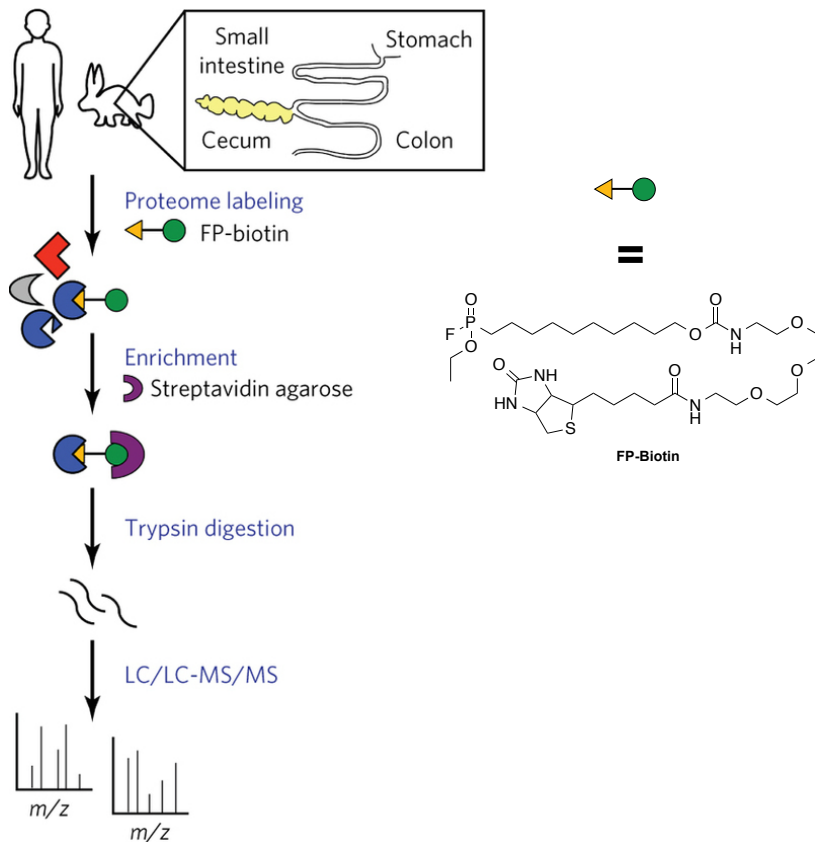


**Figure 5-1.** Workflow of FP-biotin labeling human choleric stool and rabbit cecal fluid with the structure of FP-biotin also shown.

### **ABPP identifies serine hydrolases active in cholera**

Inoculation of rabbits with *V. cholerae* leads to a disease that closely resembles human cholera<sup>5</sup>. Infected rabbits routinely accumulate 0.5–1 ml of cecal fluid, which has a chemical composition similar to that of choleric stool and contains pathogen- and host-secreted products<sup>5</sup>. Cecal fluid and choleric stool isolates were reacted with FP-biotin, enabling affinity purification of active serine hydrolases<sup>6,7</sup> (Figure 5-1). Proteins were purified in parallel from sample supernatants incubated with either FP-biotin or DMSO (to account for nonspecific protein enrichment) and analyzed by LC/LC-MS/MS. A total of 233 and 71 proteins from the cecal fluid of *V. cholerae*-infected rabbits and human choleric stool, respectively, were identified. The majority of human stool-extracted proteins were host enzymes with defined serine hydrolase activity, and many (for example, chymotrypsin-like elastases, trypsins, and pancreatic triacylglycerol lipase) are involved in digestive processes (Table 5-1). Only a few of the rabbit proteins identified have functional annotations in the UniProt database<sup>8</sup>, including the digestive enzyme aminopeptidase N and the bacterial lipopolysaccharide-inactivating enzyme acyloxyacyl hydrolase (Table 5-2). Of the 25 most abundant proteins, ~75% contain predicted serine hydrolase domains, and there was considerable (~45%) overlap between the active enzymes identified in human stool and rabbit cecal fluid.

UniProt ID	Human Proteins	FPB	DMSO
P08217	CELA2A Chymotrypsin-like elastase family member 2A	2751	11
P09093	CELA3A Chymotrypsin-like elastase family member 3A	2077	4
P08861	CELA3B Chymotrypsin-like elastase family member 3B	1702	0
P07478	PRSS2 Trypsin-2	1014	0
Q99895	CTRC Chymotrypsin-C	927	0
P07477	PRSS1 Trypsin-1	777	0
P27487	DPP4 Dipeptidyl peptidase 4	757	0
P54317	PNLIPRP2 Pancreatic lipase-related protein 2	700	0
P08218	CELA2B Chymotrypsin-like elastase family member 2B	612	0
P17538	CTRB1 Chymotrypsinogen B	592	0
P35030	PRSS3 Trypsin-3	160	4
P16233	PNLIP Pancreatic triacylglycerol lipase	127	7
P00326	ADH1C Alcohol dehydrogenase 1C	94	0
P24158	PRTN3 Myeloblastin	66	0
P02768	ALB Serum albumin	58	4
P13798	APEH Acylamino-acid-releasing enzyme	50	0
P08246	ELANE Neutrophil elastase	43	0
P12821	ACE Angiotensin-converting enzyme	39	0
P40313	CTRL Chymotrypsin-like protease CTRL-1	37	0
Q9HAT2	SIAE Sialate O-acetyltransferase	35	0
UniProt ID	<i>V. cholerae</i> Proteins	FPB	DMSO
Q9KVI8	Alkaline serine protease IvaP (VC0157)	2	0

**Table 5-1.** Human and *V. cholerae* proteins enriched with FP-biotin from choleric stool.

Only 14 affinity-purified proteins were detected from *V. cholerae* in cecal fluid and one in human choleric stool (Table 5-3, Table 5-1); of these, 10 contain predicted serine hydrolase domains. Four of these enzymes (VC0157, VCA0812, VCA0803 and VC1200) were detected in nearly all of the cecal fluid samples tested. Additional ABPP analyses indicated that all four of these enzymes were also active in the cell-free supernatants of *V. cholerae* biofilms. VC0157, renamed IvaP, was the most abundant *V. cholerae* protein identified in infected rabbits and biofilms and, notably, was the only active *V. cholerae* enzyme detected in human choleric stool. IvaP, VCA0812, VCA0803 and VC1200 are putative secreted serine proteases: VCA0803 (VesA) and VC1200 (VesB) have trypsin-like activity and VCA0812 contains a trypsin-like domain. These three enzymes are putative substrates of the type II secretion system of *V. cholerae* and play a role in the cleavage of the cholera toxin virulence factor. Relatively little is known about IvaP except that it is a putative alkaline serine protease that contains a subtilisin-

like S8 peptidase domain and several predicted protein domains that are typically sites of post-translational processing that could regulate its activity. Upon investigation of the expression, proteolytic processing, and activity of IvaP in supernatants from various growth conditions, it was discovered that IvaP was indeed processed into several active forms, including autoproteolysis via its catalytic serine (Ser361).

UniProt ID	Rabbit Proteins in Cecal Fluid	Sample A		Sample B		Sample C	
		FPB	DMSO	FPB	DMSO	FPB	DMSO
G1T8X5	Serine protease, putative	1329	0	1628	181	828	0
G1SGH0	Serine protease, putative	1019	11	1213	21	818	0
G1T1C1	Dipeptidyl peptidase 5, putative	855	0	576	7	1224	0
G1U8F6	Serine protease, putative	491	0	524	6	607	0
G1U7Y9	Serine protease, putative	485	0	669	6	311	0
G1U9S2	Serum albumin	225	3	114	2	894	0
G1SQ70	Alpha-2-macroglobulin, putative	187	0	179	2	449	0
G1SIW9	Sialate O-acetyltransferase, putative	149	0	44	0	100	0
G1TAR5	Serine protease, putative	144	0	499	4	693	0
P01840	Ig kappa-b4 chain C region	79	2	168	3	92	2
G1U2Q8	Serine protease, putative	74	0	40	0	51	0
G1THZ6	Uncharacterized protein	69	6	55	3	66	7
G1TEF4	Angiotensin-converting enzyme 2, putative	56	0	11	0	71	0
G1TDD9	Serine protease, putative	52	0	245	0	39	0
G1SMY7	Acylamino-acid-releasing enzyme	47	0	6	0	23	0
G1U1W4	Acylamino-acid-releasing enzyme	47	0	6	0	23	0
G1TOM4	Serine protease, putative	44	0	90	0	27	0
G1SCT1	Prolyl endopeptidase, putative	41	0	7	0	34	0
G1SUW7	Chymotrypsin-like elastase, putative	41	0	6	0	29	0
G1T9G2	Calcium-activated chloride channel regulator 4, putative	28	0	14	0	148	0

**Table 5-2.** Rabbit proteins enriched with FP-biotin from *V. cholerae* infected rabbit cecal fluid.

UniProt ID	<i>V. cholerae</i> Proteins in Rabbit Cecal Fluid	Sample A		Sample B		Sample C	
		FPB	DMSO	FPB	DMSO	FPB	DMSO
Q9KV18	Alkaline serine protease IvaP (VC0157)	76	0	128	0	30	0
Q9KLE3	Serine protease VesA (VCA0803)	13	0	4	0	6	0
Q9KSQ6	Trypsin-like serine protease VesB (VC1200)	12	0	7	0	4	0
Q9KLD4	Leucine aminopeptidase-related protein VCA0812	6	0	8	0	8	0
Q9KUF5	Protease DO VC0566	23	0	4	0	0	0
P01556	Cholera enterotoxin subunit B ctxB	4	0	2	0	0	0
Q9KMOV0	Thermolabile hemolysin VCA0218	8	0	0	0	7	0
Q9KUB9	Putative uncharacterized protein VC0603	11	0	0	0	0	0
Q9KLG1	Arylesterase VCA0783	6	0	0	0	0	0
Q9KQJ6	Putative uncharacterized protein VC2002	4	0	0	0	0	0
Q9KUG7	Protease, insulinase family VC0554	4	0	0	0	0	0
P01555	Cholera enterotoxin subunit A ctxA	3	0	0	0	0	0
P15493	Lipase lipA	0	0	5	0	0	0
Q9KLP3	Chitodextrinase VCA0700	0	0	0	0	2	0

**Table 5-3.** *V. cholerae* proteins enriched with FP-biotin from *V. cholerae* infected rabbit cecal fluid.

## IvaP influences the activity of other serine hydrolases

To determine if IvaP proteolytic activity regulates the activity of other SHs, we compared the FP-Biotin enrichment of SHs in cecal fluid of rabbits infected with either wild-type *V. cholerae* or *V. cholerae* expressing IvaP<sup>S361A</sup>. We identified four *V. cholerae* serine hydrolases, in addition to IvaP, whose activity was higher (>5-fold change in spectral counts,  $P \leq 0.05$ ) in the cecal fluid of rabbits infected with wild-type than in those infected with mutant *V. cholerae* (Table 5-4). These were VCA0812 and VesB; VCA0218, which has phospholipase activity *in vitro*<sup>9</sup>; and VolA (VCA0863) an outer membrane-associated phospholipase that may facilitate bacterial uptake of host-derived fatty acids<sup>9</sup>. Additionally, we identified two rabbit serine hydrolases that were less active in rabbits infected with wild-type *V. cholerae*: kallikrein 1 (KLK1), a trypsin-like peptidase that regulates vascular tone<sup>10</sup>, and cholesterol esterase, a digestive enzyme that hydrolyzes triglycerides and other lipid esters in the intestine<sup>11</sup> (Table 5-4). Collectively, these findings suggest IvaP influences the activity of other pathogen-secreted and host serine hydrolases that may shape the intestinal niche of *V. cholerae*.

UniProt ID	<i>V. cholerae</i> Proteins in Rabbit Cecal Fluid	WT <i>V. cholerae</i>			IvaP S361A		Fold Change	p-value
		A	B	C	A	B		
Q9KVI8	Alkaline serine protease IvaP (VC0157)	107	68	50	0	0	76	< 0.00004
Q9KLD4	Leucine aminopeptidase-related protein VCA0812	78	21	7	0	0	36.33333	0.00029
Q9KL83	Lipase VolA (VCA0863)	11	2	3	0	0	6.33333	0.02648
Q9KMOV0	Thermolabile hemolysin VCA0218	34	9	0	0	2	7.66667	0.03984
Q9KSQL6	Trypsin-like serine protease VesB (VC1200)	26	9	0	2	0	6.33333	0.04816
UniProt ID	Rabbit Proteins in Rabbit Cecal Fluid	A	B	C	A	B	Fold Change	p-value
A5A2M0	Kallikrein 1	7	2	0	25	16	0.18605	< 0.00004
Q28681	Cholesterol esterase	12	0	0	59	27	0.11364	0.004

**Table 5-4.** Comparison of *V. cholerae* and rabbit proteins enriched from cecal fluid infected with WT and IvaP<sup>S361A</sup> mutant *V. cholerae*.

### ***V. cholerae* proteases alter host protein abundance**

To identify additional secreted and cell-associated bacterial and host proteins present in the context of an infection, we conducted proteomic analyses of unfractionated cecal fluid from rabbits infected with wild-type *V. cholerae* and unfractionated human choleric stool. In the cecal fluid of wild-type–infected rabbits, we detected 1,330 proteins (405 *V. cholerae*, 925 rabbit) with  $\geq 2$  spectral counts. The *V. cholerae* proteins included key contributors to virulence such as both subunits of cholera toxin and TcpA, the major subunit of a pilus that is *V. cholerae*'s principal intestinal colonization factor<sup>4</sup> (Table 5-5). Notably, we did not detect IvaP or the other three *V. cholerae* proteases identified by ABPP in these analyses, which underscores the ability of ABPP to enhance detection of low-abundance enzymes. Host proteins included several rabbit immunoglobulins and hemoglobin subunits; however, the majority of rabbit proteins detected in cecal fluid are uncharacterized. We identified 493 proteins (29 *V. cholerae*, 464 human) in a parallel whole-proteome analysis of human choleric stool, of which 27 *V. cholerae* proteins were also present in cecal fluid (Table 5-6). We also detected immunoglobulins and several digestive proteases (for example, chymotrypsin-like elastases) in the human choleric stool.

UniProt ID	<i>V. cholerae</i> Proteins in Rabbit Cecal Fluid	Biological Replicate 1		Biological Replicate 2	
		TR 1	TR2	TR 1	TR 2
P01555	Cholera enterotoxin subunit A (ctxA)	17	28	10	22
P01556	Cholera enterotoxin subunit B (ctxB)	2	10	42	17
Q60153	Toxin coregulated pilin (tcpA)	113	183	125	72

**Table 5-5.** *V. cholerae* virulence factors identified from unfractionated rabbit cecal fluid.

UniProt ID	<i>V. cholerae</i> Proteins in Unfractionated Human Cholera Stool	TR 1	TR 2
P0C6Q6	Outer membrane protein U	66	34
Q9KV37	Elongation factor Tu-A	12	8
Q9KUZ6	Elongation factor Tu-B	12	8
Q9KUT3	Malate dehydrogenase	8	7
Q9KTZ9	Antioxidant, AhpC/Tsa family	8	5
Q9KTQ6	Accessory colonization factor AcfC	6	6
Q9KNK0	Phosphoenolpyruvate carboxykinase [ATP]	5	4
Q9KQF3	Superoxide dismutase	4	5
Q9KL05	Maltose ABC transporter, periplasmic maltose-binding protein	4	5
P0C6Q3	Phosphoglycerate kinase	4	0
Q9KUS9	50S ribosomal protein L27	4	0
Q9KT14	Oligopeptide ABC transporter, periplasmic oligopeptide-binding protein	0	4
Q9KQT3	30S ribosomal protein S1	0	4
Q9KQB6	Succinyl-CoA ligase [ADP-forming] subunit alpha	3	0
Q9KLJ9	Glycerol kinase	0	3
Q9KUY4	Glucose-6-phosphate isomerase	0	3
Q9KN05	Tryptophanase	2	2
Q9KUN7	Fructose-bisphosphate aldolase, class II	2	2
P0C6Q1	Glutamate-tRNA ligase	2	0
Q9KNR7	60 kDa chaperonin 1	2	0
Q9KNY7	50S ribosomal protein L2	2	0
Q9KSF2	Fumarate hydratase, class I, putative	2	0
Q9KPR1	Outer membrane protein OmpK	2	0
Q9KV31	50S ribosomal protein L7/L12	0	2
Q9KP08	DNA-directed RNA polymerase subunit alpha	0	2
Q9KUR5	Membrane-bound lytic murein transglycosylase C	0	2
Q9KUB8	Aconitate hydratase 2	0	2
Q9KQJ8	Glyceraldehyde 3-phosphate dehydrogenase	0	2
Q9KNS5	Fumarate reductase, flavoprotein subunit	0	2

**Table 5-6.** *V. cholerae* proteins identified from unfractionated human choleric stool. All proteins but the two highlighted in gray were also detected in rabbit cecal fluid.

A  $\Delta$ quad *V. cholerae* mutant was created, which lacks all four secreted proteases active *in vivo* (ivaP, vesA, vesB and VCA0812), to maximize potential protease-dependent phenotypes. Comparative whole-proteome analyses of cecal fluid revealed nine host proteins that were significantly more abundant in rabbits infected with the  $\Delta$ quad mutant than in those infected with wild-type *V. cholerae*, suggesting that these proteins are degraded by one or more of the deleted enzymes; we did not detect any bacterial proteins that were significantly enriched in these mutant samples (Table 5-7).

The host proteins we identified included a putative cathepsin Z protease; the phospholipid-binding protein annexin A1; a putative chymotrypsin-like elastase (serine-type protease) and a galactoside-binding galectin. In addition, we identified an uncharacterized rabbit protein (UniProt G1U048) with 88% amino acid sequence identity to human intelectin, an intestinally secreted D-galactofuranosyl-binding protein<sup>12</sup>. Because galactofuranose is found in a variety of microbial, but not mammalian, glycoconjugates<sup>13</sup>, intelectin has been proposed to facilitate mucosal adhesion and/or phagocytic uptake of bacterial pathogens in the host and may therefore be a rational target for secreted bacterial proteases. Our proteomic data suggest that secreted *V. cholerae* serine proteases regulate host factors that may modulate pathogen metabolism and interactions with the infected host.

UniProt ID	Rabbit Proteins in Unfractionated Cecal Fluid	WT <i>V. cholerae</i>				$\Delta$ quad <i>V. cholerae</i>				Fold Change
		Bio Rep 1		Bio Rep 2		Bio Rep 1		Bio Rep 2		
		TR 1	TR 2	TR 1	TR 2	TR 1	TR 2	TR 1	TR 2	
G1SPI0	Nucleoside transport protein, putative (SLC28A3)	5	4	0	0	11	18	95	65	12.59745
G1TRH3	Cathepsin Z, putative (CTSZ)	0	0	0	0	6	6	14	16	10.61119
G1TIS5	Annexin A1 (ANXA1)	0	0	0	0	0	10	15	13	10.11268
G1U048	Intelectin, putative	21	20	43	42	97	120	978	558	9.79515
G1T8X5	Chymotrypsin-like elastase, putative	12	18	42	47	168	192	443	345	9.30985
G1TUQ2	Ig kappa chain V region protein, putative	0	0	0	9	18	30	23	19	7.23077
G1TRK9	Uncharacterized protein	0	3	0	0	19	21	4	6	6.87471
G1TVQ8	Olfactomedin-4, putative (OLFM4)	0	0	0	4	3	6	20	16	5.5879
G1TPZ1	Galectin (LGALS1)	2	0	0	0	10	4	7	8	5.5

**Table 5-7.** The nine rabbit proteins identified from unfractionated cecal that were more abundant in the  $\Delta$ quad mutant *V. cholerae*.

### Intelectin binds *V. cholerae* and other enteric bacteria

Human intelectin consists of two isoforms (intelectin-1 and intelectin-2) with 91% amino acid sequence identity<sup>14</sup>. Previous studies have shown that intelectin-1 is constitutively expressed at high levels in the mouse small intestine, whereas expression of intelectin-2 is strongly induced by intestinal nematodes, suggesting its role in the

intestinal innate immune response<sup>15, 16</sup>. Human intelectin-1 has been shown to bind *Mycobacterium bovis* bacillus Calmette–Guérin (BCG)<sup>17</sup> and *Streptococcus pneumoniae*<sup>18</sup> in a Ca<sup>2+</sup>-dependent manner *in vitro*<sup>17</sup>; however, intelectin binding to *V. cholerae* or other enteric bacteria has not been demonstrated. An *in vitro* assay was developed using *V. cholerae* treated with purified human intelectin-1 to assess whether this protein binds *V. cholerae* or other enteric pathogens. It was demonstrated that intelectin binds *V. cholerae* in a Ca<sup>2+</sup>-dependent manner, as well as all other bacteria assayed, including Gram-negative (*Escherichia coli*, *Vibrio parahaemolyticus* and *Salmonella enterica*) and Gram-positive (*Listeria monocytogenes* and *Staphylococcus aureus*) species.

#### ***V. cholerae* proteases decrease intelectin binding *in vivo***

Immunoblot analyses of proteins associated with *V. cholerae* cells isolated from the ceca of infected rabbits suggested that intelectin also binds to *V. cholerae* during infection. Evidence suggested that most intelectin in the ceca of *V. cholerae*-infected rabbits is cell-associated. Bacteria-associated intelectin was analyzed using  $\Delta$ quad *V. cholerae* isolated from infected rabbits. As in our proteomic analyses, which detected greater amounts of cecal intelectin in rabbits infected with  $\Delta$ quad than in those infected with wild-type *V. cholerae*, a consistent and substantial (~4- to 9-fold) higher amount of EDTA-eluted intelectin from  $\Delta$ quad *V. cholerae* than from wild-type bacterial cells was observed. Notably, wild-type and  $\Delta$ quad *V. cholerae* grown *in vitro* showed approximately equal intelectin binding, suggesting that these strains have similar cell surfaces. Collectively, these observations suggest that less intelectin degradation occurs

when the secreted *V. cholerae* serine proteases are absent, and this may, in turn, enable increased intelectin binding to *V. cholerae* cells.

Monitoring the proteolysis of recombinant human intelectin-1 in the presence of cell-free cecal fluid supernatants from rabbits infected with wild-type or  $\Delta$ quad *V. cholerae* was done to determine whether intelectin degradation is enhanced by the *V. cholerae* proteases. Immunoblot analysis revealed that intelectin was degraded more rapidly in cecal fluid from rabbits infected with wild-type *V. cholerae*; however, incubation with either extract induced a nominal decrease in the molecular weight of the protein, and cecal fluid lacking the *V. cholerae* proteases was still capable of degrading intelectin, albeit more slowly. Taken together, these data suggest that the *V. cholerae* proteases accelerate intelectin degradation *in vitro*.

## **Conclusion**

This work demonstrates the use of activity-based proteomics to investigate enzyme-mediated interactions between a pathogen and its host in an animal model of infection. By capturing enzymes active in *V. cholerae*-infected rabbits, we identified four pathogen-secreted proteases that alter the biochemical composition of cecal fluid, decrease the activity of host serine hydrolases, and inhibit bacterial binding by a host-secreted lectin. Our findings highlight the ability of ABPP to dissect complex enzymatic crosstalk at the host-pathogen interface and suggest that application of this approach to other animal models of microbial infection could yield important insights into the underlying enzymology of diverse infectious diseases.

## **Experimental Procedures**

### **Probe labeling and affinity purification of labeled proteins for ABPP-MudPIT.**

Cell-free supernatants from biofilm cultures (300  $\mu$ L, 1 mg/ml), human choleric stool (650  $\mu$ L, 0.25 mg/ml), and cell lysates from exponential- and stationary-phase *V. cholerae* cultures (500  $\mu$ L, 1 mg/ml) were labeled with FP-biotin (5  $\mu$ M) or DMSO for 1 h at RT. Pooled cecal fluid isolates from wild-type *V. cholerae*-infected rabbits (Sample A: 245  $\mu$ L, 0.5 mg/ml; Sample B: 1.9 ml, 0.3 mg/ml; Sample C: 210  $\mu$ L, 0.4 mg/ml) and individual isolates for comparative analyses of wild-type and S361A *V. cholerae*-infected rabbits (450  $\mu$ L, 0.3 mg/ml) were similarly labeled with probe. A NAP-5 column (GE Healthcare) was used to remove the unreacted probe from each sample. The resulting probe-labeled protein was added to a solution of SDS/PBS (1.2% (w/v) final SDS concentration), heated for 5 min at 90 °C, and diluted to a final SDS concentration of 0.2% with PBS. The solutions were incubated with 100  $\mu$ L streptavidin-agarose beads (Thermo Scientific) at 4 °C for 16 h and at RT for 3 h. The beads were washed with 0.2% SDS in PBS (5 ml), PBS (3  $\times$  5 ml), and water (3  $\times$  5 ml). The beads were pelleted by centrifugation (1,400  $\times$  g, 4 °C, 3 min) between washes.

### **On-bead trypsin digestion.**

The washed beads were suspended in 6 M urea in PBS (500  $\mu$ L) and DTT (10 mM final concentration, diluted from a 20 $\times$  stock in water) and incubated at 65 °C for 15 min. Iodoacetamide (20 mM final concentration, diluted from a 20 $\times$  stock in water) was then reacted with the samples at 37 °C for 30 min. After reduction and alkylation, the beads were pelleted by centrifugation (1,400  $\times$  g, 4 °C, 3 min) and suspended in 200  $\mu$ L

of 2 M urea, 1 mM CaCl<sub>2</sub> (diluted from a 100× stock in water), and sequencing-grade modified trypsin (2 µg; Promega) in PBS. The digestion was allowed to proceed overnight at 37 °C. The digested peptides were separated from the beads using a Micro Bio-Spin column (BioRad). The beads were washed twice with 50 µL ultrapure water, and formic acid (15 µL) was added to the eluted peptides, which were stored at −20 °C until MS analysis.

### **In-solution trypsin digestion.**

Unfractionated cecal fluid and human choleric stool samples were vortexed with 1/10 volume of 100% (w/v) trichloroacetic acid in PBS and frozen overnight at −80 °C. Samples were thawed on ice, centrifuged (20,817 × g, 4 °C, 10 min), and washed three times with cold acetone (500 µL). Samples were sonicated and centrifuged (2,655 × g, 4 °C, 10 min) between washes. Acetone-washed pellets were air dried and resuspended by sonication in 100 µL PBS containing 2.4 M urea and 70 mM ammonium bicarbonate, treated with 15 mM DTT, and incubated at 65 °C for 15 min. Iodoacetamide (12.5 mM final concentration) was then reacted with the samples for 30 min at RT. PBS (120 µL) was added to each sample, and protein concentrations were measured using the Pierce Coomassie Plus (Bradford) Assay Kit (Life Technologies). Samples were adjusted to 0.5 mg/ml in PBS and divided into two technical replicates of equal volume (90 µL). Samples were incubated with sequencing-grade modified trypsin (2 µg; Promega) and 1 mM CaCl<sub>2</sub> and digested overnight at 37 °C. Digested peptides were treated with formic acid (5 µL) and centrifuged (100,000 × g, 4 °C, 1 h) to remove any remaining

particulates. Supernatants were transferred to new tubes and stored at  $-20\text{ }^{\circ}\text{C}$  until MS analysis.

### **Liquid chromatography-MS (LC-MS) analysis.**

LC-MS analysis was performed on an LTQ Orbitrap Discovery mass spectrometer (ThermoFisher) coupled to an Agilent 1200 series HPLC. Digests were pressure-loaded onto a 250- $\mu\text{m}$  fused silica desalting column packed with 4 cm of Aqua C18 reverse phase resin (Phenomenex). Digests of affinity-purified samples were loaded in their entirety, whereas unfractionated sample digests were centrifuged ( $16,873 \times g$ ,  $4\text{ }^{\circ}\text{C}$ , 2 min) before loading half of each sample onto the column. The peptides were eluted onto a biphasic column (100- $\mu\text{m}$  fused silica with a 5- $\mu\text{m}$  tip, packed with 10-cm C18 and 3-cm Partisphere strong cation exchange resin (SCX, Whatman)). The peptides were eluted from the SCX onto the C18 resin and into the mass spectrometer as previously described.

### **MS data analysis.**

For the *V. cholerae* data, MS/MS data were searched using the SEQUEST algorithm against a combined rabbit (or human) and *V. cholerae* UniProt database using the *V. cholerae* serotype O1 (strain ATCC 39315/EI Tor Inaba N16961) proteome (UniProt proteome ID UP000000584). A static modification of  $+57.0215m/z$  on cysteine was specified to account for iodoacetamide alkylation. The SEQUEST output files generated from the digests were filtered using DTASelect (v2.0.39). MS data files have been deposited to the ProteomeXchange Consortium via the PRIDE partner repository

with the data set identifier PXD003000. MS data are presented in the form of spectral counts, which is standard for ABPP-MudPIT analyses with FP-biotin.

## References

1. Ivarsson, M. E.; Leroux, J. C.; Castagner, B., Targeting bacterial toxins. *Angewandte Chemie* **2012**, *51* (17), 4024-45.
2. Kilian, M.; Mestecky, J.; Russell, M. W., Defense mechanisms involving Fc-dependent functions of immunoglobulin A and their subversion by bacterial immunoglobulin A proteases. *Microbiological reviews* **1988**, *52* (2), 296-303.
3. Ruiz-Perez, F.; Nataro, J. P., Bacterial serine proteases secreted by the autotransporter pathway: classification, specificity, and role in virulence. *Cellular and molecular life sciences : CMLS* **2014**, *71* (5), 745-70.
4. Ritchie, J. M.; Waldor, M. K., *Vibrio cholerae* interactions with the gastrointestinal tract: lessons from animal studies. *Current topics in microbiology and immunology* **2009**, *337*, 37-59.
5. Ritchie, J. M.; Rui, H.; Bronson, R. T.; Waldor, M. K., Back to the future: studying cholera pathogenesis using infant rabbits. *mBio* **2010**, *1* (1).
6. Kidd, D.; Liu, Y.; Cravatt, B. F., Profiling serine hydrolase activities in complex proteomes. *Biochemistry* **2001**, *40* (13), 4005-15.
7. Bachovchin, D. A.; Ji, T.; Li, W.; Simon, G. M.; Blankman, J. L.; Adibekian, A.; Hoover, H.; Niessen, S.; Cravatt, B. F., Superfamily-wide portrait of serine hydrolase

- inhibition achieved by library-versus-library screening. *Proceedings of the National Academy of Sciences of the United States of America* **2010**, *107* (49), 20941-6.
8. UniProt, C., UniProt: a hub for protein information. *Nucleic acids research* **2015**, *43* (Database issue), D204-12.
  9. Fiore, A. E.; Michalski, J. M.; Russell, R. G.; Sears, C. L.; Kaper, J. B., Cloning, characterization, and chromosomal mapping of a phospholipase (lecithinase) produced by *Vibrio cholerae*. *Infection and immunity* **1997**, *65* (8), 3112-7.
  10. Lundwall, A.; Brattsand, M., Kallikrein-related peptidases. *Cellular and molecular life sciences : CMLS* **2008**, *65* (13), 2019-38.
  11. Holmes, R. S.; Cox, L. A., Comparative Structures and Evolution of Vertebrate Carboxyl Ester Lipase (CEL) Genes and Proteins with a Major Role in Reverse Cholesterol Transport. *Cholesterol* **2011**, *2011*, 781643.
  12. Tsuji, S.; Uehori, J.; Matsumoto, M.; Suzuki, Y.; Matsuhisa, A.; Toyoshima, K.; Seya, T., Human intelectin is a novel soluble lectin that recognizes galactofuranose in carbohydrate chains of bacterial cell wall. *The Journal of biological chemistry* **2001**, *276* (26), 23456-63.
  13. Pedersen, L. L.; Turco, S. J., Galactofuranose metabolism: a potential target for antimicrobial chemotherapy. *Cellular and molecular life sciences : CMLS* **2003**, *60* (2), 259-66.
  14. Wrackmeyer, U.; Hansen, G. H.; Seya, T.; Danielsen, E. M., Intelectin: a novel lipid raft-associated protein in the enterocyte brush border. *Biochemistry* **2006**, *45* (30), 9188-97.

15. Pemberton, A. D.; Knight, P. A.; Gamble, J.; Colledge, W. H.; Lee, J. K.; Pierce, M.; Miller, H. R., Innate BALB/c enteric epithelial responses to *Trichinella spiralis*: inducible expression of a novel goblet cell lectin, intelectin-2, and its natural deletion in C57BL/10 mice. *Journal of immunology* **2004**, *173* (3), 1894-901.
16. Voehringer, D.; Stanley, S. A.; Cox, J. S.; Completo, G. C.; Lowary, T. L.; Locksley, R. M., *Nippostrongylus brasiliensis*: identification of intelectin-1 and -2 as Stat6-dependent genes expressed in lung and intestine during infection. *Experimental parasitology* **2007**, *116* (4), 458-66.
17. Tsuji, S.; Yamashita, M.; Hoffman, D. R.; Nishiyama, A.; Shinohara, T.; Ohtsu, T.; Shibata, Y., Capture of heat-killed *Mycobacterium bovis* bacillus Calmette-Guerin by intelectin-1 deposited on cell surfaces. *Glycobiology* **2009**, *19* (5), 518-26.
18. Wesener, D. A.; Wangkanont, K.; McBride, R.; Song, X.; Kraft, M. B.; Hodges, H. L.; Zarling, L. C.; Splain, R. A.; Smith, D. F.; Cummings, R. D.; Paulson, J. C.; Forest, K. T.; Kiessling, L. L., Recognition of microbial glycans by human intelectin-1. *Nature structural & molecular biology* **2015**, *22* (8), 603-10.

## Chapter 6

### Chemical Proteomic Platform to Identify Citrullinated Proteins

A significant portion of the work described in this chapter has been published in:

Lewallen, D.M., Bicker, K.L., Subramanian, V., Clancy, K.W., Slade, D.J., Martell, J., Dreyton, C.J., Sokolove, J., Weerapana, E., Thompson, P.R. Chemical Proteomic Platform To Identify Citrullinated Proteins. *ACS Chem. Biol.* **2015**, *10*, 2520-2528.

Sample preparation, including probe labeling and precipitation, were performed in the Thompson Lab. All mass-spectrometry experiments and data analysis were performed by me.

## Introduction

The importance of protein citrullination to human pathology was first recognized in rheumatoid arthritis<sup>1</sup> (RA, which will be discussed further later in this chapter), and more recent studies indicate that dysregulated citrullination is a general feature of autoimmunity and cancer<sup>2-5</sup>. This post-translational modification is catalyzed by the protein arginine deiminases (PADs), a small family of calcium-dependent enzymes that hydrolyze the positively-charged side chain guanidinium of arginine residues to form the noncoded, neutral amino acid citrulline<sup>6</sup>. This change in net charge can induce conformational changes that can affect the structure and activity of the modified protein<sup>7</sup>. Citrullination has an important role in the normal function of the immune system, skin keratinization, the insulation of neurons, and its essential role in gene regulation<sup>8</sup>. How PADs contribute to such a diverse set of pathologies is unclear, but one common feature of this enzyme family is their ability to citrullinate histones. Histone citrullination is known to modulate the chromatin architecture with consequent downstream effects on gene transcription, differentiation, and pluripotency<sup>9-11</sup>. For example, PAD4 citrullinates histones H3 and H4, and this activity is generally associated with increased expression of growth-promoting genes and decreased expression of growth-inhibiting genes<sup>10, 12</sup>.

In addition to modulating gene expression, the histone modifying activity of PADs is required for the formation of neutrophil and macrophage extracellular traps (NETs and METs)<sup>5, 13, 14</sup>. For example, in response to stimuli of bacterial or immunological origin, neutrophils decondense and externalize their chromatin to form web-like structures to capture pathogens. PAD4 activity appears to be critical for this process, as PAD4<sup>-/-</sup> knockout mice do not form NETs and PAD inhibitors, e.g., Cl-

amidine and BB-CI-amidine<sup>15,16</sup>, block this pro-inflammatory form of programmed cell death. Although NET formation is a normal and essential component of the innate immune response<sup>17</sup>, aberrantly increased NET formation is a hallmark of RA<sup>18</sup>, lupus<sup>19</sup>, colitis<sup>20</sup>, atherosclerosis<sup>21</sup>, and a variety of cancers<sup>22</sup>. As such, aberrant NET formation is thought to be a key driver of these diseases. The specific protein substrates targeted by PADs in these diseases remain mostly unknown. Identifying these proteins will not only further our understanding of how PADs contribute to disease pathology but also lay the foundation for identifying novel biomarkers to expedite disease diagnosis and treatment. Although a number of citrulline-specific antibodies and proteomic methods have been described<sup>23-26</sup>, these methods suffer from a number of limitations, most especially the need to chemically derivatize citrullinated proteins after transfer to a membrane in western blotting applications or post-tryptic digestion for proteomic detection, which necessitates protein identifications based on a single peptide.

Building on the recent development of a fluorescent citrulline-specific probe (i.e., rhodamine-conjugated phenyl- glyoxal, Rh-PG) that is used to visualize protein citrullination<sup>27</sup>, a biotin-conjugated phenylglyoxal (biotin-PG, Figure 6-1a) was designed and synthesized. Here we describe the use of biotin-PG as a chemical handle to enrich and isolate PAD substrates from complex mixtures for mass spectrometry identification (Figure 6-1b). Biotin-PG was used to identify more than 50 proteins that are citrullinated in cells. Enriched among these proteins are several mRNA splicing and processing proteins, suggesting, for the first time, that PAD activity modulates RNA biology and highlighting the use of biotin-PG in furthering the understanding of PAD biology.

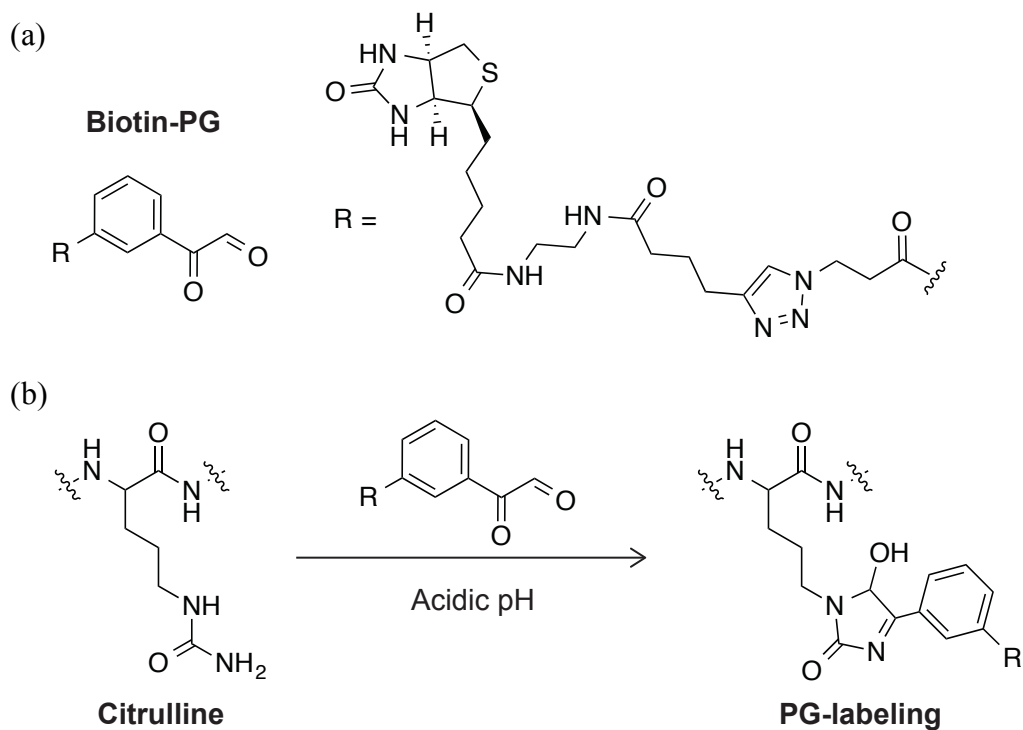


**Figure 6-1.** (a) Structure of Biotin-PG. (b) Biotin-PG labeling of citrulline residues.

Figure adapted from Bicker *et al.*<sup>27</sup>

### Characterization of the PAD2 citrullinome

To showcase the utility of the biotin-PG probe in a physiologically relevant system and identify novel PAD substrates, PAD activity was stimulated by the addition of ionomycin to a stable PAD2 overexpressing HEK293T cells (HEK293T·PAD2) as well as the parent HEK293T cells, which express very low levels of PADs, as a control. After lysis, the soluble protein fraction was incubated with TCA and labeled with biotin-PG for 30 minutes at 37 °C. Samples were cooled on ice for 30 minutes to TCA precipitate the proteins and then washed with cold acetone. The samples were re-solubilized in SDS/PBS and citrullinated proteins were then isolated on streptavidin-agarose. After thorough washing, bound proteins were subjected to on-bead tryptic

digestion and subsequently analyzed by LC-MS/MS. Using this streamlined workflow, we identified more than 50 citrullinated proteins that were significantly enriched by at least 2-fold in the PAD2 overexpressing cell line versus the controls (Table 6-1). A 2-fold cutoff was chosen because this is an acceptable fold-change that can be quantified through spectral counting<sup>28</sup>. Notably, we isolated PAD2, which is known to autocitrullinate, from the overexpressing cell line but not control HEK293T cells, thereby confirming the selectivity of this methodology.

Protein Name and Uniprot ID	Fold Change	Protein Name and Uniprot ID	Fold Change
SRSF7 Serine/arginine - rich splicing factor 7	>>25	TRA2A Transformer-2 protein homolog alpha	>>25
RBMX RNA-binding motif protein, X chromosome	>>25	MYH9 Myosin-9	>>25
U2AF2 Splicing factor U2AF 65 kDa subunit	>>25	PDIA6 Protein disulfide-isomerase A6	>>25
EIF4H Eukaryotic translation initiation factor 4H	>>25	DNAJA1 DnaJ homolog subfamily A member 1	>>25
SRSF1 Serine/arginine-rich splicing factor 1	>>25	HMGB1 High mobility group protein B1	>>25
MCM2 DNA replication licensing factor MCM2	>>25	PTBP1 Polypyrimidine tract-binding protein 1	>>25
PCBP2 Poly(rC)-binding protein 2	>>25	TRA2B Transformer-2 protein homolog beta	>>25
DDX21 Nucleolar RNA helicase 2	>>25	PADI2 Protein-arginine deiminase type	>>25
PCBP1 Poly(rC)-binding protein 1	>>25	SRSF3 Serine/arginine-rich splicing factor 3	4.8
CPSF6 Cleavage and polyadenylation specificity factor subunit 6	>>25	HNRNPA3 Heterogeneous nuclear ribonucleoprotein A3	3.7
RBM39 RNA-binding protein 39	>>25	VIM Vimentin	3.6
RPS10 40S ribosomal protein S10	>>25	SFPQ Splicing factor, proline-and glutamine-rich	3.6
FLNB Filamin -B	>>25	HNRNPA1 Heterogeneous nuclear ribonucleoprotein A1	3.3
LMNB1 Lamin-B1	>>25	HNRNPC Heterogeneous nuclear ribonucleoproteins C1/C2	3.0
POTEE POTE ankyrin domain family member E	>>25	HNRNPH1 Heterogeneous nuclear ribonucleoprotein H	2.9
MCM3 DNA replication licensing factor MCM3	>>25	MCM5 DNA replication licensing factor MCM5	2.4
TAGLN2 Transgelin-2	>>25	NPM1 Nucleophosmin	2.4
HNRNPAB Heterogeneous nuclear ribonucleoprotein A/B	>>25	DDX5 Probable ATP-dependent RNA helicase DDX5	2.4
G3BP2 Ras GTPase-activating protein-inactivating protein-binding protein 2	>>25	HNRNPF Heterogeneous nuclear ribonucleoprotein F	2.4
DNAJB1 DnaJ homolog subfamily B member 1	>>25	YBX1 Nuclease-sensitive element-binding protein 1	2.4
SNRNP200 U5 small nuclear ribonucleoprotein 200 kDa helicase	>>25	G3BP1 Ras GTPase-activating protein-binding protein 1	2.3
HNRNPH3 Heterogeneous nuclear ribonucleoprotein H3	>>25	NONO Non-POU domain-containing octamer-binding protein	2.3
PRPF8 Pre-mRNA-processing-splicing factor 8	>>25	MATR3 Matrin-3	2.2
EZR Ezrin	>>25	HNRNPA2B1 Heterogeneous nuclear ribonucleoproteins A2/B1	2.1
HNRPDL Heterogeneous nuclear ribonucleoprotein D-like	>>25	HNRNPH2 Heterogeneous nuclear ribonucleoprotein H2	2.1
EIF3LC Eukaryotic translation initiation factor 3 subunit C	>>25	DDX17 Probable ATP-dependent RNA helicase DDX17	2.1

**Table 6-1.** Proteins identified with a greater than 2-fold change in PAD2 overexpressing cells versus parental cells.

Among the various other citrullinated proteins enriched were several chromatin binding proteins, ribosomal proteins, and lamin B1. Additionally, almost half of the isolated proteins are components of the mRNA splicing and processing machinery. These proteins include several heterogeneous nuclear ribonucleoproteins (e.g., hnRNPs C, A3,

and AB), RNA helicases (e.g., DDX5 and DDX21), the nucleolar protein nucleophosmin (NPM1), and SNRNP200, an essential component of the U5 spliceosome complex. To validate these findings, HEK293T·PAD2 cells were treated in the absence and presence of ionomycin, and the cell lysates were labeled with biotin-PG. Subsequently, the biotin-PG tagged proteins were isolated on streptavidin-agarose, and then the bound proteins were eluted and the inputs and eluents were probed for PAD2, HNRNPA1, and HNRNPC (Figure 6-2). The results of these studies confirmed that all three proteins were enriched in the ionomycin treated cells, thereby confirming the mass spectrometry data showing that these proteins are citrullinated *in vivo*. While further work is needed to determine how citrullination affects RNA splicing, it is noteworthy that arginine methylation of a similar set of mRNA processing factors can modulate spliceosome activity<sup>29</sup>. Since citrullination antagonizes arginine methylation<sup>30</sup>, these results suggest that the effects of citrullination, particularly when dysregulated, may act beyond the level of regulating the chromatin architecture and also impact mRNA splicing.

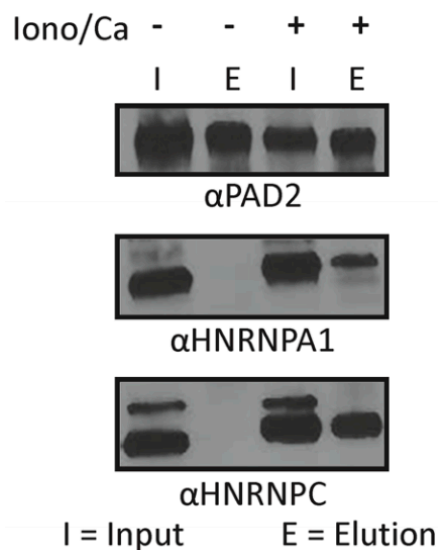


**Figure 6-2.** HEK294T-PAD2 cells treated with or without ionomycin and calcium, labeled with biotin-PG, and enriched on streptavidin beads. Bound proteins were eluted from the beads and the inputs and eluents were probed by western blotting using antibodies against PAD2, HNRNPA1, and HNRNPC. Figure from Lewallen *et al.*<sup>31</sup>

### **The use of biotin-PG to identify dysregulated citrullination in RA**

RA is a common auto-immune disease that is characterized by chronic inflammation of the synovial joints leading to joint damage and disability, but the cause of RA remains unknown<sup>32</sup>. Several factors have been proposed to play a role in the pathogenesis of RA, including environmental (e.g., smoking), genetic (e.g., HLA-DRB1 shared-epitope alleles), and hormonal (female sex) factors<sup>33</sup>. Many studies have indicated that the citrullinated proteins produced by enzymatic deimination are particularly important for RA pathogenesis. For example, the PAD4 gene has a genetic variant that increases susceptibility to RA by increasing PAD4 activity<sup>34</sup>. A specific feature of the immune response in RA is the presence of anti-citrullinated protein antibodies (ACPAs) in patient sera<sup>33</sup>. Proteins known to be targeted by ACPAs such as antithrombin,  $\alpha$ -enolase, filaggrin, fibronectin, fibrin, collagen, and vimentin, change their structural properties following this post-translational modification and can consequently promote autoimmunity as well as tissue destruction of the diseased joint<sup>35</sup>.

Several MS-based experiments have been done to identify differentially expressed proteins in RA<sup>36</sup>, as well as citrullinated proteins residues in synovial fluid from RA patients<sup>24, 33, 37</sup>. Since these studies aimed at identifying citrulline-modified arginine residues from whole RA proteomes, we were interested in comparing that data with

proteins enriched from RA sera using the biotin-PG probe. Sera from healthy and RA patients were treated with PG-biotin to enrich citrullinated proteins, or DMSO as a control. Samples were enriched with streptavidin beads, tryptically digested on the beads, and analyzed by LC/LC-MS/MS. Highly abundant serum albumin and IgG are known to be heavily citrullinated in normal physiology<sup>37</sup> (as observed in our data, Table 6A-1) and were therefore removed from further analysis. Keratin is another highly abundant protein whose citrullination plays a role in normal physiology by helping to create a keratin matrix involved in strengthening the skin, hair, and nails<sup>7</sup>. One study investigated the amount of citrullinated keratin in synovial tissues from RA patients compared with osteoarthritis patients and found that while the amount of keratin in RA patients was lower, the amount of keratin citrullination was roughly three times higher (detected by western blot using an anti-keratin and anti-citrulline antibody)<sup>38</sup>.

Unfortunately, keratin is a common contaminate in MS-based proteomic experiments as it is highly abundant on the outer layer of skin, hair, nails, and wool clothing<sup>39</sup>. In our data, the majority of keratin with high spectral counts in PG-biotin-treated samples also had high spectral counts in untreated samples (Table 6A-1), preventing substantial interpretation of the data in regards to citrullination of keratin in RA. There were, however, 5 keratin proteins that did show a greater than 2-fold increase in one of the RA samples over the healthy samples and no spectral counts in the untreated samples (Table 6A-1). KRT85 and KRT86 is a type II hair keratin that heterodimerizes with type I keratins to form hair and nails. KRT71 is a type II cytoskeletal keratin that plays a central role in hair formation that is expressed in the inner root sheath of hair follicles. Their function in hair structure suggests they are more likely contaminants than

relevant increases of citrullination in RA. KRT17 and KRT13 are type I cytoskeletal keratins and interestingly, an increase of autoantigens for both proteins have been seen in psoriasis patients<sup>40, 41</sup>. While maintaining keratin-free environments are challenging, it would be interesting to try and investigate the role these highly citrullinated proteins have in RA pathology.

Due to multiple factors such as an increase in proteolytic activity in RA, heterogeneity of the composition of RA sera among patients is common<sup>33</sup>. Another problem associated with identifying citrullinated peptides via MS is the inability of trypsin to cleave after a citrulline residue, resulting in large peptides that are difficult to characterize by MS<sup>26</sup>. It is not surprising that citrullination patterns differ between the two RA samples, therefore increases in the citrullination of a protein in one RA sample over the other was still considered. We identified 363 biotin-PG-labeled proteins, with 150 proteins having at least 5 spectral counts in at least one run and an at least 2-fold greater average spectral count than the control samples (Table 6A-1). Of those, 17 proteins showed a significant increase in citrullination in at least one RA sample over the healthy samples, having at least 10 spectra counts in one RA sample and an at least 2-fold increase in average spectral counts over the healthy sample (Table 6-2). Only two of these proteins, filaggrin<sup>42</sup> and fibronectin<sup>43</sup>, are well known PAD targets associated with RA. While two other RA-related citrullinated proteins,  $\alpha$ -enolase and antithrombin, were identified in our data but did not pass the criteria, we were not able to identify any other known RA-related proteins (vimentin and fibrin) or even any PAD enzymes. Albumin, IgG, antitrypsin, IgA, transferrin, and haptoglobin make up roughly 85-90% of the total

protein mass<sup>37</sup>, therefore removal of these proteins prior to biotin-PG enrichment may help enrich lower abundant and more relevant proteins.

Protein	Healthy		RA 1		RA 2			RA1 Fold Change	RA2 Fold Change
	1	2	1	2	1	2	3		
GAPDH Glyceraldehyde-3-phosphate dehydrogenase	0	0	0	13	0	0	0	13	0
ACTB Actin, cytoplasmic 1	0	0	0	11	0	0	0	11	0
FLG2 Filaggrin-2	0	4	0	16	0	0	0	4	0.25
APOD Apolipoprotein D	3	0	12	0	0	9	9	4	3
HRNR Hornerin	0	0	0	130	0	7	0	130	7
JUP Junction plakoglobin	2	8	0	115	0	6	0	23	1.2
ARG1 Arginase-1	0	0	0	23	0	0	0	23	0
SERPINB12 Serpin B12	0	0	0	18	0	2	0	18	2
TGM3 Protein-glutamine gamma-glutamyltransferase E	0	0	0	17	0	0	0	17	0
DSP Desmoplakin	0	8	0	106	2	9	2	13.25	0.5417
PKP1 Plakophilin-1	0	0	0	13	0	0	0	13	0
SAA2 Serum amyloid A-2 protein	0	0	9	14	0	0	0	11.5	0
DSG1 Desmoglein-1	0	0	0	33	0	3	0	33	3
HPR Haptoglobin-related protein	49	30	92	71	46	54	43	2.063	1.207
CFB Complement factor B	0	0	0	46	40	0	0	46	40
SAA4 Serum amyloid A-4 protein	4	0	10	16	4	0	8	3.25	1.5
FN1 Fibronectin	36	29	61	49	77	184	97	1.692	3.672

**Table 6-2.** Citrullinated proteins showing the most significant changes in RA versus healthy sera. Proteins that are not known targets of ACPAs nor were identified in previous MS-based proteomic studies are highlighted in red.

Among the proteins showing a significant increase in RA sera, 11 proteins were also identified in at least 2 of the previously mentioned MS-based proteomic experiments (Table 6-2). The remaining 7 proteins were investigated further for their role in RA pathology. Hornerin plays a role in the keratinization process and exists in the outer layer of human skin<sup>44</sup>. It is likely that this, similar to keratin, is a result of dust contamination and probably not involved in RA, especially since it was only identified in a single RA sample. Desmosomes are cell structures specialized for cell-to-cell adhesion.

Desmoplakin is a desmosomal protein that helps the keratin matrix to extend transcellularly and attach to cadherins (such as desmoglein) via plakophilin and plakoglobin<sup>45</sup>. As citrullination of keratins help them bind to desmoplakin<sup>46</sup>, it is possible that the desmoglein, desmoplakin, plakophilin, and plakoglobin identified in our data are a result of contamination or remain attached to enriched keratin. However, recently, anti-citrullinated protein antibodies were created from antibody repertoires of RA-patients with the goal of treating RA by masking citrullinated epitopes from the immune system. One particular antibody showed anti-inflammatory effects in mice models of RA. Immunoprecipitation of proteins that bind to this antibody revealed that both citrullinated desmoplakin and plakoglobin are targets, suggesting a role of these proteins in inducing the damaging immune response in RA.

While the citrullination of arginase has not been observed, a correlation between arginase levels and RA has been previously identified<sup>47</sup>. The study showed that RA synovium fluid had significantly higher arginase activity and protein levels compared to healthy patients or patients with other auto-immune diseases (e.g. lupus erythematosus) or osteoarthritis. There was also a significant correlation between concentrations of arginase protein and rheumatoid factor<sup>47</sup>. We also identified the transglutaminase TGM3 as having higher citrullination in RA sera than healthy, despite no evidence indicating that it is a PAD substrate. However, studies have shown increased antibodies against transglutaminase (TG) in almost half of the RA patients used in the experiment<sup>48</sup>. Additionally, the administration of TG to mice models of RA enhanced the severity of the disease compared to control mice treated with PBS<sup>49</sup>. While not able to identify novel regulators of RA, these data help to highlight the utility of biotin-PG in identifying and

quantifying relevant targets of PADs while also possibly identifying previously unknown targets.

## **Conclusion**

Overall, this single diagnostic platform has the potential to revolutionize our understanding of PAD biology by uncovering the full scope of the substrates modified by these enzymes in response to a variety of cell signaling paradigms. Additionally, extension of this methodology to diseases in which PAD activity is dysregulated promises to uncover biomarkers associated with a wide range of human ailments.

## **Experimental Procedures**

### **PG-Biotin labeling and affinity purification of labeled proteins for MS analysis**

Cell lysates or human sera were incubated with 20% trichloroacetic acid (TCA; 5  $\mu$ L of 100% TCA) and 0.1 mM biotin-PG (0.5  $\mu$ L of a 5 mM stock) for 30 min at 37 °C. Solutions were quenched by the addition of citrulline to the acidic solution (5  $\mu$ L of a 500 mM stock, 100 mM final). The sample was then cooled on ice for 30 min and centrifuged at 13, 200 g for 15 min at 4 °C to TCA precipitate the protein. The supernatant was removed, and precipitates were washed with cold acetone and dried. Acetone-washed pellets were solubilized in PBS containing 1.2% SDS via sonication and heating (5 min, 80 °C). The SDS-solubilized samples were diluted with PBS (5 mL) for a final SDS concentration of 0.2%. The solutions were incubated with 100  $\mu$ L of streptavidin- agarose

beads (Thermo Scientific) at 4 °C for 16 h. The solutions were then incubated at rt for 3 h. The beads were washed with 0.2% SDS/PBS (5 mL), PBS (3 × 5 mL), and water (3 × 5 mL). The beads were pelleted by centrifugation (1400g, 3 min) between washes. The washed beads were suspended in 6 M urea in PBS (500 µL) and 10 mM dithiothreitol (from 20× stock in water) and placed in a 65 °C heat block for 15 min. Iodoacetamide (20 mM, from 20× stock in water) was then added to the samples and allowed to react at 37 °C for 30 min. Following reduction and alkylation, the beads were pelleted by centrifugation (1400g, 3 min) and resuspended in a premixed solution of 2 M urea in PBS (200 µL), 100 mM CaCl<sub>2</sub> in water (2 µL), and trypsin (4 µL of 20 mg reconstituted in 40 µL of trypsin buffer). The digestion was allowed to proceed overnight at 37 °C. The digested peptides were separated from the beads using a Micro Bio-Spin column (Bio-Rad), and the beads were washed twice with 50 µL of H<sub>2</sub>O. Formic acid (15 µL) was added to the samples, and the samples were stored at -20 °C until MS analysis. LC/LC-MS/MS analysis was performed on an LTQ Orbitrap Discovery mass spectrometer as described in previous chapters.

## References

1. Schellekens, G. A.; de Jong, B. A.; van den Hoogen, F. H.; van de Putte, L. B.; van Venrooij, W. J., Citrulline is an essential constituent of antigenic determinants recognized by rheumatoid arthritis-specific autoantibodies. *The Journal of clinical investigation* **1998**, *101* (1), 273-81.

2. McElwee, J. L.; Mohanan, S.; Griffith, O. L.; Breuer, H. C.; Anguish, L. J.; Cherrington, B. D.; Palmer, A. M.; Howe, L. R.; Subramanian, V.; Causey, C. P.; Thompson, P. R.; Gray, J. W.; Coonrod, S. A., Identification of PADI2 as a potential breast cancer biomarker and therapeutic target. *BMC cancer* **2012**, *12*, 500.
3. Mohanan, S.; Cherrington, B. D.; Horibata, S.; McElwee, J. L.; Thompson, P. R.; Coonrod, S. A., Potential role of peptidylarginine deiminase enzymes and protein citrullination in cancer pathogenesis. *Biochemistry research international* **2012**, *2012*, 895343.
4. Romero, V.; Fert-Bober, J.; Nigrovic, P. A.; Darrah, E.; Haque, U. J.; Lee, D. M.; van Eyk, J.; Rosen, A.; Andrade, F., Immune-mediated pore-forming pathways induce cellular hypercitrullination and generate citrullinated autoantigens in rheumatoid arthritis. *Science translational medicine* **2013**, *5* (209), 209ra150.
5. Wang, Y.; Li, M.; Stadler, S.; Correll, S.; Li, P.; Wang, D.; Hayama, R.; Leonelli, L.; Han, H.; Grigoryev, S. A.; Allis, C. D.; Coonrod, S. A., Histone hypercitrullination mediates chromatin decondensation and neutrophil extracellular trap formation. *The Journal of cell biology* **2009**, *184* (2), 205-13.
6. Vossenaar, E. R.; Zendman, A. J.; van Venrooij, W. J.; Pruijn, G. J., PAD, a growing family of citrullinating enzymes: genes, features and involvement in disease. *BioEssays : news and reviews in molecular, cellular and developmental biology* **2003**, *25* (11), 1106-18.
7. Chirivi, R. G., Jenniskens, G. J., Raats, J.M., Anti-Citrullinated Protein Antibodies as Novel Therapeutic Drugs in Rheumatoid Arthritis. *Journal Clinical & Cellular Immunology* **2013**, *4* (S6).

8. Baka, Z.; Gyorgy, B.; Geher, P.; Buzas, E. I.; Falus, A.; Nagy, G., Citrullination under physiological and pathological conditions. *Joint, bone, spine : revue du rhumatisme* **2012**, *79* (5), 431-6.
9. Christophorou, M. A.; Castelo-Branco, G.; Halley-Stott, R. P.; Oliveira, C. S.; Loos, R.; Radzsheuskaya, A.; Mowen, K. A.; Bertone, P.; Silva, J. C.; Zernicka-Goetz, M.; Nielsen, M. L.; Gurdon, J. B.; Kouzarides, T., Citrullination regulates pluripotency and histone H1 binding to chromatin. *Nature* **2014**, *507* (7490), 104-8.
10. Li, P.; Yao, H.; Zhang, Z.; Li, M.; Luo, Y.; Thompson, P. R.; Gilmour, D. S.; Wang, Y., Regulation of p53 target gene expression by peptidylarginine deiminase 4. *Molecular and cellular biology* **2008**, *28* (15), 4745-58.
11. Slack, J. L.; Causey, C. P.; Thompson, P. R., Protein arginine deiminase 4: a target for an epigenetic cancer therapy. *Cellular and molecular life sciences : CMLS* **2011**, *68* (4), 709-20.
12. Zhang, X.; Gamble, M. J.; Stadler, S.; Cherrington, B. D.; Causey, C. P.; Thompson, P. R.; Roberson, M. S.; Kraus, W. L.; Coonrod, S. A., Genome-wide analysis reveals PADI4 cooperates with Elk-1 to activate c-Fos expression in breast cancer cells. *PLoS genetics* **2011**, *7* (6), e1002112.
13. Mohanan, S.; Horibata, S.; McElwee, J. L.; Dannenberg, A. J.; Coonrod, S. A., Identification of macrophage extracellular trap-like structures in mammary gland adipose tissue: a preliminary study. *Frontiers in immunology* **2013**, *4*, 67.
14. Rohrbach, A. S.; Slade, D. J.; Thompson, P. R.; Mowen, K. A., Activation of PAD4 in NET formation. *Frontiers in immunology* **2012**, *3*, 360.

15. Knight, J. S.; Subramanian, V.; O'Dell, A. A.; Yalavarthi, S.; Zhao, W.; Smith, C. K.; Hodgin, J. B.; Thompson, P. R.; Kaplan, M. J., Peptidylarginine deiminase inhibition disrupts NET formation and protects against kidney, skin and vascular disease in lupus-prone MRL/lpr mice. *Annals of the rheumatic diseases* **2015**, *74* (12), 2199-206.
16. Luo, Y.; Arita, K.; Bhatia, M.; Knuckley, B.; Lee, Y. H.; Stallcup, M. R.; Sato, M.; Thompson, P. R., Inhibitors and inactivators of protein arginine deiminase 4: functional and structural characterization. *Biochemistry* **2006**, *45* (39), 11727-36.
17. Neeli, I.; Khan, S. N.; Radic, M., Histone deimination as a response to inflammatory stimuli in neutrophils. *Journal of immunology* **2008**, *180* (3), 1895-902.
18. Khandpur, R.; Carmona-Rivera, C.; Vivekanandan-Giri, A.; Gizinski, A.; Yalavarthi, S.; Knight, J. S.; Friday, S.; Li, S.; Patel, R. M.; Subramanian, V.; Thompson, P.; Chen, P.; Fox, D. A.; Pennathur, S.; Kaplan, M. J., NETs are a source of citrullinated autoantigens and stimulate inflammatory responses in rheumatoid arthritis. *Science translational medicine* **2013**, *5* (178), 178ra40.
19. Leffler, J.; Martin, M.; Gullstrand, B.; Tyden, H.; Lood, C.; Truedsson, L.; Bengtsson, A. A.; Blom, A. M., Neutrophil extracellular traps that are not degraded in systemic lupus erythematosus activate complement exacerbating the disease. *Journal of immunology* **2012**, *188* (7), 3522-31.
20. Savchenko, A. S.; Inoue, A.; Ohashi, R.; Jiang, S.; Hasegawa, G.; Tanaka, T.; Hamakubo, T.; Kodama, T.; Aoyagi, Y.; Ushiki, T.; Naito, M., Long pentraxin 3 (PTX3) expression and release by neutrophils in vitro and in ulcerative colitis. *Pathology international* **2011**, *61* (5), 290-7.

21. Knight, J. S.; Zhao, W.; Luo, W.; Subramanian, V.; O'Dell, A. A.; Yalavarthi, S.; Hodgins, J. B.; Eitzman, D. T.; Thompson, P. R.; Kaplan, M. J., Peptidylarginine deiminase inhibition is immunomodulatory and vasculoprotective in murine lupus. *The Journal of clinical investigation* **2013**, *123* (7), 2981-93.
22. Demers, M.; Krause, D. S.; Schatzberg, D.; Martinod, K.; Voorhees, J. R.; Fuchs, T. A.; Scadden, D. T.; Wagner, D. D., Cancers predispose neutrophils to release extracellular DNA traps that contribute to cancer-associated thrombosis. *Proceedings of the National Academy of Sciences of the United States of America* **2012**, *109* (32), 13076-81.
23. Slade, D. J.; Subramanian, V.; Fuhrmann, J.; Thompson, P. R., Chemical and biological methods to detect post-translational modifications of arginine. *Biopolymers* **2014**, *101* (2), 133-43.
24. Tuttunen, A. E.; Fleckenstein, B.; de Souza, G. A., Assessing the citrullinome in rheumatoid arthritis synovial fluid with and without enrichment of citrullinated peptides. *Journal of proteome research* **2014**, *13* (6), 2867-73.
25. Holm, A.; Rise, F.; Sessler, N.; Sollid, L. M.; Undheim, K.; Fleckenstein, B., Specific modification of peptide-bound citrulline residues. *Analytical biochemistry* **2006**, *352* (1), 68-76.
26. Bennike, T. L., KB. Olesen, MK. Andersen, V. Birkelund, S. Stensballe, A., Optimizing the Identification of Citrullinated Peptides by Mass Spectrometry: Utilizing the Inability of Trypsin to Cleave after Citrullinated Amino Acids. *J Proteomics Bioinform* **2013**, *6*, 288-295.

27. Bicker, K. L.; Subramanian, V.; Chumanevich, A. A.; Hofseth, L. J.; Thompson, P. R., Seeing citrulline: development of a phenylglyoxal-based probe to visualize protein citrullination. *Journal of the American Chemical Society* **2012**, *134* (41), 17015-8.
28. Liu, H.; Sadygov, R. G.; Yates, J. R., 3rd, A model for random sampling and estimation of relative protein abundance in shotgun proteomics. *Analytical chemistry* **2004**, *76* (14), 4193-201.
29. Bedford, M. T.; Clarke, S. G., Protein arginine methylation in mammals: who, what, and why. *Molecular cell* **2009**, *33* (1), 1-13.
30. Cuthbert, G. L.; Daujat, S.; Snowden, A. W.; Erdjument-Bromage, H.; Hagiwara, T.; Yamada, M.; Schneider, R.; Gregory, P. D.; Tempst, P.; Bannister, A. J.; Kouzarides, T., Histone deimination antagonizes arginine methylation. *Cell* **2004**, *118* (5), 545-53.
31. Lewallen, D. M.; Bicker, K. L.; Subramanian, V.; Clancy, K. W.; Slade, D. J.; Martell, J.; Dreyton, C. J.; Sokolove, J.; Weerapana, E.; Thompson, P. R., Chemical Proteomic Platform To Identify Citrullinated Proteins. *ACS chemical biology* **2015**, *10* (11), 2520-8.
32. Scott, D. L.; Wolfe, F.; Huizinga, T. W., Rheumatoid arthritis. *Lancet* **2010**, *376* (9746), 1094-108.
33. van Beers, J. J.; Schwarte, C. M.; Stammen-Vogelzangs, J.; Oosterink, E.; Bozic, B.; Pruijn, G. J., The rheumatoid arthritis synovial fluid citrullinome reveals novel citrullinated epitopes in apolipoprotein E, myeloid nuclear differentiation antigen, and beta-actin. *Arthritis and rheumatism* **2013**, *65* (1), 69-80.

34. Yamada, R.; Suzuki, A.; Chang, X.; Yamamoto, K., Citrullinated proteins in rheumatoid arthritis. *Frontiers in bioscience : a journal and virtual library* **2005**, *10*, 54-64.
35. Cantaert, T.; De Rycke, L.; Bongartz, T.; Matteson, E. L.; Tak, P. P.; Nicholas, A. P.; Baeten, D., Citrullinated proteins in rheumatoid arthritis: crucial...but not sufficient! *Arthritis and rheumatism* **2006**, *54* (11), 3381-9.
36. Cheng, Y.; Chen, Y.; Sun, X.; Li, Y.; Huang, C.; Deng, H.; Li, Z., Identification of potential serum biomarkers for rheumatoid arthritis by high-resolution quantitative proteomic analysis. *Inflammation* **2014**, *37* (5), 1459-67.
37. Cano, L., Arkfeld, D.G., Targeted Synovial Fluid Proteomics for Biomarker Discovery in Rheumatoid Arthritis. *Clinical Proteomics* **2009**, *5* (2), 75-102.
38. Chang, X.; Jian, X.; Yan, X., Expression and citrullination of keratin in synovial tissue of rheumatoid arthritis. *Rheumatology international* **2009**, *29* (11), 1337-42.
39. Hodge, K.; Have, S. T.; Hutton, L.; Lamond, A. I., Cleaning up the masses: exclusion lists to reduce contamination with HPLC-MS/MS. *Journal of proteomics* **2013**, *88*, 92-103.
40. Jones, D. A.; Yawalkar, N.; Suh, K. Y.; Sadat, S.; Rich, B.; Kupper, T. S., Identification of autoantigens in psoriatic plaques using expression cloning. *The Journal of investigative dermatology* **2004**, *123* (1), 93-100.
41. Maejima, H.; Nagashio, R.; Yanagita, K.; Hamada, Y.; Amoh, Y.; Sato, Y.; Katsuoka, K., Moesin and stress-induced phosphoprotein-1 are possible sero-diagnostic markers of psoriasis. *PloS one* **2014**, *9* (7), e101773.

42. Girbal-Neuhauser, E.; Durieux, J. J.; Arnaud, M.; Dalbon, P.; Sebbag, M.; Vincent, C.; Simon, M.; Senshu, T.; Masson-Bessiere, C.; Jolivet-Reynaud, C.; Jolivet, M.; Serre, G., The epitopes targeted by the rheumatoid arthritis-associated antifilaggrin autoantibodies are posttranslationally generated on various sites of (pro)filaggrin by deimination of arginine residues. *Journal of immunology* **1999**, *162* (1), 585-94.
43. Chang, X.; Yamada, R.; Suzuki, A.; Kochi, Y.; Sawada, T.; Yamamoto, K., Citrullination of fibronectin in rheumatoid arthritis synovial tissue. *Rheumatology* **2005**, *44* (11), 1374-82.
44. Henry, J.; Hsu, C. Y.; Haftek, M.; Nachat, R.; de Koning, H. D.; Gardinal-Galera, I.; Hitomi, K.; Balica, S.; Jean-Decoster, C.; Schmitt, A. M.; Paul, C.; Serre, G.; Simon, M., Hornerin is a component of the epidermal cornified cell envelopes. *Faseb J* **2011**, *25* (5), 1567-76.
45. Bornslaeger, E. A.; Corcoran, C. M.; Stappenbeck, T. S.; Green, K. J., Breaking the connection: displacement of the desmosomal plaque protein desmoplakin from cell-cell interfaces disrupts anchorage of intermediate filament bundles and alters intercellular junction assembly. *The Journal of cell biology* **1996**, *134* (4), 985-1001.
46. Chirivi, R. G., van Rosmalen, J. W., Jenniskens, G. J., Pruijn, G.J., Raats, J.M., Citrullination: A Target for Disease Intervention in Multiple Sclerosis and other Inflammatory Diseases? *Journal Clinical & Cellular Immunology* **2013**, *4*.
47. Huang, L. W.; Chang, K. L.; Chen, C. J.; Liu, H. W., Arginase levels are increased in patients with rheumatoid arthritis. *The Kaohsiung journal of medical sciences* **2001**, *17* (7), 358-63.

48. Picarelli, A.; Di Tola, M.; Sabbatella, L.; Vetrano, S.; Anania, M. C.; Spadaro, A.; Sorgi, M. L.; Taccari, E., Anti-tissue transglutaminase antibodies in arthritic patients: a disease-specific finding? *Clinical chemistry* **2003**, *49* (12), 2091-4.
49. Dzhambazov, B.; Lindh, I.; Engstrom, A.; Holmdahl, R., Tissue transglutaminase enhances collagen type II-induced arthritis and modifies the immunodominant T-cell epitope CII260-270. *European journal of immunology* **2009**, *39* (9), 2412-23.

## **Appendix I.**

*C. elegans* lifespan data

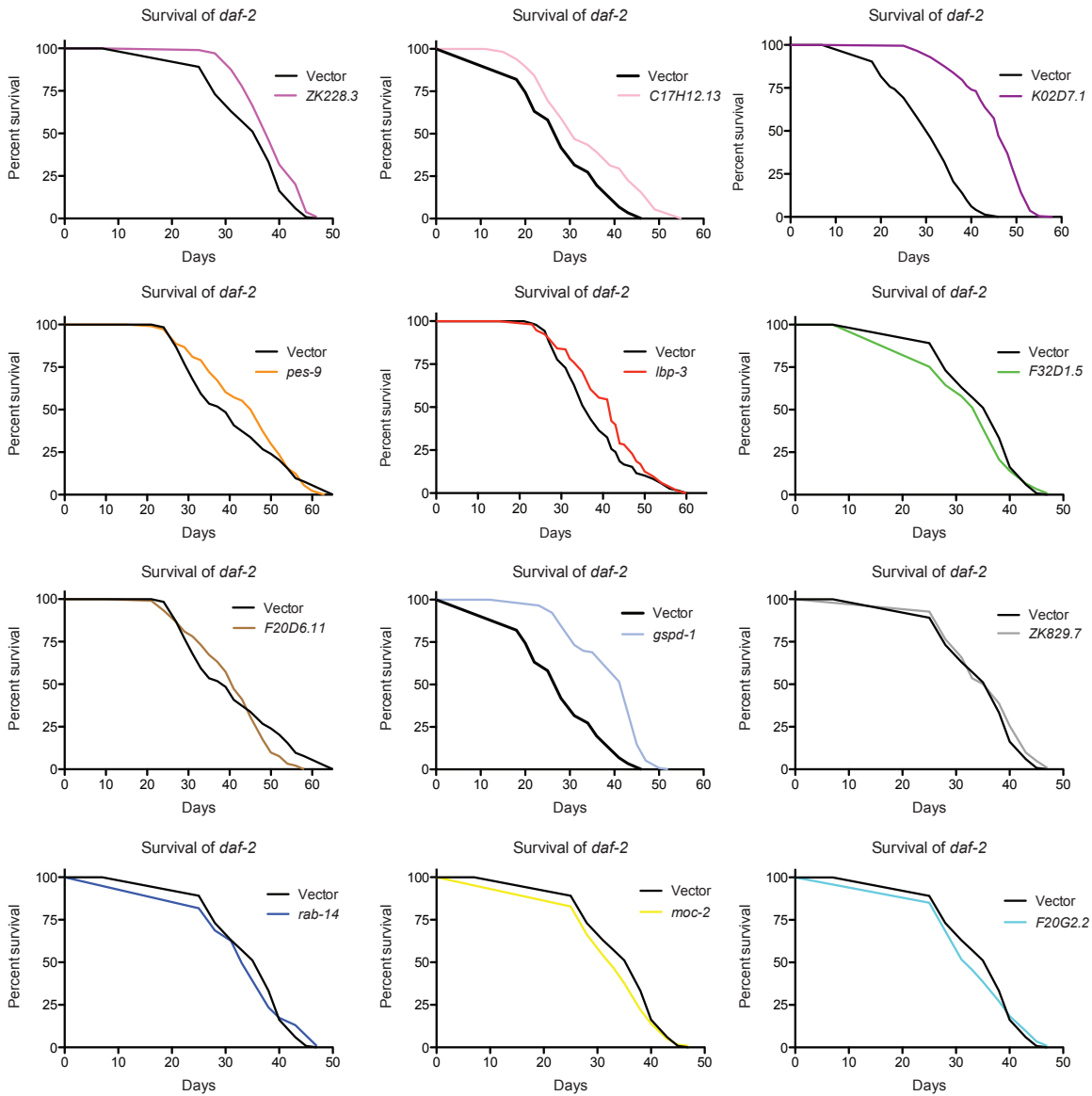


**Figure 3A-1.** Lifespan assays on RNAi-mediated knockdown of cysteine-containing proteins with the greatest reactivity change between *daf-2* and *daf-16;daf-2* mutants.

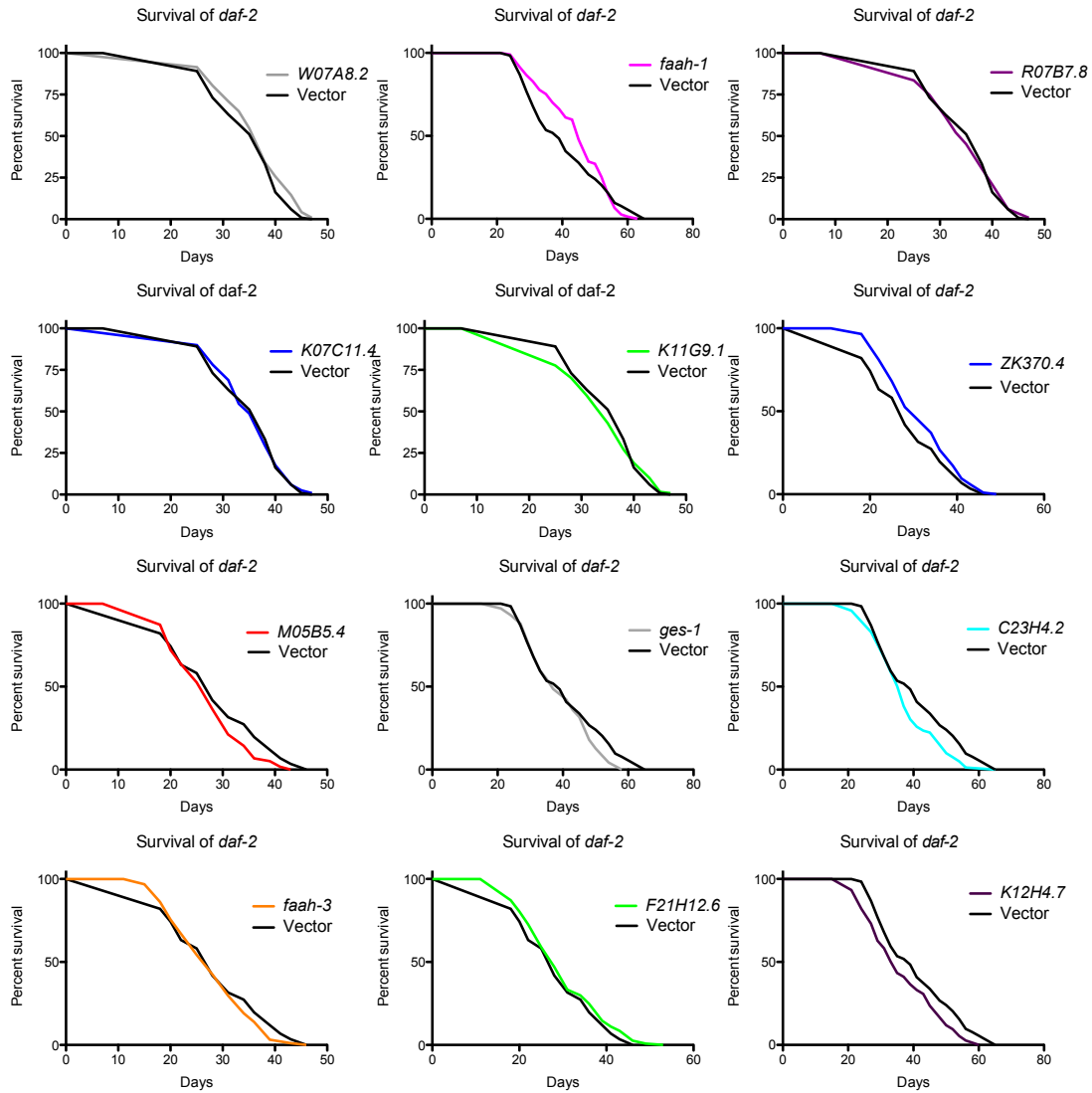


**Figure 4A-1.** Lifespan assays on RNAi-mediated knockdown of serine hydrolases labeled by FP-biotin with the greatest activity changes between *daf-2* and *daf-16;daf-2* mutants.



## **Appendix II.**

### Mass Spectrometry Tables

**Table 3A-1.** MS results showing the 578 cysteine-containing peptides identified in the daf-2 lysates. The cysteines are ranked by reactivity based on their average light:heavy ratios (R) from R~1 (high reactivity) to R>>1(low reactivity). The closest human homologue for each cysteine-containing protein was determined by performing a BLAST search against the human UniProt database. Cysteine-containing proteins with good homology (E-value  $\leq 1.0E-05$ ) to human proteins were identified and their conservation and function in humans were determined. Identified cysteines with an annotated biological function in *C. elegans* are shown. Cysteines with unknown function in *C. elegans* but are conserved in a human homologue that is annotated as functional are indicated in bold. To establish if these cysteines are conserved across other species, a BLAST search of each cysteine-containing protein was performed against the mouse, fly, yeast, and mustard UniProt databases.

Run 1	Run 2	Average	<i>C. elegans</i>			
			Uniprot ID	Description	Sequence	Function
0	1.13	1.13	O45552	F53A2.7 Protein F53A2.7	R.LC*GSGFQAVVNAAQ AIK.L	Acyl-thioester intermediate
0	1.3	1.3	Q22101	T02G5.7 Protein T02G5.7	K.VC*SSSMK.A	Acyl-thioester intermediate
1.33	1.31	1.32	O46009	ZK228.3 Protein ZK228.3	R.DGVVYSVAC*STHQF V.-	
0	1.42	1.42	H2KZ24	C27H5.2 Protein C27H5.2, isoform a	R.ELSPLEQQFLDLC*R.I	
1.55	0	1.55	O45352	gst-44 Protein GST-44	R.FC*PAAQR.A	<b>Active site nucleophile</b>
1.51	1.6	1.555	O17234	gsto-3 Protein GSTO-3, isoform a	R.FC*PYAQR.V	<b>Active site nucleophile</b>
1.57	1.58	1.575	Q22100	kat-1 Protein KAT-1	K.VC*SSGLK.A	Acyl-thioester intermediate
1.58	1.74	1.66	Q21307	mek-1 Protein MEK-1, isoform a	R.VCMECMATC*LDR.L	
1.64	1.71	1.675	Q22392	dhs-19 Protein DHS-19	K.TGC*VGLVDYCASK. H	
1.95	0	1.95	P46562	alh-9 Putative aldehyde dehydrogenase family 7 member A1	K.GSDC*GIVNVNIPTSG AEIGGAFGGEK.E	
2.27	2.23	2.25	Q3Y400	glrx-22 Protein GLRX-22	K.DGC*GYCVK.A	<b>S-glutathionyl cysteine/ Redox-active disulfide</b>
2.34	2.4	2.37	G5ECV9	alh-3 Protein ALH-3	K.GENC*IAAGR.V	<b>Active site</b>
2.67	2.42	2.545	Q95Y85	Y110A7A.6 Protein Y110A7A.6, isoform b	R.VFFVESVC*DDPDIIN SNITEVK.I	<b>Active site</b>
2.7	2.48	2.59	D7SFI3	C02D5.4 Protein C02D5.4	R.FC*PWAQR.A	<b>Active site nucleophile</b>
0	2.77	2.77	Q21284	K07E3.4 Protein K07E3.4, isoform a	K.LPIC*MAK.T	
2.97	2.67	2.82	Q21589	M7.8 Protein M7.8	K.C*LDGALDR.A	
4.13	1.59	2.86	Q19297	F10D7.3 Uncharacterized monothiol glutaredoxin F10D7.3	K.TYC*PWSK.R	Iron-Sulfur (2Fe-2S)
2.93	0	2.93	O44658	cyp-34a8 Protein CYP-34A8	R.AC*PGESLAR.A	<b>Iron-binding</b>
2.99	2.95	2.97	O16228	djr-1.2 Protein DJR-1.2	K.LAEC*PVIGELK.T	
0	2.99	2.99	Q18758	klo-1 Protein KLO-1	R.FC*LPASDSPADLDAC NR.A	
2.99	0	2.99	G5EE42	ZK1098.11 Protein ZK1098.11	K.YLVQPTC*WYVAK.Y	
0	3.01	3.01	Q09657	ZK1320.9 Protein ZK1320.9	K.IQNNSLFIC*PGNR.K	

Human			Conserved Cysteine				
Uniprot ID	E-value	Description	Human	Mouse	Fly	Yeast	Mustard
P42765	2.00E-163	3-ketoacyl-CoA thiolase, mitochondrial	Yes	Yes	Yes	Yes	Yes
P24752	1.00E-127	Acetyl-CoA acetyltransferase, mitochondrial	Yes	Yes	Yes	Yes	Yes
Q96M93	0.92	Adenosine deaminase domain-containing protein 1	--	--	--	--	--
H0YNH8	0.093	Uveal autoantigen with coiled-coil domains and ankyrin repeats	--	--	--	--	--
P78417	2.00E-43	Glutathione S-transferase omega-1	Yes	Yes	Yes	--	--
P78417	1.00E-38	Glutathione S-transferase omega-1	Yes	Yes	Yes	No	No
P24752	2.00E-155	Acetyl-CoA acetyltransferase, mitochondrial	Yes	Yes	Yes	Yes	Yes
O14733	1.00E-111	Dual specificity mitogen-activated protein kinase kinase 7	Yes	Yes	Yes	No	No
Q8N3Y7	1.00E-98	Epidermal retinol dehydrogenase 2	No	No	No	No	No
P49419	0	Alpha-aminoadipic semialdehyde dehydrogenase	Yes	Yes	Yes	No	Yes
Q9NS18	3.00E-10	Glutaredoxin-2, mitochondrial	Yes	Yes	Yes	Yes	Yes
Q3SY69	0	Mitochondrial 10-formyltetrahydrofolate dehydrogenase	Yes	Yes	Yes	Yes	Yes
O60825	6.70E-159	6-phosphofructo-2-kinase/fructose-2, 6-bisphosphatase 2 transcript variant 3	Yes	Yes	Yes	No	Yes
P78417	2.00E-40	Glutathione S-transferase omega-1	Yes	Yes	Yes	--	No
P11586	0	C-1-tetrahydrofolate synthase, cytoplasmic	Yes	Yes	Yes	Yes	Yes
F8W808	1.1	N-alpha-acetyltransferase 10	--	--	No	--	--
P35754	1.00E-12	Glutaredoxin-1	Yes	Yes	Yes	Yes	Yes
P11509	2.00E-74	Cytochrome P450 2A6	Yes	Yes	Yes	Yes	Yes
Q99497	5.00E-42	Protein deglycase DJ-1	No	No	No	--	Yes
Q9H227	2.00E-95	Cytosolic beta-glucosidase	No	No	No	--	No
H3BMV2	1.00E-12	N-acetyltransferase domain-containing protein 1	Yes	Yes	--	--	--
Q8N6N6	5.8	N-acetyltransferase domain-containing protein 1	No	--	No	--	--

2.73	3.47	3.1	P91500	T27A3.6 Protein T27A3.6	K.AYVLALAGC*TNSGK.S	
3.75	2.96	3.355	P91502	T27A3.2 Ubiquitin carboxyl-terminal hydrolase	R.YGEGQLETLVNC*PLDK.L	
4.39	3.42	3.905	P49041	rps-5 40S ribosomal protein S5	K.AAC*PIVER.L	
0	3.91	3.91	Q27513	cyp-13A4 Putative cytochrome P450 CYP13A4	R.IC*IGMR.L	Iron-binding
3.71	4.18	3.945	Q21962	R12C12.1 Protein R12C12.1, isoform a	R.NLVC*TCPPIESYQ.-	
4.56	3.39	3.975	H2KZ06	clec-266 Protein CLEC-266, isoform a	K.FYSIC*ER.N	
4.03	3.92	3.975	Q20655	ftt-2 14-3-3-like protein 2	R.DIC*QDVLNLLDK.F	
3.75	4.39	4.07	Q9XW92	vha-13 V-type proton ATPase catalytic subunit A	K.YSNSDAIIYVGC*GER.G	
4.1	0	4.1	Q6IMP3	anc-1 ANC-1	R.LQNFC*DAVK.I	
4.52	3.86	4.19	O76258	tsg-101 Protein TSG-101	K.DLTC*DDVIYSLGQS.LK.K	
4.3	4.2	4.25	P62784	his-1 Histone H4	R.DAVTYC*EHAK.R	
4.45	4.15	4.3	Q9N456	glrx-10 Protein GLRX-10	K.SYC*PYCHK.A	Redox-active disulfide
0	4.42	4.42	O17643	idh-2 Isocitrate dehydrogenase [NADP]	K.SSGGFVWAC*K.N	
4.42	0	4.42	P48583	erd-2 ER lumen protein retaining receptor	R.SC*EGISGR.S	
4.57	4.32	4.445	O44650	cyp-35b1 Protein CYP-35B1	R.SC*VGENIAK.S	Iron-binding
4.71	4.25	4.48	Q09512	ttl-12 Tubulin--tyrosine ligase-like protein 12	K.C*ENFIETIEK.A	
4.4	4.67	4.535	Q21193	pfn-3 Profilin-3	K.GLQPEMC*SK.T	
4.55	4.56	4.555	Q9BL27	Y71H2AR.1 Protein Y71H2AR.1	K.ILTTGESWC*PDCVV.AEPPVVEEVK.D	Active site nucleophile
0	4.58	4.58	Q965W3	Y40B10A.2 Protein Y40B10A.2	K.SSDPVIAYC*SEHTTI.QSPLQAE LLK.E	
0	4.62	4.62	Q20166	cpin-1 Protein CPIN-1	K.LGANVSIC*PCTEGY.LGDGIPR.I	
4.92	4.45	4.685	Q10457	B0286.3 Probable multifunctional protein ADE2	R.MPNGIGC*TTVLDPS.EAALAAAK.I	
5.12	4.27	4.695	O18240	rps-18 Protein RPS-18	R.FAFVC*CR.K	
5.2	4.21	4.705	Q21746	sgt-1 Protein SGT-1	R.LEQYDLAIQDC*R.T	
4.5	4.91	4.705	G5ECA7	T02D1.8 Protein T02D1.8	K.SC*MFGNQAIVDSFK.G	
5.14	4.37	4.755	O61217	K02D7.1 Protein K02D7.1	K.TVGADALGMSTC*H.EVTVAR.Q	
4.88	4.68	4.78	A7DTF0	mrg-1 Protein MRG-1, isoform b	K.ITNLALIC*TAR.G	
5.65	4.04	4.845	O18229	Y57G11C.3 Putative 6-phosphogluconolactonase	K.NVAFIIC*GK.Q	
4.53	5.16	4.845	Q23570	ZK669.3 GILT-like protein ZK669.3	R.C*SDTSYWMK.W	Redox-active disulfide
4.84	4.96	4.9	Q18075	C18B2.4 Protein C18B2.4	K.GGC*IEFGEALLR.A	
6.27	3.58	4.925	O17953	dld-1 Dihydrolipoyl dehydrogenase	R.EANLAAYC*GK.A	
4.98	0	4.98	Q18758	klo-1 Protein KLO-1	K.FADLC*FQK.F	
4.99	0	4.99	Q86DB5	gsr-1 Protein GSR-1, isoform b	R.LGGTC*VNVGCVPK.K	FAD-binding/Redox-active disulfide
5.01	0	5.01	P28548	kin-10 Casein kinase II subunit beta	R.GNEFFC*EVDEEYIQ.DR.F	
5.01	0	5.01	Q27512	nex-2 Annexin	K.VISILC*QR.T	
5.03	0	5.03	Q21307	mek-1 Protein MEK-1, isoform a	K.ELQFVEDIGHGSC*G.TVTK.C	ATP-binding

O96007	6.00E-32	Molybdopterin synthase catalytic subunit	No	--	--	Yes	--
P45974	4.00E-161	Ubiquitin carboxyl-terminal hydrolase 5	No	No	No	No	No
P46782	3.00E-125	40S ribosomal protein S5	Yes	Yes	Yes	Yes	Yes
P20815	2.00E-71	Cytochrome P450 3A5	Yes	Yes	Yes	Yes	Yes
P23378	0	Glycine dehydrogenase (decarboxylating), mitochondrial	Yes	Yes	Yes	Yes	Yes
J3KR22	3.00E-11	C-type lectin domain family 10 member A	No	--	--	--	--
P63104	2.00E-145	14-3-3 protein zeta/delta	Yes	Yes	Yes	No	Yes
P38606	0	V-type proton ATPase catalytic subunit A	Yes	Yes	Yes	Yes	Yes
F5GYQ7	2.00E-54	Nesprin-1	No	--	--	--	--
Q99816	2.00E-87	Tumor susceptibility gene 101 protein	No	No	No	--	--
P62805	4.00E-66	Histone H4	No	No	No	No	No
P35754	2.00E-26	Glutaredoxin-1	Yes	Yes	Yes	Yes	Yes
P48735	0	Isocitrate dehydrogenase [NADP], mitochondrial	Yes	Yes	Yes	No	Yes
P33947	7.00E-104	ER lumen protein-retaining receptor 2	Yes	Yes	Yes	No	Yes
P11509	2.00E-54	Cytochrome P450 2A6	Yes	Yes	Yes	Yes	Yes
Q14166	2.00E-119	Tubulin--tyrosine ligase-like protein 12	Yes	No	Yes	--	No
P07737	0.81	Profilin-1	No	--	No	No	Yes
Q9BRA2	4.00E-20	Thioredoxin domain-containing protein 17	Yes	Yes	Yes	--	Yes
R4GNF4	4.00E-32	Catechol O-methyltransferase domain-containing protein 1	No	--	--	--	No
Q9Y2T3	1.00E-09	Guanine deaminase	Yes	Yes	Yes	Yes	--
P22234	9.00E-148	Multifunctional protein ADE2	Yes	Yes	Yes	No	--
P62269	2.00E-86	40S ribosomal protein S18	No	No	No	No	No
O43765	5.00E-61	Small glutamine-rich tetratricopeptide repeat-containing protein alpha	Yes	Yes	Yes	No	Yes
F8W717	1.4	Echinoderm microtubule-associated protein-like 1	--	--	--	--	--
P00491	2.00E-79	Purine nucleoside phosphorylase	No	No	No	No	--
B3KTM8	2.00E-25	Mortality factor 4-like protein 1	No	No	No	Yes	No
O95336	3.00E-26	6-phosphogluconolactonase	No	No	No	No	Yes
P13284	1.00E-13	Gamma-interferon-inducible lysosomal thiol reductase	Yes	Yes	Yes	--	--
K7ENL2	1.00E-30	WW domain-binding protein 2	No	No	No	--	Yes
P09622	0	Dihydrolipoyl dehydrogenase, mitochondrial	No	No	No	No	--
Q9H227	2.00E-95	Cytosolic beta-glucosidase	Yes	No	No	--	Yes
P00390	0	Glutathione reductase, mitochondrial	Yes	Yes	Yes	Yes	Yes
Q5SRQ6	3.00E-126	Casein kinase II subunit beta	Yes	Yes	Yes	Yes	Yes
P20073	1.00E-108	Annexin A7	No	No	Yes	--	No
O14733	1.00E-111	Dual specificity mitogen-activated protein kinase kinase 7	Yes	Yes	No	No	No

5.05	0	5.05	G4S185	C17H12.13 Protein C17H12.13, isoform b	R.DLVQDSLQC*SSTCVI R.D	
5.1	5.07	5.085	P52015	cyn-7 Peptidyl-prolyl cis-trans isomerase 7	K.SEC*LIADCGQL.-	
5.4	4.8	5.1	O01504	rpa-2 60S acidic ribosomal protein P2	K.VLEAGGLDC*DMEN ANSVVDALK.G	
4.99	5.21	5.1	Q22100	kat-1 Protein KAT-1	K.SGQIGVAAIC*NGGG GSSGMVIQK.L	Active site (proton acceptor)
4.93	5.29	5.11	Q22799	dlc-1 Dynein light chain 1, cytoplasmic	K.NADMSDDMQQDAID C*ATQALEK.Y	
4.89	5.38	5.135	O44156	pas-6 Proteasome subunit alpha type-1	R.YLQTEC*SSWR.W	
4.9	5.39	5.145	Q7Z139	hyl-2 Protein HYL-2	R.MAEC*AMR.A	
5.05	5.28	5.165	P06582	hsp-16.2 Heat shock protein Hsp-16.2	R.QFAPVC*R.I	
5.25	5.14	5.195	P53588	F47B10.1 Probable succinyl-CoA ligase [ADP-forming] subunit	K.DC*EQQASEHEK.L	
5.58	4.93	5.255	Q2AAC3	glrx-21 Protein GLRX-21, isoform b	K.TSC*TFCNR.A	<b>S-glutathionyl cysteine/Redox-active disulfide</b>
5.27	0	5.27	Q20627	pam-1 Protein PAM-1, isoform a	R.AVEFQDFFC*NCNVL SDTDR.Q	
5.27	0	5.27	Q10663	gei-7 Bifunctional glyoxylate cycle protein	R.GTGC*VPLYNLMEDA ATAEISR.A	
4.52	6.03	5.275	Q20222	lbp-3 Fatty acid-binding protein homolog 3	K.MVNNGITC*R.R	<b>Disulfide</b>
5.01	5.57	5.29	O44906	W05G11.6 Protein W05G11.6, isoform a	K.FIAAAFPSAC*GK.T	<b>GTP-binding</b>
5.26	5.34	5.3	P48152	rps-3 40S ribosomal protein S3	R.AC*YGVLR.F	
5.38	5.25	5.315	Q9U3M0	C46C2.5 Protein C46C2.5	K.ENLESLFMSC*AR.E	
4.95	5.76	5.355	P34696	hsp-16.1 Heat shock protein Hsp-16.1/Hsp-16.11	R.QFTPVC*R.G	
5.17	5.62	5.395	P48152	rps-3 40S ribosomal protein S3	R.GLC*AVAQCESLR.Y	
5.24	5.57	5.405	H2LOB0	nhr-104 Protein NHR-104, isoform a	K.SEGLLC*K.K	
0	5.41	5.41	O17071	rpt-4 Probable 26S protease regulatory subunit 10B	R.AVASQLDC*NFLK.V	
4.75	6.08	5.415	P17329	gpd-2 Glyceraldehyde-3-phosphate dehydrogenase 2	K.YDHANDHIISNASC* TTNCLAPLAK.V	Active site nucleophile
5.93	4.94	5.435	Q95Y96	M04F3.4 Protein M04F3.4, isoform a	R.YINDWTNC*FR.G	
5.23	5.65	5.44	Q9XUY0	F56G4.6 Protein F56G4.6	R.NC*YGVIR.C	
6.46	4.49	5.475	Q95QW0	eif-3.L Eukaryotic translation initiation factor 3 subunit	R.NAFATGC*PK.F	
5.38	5.58	5.48	Q21032	idh-1 Isocitrate dehydrogenase [NADP]	K.SDGGFVWAC*K.N	
5.19	5.78	5.485	P53588	F47B10.1 Probable succinyl-CoA ligase [ADP-forming] subunit	R.ILPC*DNLDEAAK.M	
5.87	5.17	5.52	Q23621	gdh-1 Glutamate dehydrogenase	K.C*AVVDVPPFGGAK.G	<b>ADP-ribosylcysteine</b>
5.53	0	5.53	Q17348	snr-1 Small nuclear ribonucleoprotein Sm D3	K.LSEAEDNMNC*QLAE TVVTFR.D	
0	5.57	5.57	Q21746	sgt-1 Protein SGT-1	K.LNRDPVYFC*NR.A	
5.57	0	5.57	O44906	W05G11.6 Protein W05G11.6, isoform a	K.VINHWPC*NPEK.V	
5.46	5.71	5.585	Q93576	ndk-1 Nucleoside diphosphate kinase	R.GDFC*IQTGR.N	
5.59	0	5.59	Q23588	upp-1 Protein UPP-1	K.FVC*TTGGSPGR.F	
5.46	5.76	5.61	P41932	par-5 14-3-3-like protein 1	K.VEQELNDIC*QDVLK. L	
5.29	5.97	5.63	P91856	F26H9.5 Probable phosphoserine aminotransferase	R.SIMNVC*FR.I	

E9PD17	0.47	UDP-glucuronosyltransferase 3A1	--	--	--	--	--
P30405	1.00E-78	Peptidyl-prolyl cis-trans isomerase F, mitochondrial	No	No	No	No	No
P05387	2.00E-17	60S acidic ribosomal protein P2	No	No	No	No	No
P24752	2.00E-155	Acetyl-CoA acetyltransferase, mitochondrial	Yes	Yes	Yes	Yes	Yes
Q96FJ2	2.00E-60	Dynein light chain 2, cytoplasmic	Yes	Yes	Yes	No	No
P25786	1.00E-97	Proteasome subunit alpha type-1	Yes	Yes	Yes	Yes	No
Q96G23	2.00E-39	Ceramide synthase 2	No	No	No	No	No
E9PR44	2.00E-11	Heat shock protein beta-2	No	No	No	--	--
Q9P2R7	0	Succinyl-CoA ligase [ADP-forming] subunit beta, mitochondrial	No	No	No	No	No
Q9NS18	1.00E-14	Glutaredoxin-2, mitochondrial	Yes	Yes	Yes	--	Yes
E9PLK3	0	Puromycin-sensitive aminopeptidase	No	No	No	No	No
Q9Y4D2	3.7	Sn1-specific diacylglycerol lipase alpha	--	--	--	Yes	No
Q01469	4.00E-08	Fatty acid-binding protein, epidermal	Yes	Yes	--	--	--
Q16822	0	Phosphoenolpyruvate carboxykinase [GTP], mitochondrial	Yes	Yes	Yes	--	--
P23396	1.00E-127	40S ribosomal protein S3	Yes	Yes	Yes	No	Yes
Q5T321	6.3	Neurobeachin	--	--	--	--	--
E9PR44	9.00E-12	Heat shock protein beta-2	No	No	No	--	No
P23396	1.00E-127	40S ribosomal protein S3	Yes	Yes	Yes	No	Yes
B3KY83	2.00E-18	Retinoic acid receptor RXR-alpha	Yes	Yes	Yes	--	--
P62333	0	26S protease regulatory subunit 10B	Yes	Yes	No	No	No
P04406	0	Glyceraldehyde-3-phosphate dehydrogenase	Yes	Yes	Yes	Yes	Yes
O75340	2.00E-65	Programmed cell death protein 6	No	No	Yes	No	No
Q9Y282	3.2	Endoplasmic reticulum-Golgi intermediate compartment protein 3	--	--	--	--	--
Q9Y262	1.00E-144	Eukaryotic translation initiation factor 3 subunit L	Yes	Yes	Yes	--	Yes
O75874	0	Isocitrate dehydrogenase [NADP] cytoplasmic	Yes	Yes	Yes	No	Yes
Q9P2R7	0	Succinyl-CoA ligase [ADP-forming] subunit beta, mitochondrial	Yes	Yes	No	No	No
P00367	0	Glutamate dehydrogenase 1, mitochondrial	Yes	Yes	Yes	No	No
B4DJP7	5.00E-44	Small nuclear ribonucleoprotein Sm D3	Yes	Yes	Yes	No	Yes
O43765	5.00E-61	Small glutamine-rich tetratricopeptide repeat-containing protein alpha	Yes	Yes	Yes	No	Yes
Q16822	0	Phosphoenolpyruvate carboxykinase [GTP], mitochondrial	Yes	Yes	Yes	--	--
P22392	8.00E-75	Nucleoside diphosphate kinase B	Yes	Yes	Yes	No	No
O95045	4.00E-85	Uridine phosphorylase 2	Yes	Yes	Yes	--	--
P63104	3.00E-135	14-3-3 protein zeta/delta	Yes	Yes	Yes	No	Yes
Q9Y617	4.00E-139	Phosphoserine aminotransferase	No	No	No	No	No

0	5.64	5.64	P49041	rps-5 40S ribosomal protein S5	R.VNQAIWLLC*TGAR.E	
5.66	0	5.66	D1MN62	F54C8.7 Protein F54C8.7, isoform c	K.TVDPEFEAQC*EVLK.D	
0	5.72	5.72	Q9N4L8	lpd-5 Protein LPD-5	K.EDAIAFC*EK.N	
0	5.72	5.72	P90868	pbs-7 Protein PBS-7	K.IIGDWSIAETNC*QYE.-	
5.69	5.78	5.735	Q20627	pam-1 Protein PAM-1, isoform a	R.YAFPC*FDEPIYK.A	
5.69	5.83	5.76	Q19626	vha-12 Probable V-type proton ATPase subunit B	R.EDHSDVSNQLYAC*YAIGK.D	
5.17	6.37	5.77	Q9N3C9	rpb-7 Protein RPB-7	K.LFNEVEGTC*TGK.Y	
5.41	6.15	5.78	G5ECL1	M05D6.2 Protein M05D6.2	K.FLIENPNGC*YFAR.Q	
0	5.81	5.81	H2KYZ9	dhs-2 Protein DHS-2, isoform b	R.VVTVASIC*AR.V	
5.84	5.82	5.83	P50432	mel-32 Serine hydroxymethyltransferase	K.AIIAGVSC*YAR.H	
5.6	6.06	5.83	Q94272	fah-1 Protein FAH-1	R.IQQLSEDC*AVLR.D	
5.83	5.85	5.84	Q86MI3	Y71H10B.1 Protein Y71H10B.1, isoform c	K.LTNQMDEEYGC*LGS LFR.T	
5.85	0	5.85	B3GWB2	C08H9.2 Protein C08H9.2, isoform b	K.ANEC*AAAIEEMISEL R.S	
5.45	6.26	5.855	Q10657	tpi-1 Triosephosphate isomerase	K.AGVLVAAQNC*YK.V	
3.87	7.85	5.86	O01685	C32F10.8 Protein C32F10.8, isoform a	R.DGGIPC*NSEDVCLSGGASESIR.N	
5.86	0	5.86	P41938	B0272.3 Probable 3-hydroxyacyl-CoA dehydrogenase B0272.3	K.TTVAC*KDTPGFIVN R.L	
5.73	6	5.865	Q21824	prdx-3 Probable peroxiredoxin prdx-3	R.HTTC*NNDLPVGR.S	
5.71	6.05	5.88	G5EE16	C44H4.4 Protein C44H4.4	R.ITC*SETNR.T	
7.45	4.39	5.92	P90889	F55H12.4 Protein F55H12.4	R.GSTGHC*YK.K	
6.87	5.08	5.975	Q23621	gdh-1 Glutamate dehydrogenase	K.VIGIQEYDC*AVYNPDGIHPK.E	
5.97	6	5.985	Q22053	fib-1 rRNA 2-O-methyltransferase fibrillar	K.ANC*IDSTAEPEAVFA GEVNL.L	
6	0	6	G5EE04	hip-1 Protein HIP-1	K.RPVAAIADC*DK.A	
5.84	6.17	6.005	Q9N599	pas-3 Proteasome subunit alpha type-4	R.NSYGEEMPVEQLVQ NLC*NEK.Q	
5.81	6.21	6.01	Q93572	rpa-0 60S acidic ribosomal protein P0	K.C*LLVGVDNVGSK.Q	
0	6.02	6.02	O01576	npp-11 Protein NPP-11	K.C*ADFLLDQITK.S	
4.52	7.52	6.02	O01685	C32F10.8 Protein C32F10.8, isoform a	K.GYMGEC*GMR.G	
6.1	5.95	6.025	O02089	msra-1 Protein MSRA-1	K.LNAYC*AGFQDFHDL ER.L	
6.03	0	6.03	G5EGP8	cpz-1 Cathepsin Z-like enzyme	K.GPIAC*GIAATK.A	<b>Disulfide</b>
6.03	0	6.03	H2L0N0	unc-132 Protein UNC-132, isoform c	K.IVLTGGPC*GGK.T	
6.04	0	6.04	Q11190	let-721 Electron transfer flavoprotein-ubiquinone oxidore	R.FC*PAGVYEFVPSEADESK.K	Iron-Sulfur (4Fe-4S)
5.25	6.85	6.05	Q95Y90	rpl-9 60S ribosomal protein L9	R.TVC*SHIK.N	
6.06	0	6.06	Q9U1X8	Y62E10A.2 Protein Y62E10A.2	K.SDIQTSTVQC*TDDIV SLLDLLQSETR.H	
5.65	6.52	6.085	P30627	glb-1 Globin-like protein	R.QEISDLC*VK.S	
5.86	6.34	6.1	G5EFZ1	F57B10.3 Cofactor-independent phosphoglycerate mutase	K.AC*EATDIAIGR.I	

P46782	3.00E-125	40S ribosomal protein S5	Yes	Yes	Yes	No	No
P53367	2.00E-42	Arfaptin-1	No	No	No	--	--
O43181	4.00E-44	NADH dehydrogenase [ubiquinone] iron-sulfur protein 4, mitochondrial	No	No	Yes	--	No
P28070	8.00E-42	Proteasome subunit beta type-4	No	No	--	--	--
E9PLK3	0	Puromycin-sensitive aminopeptidase	Yes	Yes	Yes	Yes	Yes
P21281	0	V-type proton ATPase subunit B, brain isoform	Yes	Yes	Yes	No	No
P62487	2.00E-98	DNA-directed RNA polymerase II subunit RPB7	Yes	Yes	Yes	Yes	Yes
Q9NUJ3	1.00E-62	T-complex protein 11-like protein 1	No	No	No	No	--
O75452	5.00E-28	Retinol dehydrogenase 16	No	No	Yes	No	No
P34896	0	Serine hydroxymethyltransferase, cytosolic	Yes	Yes	Yes	No	No
P16930	0	Fumarylacetoacetase	No	No	No	--	No
B7Z382	6.00E-152	Cytosolic purine 5'-nucleotidase	No	No	No	--	No
Q00341	6.00E-134	Vigilin	No	No	No	--	--
P60174	2.00E-107	Triosephosphate isomerase	Yes	Yes	No	No	No
P24298	0	Alanine aminotransferase 1	No	No	No	No	No
Q16836	5.00E-113	Hydroxyacyl-coenzyme A dehydrogenase, mitochondrial	Yes	Yes	No	--	No
E9PH29	5.00E-94	Thioredoxin-dependent peroxide reductase, mitochondrial	No	No	No	No	No
H7C1J4	2.00E-81	Chromosome 6 open reading frame 107, isoform CRA b	No	No	No	--	--
B2RXH2	7.6	Lysine-specific demethylase 4E	--	--	--	--	--
P00367	0	Glutamate dehydrogenase 1, mitochondrial	No	No	No	No	No
P22087	6.00E-133	rRNA 2'-O-methyltransferase fibrillarin	Yes	Yes	Yes	--	Yes
P50502	5.00E-78	Hsc70-interacting protein	Yes	Yes	Yes	No	No
P25789	1.00E-115	Proteasome subunit alpha type-4	Yes	Yes	Yes	No	Yes
P05388	2.00E-133	60S acidic ribosomal protein P0	Yes	Yes	Yes	No	No
P98088	1.70E-47	Mucin-5AC	No	No	No	--	--
P24298	0	Alanine aminotransferase 1	Yes	Yes	Yes	Yes	Yes
Q9UJ68	7.00E-21	Mitochondrial peptide methionine sulfoxide reductase	No	No	No	No	No
Q9UBR2	1.00E-105	Cathepsin Z	Yes	Yes	No	--	No
Q8IZ41	0.99	Ras and EF-hand domain-containing protein	--	--	Yes	--	--
Q16134	0	Electron transfer flavoprotein-ubiquinone oxidoreductase, mitochondrial	Yes	Yes	Yes	Yes	Yes
P32969	3.00E-84	60S ribosomal protein L9	Yes	Yes	Yes	No	No
C9JYM0	2.00E-17	Ribonuclease P protein subunit p20	No	No	No	--	--
Q9ULR3	0.39	Protein phosphatase 1H	--	--	--	--	--
Q6UWY0	0.026	Arylsulfatase K	--	--	--	--	Yes

5.78	6.42	6.1	P91998	F53F1.3 Protein F53F1.3	K.LNTGYDC*PLIGLGT YK.I	
6.1	0	6.1	Q20627	pam-1 Protein PAM-1, isoform a	R.MLC*YYLSEPVFQK. G	
5.86	6.38	6.12	P46769	rps-0 40S ribosomal protein SA	K.LIDIGVPC*NNK.G	
6	6.25	6.125	Q22993	pmt-2 Protein PMT-2	R.DC*IQHHPDTEK.L	
6.14	0	6.14	Reverse_Q 9XWD4	fbxa-216 Reverse sequence, was Protein FBXA-216	K.C*TLNADGNGIK.Y	
6.2	6.08	6.14	Q9XW92	vha-13 V-type proton ATPase catalytic subunit A	K.YDRFC*PFYK.T	
6.64	5.67	6.155	O01804	got-2.1 Aspartate aminotransferase	R.VGAFSIVC*DSAEAAI R.V	
6.22	6.1	6.16	Q22101	T02G5.7 Protein T02G5.7	K.IEEVIGGC*VLPAGLG QNVTR.Q	
0	6.16	6.16	Q18115	rpn-2 26S proteasome non-ATPase regulatory subunit 1	K.VYFC*LEQYER.A	
5.62	6.7	6.16	O61742	rpn-10 Protein RPN-10	K.C*NFIAGIK.I	
4.79	7.53	6.16	Q9N4A5	Y77E11A.1 Protein Y77E11A.1	K.FELVPADEGSC*QGA ALIAVAER.L	
6.17	0	6.17	Q22620	pars-1 Protein PARS-1, isoform a	K.STTC*IEEFKK.L	
6.14	6.21	6.175	O01974	eif-3.H Eukaryotic translation initiation factor 3 subunit	R.LEITNC*FPTVR.N	
5.59	6.79	6.19	O17695	hda-1 Histone deacetylase 1	R.FDPC*AVVLQCGADS LNGDR.L	
6.2	0	6.2	Q93545	F20G2.2 Protein F20G2.2	R.LHILPLDIDC*DESISK .L	
6.08	6.34	6.21	Q09607	gst-36 Probable glutathione S- transferase gst-36	R.AGTNAVDC*AR.L	
6.08	6.34	6.21	P34339	egl-45 Eukaryotic translation initiation factor 3 subunit	R.FGSSDATLAGGVDEC *DNNEGFTGDDTQLGV EGVR.N	
6.28	6.15	6.215	Q22494	vha-15 Probable V-type proton ATPase subunit H 2	K.LAC*FGTTR.M	
6	6.43	6.215	Q03577	drs-1 Aspartate--tRNA ligase, cytoplasmic	R.IQAGIC*NQFR.N	
6.29	6.16	6.225	Q9N4A5	Y77E11A.1 Protein Y77E11A.1	K.GFDIKDC*LQR.D	
6.01	6.49	6.25	P52015	cyn-7 Peptidyl-prolyl cis-trans isomerase 7	R.ALC*TGEK.G	
6.25	0	6.25	P53588	F47B10.1 Probable succinyl-CoA ligase [ADP-forming] subunit	K.GSDATLVEINPMAED VNGDVYC*MDCK.L	
6.26	0	6.26	Q95XJ0	Y69A2AR.18 ATP synthase gamma chain	R.ELIEHSGAAC*V.-	
6.26	0	6.26	Q8I419	F43G6.11 Protein F43G6.11, isoform a	R.LLSQIC*PGK.I	
6.24	6.29	6.265	Q9UAQ6	rab-1 Protein RAB-1	R.YAC*ENVNK.L	
6	6.55	6.275	P18948	vit-6 Vitellogenin-6	R.VIC*PIAEVGTK.F	
5.49	7.07	6.28	P49196	rps-12 40S ribosomal protein S12	K.IIGEYC*GLCK.Y	
6.28	0	6.28	Q23652	ZK863.4 Protein ZK863.4	R.VNEYNFDTLFGDYC* K.F	
6.21	6.37	6.29	O17915	ran-1 GTP-binding nuclear protein ran- 1	R.VC*ENIPIVLCGNK.V	
6.31	0	6.31	Q95QQ4	C55F2.1 Protein C55F2.1, isoform b	R.VSVIC*DPADYDHIIS ELK.S	
6.33	0	6.33	O02115	pen-1 Proliferating cell nuclear antigen	K.MMDIDSEHLGIPDQD YAVVC*EMPAGEFQK.T	
7.2	5.49	6.345	G5EDD4	tba-4 Protein TBA-4	K.AYHEALSVNDITNSC *FEPANQMVK.C	
6.4	6.29	6.345	P04970	gpd-1 Glyceraldehyde-3-phosphate dehydrogenase 1	K.YDASNDHVVSNASC *TTNCLAPLAK.V	Active site nucleophile

Q04828	4.00E-49	Aldo-keto reductase family 1 member C1	No	No	No	No	No
E9PLK3	0	Puromycin-sensitive aminopeptidase	No	No	No	No	No
P08865	6.00E-107	40S ribosomal protein SA	Yes	Yes	Yes	Yes	No
Q9NZJ6	2.00E-05	Ubiquinone biosynthesis O-methyltransferase, mitochondrial	No	No	No	No	No
			--	--	--	--	--
P38606	0	V-type proton ATPase catalytic subunit A	Yes	Yes	Yes	Yes	Yes
P00505	0	Aspartate aminotransferase, mitochondrial	Yes	Yes	Yes	No	Yes
P24752	1.00E-127	Acetyl-CoA acetyltransferase, mitochondrial	No	No	No	No	No
Q99460	0	26S proteasome non-ATPase regulatory subunit 1	No	No	No	No	No
P55036	3.00E-96	26S proteasome non-ATPase regulatory subunit 4	No	No	No	No	No
Q2TB90	1.00E-93	Putative hexokinase HKDC1	No	No	No	No	No
P07814	0	Bifunctional glutamate/proline--tRNA ligase	No	No	No	No	No
O15372	8.00E-63	Eukaryotic translation initiation factor 3 subunit H	Yes	Yes	Yes	--	Yes
Q13547	0	Histone deacetylase 1	No	No	No	No	No
O14756	2.00E-16	17-beta-hydroxysteroid dehydrogenase type 6	No	No	No	No	No
O60760	8.00E-31	Hematopoietic prostaglandin D synthase	No	No	No	--	Yes
Q14152	2.00E-173	Eukaryotic translation initiation factor 3 subunit A	No	No	No	--	No
Q9UI12	9.00E-167	V-type proton ATPase subunit H	No	No	Yes	--	No
P14868	0	Aspartate--tRNA ligase, cytoplasmic	Yes	Yes	Yes	Yes	No
Q2TB90	1.00E-93	Putative hexokinase HKDC1	Yes	Yes	No	No	No
P30405	1.00E-78	Peptidyl-prolyl cis-trans isomerase F, mitochondrial	Yes	Yes	Yes	Yes	Yes
Q9P2R7	0	Succinyl-CoA ligase [ADP-forming] subunit beta, mitochondrial	Yes	Yes	No	Yes	No
P36542	1.00E-111	ATP synthase subunit gamma, mitochondrial	No	No	No	No	No
Q969S8	2.00E-55	Histone deacetylase 10	No	No	No	No	No
P62820	1.00E-120	Ras-related protein Rab-1A	No	No	Yes	No	No
Q8N8U9	8.00E-05	BMP-binding endothelial regulator protein	--	No	--	--	--
P25398	2.00E-47	40S ribosomal protein S12	No	No	No	No	No
Q9NVV4	3.00E-06	Poly(A) RNA polymerase, mitochondrial	No	Yes	No	--	--
P62826	2.00E-139	GTP-binding nuclear protein Ran	Yes	Yes	Yes	Yes	Yes
P31939	0	Bifunctional purine biosynthesis protein PURH	Yes	Yes	Yes	No	No
P12004	2.00E-90	Proliferating cell nuclear antigen	No	No	No	No	No
Q9BQE3	0	Tubulin alpha-1C chain	Yes	Yes	Yes	Yes	No
P04406	0	Glyceraldehyde-3-phosphate dehydrogenase	Yes	Yes	Yes	Yes	Yes

6.7	6.07	6.385	P52011	cyn-3 Peptidyl-prolyl cis-trans isomerase 3	R.ALC*TGENGIGK.S	
6.28	6.49	6.385	P54216	aldo-1 Fructose-bisphosphate aldolase 1	R.ALQASC*LAK.W	
5.56	7.21	6.385	Q18066	dim-1 Disorganized muscle protein 1	R.QNDDGSLELEC*FVD ANPTQVK.W	Disulfide
0	6.39	6.39	B2D6P1	rmd-2 Protein RMD-2, isoform c	K.FC*NEIGNRVEK.D	
6.39	0	6.39	O45622	erfa-3 Protein ERFA-3, isoform a	K.MESGC*VQK.G	
6.44	6.34	6.39	P42170	rnr-2 Ribonucleoside-diphosphate reductase small chain	R.DFAC*LLYSK.L	
5.78	7	6.39	Q21215	rack-1 Guanine nucleotide-binding protein subunit beta-2-	K.VWNLGNC*R.L	
5.91	6.88	6.395	P91917	tag-210 Putative GTP-binding protein tag-210	K.SEAQAENFPFC*TIDP NESR.V	
6.26	6.57	6.415	P46769	rps-0 40S ribosomal protein SA	R.FSPGC*LTNQIQK.T	
6.46	6.38	6.42	Q86B36	fars-1 Protein FARS-1, isoform b	K.IDLNVVYNNPIC*R.L	
4.88	8	6.44	Q9N5V3	imb-3 Protein IMB-3	R.TASAEIMPC*LLTCVE K.Q	
6.18	6.72	6.45	O44451	C04C3.3 Pyruvate dehydrogenase E1 component subunit beta,	K.VVC*PYSAEAK.G	
6.04	6.87	6.455	O02286	R11A5.4 Protein R11A5.4, isoform a	R.GIFIC*DGSQHEADEL IDK.L	
6.14	6.79	6.465	O44906	W05G11.6 Protein W05G11.6, isoform a	K.AELMNPAGIYIC*DG SQK.E	
5.89	7.07	6.48	Q18496	acs-19 Protein ACS-19, isoform a	R.VIEGPGEGSLC*FDR. A	
6.49	0	6.49	P18948	vit-6 Vitellogenin-6	R.SYANNESPC*EQTFSS R.V	
6.42	6.58	6.5	A3QMC5	rpl-34 Protein RPL-34	R.AYGGC*LSPNAVK.E	
5.51	7.51	6.51	G5EFS5	F45D11.15 Protein F45D11.15	R.AFEHSEYTC*GQYW K.K	
6.51	0	6.51	Q03604	rnr-1 Ribonucleoside-diphosphate reductase large subunit	K.TNQAETPATVAESQ DEGC*LMCSG.-	Interacts with thioredoxin/glutaredoxin
6.35	6.7	6.525	Q22067	T01C8.5 Probable aspartate aminotransferase, cytoplasmic	R.INIC*GLNTK.N	
6.72	6.39	6.555	P50093	phb-2 Mitochondrial prohibitin complex protein 2	R.VLPSIC*NEVLK.G	
6.48	6.64	6.56	P34286	pbs-6 Proteasome subunit beta type-1	K.GAVFSYDPIGC*IER.L	
5.64	7.49	6.565	O17607	ruvb-1 Protein RUVB-1	R.LCAQTC*GR.E	
6.58	6.56	6.57	O45924	Y39E4A.3 Protein Y39E4A.3, isoform a	R.GYTMENFMNQC*YG NADDLGK.G	
6.58	0	6.58	P51875	goa-1 Guanine nucleotide-binding protein G(o) subunit al	K.SPLTIC*FPEYSGR.Q	
6.79	6.38	6.585	O45495	uev-1 Protein UEV-1	R.IYNLQIQC*GGNYPR. E	
6.59	0	6.59	G3MU41	ncbp-2 Protein NCBP-2, isoform a	R.TSC*TLYVGNLSYYT K.E	
7.19	6	6.595	Q7Z071	tnt-2 Protein TNT-2, isoform b	R.AFLNVVC*K.A	
6.6	0	6.6	Q17350	Polyadenylate-binding Polyadenylate-binding protein	K.GFGFVC*FEKPEEATS AVTEMNSK.M	
6.63	6.59	6.61	Q9N358	cct-8 T-complex protein 1 subunit theta	K.AC*VTTCPANSFNFN VDNIR.I	
6.45	6.78	6.615	Q27389	rpl-16 60S ribosomal protein L13a	R.C*NINPAR.G	
0	6.62	6.62	Q95Y97	rpa-2 Protein RPA-2	K.DISQDGTTYTYDLC* DPNNTMEYR.T	
6.11	7.13	6.62	O02056	rpl-4 60S ribosomal protein L4	K.LGPVVIYGQDAEC*A R.A	

P30405	1.00E-77	Peptidyl-prolyl cis-trans isomerase F, mitochondrial	Yes	Yes	Yes	Yes	Yes
P04075	3.00E-166	Fructose-bisphosphate aldolase A	No	No	No	--	No
Q8WZ42	7.00E-20	Titin	Yes	Yes	Yes	--	--
Q96DB5	6.00E-27	Regulator of microtubule dynamics protein 1	No	No	--	--	--
Q8IYD1	0	Eukaryotic peptide chain release factor GTP-binding subunit ERF3B	No	No	No	No	No
P31350	5.00E-169	Ribonucleoside-diphosphate reductase subunit M2	Yes	Yes	No	Yes	Yes
P63244	5.00E-168	Guanine nucleotide-binding protein subunit beta-2-like 1	Yes	Yes	Yes	No	Yes
Q9NTK5	0	Obg-like ATPase 1	Yes	Yes	Yes	No	Yes
P08865	6.00E-107	40S ribosomal protein SA	No	No	No	No	No
Q9Y285	0	Phenylalanine--tRNA ligase alpha subunit	Yes	Yes	Yes	No	Yes
O00410	0	Importin-5	No	No	No	No	No
P11177	1.00E-172	Pyruvate dehydrogenase E1 component subunit beta, mitochondrial	No	No	No	No	No
Q16822	0	Phosphoenolpyruvate carboxykinase [GTP], mitochondrial	Yes	Yes	Yes	--	--
Q16822	0	Phosphoenolpyruvate carboxykinase [GTP], mitochondrial	Yes	Yes	Yes	--	--
Q9NR19	0	Acetyl-coenzyme A synthetase, cytoplasmic	No	No	No	No	Yes
Q8N8U9	8.00E-05	BMP-binding endothelial regulator protein	--	No	Yes	--	--
P49207	2.00E-29	60S ribosomal protein L34	No	No	No	No	No
E7EUI1	0.44	Zinc finger protein Helios	--	--	--	--	--
P23921	0	Ribonucleoside-diphosphate reductase large subunit	Yes	Yes	--	--	No
P17174	1.00E-157	Aspartate aminotransferase, cytoplasmic	No	Yes	No	No	No
J3KPX7	2.00E-132	Prohibitin-2	No	No	Yes	No	No
P20618	7.00E-55	Proteasome subunit beta type-1	No	No	No	No	No
Q9Y265	0	RuvB-like 1	No	No	No	No	No
P12694	0	2-oxoisovalerate dehydrogenase subunit alpha, mitochondrial	Yes	Yes	Yes	No	Yes
P09471	0	Guanine nucleotide-binding protein G(o) subunit alpha	Yes	Yes	Yes	No	Yes
Q13404	1.00E-64	Ubiquitin-conjugating enzyme E2 variant 1	Yes	Yes	Yes	Yes	Yes
P52298	4.00E-66	Nuclear cap-binding protein subunit 2	Yes	Yes	Yes	No	No
F8WAF6	0.3	Troponin T cardiac isoform	--	--	No	--	--
P11940	0	Polyadenylate-binding protein 1	Yes	Yes	Yes	Yes	No
P50990	0	T-complex protein 1 subunit theta	Yes	Yes	Yes	No	Yes
P40429	3.00E-73	60S ribosomal protein L13a	No	No	Yes	No	No
P15927	4.00E-11	Replication protein A 32 kDa subunit	No	No	--	--	No
P36578	1.00E-133	60S ribosomal protein L4	No	No	No	No	No

6.62	0	6.62	Q9GYJ9	snx-1 Protein SNX-1	K.ALSMLAAC*EESTSL SR.A	
6.47	6.8	6.635	F5GUA3	T14G10.5 Coatomer subunit gamma	R.SPYAVC*YLIR.I	
6.18	7.09	6.635	G8JYF5	hsp-60 Protein HSP-60, isoform b	R.VTDALC*ATR.A	
4.69	8.58	6.635	Q95ZQ4	aak-2 5-AMP-activated protein kinase catalytic subunit	R.TSC*GSPNYAAPEVIS GK.L	
0	6.65	6.65	Q94055	T14D7.1 Protein T14D7.1	R.LPC*LTTVK.V	
6.44	6.88	6.66	Q22633	hpd-1 4-hydroxyphenylpyruvate dioxygenase	R.GC*EFLSIPSSYYDNL K.E	
5.53	7.8	6.665	G5EE04	hip-1 Protein HIP-1	K.TDLATAC*K.L	
6.67	0	6.67	Q21993	pfd-5 Probable prefoldin subunit 5	K.NC*EQELNFFQESFN ALK.G	
6.67	0	6.67	Q9TZ33	ucr-2.3 Protein UCR-2.3	R.TTQVQDIEGC*K.R	
6.68	0	6.68	Q18066	dim-1 Disorganized muscle protein 1	K.DSGTYTC*NIK.N	
7.5	5.87	6.685	P37165	ubl-1 Ubiquitin-like protein 1-40S ribosomal protein S27	K.ECQQPSC*GGGVFM AQHANR.H	
6.18	7.19	6.685	Q21217	gta-1 Probable 4-aminobutyrate aminotransferase, mitocho	K.AVQTMLC*GTSANEN AIK.T	<b>Iron-Sulfur (2Fe-2S)</b>
6.36	7.03	6.695	Q27389	rpl-16 60S ribosomal protein L13a	K.FC*VVGR.L	
0	6.7	6.7	A9UJN4	pptr-2 Protein PPTR-2, isoform c	R.FLEC*PDFQSQVAK.R	
6.04	7.36	6.7	Q95YF3	cgh-1 ATP-dependent RNA helicase cgh-1	K.TGAYC*IPVIEK.I	
6.7	0	6.7	Q95XN1	Y71G12B.10 Protein Y71G12B.10	R.SADSSIAGLGGC*PYA K.G	<b>Active site</b>
0	6.72	6.72	Q23069	moc-2 Protein MOC-2	R.VCVITVSDTC*SAGT R.T	
6.43	7.09	6.76	G5EF01	tbb-6 Protein TBB-6	K.EIINVQVGQC*GNQIG AK.F	
5.22	8.33	6.775	G8JYF5	hsp-60 Protein HSP-60, isoform b	K.ANEEAGDGTTTC*ATV LAR.A	
6.78	0	6.78	Q9NF11	Y105E8B.5 Protein Y105E8B.5	R.SSC*PEPMTVDFIR.V	
6.79	0	6.79	Q19289	ifb-1 Intermediate filament protein ifb- 1	K.GNVTISEC*DPNGK.F	
0	6.82	6.82	P18948	vit-6 Vitellogenin-6	K.TEEGLIC*R.V	
5.47	8.17	6.82	Q9XTQ5	gob-1 Trehalose-phosphatase	K.LC*DLPGLLSK.F	
6.83	0	6.83	Q22067	T01C8.5 Probable aspartate aminotransferase, cytoplasmic	R.SFGVQC*LSGTGALR. A	
6.84	6.84	6.84	Q8WTM6	arx-4 Probable actin-related protein 2/3 complex subunit	R.NC*FASVFEK.Y	
0	6.84	6.84	Q93934	R07H5.8 Protein R07H5.8	K.ANGWETTC*VK.E	
7.02	6.67	6.845	P50432	mel-32 Serine hydroxymethyltransferase	R.YYGGNEFIDQMELLC *QK.R	
6.38	7.31	6.845	Q9XW92	vha-13 V-type proton ATPase catalytic subunit A	K.C*LGSPER.E	
0	6.85	6.85	Q22285	ttr-46 Transthyretin-like protein 46	R.LLC*GNGPAANVR.V	
6.73	6.97	6.85	Q17763	atp-5 Protein ATP-5	R.IPDPC*NIGLNETPEIE NR.F	
6.67	7.04	6.855	Q93619	tag-173 Protein TAG-173	R.SGNQFDC*GK.L	
6.67	7.04	6.855	G3MU53	eef-2 Protein EEF-2, isoform b	K.TC*DPNGPLMMYISK .M	
6.69	7.03	6.86	Q95XQ8	mcm-4 Protein MCM-4	R.IC*VADVQR.S	
7.41	6.32	6.865	P53588	F47B10.1 Probable succinyl-CoA ligase [ADP-forming] subunit	R.C*DVI AQGIIQAAR.E	
7.08	6.66	6.87	Q10454	F46H5.3 Probable arginine kinase F46H5.3	R.SLQGYPFNPC*LSEA NYLEMESK.V	

O60749	4.00E-95	Sorting nexin-2	No	No	Yes	No	Yes
Q9UBF2	0	Coatomer subunit gamma-2	Yes	Yes	Yes	No	Yes
P10809	1.00E-81	60 kDa heat shock protein, mitochondrial	No	No	No	No	No
P54646	0	5'-AMP-activated protein kinase catalytic subunit alpha-2	Yes	Yes	Yes	Yes	Yes
P21549	3.00E-117	Serine--pyruvate aminotransferase	No	No	No	No	No
P32754	2.00E-173	4-hydroxyphenylpyruvate dioxygenase	No	No	No	--	No
P50502	5.00E-78	Hsc70-interacting protein	Yes	Yes	Yes	No	No
Q99471	2.00E-19	Prefoldin subunit 5	No	No	No	No	No
P22695	1.00E-34	Cytochrome b-c1 complex subunit 2, mitochondrial	No	No	No	No	No
Q8WZ42	7.00E-20	Titin	Yes	Yes	Yes	--	--
P62979	4.00E-43	Ubiquitin-40S ribosomal protein S27a	Yes	Yes	Yes	Yes	Yes
P80404	8.00E-168	4-aminobutyrate aminotransferase, mitochondrial	Yes	Yes	Yes	No	No
P40429	3.00E-73	60S ribosomal protein L13a	No	No	Yes	No	Yes
E9PFR3	0	Serine/threonine-protein phosphatase 2A 56 kDa regulatory subunit delta isoform	No	No	No	No	No
P26196	0	Probable ATP-dependent RNA helicase DDX6	No	No	Yes	No	Yes
P35914	1.00E-113	Hydroxymethylglutaryl-CoA lyase, mitochondrial	Yes	Yes	Yes	--	Yes
Q9NQX3	6.00E-37	Gephyrin	Yes	Yes	Yes	--	No
P68371	1.00E-175	Tubulin beta-4B chain	Yes	Yes	Yes	Yes	Yes
P10809	1.00E-81	60 kDa heat shock protein, mitochondrial	No	No	No	No	No
P00492	5.00E-61	Hypoxanthine-guanine phosphoribosyltransferase	No	No	--	--	No
P02545	2.00E-55	Prelamin-A/C	No	No	No	--	--
Q8N8U9	8.00E-05	BMP-binding endothelial regulator protein	--	--	--	--	--
H0YCT9	2.3	Sororin	--	--	--	--	--
P17174	1.00E-157	Aspartate aminotransferase, cytoplasmic	No	No	No	No	Yes
O15144	2.00E-156	Actin-related protein 2/3 complex subunit 2	Yes	Yes	Yes	No	No
P55263	8.00E-120	Adenosine kinase	No	No	No	Yes	No
P34896	0	Serine hydroxymethyltransferase, cytosolic	Yes	Yes	No	Yes	Yes
P38606	0	V-type proton ATPase catalytic subunit A	Yes	Yes	Yes	No	Yes
J3QT39	2.5	Coiled-coil domain containing 14, isoform CRA_c	--	--	--	--	--
E7EVL6	0.17	Replication initiator 1	--	--	--	--	--
P21953	4.00E-176	2-oxoisovalerate dehydrogenase subunit beta, mitochondrial	Yes	Yes	Yes	Yes	Yes
P13639	0	Elongation factor 2	Yes	Yes	Yes	Yes	Yes
P33991	0	DNA replication licensing factor MCM4	No	No	No	No	No
Q9P2R7	0	Succinyl-CoA ligase [ADP-forming] subunit beta, mitochondrial	Yes	Yes	Yes	Yes	Yes
P06732	4.00E-82	Creatine kinase M-type	No	No	Yes	--	--

6.52	7.23	6.875	Q19246	dhs-25 Protein DHS-25	K.TPMTEAMPPTVLAEIC*K.G	
0	6.89	6.89	P54216	aldo-1 Fructose-bisphosphate aldolase 1	R.YASIC*QONGLVPIVEPEILPDGEHCLAR.G	
6.84	6.94	6.89	O02056	rpl-4 60S ribosomal protein L4	R.SGQGAFGNMC*R.G	
6.46	7.33	6.895	Q93573	tct-1 Translationally-controlled tumor protein homolog	K.LVEMNC*YEDASMF K.A	
7.29	6.51	6.9	P48158	rpl-23 60S ribosomal protein L23	R.ISLGLPVGAVMNC*A DNTGAK.N	
6.61	7.19	6.9	Q23027	inx-5 Innexin-5	R.TFNESC*ELK.I	
8.59	5.24	6.915	O16259	sti-1 Protein STI-1	K.AAC*LVAMR.E	
7.37	6.46	6.915	G5EF87	swn-1 Protein SWSN-1	K.GVQAAAASC*LAAA AVK.A	
6.92	6.91	6.915	Q17334	sodh-1 Alcohol dehydrogenase 1	K.LMNFNC*LNCEFCK.K	Zinc-binding
6.29	7.54	6.915	G5EES6	ufd-3 Protein UFD-3, isoform b	K.ALAVTQGGC*LISGG R.D	
7.14	6.72	6.93	P46562	alh-9 Putative aldehyde dehydrogenase family 7 member A1	R.STC*TINYSK.E	
7.07	6.81	6.94	Q10663	gei-7 Bifunctional glyoxylate cycle protein	K.DNIVGLNC*GR.W	
0	6.94	6.94	Q19057	acd-12 Protein ACDH-12, isoform a	R.FGIPAAC*TGAMK.H	
0	6.94	6.94	Q5CCJ2	H06I04.3 Protein H06I04.3, isoform c	R.SNDYSC*LIR.V	
6.93	6.96	6.945	G5EGR8	W02A11.1 Protein W02A11.1	R.LVSFSPC*LEQVQR.A	
7.56	6.34	6.95	C1P636	uba-1 Protein UBA-1, isoform c	K.DALIDARPSSAEDC*I R.W	
6.95	0	6.95	Q9N3X2	rps-4 40S ribosomal protein S4	R.IQAAEADFKLC*K.V	
6.95	0	6.95	G5EDZ9	cpi-1 Cystatin	R.QGSVQASQVTAANC* PLK.S	Disulfide
6.58	7.34	6.96	P34455	aco-2 Probable aconitate hydratase, mitochondrial	K.VSLIGSC*TNSSYED MTR.A	Iron-Sulfur (4Fe-4S)
6.96	0	6.96	Q9XW17	car-1 Protein CAR-1	K.TSFFDNISC*ESLEK.A	
6.86	7.07	6.965	O45812	T23G11.7 Protein T23G11.7, isoform b	K.STQIFTC*LR.D	
0	6.98	6.98	Q18036	C16A3.5 Protein C16A3.5	K.SQILLADGC*R.Q	
0	7	7	O16294	F32D1.5 Probable GMP reductase	R.SAC*TYTGAK.H	NADP-binding
6.83	7.19	7.01	Q21276	K07C5.4 Uncharacterized NOP5 family protein K07C5.4	R.VDC*FSETPVSTYGEF LR.Q	
7.01	0	7.01	P52899	T05H10.6 Probable pyruvate dehydrogenase E1 component subun	R.GFCHLYSGQEAC*AV GMK.A	
7.23	6.8	7.015	Q8WQA4	exc-4 Chloride intracellular channel exc-4	R.VC*EQLSNIDQLLSER .K	
7.06	6.98	7.02	P34659	snr-5 Probable small nuclear ribonucleoprotein F	R.C*NNVLYVGGVDGE NETSA.-	
6.8	7.24	7.02	Q9U2X0	prmt-1 Protein PRMT-1	R.LYVC*AIEDR.Q	
6.97	7.09	7.03	Q18678	srs-2 Probable serine--tRNA ligase, cytoplasmic	R.ELVSC*SNCLDYQSR. R	
0	7.04	7.04	P54811	cdc-48.1 Transitional endoplasmic reticulum ATPase homolog	K.NTVGFSGADLTEIC* QR.A	
6.89	7.19	7.04	Q9XUV0	pbs-5 Proteasome subunit beta type	K.YC*TLYELR.E	
6.5	7.6	7.05	Q9XW92	vha-13 V-type proton ATPase catalytic subunit A	K.LAANNPLLC*GQR.V	
7.05	0	7.05	P27798	crt-1 Calreticulin	R.ADADLGDFHGETPY NVMFGPDIC*GPTR.R	Disulfide

Q92506	2.00E-76	Estradiol 17-beta-dehydrogenase 8	No	No	No	No	No
P04075	3.00E-166	Fructose-bisphosphate aldolase A	Yes	Yes	Yes	--	Yes
P36578	1.00E-133	60S ribosomal protein L4	Yes	Yes	Yes	Yes	Yes
P13693	2.00E-24	Translationally-controlled tumor protein	No	No	No	No	No
P62829	4.00E-85	60S ribosomal protein L23	Yes	Yes	Yes	Yes	Yes
Q96RD6	0.014	Pannexin-2	--	--	No	--	--
F5H0T1	6.00E-125	Stress-induced-phosphoprotein 1	No	No	No	No	No
Q8TAQ2	4.00E-133	SWI/SNF complex subunit SMARCC2	No	No	--	No	No
P08319	7.00E-20	Alcohol dehydrogenase 4	Yes	Yes	Yes	Yes	Yes
Q9Y263	5.00E-75	Phospholipase A-2-activating protein	No	No	No	No	No
P49419	0	Alpha-aminoadipic semialdehyde dehydrogenase	Yes	Yes	No	--	Yes
Q9Y4D2	3.7	Sn1-specific diacylglycerol lipase alpha	--	--	--	Yes	Yes
P49748	0	Very long-chain specific acyl-CoA dehydrogenase, mitochondrial	No	No	No	No	No
J3KS36	9.00E-69	pre-rRNA-processing protein FTSJ3	No	No	No	No	--
Q96FX7	5.00E-77	tRNA (adenine(58)-N(1))-methyltransferase catalytic subunit TRMT61A	Yes	Yes	Yes	Yes	Yes
P22314	0	Ubiquitin-like modifier-activating enzyme 1	Yes	Yes	Yes	Yes	Yes
P62701	6.00E-123	40S ribosomal protein S4, X isoform	Yes	Yes	Yes	No	Yes
P28325	5.00E-08	Cystatin-D	Yes	Yes	--	--	No
Q99798	0	Aconitate hydratase, mitochondrial	Yes	Yes	Yes	Yes	Yes
I3L4Q1	5.00E-39	Protein LSM14 homolog A	Yes	Yes	--	No	--
Q9NP79	2.00E-51	Vacuolar protein sorting-associated protein VTA1 homolog	Yes	Yes	Yes	--	No
Q9Y6M9	3.00E-22	NADH dehydrogenase [ubiquinone] 1 beta subcomplex subunit 9	No	No	No	--	No
P36959	0	GMP reductase 1	Yes	Yes	Yes	Yes	No
O00567	0	Nucleolar protein 56	Yes	Yes	Yes	No	Yes
P08559	2.00E-159	Pyruvate dehydrogenase E1 component subunit alpha, somatic form, mitochondrial	Yes	Yes	Yes	No	No
Q9Y696	4.00E-15	Chloride intracellular channel protein 4	No	No	No	--	--
P62306	3.00E-34	Small nuclear ribonucleoprotein F	Yes	Yes	Yes	Yes	Yes
Q99873	1.00E-170	Protein arginine N-methyltransferase 1	No	No	No	No	No
P49591	0	Serine--tRNA ligase, cytoplasmic	Yes	Yes	Yes	Yes	Yes
P55072	0	Transitional endoplasmic reticulum ATPase	Yes	Yes	Yes	No	Yes
P28062	4.00E-64	Proteasome subunit beta type-8	Yes	Yes	Yes	Yes	Yes
P38606	0	V-type proton ATPase catalytic subunit A	No	No	No	--	No
P27797	4.00E-168	Calreticulin	Yes	Yes	Yes	Yes	Yes

7.05	0	7.05	Q21831	snfc-5 Protein SNFC-5	R.TYAFSESPLATVDC*PFR.T	
7.06	0	7.06	G5ECW7	F02E9.9 Protein F02E9.9, isoform b	R.SLYIIPNETPVC*QLDAADAFK.T	
6.8	7.32	7.06	G5ECU5	F44E5.4 Protein F44E5.4	R.ARFEELC*ADLFR.S	
6.78	7.37	7.075	Q23621	gdh-1 Glutamate dehydrogenase	K.C*DIFVPAACEK.S	
7.55	6.61	7.08	P49596	T23F11.1 Probable protein phosphatase 2C T23F11.1	K.RDPQISC*EELLTR.C	
7	7.16	7.08	Q18678	srs-2 Probable serine--tRNA ligase, cytoplasmic	K.YAGVSTC*FR.Q	
7.08	0	7.08	Q93353	C37E2.1 Probable isocitrate dehydrogenase [NAD] subunit be	R.EQTEGEYSSLEHELVPGVIEC*LK.I	
7.08	0	7.08	Q9BL43	Y71H2AM.13 Protein Y71H2AM.13	R.PLNAC*R.N	
7.08	0	7.08	O61199	T22B11.5 2-oxoglutarate dehydrogenase, mitochondrial	R.VEQLSPFPYDLVQQEC*R.K	
7.09	0	7.09	O61790	R12E2.11 Protein R12E2.11	R.MAAQAMC*EK.I	
7.1	0	7.1	Q9N456	glrx-10 Protein GLRX-10	K.DC*NEIQDYLGSLTGAR.S	
9.58	4.63	7.105	P47207	cct-2 T-complex protein 1 subunit beta	K.LC*MVSSAAEATEQILR.V	
0	7.11	7.11	O17626	C31C9.2 Protein C31C9.2	K.VLIADDIEQEC*VDILK.Q	
7.11	0	7.11	Q17569	C01G5.6 Protein C01G5.6	K.VEDAHFSC*PFEVMA R.R	
7.2	7.03	7.115	O17921	tbb-1 Protein TBB-1	R.EIVHVQAGQC*GNQIGSK.F	
6.58	7.65	7.115	G3MU14	gsp-1 Serine/threonine-protein phosphatase	R.GNHEC*ASINR.I	
6.71	7.53	7.12	Q21032	idh-1 Isocitrate dehydrogenase [NADP]	K.DLAIC*VK.G	
7.2	7.05	7.125	Q17543	C01B10.3 Protein C01B10.3	R.TLC*PAWSDR.I	
6.93	7.38	7.155	Q22038	rho-1 Ras-like GTP-binding protein rhoA	K.KLVIVGDGAC*GK.T	GTP-binding
6.77	7.56	7.165	Q27464	gspd-1 Glucose-6-phosphate 1-dehydrogenase	K.SSC*ELSTHLAK.L	
7.48	6.85	7.165	Q22054	rps-16 40S ribosomal protein S16	K.TATAVAHC*K.K	
7.17	0	7.17	Q9TY0	M57.2 Protein M57.2	R.LVFC*ETPLVEK.T	
7.07	7.28	7.175	G8JY38	vit-2 Protein VIT-2, isoform b	R.VAIVC*SK.V	
7.43	6.94	7.185	P52819	rpl-22 60S ribosomal protein L22	K.FNVEC*KNPVEDGILR.I	
5.28	9.09	7.185	P48158	rpl-23 60S ribosomal protein L23	R.LPSAGVGD MFVC*SVK.K	
6.99	7.4	7.195	Q93572	rpa-0 60S acidic ribosomal protein P0	K.AGAIAPC*DVK.L	
7.18	7.22	7.2	Q95QH4	F32A5.8 Protein F32A5.8	K.IDFISC*DLNSLQSAK.A	
6.79	7.62	7.205	Q3LFN1	lbp-9 Protein LBP-9, isoform b	K.LVIVC*TCNGVK.C	
0	7.21	7.21	Q17335	H24K24.3 Alcohol dehydrogenase class-3	K.FFGATEC*INPK.S	
6.75	7.68	7.215	G5ECR7	elb-1 Protein ELB-1	K.AQC*PAALGLR.L	
7.22	0	7.22	Q21742	R05F9.6 Protein R05F9.6	K.DLEC*DFTQVGR.Y	
7.27	7.21	7.24	P49196	rps-12 40S ribosomal protein S12	K.GLHETC*K.A	
7.17	7.31	7.24	P18948	vit-6 Vitellogenin-6	R.NQFTPC*YSVLAK.D	
6.81	7.7	7.255	Q9N5B3	W08E12.7 Protein W08E12.7	K.MGVVEC*EK.Y	
8.14	6.38	7.26	Q9N5K2	rpb-5 DNA-directed RNA polymerases I, II, and III subunit	R.IQQC*DPVAR.Y	
7.53	7	7.265	Q9NLD1	hrp-2 Protein HRP-2, isoform a	R.GYAFVTYC*NK.E	

Q12824	1.00E-127	SWI/SNF-related matrix-associated actin-dependent regulator of chromatin subfamily B member 1	No	No	No	No	--
G3V1D3	0	Dipeptidyl peptidase 3	No	No	No	No	--
P11142	0	Heat shock cognate 71 kDa protein	No	Yes	Yes	Yes	No
P00367	0	Glutamate dehydrogenase 1, mitochondrial	Yes	Yes	Yes	No	Yes
P35813	9.00E-65	Protein phosphatase 1A	Yes	Yes	Yes	No	Yes
P49591	0	Serine--tRNA ligase, cytoplasmic	Yes	Yes	Yes	Yes	Yes
O43837	2.00E-142	Isocitrate dehydrogenase [NAD] subunit beta, mitochondrial	Yes	Yes	Yes	No	No
P23141	2.00E-53	Liver carboxylesterase 1	No	No	No	--	No
Q02218	0	2-oxoglutarate dehydrogenase, mitochondrial	No	No	No	No	No
E9PFD2	8.00E-50	Uridine 5'-monophosphate synthase	No	No	No	No	No
P35754	2.00E-26	Glutaredoxin-1	No	No	No	No	No
P78371	0	T-complex protein 1 subunit beta	No	No	No	No	No
O43175	3.00E-115	D-3-phosphoglycerate dehydrogenase	Yes	Yes	Yes	No	No
Q8WTU0	3.00E-40	Protein DDI1 homolog 1	Yes	Yes	No	Yes	Yes
P07437	0	Tubulin beta chain	Yes	Yes	Yes	Yes	Yes
P62140	0	Serine/threonine-protein phosphatase PP1-beta catalytic subunit	Yes	Yes	Yes	Yes	Yes
O75874	0	Isocitrate dehydrogenase [NADP] cytoplasmic	Yes	Yes	Yes	No	No
Q14642	6.00E-14	Type I inositol 1,4,5-trisphosphate 5-phosphatase	Yes	Yes	Yes	--	--
P61586	8.00E-125	Transforming protein RhoA	Yes	Yes	Yes	Yes	No
P11413	0	Glucose-6-phosphate 1-dehydrogenase	No	No	No	No	No
P62249	2.00E-76	40S ribosomal protein S16	Yes	Yes	Yes	No	Yes
Q92696	5.00E-68	Geranylgeranyl transferase type-2 subunit alpha	No	--	--	--	--
Q8N8U9	0.003	BMP-binding endothelial regulator protein	--	--	No	--	--
P35268	2.00E-31	60S ribosomal protein L22	Yes	Yes	Yes	No	Yes
P62829	4.00E-85	60S ribosomal protein L23	No	No	No	No	No
P05388	2.00E-133	60S acidic ribosomal protein P0	Yes	Yes	No	No	No
Q9NZC7	5.00E-40	WW domain-containing oxidoreductase	No	No	No	No	No
P15090	3.00E-33	Fatty acid-binding protein, adipocyte	Yes	Yes	No	--	--
P11766	0	Alcohol dehydrogenase class-3	Yes	Yes	No	No	No
Q15370	5.00E-19	Transcription elongation factor B polypeptide 2	No	No	No	--	--
P36871	0	Phosphoglucomutase-1	No	No	No	No	No
P25398	2.00E-47	40S ribosomal protein S12	No	No	Yes	No	No
Q8N8U9	8.00E-05	BMP-binding endothelial regulator protein	--	--	--	--	--
Q9UQ80	1.00E-128	Proliferation-associated protein 2G4	Yes	Yes	Yes	No	Yes
P19388	2.00E-122	DNA-directed RNA polymerases I, II, and III subunit RPABC1	No	No	No	No	No
O60506	8.00E-131	Heterogeneous nuclear ribonucleoprotein Q	Yes	Yes	No	No	No

0	7.27	7.27	P53596	C05G5.4 Probable succinyl-CoA ligase [ADP/GDP-forming] sub	R.LVGPNC*PGIISADQC K.I	
6.94	7.62	7.28	Q19626	vha-12 Probable V-type proton ATPase subunit B	K.NTIC*EFTGDILR.T	
7.28	0	7.28	Q9XUV0	pbs-5 Proteasome subunit beta type	R.MVATMAGGAADC*Q FWTR.I	
7.11	7.48	7.295	G5EF87	swn-1 Protein SWSN-1	R.LNPFEYVSATAC*R.R	
6.72	7.89	7.305	Q27371	mup-2 Troponin T	R.NFLAAVC*R.V	
7.31	0	7.31	P52899	T05H10.6 Probable pyruvate dehydrogenase E1 component subun	K.EYC*DSGKGPLMME MATYR.Y	
7.3	7.32	7.31	Q09979	dhs-6 Protein DHS-6	K.ALPC*IVDVR.D	
6.57	8.05	7.31	Q9U2K8	abce-1 Protein ABCE-1	R.VALALC*LGK.T	
7.48	7.15	7.315	O02286	R11A5.4 Protein R11A5.4, isoform a	K.LEAYENNYIC*R.T	
6.85	7.79	7.32	A3QMC5	rpl-34 Protein RPL-34	K.C*RDTGVK.L	
7.54	7.11	7.325	Q17334	sodh-1 Alcohol dehydrogenase 1	K.DTNLAAAAAPILC*AG VTVYK.A	Zinc-binding (Catalytic)
0	7.34	7.34	Q9U3N5	C35C5.3 Putative selT-like protein C35C5.3	R.IFYCVSC*GYK.Q	Redox-active disulfide
7.1	7.58	7.34	Q8WQA8	rps-20 Protein RPS-20	R.KTPC*GEGSK.T	
7.43	7.26	7.345	Q09533	rpl-10 60S ribosomal protein L10	K.MLSC*AGADR.L	
7	7.71	7.355	O17953	dld-1 Dihydrolipoyl dehydrogenase	R.GIDC*TASLNLPK.M	
5.25	9.46	7.355	P17331	gpd-4 Glyceraldehyde-3-phosphate dehydrogenase 4	K.YDASNDHVISNASC* TTNCLAPLAK.V	Active site nucleophile
7.38	0	7.38	Q18217	ula-1 NEDD8-activating enzyme E1 regulatory subunit	K.VTDTAIAEIC*R.F	
6.98	7.79	7.385	Q966I8	pbs-1 Proteasome subunit beta type	K.ITPITDNMVVC*R.S	
7.14	7.65	7.395	P47209	cct-5 T-complex protein 1 subunit epsilon	R.MLSIEQC*PNNK.A	
7.21	7.59	7.4	P49197	rps-21 40S ribosomal protein S21	R.YAIC*GAIR.R	
7.1	7.7	7.4	O17612	ech-1 Protein ECH-1	K.DC*PGFFVVR.C	
6.7	8.11	7.405	G8JY05	nmt-1 Glycylpeptide N-tetradecanoyltransferase	K.C*ADMKPSQIGLVLQ.	
7.04	7.78	7.41	Q21215	rack-1 Guanine nucleotide-binding protein subunit beta-2-	K.LWNTLAQC*K.Y	
7.41	0	7.41	Q9N4E9	ppfr-4 Protein PFR-4	R.C*YEELQAIDDELPLL K.M	
7.61	7.23	7.42	O01692	rps-17 40S ribosomal protein S17	R.VC*DEVAIIGSK.P	
6.93	7.91	7.42	O76449	ZK1055.7 Protein ZK1055.7	K.EDWTSAPLVLSTAQP C*LAGR.I	
9	5.86	7.43	P37165	ubl-1 Ubiquitin-like protein 1-40S ribosomal protein S27	R.C*HDTLVVDTATAAA TSGEK.G	
0	7.43	7.43	H2KYJ5	mtch-1 Protein MTCH-1, isoform a	K.YTTC*AQALAVIGK.Q	
7.93	6.96	7.445	Q17334	sodh-1 Alcohol dehydrogenase 1	K.DMSVC*PLVGGHEG AGSVVQIGK.N	
7.45	0	7.45	G5EDW8	VF13D12L.3 Protein VF13D12L.3	R.FMVEC*MTK.V	
7.52	7.4	7.46	Q9TXP0	rps-27 40S ribosomal protein S27	K.LTEGC*SFR.K	
6.52	8.41	7.465	O44549	acd-3 Protein ACDH-3	K.YAIEC*LNAGR.I	
6.5	8.44	7.47	Q9XWS4	rpl-30 Protein RPL-30	R.VC*TLAVTDAGDSDII LSVPSESA.-	
7.4	7.54	7.47	Q21217	gta-1 Probable 4-aminobutyrate aminotransferase, mitocho	R.SLC*MLSVTR.S	
7.17	7.78	7.475	G5ECU1	skr-1 Protein SKR-1	K.GLLDVTC*K.T	

P53597	5.00E-132	Succinyl-CoA ligase [ADP/GDP-forming] subunit alpha, mitochondrial	Yes	Yes	Yes	Yes	Yes
P21281	0	V-type proton ATPase subunit B, brain isoform	Yes	Yes	Yes	No	No
P28062	4.00E-64	Proteasome subunit beta type-8	Yes	Yes	Yes	Yes	Yes
Q8TAQ2	4.00E-133	SWI/SNF complex subunit SMARCC2	Yes	Yes	Yes	No	Yes
P45379	1.60E-20	Troponin T, cardiac muscle	No	No	No	--	--
P08559	2.00E-159	Pyruvate dehydrogenase E1 component subunit alpha, somatic form, mitochondrial	Yes	Yes	No	Yes	No
Q6YN16	1.00E-141	Hydroxysteroid dehydrogenase-like protein 2	Yes	Yes	Yes	No	No
P61221	0	ATP-binding cassette sub-family E member 1	Yes	Yes	Yes	No	Yes
Q16822	0	Phosphoenolpyruvate carboxykinase [GTP], mitochondrial	No	No	No	--	--
P49207	2.00E-29	60S ribosomal protein L34	Yes	Yes	Yes	Yes	Yes
P08319	7.00E-20	Alcohol dehydrogenase 4	Yes	Yes	Yes	Yes	Yes
P62341	8.00E-34	Selenoprotein T	No	No	Yes	--	Yes
P60866	8.00E-56	40S ribosomal protein S20	Yes	Yes	Yes	No	Yes
P27635	3.00E-111	60S ribosomal protein L10	Yes	Yes	Yes	Yes	Yes
P09622	0	Dihydrolipoyl dehydrogenase, mitochondrial	No	No	Yes	No	No
P04406	0	Glyceraldehyde-3-phosphate dehydrogenase	Yes	Yes	Yes	Yes	Yes
Q13564	3.00E-109	NEDD8-activating enzyme E1 regulatory subunit	Yes	Yes	Yes	--	Yes
P28072	2.00E-66	Proteasome subunit beta type-6	Yes	Yes	Yes	Yes	Yes
P48643	0	T-complex protein 1 subunit epsilon	Yes	Yes	Yes	No	Yes
P63220	1.00E-35	40S ribosomal protein S21	Yes	Yes	Yes	No	Yes
P40939	0	Trifunctional enzyme subunit alpha, mitochondrial	No	No	No	--	Yes
F5H594	2.00E-170	Bad ID	Yes	Yes	Yes	No	No
P63244	5.00E-168	Guanine nucleotide-binding protein subunit beta-2-like 1	Yes	Yes	Yes	Yes	Yes
P78318	3.00E-40	Immunoglobulin-binding protein 1	No	No	No	No	--
P08708	1.00E-55	40S ribosomal protein S17	Yes	Yes	Yes	Yes	No
Q9Y6X9	4.8	MORC family CW-type zinc finger protein 2	No	No	--	--	--
P62979	4.00E-43	Ubiquitin-40S ribosomal protein S27a	Yes	Yes	Yes	Yes	Yes
Q9Y6C9	9.00E-36	Mitochondrial carrier homolog 2	No	No	No	--	--
P08319	7.00E-20	Alcohol dehydrogenase 4	No	No	No	No	No
P00966	2.6	Argininosuccinate synthase	--	--	Yes	--	--
P42677	8.00E-38	40S ribosomal protein S27	Yes	Yes	Yes	No	Yes
P45954	3.00E-178	Short/branched chain specific acyl-CoA dehydrogenase, mitochondrial	No	No	No	No	No
P62888	1.00E-55	60S ribosomal protein L30	Yes	Yes	Yes	No	No
P80404	8.00E-168	4-aminobutyrate aminotransferase, mitochondrial	No	No	No	No	No
P63208	3.00E-73	S-phase kinase-associated protein 1	Yes	Yes	Yes	Yes	Yes

6.58	8.37	7.475	Q17761	T25B9.9 6-phosphogluconate dehydrogenase, decarboxylating	K.SNGEPC*CDWVGNA GSGHFVK.M	
7.48	0	7.48	Q09545	sdhb-1 Succinate dehydrogenase [ubiquinone] iron-sulfur s	K.C*HTIMNCTK.T	Iron-sulfur 3 (3Fe-4S)
7.11	7.86	7.485	Q9BKU5	Y37E3.8 Protein Y37E3.8, isoform a	K.NQHYC*PTVNVER.L	
6.59	8.38	7.485	O02141	C46G7.2 Protein C46G7.2	K.SDSVSTLAPSLALPQ YC*R.E	
7.52	0	7.52	Q10663	gei-7 Bifunctional glyoxylate cycle protein	R.ANC*TKEDLTVIPEGT R.T	
7.52	0	7.52	Q17489	unc-44 Protein UNC-44, isoform a	K.DGSSPFDNQEEDEPIA SC*K.Q	
7.67	7.38	7.525	O17214	fum-1 Probable fumarate hydratase, mitochondrial	R.C*GLGELSLPENEPGS SIMPVK.V	
0	7.53	7.53	Q09533	rpl-10 60S ribosomal protein L10	R.ANVDTFPAC*VHMM SNER.E	
7.48	7.6	7.54	Q2HQL4	gln-3 Glutamine synthetase	R.TVC*LEGAER.K	
7.51	7.59	7.55	Q10454	F46H5.3 Probable arginine kinase F46H5.3	R.FLQAANAC*R.Y	
7.31	7.8	7.555	O44549	acd-3 Protein ACDH-3	K.GITC*FLVDR.N	
7.56	0	7.56	Q19680	F21D5.1 Protein F21D5.1	R.CSGPC*LMNAAR.A	
6.62	8.52	7.57	Q9N358	cct-8 T-complex protein 1 subunit theta	R.IAVYTC*PFDLTQTET K.G	
7.81	7.35	7.58	O17586	pas-1 Proteasome subunit alpha type-6	K.NGYDMPC*ELLAK.K	
6.89	8.29	7.59	P34690	tba-2 Tubulin alpha-2 chain	K.AYHEALSVSDITNSC* FEPANQMVK.C	
6.37	8.82	7.595	Q19749	F23B12.5 Dihydrolipoyllysine-residue acetyltransferase comp	K.ASALAC*QR.V	
8.31	6.92	7.615	P41988	cct-1 T-complex protein 1 subunit alpha	K.IAC*LDFSLMK.A	
7.63	7.6	7.615	G5ECS9	cpt-2 Protein CPT-2, isoform a	K.EFVPTYESC*STAAFL K.G	
7.58	7.66	7.62	Q27527	enol-1 Enolase	K.TGAPC*R.S	
8.46	6.81	7.635	Q21154	moma-1 Protein MOMA-1	K.VVDC*AMTQTK.K	
7.7	7.57	7.635	Q93874	rab-14 Protein RAB-14	K.AFAEENGLTFLEC*SA K.T	
7.14	8.17	7.655	Q9TZS5	cct-7 Protein CCT-7, isoform a	K.GQIISNINAC*QVVAD SIR.T	
7.41	7.9	7.655	O02640	mdh-1 Probable malate dehydrogenase, mitochondrial	K.NVQC*AYVASDAVK. G	
0	7.66	7.66	Q22347	acd-10 Probable medium-chain specific acyl-CoA dehydrogen	R.C*LDESAK.Y	
0	7.66	7.66	G5EDZ7	cdr-4 Cadmium-inducible lysosomal protein CDR-4	K.SC*PNLSPFCMK.L	
7.66	0	7.66	O17762	ech-9 Protein ECH-9	K.LSNC*DLIVESVIEDM K.L	
7.45	7.89	7.67	Q9U2M4	Y38F1A.6 Probable hydroxyacid-oxoacid transhydrogenase, mit	K.STDYAFEMVC*STLR. F	
7.66	7.69	7.675	Q8WQA8	rps-20 Protein RPS-20	K.VC*AQLIDGAK.N	
7.68	0	7.68	Q9XUV0	pbs-5 Proteasome subunit beta type	R.DSGSGGVC*NLCBIT PTEK.I	
7.69	0	7.69	Q9GRZ9	Y59A8A.3 Protein Y59A8A.3	K.TEAEPGLVIC*ER.K	
0	7.7	7.7	Q9N5V3	imb-3 Protein IMB-3	R.GC*PIHFGNR.L	
7.38	8.03	7.705	Q17761	T25B9.9 6-phosphogluconate dehydrogenase, decarboxylating	R.VVVC*AAVR.L	
7.85	7.58	7.715	P34552	alx-1 Apoptosis-linked gene 2-interacting protein X 1	K.NTNC*DIANDFLK.A	
7.72	7.71	7.715	H2L0J5	cysl-3 Protein CYSL-3, isoform c	K.VEYLNPC*SVK.D	

P52209	0	6-phosphogluconate dehydrogenase, decarboxylating	Yes	Yes	Yes	Yes	Yes
P21912	3.00E-128	Succinate dehydrogenase [ubiquinone] iron-sulfur subunit, mitochondrial	Yes	Yes	Yes	Yes	Yes
P46776	8.00E-71	60S ribosomal protein L27a	Yes	Yes	No	No	Yes
Q9UM73	0.7	ALK tyrosine kinase receptor	--	--	--	--	--
Q9Y4D2	3.7	Sn1-specific diacylglycerol lipase alpha	--	--	--	No	No
Q8N8A2	0	Serine/threonine-protein phosphatase 6 regulatory ankyrin repeat subunit B	No	No	--	--	--
P07954	0	Fumarate hydratase, mitochondrial	No	No	Yes	Yes	Yes
P27635	3.00E-111	60S ribosomal protein L10	Yes	Yes	Yes	Yes	Yes
P15104	5.00E-178	Glutamine synthetase	No	No	Yes	Yes	No
P06732	4.00E-82	Creatine kinase M-type	No	No	Yes	--	--
P45954	3.00E-178	Short/branched chain specific acyl-CoA dehydrogenase, mitochondrial	No	Yes	No	No	No
O95394	2.00E-131	Phosphoacetylglucosamine mutase	No	No	No	No	No
P50990	0	T-complex protein 1 subunit theta	Yes	Yes	Yes	Yes	No
P60900	2.00E-102	Proteasome subunit alpha type-6	No	No	No	Yes	No
Q9BQE3	0	Tubulin alpha-1C chain	Yes	Yes	Yes	Yes	No
H0YDD4	3.00E-169	Acetyltransferase component of pyruvate dehydrogenase complex	Yes	Yes	No	No	No
P17987	0	T-complex protein 1 subunit alpha	Yes	Yes	Yes	Yes	Yes
P23786	0	Carnitine O-palmitoyltransferase 2, mitochondrial	Yes	Yes	Yes	No	--
P06733	0	Alpha-enolase	Yes	Yes	Yes	No	Yes
Q6UXV4	3.00E-12	MICOS complex subunit MIC27	No	No	No	--	--
P61106	5.00E-130	Ras-related protein Rab-14	No	No	No	No	No
Q99832	0	T-complex protein 1 subunit eta	Yes	Yes	Yes	Yes	Yes
P40926	7.00E-131	Malate dehydrogenase, mitochondrial	Yes	Yes	Yes	No	Yes
P11310	3.00E-179	Medium-chain specific acyl-CoA dehydrogenase, mitochondrial	No	No	Yes	No	Yes
Q5TGI0	1.00E-19	Failed axon connections homolog	No	No	No	--	--
Q08426	4.00E-75	Peroxisomal bifunctional enzyme	No	No	No	--	No
Q81WW8	2.00E-133	Hydroxyacid-oxoacid transhydrogenase, mitochondrial	No	No	No	--	--
P60866	8.00E-56	40S ribosomal protein S20	Yes	Yes	Yes	No	Yes
P28062	4.00E-64	Proteasome subunit beta type-8	No	No	No	No	No
Q7Z7B0	3.6	Filamin-A-interacting protein 1	--	--	--	--	--
O00410	0	Importin-5	No	No	No	--	No
P52209	0	6-phosphogluconate dehydrogenase, decarboxylating	No	No	No	No	Yes
Q8WUM4	0	Programmed cell death 6-interacting protein	No	No	No	No	No
P35520	2.00E-59	Cystathionine beta-synthase	No	No	No	No	Yes

6.85	8.58	7.715	Q7YTR9	C27B7.9 Protein C27B7.9	K.VDC*AMGIIPK.V	
7.72	0	7.72	G5EF11	efl-1 EFL-1	R.C*DLNTAAEALNVR.Q	
7.83	7.62	7.725	Q69Z12	K08E3.10 Protein K08E3.10	K.KVEAAC*GR.S	
7.73	0	7.73	H2KZV8	mlp-1 Protein MLP-1, isoform b	K.LLDSC*TVAPHEAEL YCK.Q	
6.65	8.82	7.735	Q9U2A8	rpl-43 60S ribosomal protein L37a	R.YTCSFC*GK.E	
7.66	7.82	7.74	O62107	gale-1 Protein GALE-1, isoform a	K.DVPFQNVQVDC*DEA ALEK.V	
7.74	0	7.74	Q65XX1	vbh-1 Protein VBH-1, isoform c	R.TYYPC*ALVLSPTR.E	
7.15	8.34	7.745	F5GUA3	T14G10.5 Coatmer subunit gamma	K.ISEILGLVPC*ER.S	
7.75	0	7.75	P90978	uaf-1 Splicing factor U2AF 65 kDa subunit	R.GSVQSAVPVVGPSVT C*QSR.R	
7.58	7.94	7.76	O44480	rpl-20 60S ribosomal protein L18a	R.DTTVAGAVTQC*YR.D	
7.13	8.39	7.76	P50432	mel-32 Serine hydroxymethyltransferase	K.AVMDALGSAMC*NK.Y	
9.91	5.62	7.765	Q22100	kat-1 Protein KAT-1	K.DGLTDAYDKVHMGNC*GEK.T	
6.11	9.42	7.765	O02286	R11A5.4 Protein R11A5.4, isoform a	R.C*VGDDIAWMK.F	
7.52	8.02	7.77	Q18787	rpt-1 26S protease regulatory subunit 7	R.LC*PNSTGAEIR.S	
6.62	8.93	7.775	B1V8J2	Y43F8B.2 Protein Y43F8B.2, isoform c	R.SDC*MVGDFTR.L	
6.92	8.64	7.78	G5EE46	F54D5.12 Protein F54D5.12	K.C*DSGFILEDLDNK.L	
7.61	7.96	7.785	O17759	tkl-1 Protein TKT-1	R.ISSIEMTC*ASK.S	
6.08	9.49	7.785	Q9N362	Y55F3AM.13 Protein Y55F3AM.13	K.AEQILAGSC*DQSFV TR.E	
7.68	7.92	7.8	Q05036	C30C11.4 Uncharacterized protein C30C11.4	K.VSDC*VLAVPSYFTD VQR.R	
7.28	8.32	7.8	Q19264	F09E5.3 Putative deoxyribose-phosphate aldolase	R.IGASSLLDDC*LK.G	
7.89	7.76	7.825	H2L2E8	tba-1 Protein TBA-1, isoform b	R.TIQFVDWC*PTGFK.V	
7.86	7.83	7.845	P53013	eft-3 Elongation factor 1-alpha	K.QLIVAC*NK.M	
7.86	0	7.86	Q9N5B3	W08E12.7 Protein W08E12.7	K.EGAIAGDLC*DLGDK LILEK.T	<b>RNA-binding</b>
7.07	8.69	7.88	Q8IA58	F22F7.1 Protein F22F7.1, isoform b	R.ILQQYPDQC*SFYMF K.N	
7.65	8.13	7.89	Q95X44	vha-8 Protein VHA-8	R.LVEQLLPEC*LDGLQ K.E	
7.9	0	7.9	Q21484	tag-235 Protein TAG-235	R.C*DTGEGDGTVANV AGYATLKF.F	
7.15	8.66	7.905	O17921	tbb-1 Protein TBB-1	K.NMMAAC*DPR.H	
7.91	0	7.91	Q23487	ZK418.9 Protein ZK418.9, isoform a	R.NC*NVVQETTATGQ PKPLR.M	
7.91	0	7.91	P02566	unc-54 Myosin-4	K.VIC*YFAAVGASQQE GGAEVDPNK.K	
7.7	8.14	7.92	Q95005	pas-4 Proteasome subunit alpha type-7	R.IEC*QSYK.L	
7.9	7.96	7.93	O45903	W09H1.5 Probable trans-2-enoyl-CoA reductase 1, mitochondr	K.LALNC*VGGR.S	
7.6	8.27	7.935	Q23621	gdh-1 Glutamate dehydrogenase	K.AVGKDC*PVEPNAAF AAK.I	
8.06	7.81	7.935	Q17361	usp-14 Ubiquitin carboxyl-terminal hydrolase 14	K.QQDANEC*LVSIMSN VTR.I	
7.98	7.92	7.95	O02115	pcn-1 Proliferating cell nuclear antigen	R.LSLC*NDVPVVVEYPI EENGYLR.F	

H7BYS8	5	Leukocyte surface antigen CD47	--	--	--	--	--
Q16254	2.00E-40	Transcription factor E2F4	No	No	No	--	No
P14649	2.00E-17	Myosin light chain 6B	No	No	No	No	No
P50461	9.00E-29	Cysteine and glycine-rich protein 3	No	No	No	--	No
P61513	2.00E-43	60S ribosomal protein L37a	Yes	Yes	Yes	Yes	Yes
Q14376	9.00E-144	UDP-glucose 4-epimerase	No	No	No	Yes	No
B4DXX7	0	ATP-dependent RNA helicase DDX3Y	No	No	No	No	No
Q9UBF2	0	Coatomer subunit gamma-2	Yes	Yes	No	No	Yes
P26368	5.00E-148	Splicing factor U2AF 65 kDa subunit	No	No	No	No	No
Q02543	1.00E-78	60S ribosomal protein L18a	Yes	Yes	Yes	No	No
P34896	0	Serine hydroxymethyltransferase, cytosolic	No	No	No	No	No
P24752	2.00E-155	Acetyl-CoA acetyltransferase, mitochondrial	Yes	Yes	Yes	No	Yes
Q16822	0	Phosphoenolpyruvate carboxykinase [GTP], mitochondrial	Yes	Yes	Yes	--	--
P35998	0	26S protease regulatory subunit 7	Yes	Yes	Yes	Yes	Yes
Q9P0R6	2.00E-17	GSK3-beta interaction protein	No	No	No	--	--
Q8N465	3.00E-140	D-2-hydroxyglutarate dehydrogenase, mitochondrial	Yes	Yes	No	Yes	Yes
P29401	0	Transketolase	No	Yes	No	No	No
O75037	7.5	Kinesin-like protein KIF21B	--	--	--	--	--
O95757	0	Heat shock 70 kDa protein 4L	Yes	Yes	Yes	No	Yes
Q9Y315	4.00E-87	Deoxyribose-phosphate aldolase	No	No	--	--	--
Q9BQE3	0	Tubulin alpha-1C chain	Yes	Yes	Yes	Yes	Yes
Q05639	0	Elongation factor 1-alpha 2	No	No	No	No	Yes
Q9UQ80	1.00E-128	Proliferation-associated protein 2G4	Yes	Yes	Yes	No	Yes
Q8NBX0	4.00E-88	Saccharopine dehydrogenase-like oxidoreductase	No	No	No	--	No
P36543	1.00E-87	V-type proton ATPase subunit E 1	No	No	No	No	No
O14929	2.00E-72	Histone acetyltransferase type B catalytic subunit	No	No	No	No	No
P07437	0	Tubulin beta chain	Yes	Yes	Yes	No	No
Q96AE4	2.00E-56	Far upstream element-binding protein 1	No	No	No	--	--
P13533	0	Myosin-6	No	No	No	No	No
O14818	5.00E-108	Proteasome subunit alpha type-7	Yes	Yes	Yes	No	Yes
Q9BV79	5.00E-92	Trans-2-enoyl-CoA reductase, mitochondrial	Yes	Yes	Yes	No	Yes
P00367	0	Glutamate dehydrogenase 1, mitochondrial	No	No	No	No	--
P54578	2.00E-117	Ubiquitin carboxyl-terminal hydrolase 14	Yes	Yes	Yes	No	Yes
P12004	2.00E-90	Proliferating cell nuclear antigen	No	No	Yes	No	No

0	7.95	7.95	G3MU69	ant-1.1 Protein ANT-1.1, isoform d	K.GLADC*LIK.I	
7.74	8.16	7.95	O45418	fkf-6 Protein FKB-6	K.AAAQQIIVC*R.N	
7.95	0	7.95	P27639	inf-1 Eukaryotic initiation factor 4A	K.MTENQFTVSC*LHGD MDQAER.D	
7.95	0	7.95	Q17695	spdl-1 Protein SPDL-1	R.VC*HLETER.V	
8.33	7.59	7.96	Q17350	Polyadenylate-binding Polyadenylate-binding protein	K.FGNITSC*EVMTVEG K.S	
0	7.96	7.96	Q93934	R07H5.8 Protein R07H5.8	K.GVEASVTC*GSYAAQ EIIK.K	
7.99	7.96	7.975	P48150	rps-14 40S ribosomal protein S14	R.IEDVTPIPSDC*TR.R	
7.91	8.06	7.985	P02566	unc-54 Myosin-4	R.YNC*LNWLEK.N	
8.62	7.38	8	Q9TZS5	cct-7 Protein CCT-7, isoform a	K.C*AATLSSK.L	
6.73	9.28	8.005	G5EBJ8	Y59E9AR.1 Major sperm protein	R.LGVDPPC*GVLDPK.E	
7.21	8.8	8.005	Q23624	ZK829.7 Protein ZK829.7	R.AILEVC*DPSSALDAD QSGGVPIPAATSE.-	
7.77	8.25	8.01	Q27535	ZC434.8 Probable arginine kinase ZC434.8	R.SLQGYFPNPC*LSETN YK.M	
8.7	7.36	8.03	Q09359	ZK1307.1 Uncharacterized protein ZK1307.1	K.SGGACQC*LVLRL	
7.49	8.58	8.035	Q27274	rop-1 60 kDa SS-A/Ro ribonucleoprotein homolog	R.LSNVC*AR.L	
0	8.04	8.04	Q07085	F13H6.3 Esterase CM06B1	K.YGPAC*VQTGGFEQI AGPR.T	Disulfide
8.41	7.68	8.045	Q22067	T01C8.5 Probable aspartate aminotransferase, cytoplasmic	R.AGAEFLASVC*NMK. T	
7.55	8.55	8.05	G5EFZ1	F57B10.3 Cofactor-independent phosphoglycerate mutase	K.VSQFHC*AETEK.Y	
6.87	9.23	8.05	Q9TZS5	cct-7 Protein CCT-7, isoform a	R.QLC*QNAGLDALDV LNK.L	
0	8.06	8.06	O45903	W09H1.5 Probable trans-2-enoyl-CoA reductase 1, mitochondr	K.QPVDC*PTGPLIFK.D	
7.8	8.32	8.06	Q21307	mek-1 Protein MEK-1, isoform a	K.LC*DFGIAGR.L	
8.06	0	8.06	Q19722	nrs-1 Asparagine--tRNA ligase, cytoplasmic	R.IEALVC*DTVDR.L	
8.06	0	8.06	B3GWB2	C08H9.2 Protein C08H9.2, isoform b	K.TGC*VVEVPAEDSGS DQVTLIGNAQDLAK.A	
8.07	0	8.07	P47209	cct-5 T-complex protein 1 subunit epsilon	K.IADGFDLAC*KK.A	
7.99	8.17	8.08	Q9N4J8	cct-3 Protein CCT-3	R.TLIQNC*GGSTIR.K	
7.42	8.77	8.095	P48158	rpl-23 60S ribosomal protein L23	K.EC*ADLWPR.I	
7.98	8.21	8.095	P53013	eft-3 Elongation factor 1-alpha	R.GSVC*SDSKQDPAK.E	
8.68	7.52	8.1	P91277	F26B1.2 Protein F26B1.2, isoform a	K.GTEQQIHSQAQYLLQQ C*VR.N	
8.1	0	8.1	P50432	mel-32 Serine hydroxymethyltransferase	R.QC*LSEDFVQYGEQV L.K.N	
7.98	8.23	8.105	P52709	trs-1 Threonine--tRNA ligase, cytoplasmic	R.C*GPLIDLGR.G	
7.72	8.5	8.11	Q10663	gei-7 Bifunctional glyoxylate cycle protein	K.C*GHMGGK.V	
7.7	8.52	8.11	P46561	atp-2 ATP synthase subunit beta, mitochondrial	R.C*IAMDGTEGLVR.G	
8.11	0	8.11	Q09444	ubh-4 Probable ubiquitin carboxyl- terminal hydrolase ubh	R.GHC*LSNSEIR.T	
8.11	0	8.11	Q17761	T25B9.9 6-phosphogluconate dehydrogenase, decarboxylating	K.GIMFVGC*GVSGGEE GAR.F	

P12236	1.00E-117	ADP/ATP translocase 3	Yes	Yes	Yes	No	No
Q02790	8.00E-112	Peptidyl-prolyl cis-trans isomerase FKBP4	Yes	Yes	Yes	--	--
Q14240	0	Eukaryotic initiation factor 4A-II	No	No	No	No	No
E7EMX7	0.037	Laminin subunit alpha-2	--	--	--	--	--
P11940	0	Polyadenylate-binding protein 1	No	No	No	No	No
P55263	8.00E-120	Adenosine kinase	No	No	Yes	No	No
P62263	9.00E-84	40S ribosomal protein S14	No	No	No	No	No
P13533	0	Myosin-6	No	No	No	No	No
Q99832	0	T-complex protein 1 subunit eta	Yes	Yes	Yes	Yes	Yes
Q9P0L0	4.00E-07	Vesicle-associated membrane protein-associated protein A	No	No	--	--	--
Q00796	1.00E-11	Sorbitol dehydrogenase	Yes	--	No	--	--
P12277	1.00E-83	Creatine kinase B-type	No	No	Yes	--	--
O94760	0.01	N(G),N(G)-dimethylarginine dimethylaminohydrolase 1	--	--	--	--	--
P10155	5.00E-127	60 kDa SS-A/Ro ribonucleoprotein	No	No	--	--	--
Q6NT32	4.00E-61	Carboxylesterase 5A	Yes	Yes	Yes	--	--
P17174	1.00E-157	Aspartate aminotransferase, cytoplasmic	No	No	No	No	No
Q6UWY0	0.026	Arylsulfatase K	--	--	--	--	Yes
Q99832	0	T-complex protein 1 subunit eta	Yes	Yes	Yes	Yes	Yes
Q9BV79	5.00E-92	Trans-2-enoyl-CoA reductase, mitochondrial	No	No	No	No	No
O14733	1.00E-111	Dual specificity mitogen-activated protein kinase kinase 7	Yes	Yes	Yes	Yes	No
O43776	0	Asparagine--tRNA ligase, cytoplasmic	Yes	Yes	Yes	No	No
Q00341	6.00E-134	Vigilin	No	No	No	Yes	--
P48643	0	T-complex protein 1 subunit epsilon	No	No	No	No	No
P49368	0	T-complex protein 1 subunit gamma	Yes	Yes	Yes	No	Yes
P62829	4.00E-85	60S ribosomal protein L23	Yes	Yes	Yes	Yes	Yes
Q05639	0	Elongation factor 1-alpha 2	Yes	Yes	No	Yes	No
P61978	1.00E-67	Heterogeneous nuclear ribonucleoprotein K	No	No	--	No	No
P34896	0	Serine hydroxymethyltransferase, cytosolic	No	No	No	No	No
P26639	0	Threonine--tRNA ligase, cytoplasmic	Yes	Yes	Yes	Yes	Yes
Q9Y4D2	3.7	Sn1-specific diacylglycerol lipase alpha	--	--	--	--	--
P06576	0	ATP synthase subunit beta, mitochondrial	No	No	No	No	No
Q9Y5K5	1.00E-97	Ubiquitin carboxyl-terminal hydrolase isozyme L5	No	No	No	--	No
P52209	0	6-phosphogluconate dehydrogenase, decarboxylating	No	No	No	No	No

6.35	9.88	8.115	G8JY45	aldo-2 Fructose-bisphosphate aldolase	R.YASIC*QANGLVPIVE PEVLCDCGEHDLAR.A	
7.78	8.46	8.12	C1P636	uba-1 Protein UBA-1, isoform c	K.GNTQVVVYPYLTESYS SSVDPPEKEIPVC*TLK. N	<b>Glycyl thioester intermediate</b>
7.81	8.44	8.125	P61866	rpl-12 60S ribosomal protein L12	R.C*VGGEVGATSALAP K.V	
8.13	8.13	8.13	P46554	B0285.4 Probable leucine carboxyl methyltransferase 1	R.TNDDATQC*K.Y	
8.15	0	8.15	Q22792	T25G3.3 Protein T25G3.3	K.NC*NVNNATFDAMNI DNVPDAIIVR.K	
8.16	0	8.16	Q22099	krs-1 Lysine--tRNA ligase	R.DNNVDC*SAPR.T	
7.57	8.76	8.165	O44906	W05G11.6 Protein W05G11.6, isoform a	K.TNAMAMESC*R.A	
7.48	8.85	8.165	H2L023	cas-1 Protein CAS-1, isoform b	K.VAQC*EIVTSK.S	
8.96	7.38	8.17	P90900	ifa-4 Intermediate filament protein ifa- 4	R.NC*LEQNYAR.E	
5.36	10.98	8.17	HIUBK1	map-2 Protein MAP-2, isoform b	K.NFATLAFK*R.C	
8.2	8.16	8.18	Q69Z13	K08E3.5 Protein K08E3.5, isoform f	K.LNGGLGTSMGC*K.G	
8.18	0	8.18	Q9XW17	car-1 Protein CAR-1	K.ASDIKDLIVC*DTPK. M	
9.36	7.01	8.185	Q21926	irs-1 Isoleucine--tRNA ligase, cytoplasmic	K.LLDC*PNR.Q	
7.81	8.56	8.185	Q18212	hel-1 Spliceosome RNA helicase DDX39B homolog	K.YFVLDEC*DK.M	
7.82	8.56	8.19	Q19825	rrt-1 Probable arginine--tRNA ligase, cytoplasmic	R.LALC*DVTR.K	
8.55	7.84	8.195	O17643	idh-2 Isocitrate dehydrogenase [NADP]	K.C*ATITPEAR.I	
0	8.2	8.2	P46502	rpt-3 Probable 26S protease regulatory subunit 6B	R.GVLMYGPPGC*GK.T	ATP-binding
7.84	8.58	8.21	A7LPE5	gpdh-2 Protein GPDH-2, isoform c	K.NVAC*AAGFTDGL GYGDNTK.A	
8.21	0	8.21	Q10454	F46H5.3 Probable arginine kinase F46H5.3	K.TFLIWC*NEEDHLR.I	
7.47	8.96	8.215	Q21484	tag-235 Protein TAG-235	R.DYVDCVNC*MTLR.E	
8.22	0	8.22	G5EF87	swn-1 Protein SWSN-1	R.TQHEC*VLK.F	
8.16	8.29	8.225	Q2EEM8	ttr-45 Protein TTR-45	K.LLC*GTSPAK.N	
7.1	9.35	8.225	Q9N4J8	cct-3 Protein CCT-3	R.ESGHQVQIGNINAC* K.T	
8.23	0	8.23	Q9XWP7	eif-3.j Protein EIF-3.J	K.ASC*YGDMIGK.L	
7.79	8.68	8.235	Q9N585	ppw-2 Protein PPW-2	K.MGVTVC*DEPLVVK. G	
6.81	9.66	8.235	O01826	C53H9.2 Protein C53H9.2, isoform a	R.GFMASGIPDC*SR.A	
0	8.24	8.24	Q17896	C10C5.2 Protein C10C5.2	K.SETPC*QLYPFYYSY G.-	
8.24	0	8.24	Q18905	cgp-1 GTP-binding protein cgp-1	K.IDMC*PANILEETMK. N	
0	8.26	8.26	Q95YB2	acd-9 Protein ACDH-9	R.INIASC*SLGAAQR.S	
8.28	0	8.28	O76630	Y57G7A.10 Protein Y57G7A.10	K.SNPESDGILNC*LEA MK.V	
7.71	8.88	8.295	O16368	rpt-2 Probable 26S protease regulatory subunit 4	K.AMC*TEAGLLALR.E	
8.21	8.39	8.3	G5EG13	dhs-12 Protein DHS-12	R.AAIVNIGSDC*ASQAL NLR.G	
8.21	8.42	8.315	Q9BKU3	Y37E3.10 Protein Y37E3.10	K.AITEPTILDEC*DISAD IK.E	

P04075	2.00E-106	Fructose-bisphosphate aldolase A	Yes	Yes	Yes	--	Yes
P22314	0	Ubiquitin-like modifier-activating enzyme 1	Yes	Yes	Yes	Yes	Yes
P30050	3.00E-89	60S ribosomal protein L12	Yes	Yes	Yes	No	No
Q9UIC8	7.00E-75	Leucine carboxyl methyltransferase 1	Yes	Yes	Yes	Yes	No
C9JA08	0	60S ribosomal export protein NMD3	Yes	Yes	No	No	No
Q15046	0	Lysine--tRNA ligase	Yes	Yes	Yes	Yes	Yes
Q16822	0	Phosphoenolpyruvate carboxykinase [GTP], mitochondrial	No	No	No	--	--
Q01518	1.00E-108	Adenylyl cyclase-associated protein 1	Yes	Yes	No	No	No
J9JID7	5.00E-56	Lamin B2, isoform CRA_a	No	No	No	--	--
G3XA91	0	Methionine aminopeptidase 2	Yes	Yes	Yes	Yes	Yes
Q16851	0	UTP--glucose-1-phosphate uridylyltransferase	Yes	Yes	Yes	Yes	Yes
I3L4Q1	5.00E-39	Protein LSM14 homolog A	Yes	Yes	No	No	No
P41252	0	Isoleucine--tRNA ligase, cytoplasmic	No	No	No	No	No
Q13838	0	Spliceosome RNA helicase DDX39B	Yes	Yes	Yes	Yes	Yes
P54136	0	Arginine--tRNA ligase, cytoplasmic	Yes	Yes	Yes	No	Yes
P48735	0	Isocitrate dehydrogenase [NADP], mitochondrial	Yes	Yes	Yes	Yes	Yes
P43686	0	26S protease regulatory subunit 6B	Yes	Yes	Yes	No	No
P21695	2.00E-120	Glycerol-3-phosphate dehydrogenase [NAD(+)], cytoplasmic	No	No	Yes	No	No
P06732	4.00E-82	Creatine kinase M-type	No	No	Yes	--	--
O14929	2.00E-72	Histone acetyltransferase type B catalytic subunit	Yes	Yes	Yes	No	No
Q8TAQ2	4.00E-133	SWI/SNF complex subunit SMARCC2	Yes	Yes	Yes	Yes	Yes
H0YNH0	5	GMP reductase 2	--	--	--	--	--
P49368	0	T-complex protein 1 subunit gamma	No	No	No	No	No
H0YGJ7	1.1	Eukaryotic translation initiation factor 3 subunit J	--	--	--	--	--
Q9UL18	2.00E-43	Protein argonaute-1	No	No	No	--	No
Q9H089	1.00E-61	Large subunit GTPase 1 homolog	No	--	No	No	No
Q8NDV7	1.3	Trinucleotide repeat-containing gene 6A protein	--	--	--	--	--
O00178	0	GTP-binding protein 1	Yes	Yes	Yes	No	Yes
Q9UKU7	8.00E-170	Isobutyryl-CoA dehydrogenase, mitochondrial	Yes	Yes	No	--	No
Q15006	6.00E-76	ER membrane protein complex subunit 2	No	No	--	--	--
P62191	0	26S protease regulatory subunit 4	Yes	Yes	Yes	Yes	Yes
Q8NEX9	8.00E-12	Short-chain dehydrogenase/reductase family 9C member 7	No	No	No	No	No
P05198	3.00E-117	Eukaryotic translation initiation factor 2 subunit 1	No	No	Yes	No	No

10.29	6.39	8.34	G5EDZ2	umps-1 Protein UMPS-1	R.VSAC*SDLLNWTGPV NLDAK.S	
8.34	8.34	8.34	Q22101	T02G5.7 Protein T02G5.7	K.GPMGLC*AEK.T	
7.84	8.87	8.355	O45012	nol-5 Protein NOL-5	K.GLC*DQVIELSAYR.A	
8.82	7.91	8.365	Q9XVF7	rpl-8 60S ribosomal protein L8	K.AQIQIGNIVPVGTLPE GTTIC*NVENK.S	
8.07	8.69	8.38	P27639	inf-1 Eukaryotic initiation factor 4A	R.AIVPC*TTGK.D	
8.41	0	8.41	A6PVA5	C05C8.1 Protein C05C8.1, isoform b	K.FNQIAETFEDYNC*L VK.R	
8.83	8.01	8.42	Q20938	rpn-6.1 Probable 26S proteasome regulatory subunit rpn-6.1	R.DLV DLC*LK.I	
0	8.42	8.42	Q9U1Q8	Y80D3A.9 Protein Y80D3A.9	K.LFEIATC*R.T	
8.33	8.56	8.445	O01854	F32B5.1 Protein F32B5.1	K.GYPFNPC*LTQDNYL EMEGK.V	
8.46	0	8.46	P91851	F26H9.4 Uncharacterized protein F26H9.4	R.EGSNPLNTIQSMPAIS EFC*DR.I	
8.46	0	8.46	B3GWB2	C08H9.2 Protein C08H9.2, isoform b	K.LATEHIVC*PK.N	
9.46	7.53	8.495	P91477	pbs-4 Proteasome subunit beta type-2	R.FC*YAIMDR.E	
8.28	8.76	8.52	G3MU53	eef-2 Protein EEF-2, isoform b	R.LHC*TAQMPDGLAD DIEGGTVNAR.D	
8.44	8.61	8.525	Q20057	F35G12.11 Protein F35G12.11	R.C*QHPEGGEK.V	
8.53	0	8.53	P34346	let-754 Adenylate kinase 2, mitochondrial	K.LVSDEVVC*K.L	
8.53	0	8.53	Q95YF3	cgh-1 ATP-dependent RNA helicase cgh-1	R.NLVC*SDLLTR.G	
8.54	0	8.54	D0VWN5	W04G3.5 Protein W04G3.5, isoform b	K.EIQGFFSC*PVDNLR. A	
7.79	9.3	8.545	Q27888	ldh-1 L-lactate dehydrogenase	K.LC*VVTAGAR.Q	
7.93	9.2	8.565	P24894	COX2 Cytochrome c oxidase subunit 2	K.SWC*FGTME.-	
0	8.57	8.57	Q2HQL4	gln-3 Glutamine synthetase	K.NGFPGPQGPYYC*GV GANK.V	
8.57	0	8.57	O62102	pbs-2 Proteasome subunit beta type	K.GPIVPEFC*K.R	
8.37	8.79	8.58	Q8IA50	mdh-1 Protein MDH-1, isoform c	K.ELEEERDDALKAC*D DANI.-	
7.72	9.51	8.615	O16927	F25G6.8 Signal recognition particle 14 kDa protein	K.EGDEISC*IFR.A	
0	8.62	8.62	Q967F1	eif-1 Protein EIF-1	K.VGIVNESNC*R.V	
8.62	0	8.62	D7SFL2	C34F11.3 Protein C34F11.3, isoform b	R.NIC*ALNAFR.R	
9.24	8.01	8.625	P24886	ND4L NADH dehydrogenase subunit 4L (Fragment)	K.FFGSDNC*IF.-	
9.29	7.97	8.63	Q93576	ndk-1 Nucleoside diphosphate kinase	R.NIC*HGSDAVDSANR. E	
0	8.63	8.63	O45012	nol-5 Protein NOL-5	R.QNC*INTDLSSILPEEL EEK.V	
0	8.64	8.64	Q20206	rps-11 Protein RPS-11	K.C*PWAGNVPIR.G	<b>S-palmitoyl cysteine</b>
8.48	8.85	8.665	Q20585	rpn-7 26S proteasome non-ATPase regulatory subunit 6	R.LIATGQLQC*R.I	
8.67	0	8.67	Q19126	asb-2 Protein ASB-2	K.SMFEDC*NKEWSAPE PLPAIPK.D	
8.25	9.12	8.685	Q22494	vha-15 Probable V-type proton ATPase subunit H 2	R.EAALQMVQC*K.T	
8.31	9.07	8.69	Q9N537	Y32H12A.4 Protein Y32H12A.4	K.IC*LDDPAEFLK.R	
7.9	9.49	8.695	O45011	W10C8.5 Protein W10C8.5	K.LGATLYDC*IR.S	
0	8.7	8.7	O45552	F53A2.7 Protein F53A2.7	R.VVAYSAVGC*DPTIM GIGPAPAIR.E	

P11172	1.00E-99	Uridine 5'-monophosphate synthase	No	No	No	No	Yes
P24752	1.00E-127	Acetyl-CoA acetyltransferase, mitochondrial	Yes	Yes	Yes	No	Yes
Q9Y2X3	3.00E-171	Nucleolar protein 58	Yes	Yes	Yes	No	Yes
P62917	7.00E-134	60S ribosomal protein L8	Yes	Yes	Yes	No	Yes
Q14240	0	Eukaryotic initiation factor 4A-II	Yes	Yes	Yes	No	No
Q99766	9.00E-18	ATP synthase subunit s, mitochondrial	No	No	No	--	--
O00231	5.00E-146	26S proteasome non-ATPase regulatory subunit 11	No	No	No	No	No
Q6ICL3	9.00E-25	Transport and Golgi organization protein 2 homolog	No	No	No	No	No
P12277	4.00E-77	Creatine kinase B-type	No	No	Yes	--	--
Q96T66	4.00E-46	Nicotinamide/nicotinic acid mononucleotide adenylyltransferase 3	No	No	No	No	Yes
Q00341	6.00E-134	Vigilin	No	No	No	--	--
P49721	1.00E-44	Proteasome subunit beta type-2	No	No	No	No	No
P13639	0	Elongation factor 2	No	No	No	No	No
P84090	3.00E-24	Enhancer of rudimentary homolog	No	No	--	--	--
P54819	4.00E-102	Adenylate kinase 2, mitochondrial	No	No	No	No	No
P26196	0	Probable ATP-dependent RNA helicase DDX6	Yes	Yes	Yes	Yes	Yes
O60256	6.00E-140	Phosphoribosyl pyrophosphate synthase-associated protein 2	No	No	No	No	No
P07195	9.00E-148	L-lactate dehydrogenase B chain	No	No	Yes	No	Yes
P00403	1.00E-49	Cytochrome c oxidase subunit 2	No	No	No	No	No
P15104	5.00E-178	Glutamine synthetase	Yes	Yes	Yes	Yes	Yes
Q99436	2.00E-69	Proteasome subunit beta type-7	No	No	No	No	--
B9A041	1.00E-69	Malate dehydrogenase, cytoplasmic	No	No	No	--	No
P37108	2.00E-19	Signal recognition particle 14 kDa protein	Yes	Yes	--	--	Yes
O60739	2.00E-29	Eukaryotic translation initiation factor 1b	No	No	No	No	No
Q01433	0	AMP deaminase 2	No	No	No	No	No
Q6UXU4	1.2	Germ cell-specific gene 1-like protein	--	--	--	--	--
P22392	8.00E-75	Nucleoside diphosphate kinase B	No	No	No	Yes	No
Q9Y2X3	3.00E-171	Nucleolar protein 58	No	No	No	No	No
P62280	5.00E-72	40S ribosomal protein S11	Yes	Yes	Yes	Yes	Yes
Q15008	1.00E-126	26S proteasome non-ATPase regulatory subunit 6	Yes	Yes	No	Yes	Yes
P24539	4.00E-08	ATP synthase F(0) complex subunit B1, mitochondrial	No	No	No	--	--
Q9U112	9.00E-167	V-type proton ATPase subunit H	Yes	Yes	Yes	No	No
P41236	4.00E-21	Protein phosphatase inhibitor 2	No	No	--	--	--
P12277	1.00E-76	Creatine kinase B-type	No	No	No	--	--
P42765	2.00E-163	3-ketoacyl-CoA thiolase, mitochondrial	Yes	Yes	No	No	No

8.71	0	8.71	O76618	cars-1 Protein CARS-1, isoform a	K.VC*EDVVAALEHFK.T	
0	8.72	8.72	Q19969	ima-3 Importin subunit alpha-3	R.C*KDPAPSPAVR.T	
8.51	8.94	8.725	Q07749	unc-60 Actin-depolymerizing factor 2, isoform c	K.VIFVQYC*PDNAPVR.R	
9.01	8.47	8.74	Q19842	pcca-1 Propionyl-CoA carboxylase alpha chain, mitochondri	K.MADEAVC*VGEAPTAK.S	
8.6	8.91	8.755	Q20585	rpn-7 26S proteasome non-ATPase regulatory subunit 6	R.C*NEVQEQLTGGGLN.GTLIPVR.E	
8.76	0	8.76	Q9TZL8	Y71H10A.1 6-phosphofructokinase	R.LVC*IGGDGSLTGAN.TFR.L	
9.28	8.25	8.765	Q9U1Q4	vrs-2 Valine--tRNA ligase	R.DYPDGIPEC*GVDAL.R.F	
8.78	0	8.78	P91277	F26B1.2 Protein F26B1.2, isoform a	R.VC*TVTADK.T	
8.66	8.94	8.8	O45622	erfa-3 Protein ERFA-3, isoform a	K.TDITYVPC*SGLTGAF.IK.D	
9.04	8.6	8.82	Q9U1R7	arx-3 Protein ARX-3	R.VAFSPSGC*R.L	
9.68	8	8.84	Q18688	daf-21 Heat shock protein 90	K.LGLDIGDDEIEDSAVP.SSC*TAEAK.I	
8.89	8.84	8.865	O01974	eif-3.H Eukaryotic translation initiation factor 3 subunit	K.SC*SSDKYSTR.H	
9.03	8.72	8.875	Q18677	dhp-2 Dihydropyrimidinase 2	K.IFNC*YPQK.G	
7.94	9.82	8.88	Q95YF3	cgh-1 ATP-dependent RNA helicase cgh-1	K.GVEFEDFC*LGR.D	
8.89	0	8.89	Q21888	R102.2 Protein R102.2	K.DAVFIGPLHDPC*TAD.EAAK.L	
8.9	0	8.9	Q20168	F38E11.5 Probable coatomer subunit beta	K.SELLLAGEC*LGR.A	
8.23	9.59	8.91	P47207	cct-2 T-complex protein 1 subunit beta	K.LGEAC*SVVLR.G	
9.54	8.31	8.925	G5EFJ3	C08E8.4 Protein C08E8.4	R.DIMYLAC*LAK.F	
11.4	6.46	8.93	P90889	F55H12.4 Protein F55H12.4	R.QCGCGEIEGC*MGSA.TGGFMK.C	
8.87	8.99	8.93	G3MU69	ant-1.1 Protein ANT-1.1, isoform d	K.NTLDC*AKK.I	
8.64	9.24	8.94	Q18910	D1005.2 Protein D1005.2	K.NVDYIMEC*TPK.T	
8.95	0	8.95	A7LPE5	gpdh-2 Protein GPDH-2, isoform c	R.INVVEDAHTVELC*G.ALK.N	
8.95	0	8.95	Q17941	akt-1 Serine/threonine-protein kinase akt-1	R.LGGGPEDALEIC*R.A	
9.73	8.21	8.97	O16294	F32D1.5 Probable GMP reductase	K.VGIGPGSVC*TTR.K	Thioimide intermediate/Potassium-binding
9.48	8.48	8.98	Q19825	rrt-1 Probable arginine--tRNA ligase, cytoplasmic	R.STIIGDSIC*R.L	
8.98	0	8.98	Q05036	C30C11.4 Uncharacterized protein C30C11.4	R.LLDEC*ER.V	
9.58	8.41	8.995	Q94261	cif-1 COP9/Signalosome and eIF3 complex-shared subunit 1	R.LIGELEC*NLETLQDR.F	
8.45	9.56	9.005	Q9NAQ2	JC8.2 Protein JC8.2	K.GQVNVVDC*R.E	
9.8	8.21	9.005	P54811	cdc-48.1 Transitional endoplasmic reticulum ATPase homolog	K.AIANEC*QANFISIK.G	
0	9.01	9.01	P46548	nmt-1 Glycylpeptide N-tetradecanoyltransferase	K.PVSVC*R.Y	
7.72	10.31	9.015	Q20772	F54D5.7 Probable glutaryl-CoA dehydrogenase, mitochondrial	R.AITGLNGFC*.-	
0	9.02	9.02	P52709	trs-1 Threonine--tRNA ligase, cytoplasmic	R.TIC*PDDFPK.I	
8.74	9.3	9.02	P54812	cdc-48.2 Transitional endoplasmic reticulum ATPase homolog	K.AFAEC*EK.N	

P49589	0	Cysteine--tRNA ligase, cytoplasmic	No	No	No	No	--
O00629	0	Importin subunit alpha-3	No	No	No	No	No
E9PQB7	9.00E-08	Cofilin-1	No	No	Yes	No	Yes
P05165	0	Propionyl-CoA carboxylase alpha chain, mitochondrial	Yes	Yes	No	No	No
Q15008	1.00E-126	26S proteasome non-ATPase regulatory subunit 6	No	No	No	No	No
P08237	0	ATP-dependent 6-phosphofructokinase, muscle type	No	No	No	No	No
P26640	0	Valine--tRNA ligase	Yes	Yes	Yes	Yes	Yes
P61978	1.00E-67	Heterogeneous nuclear ribonucleoprotein K	No	No	No	No	No
Q8IYD1	0	Eukaryotic peptide chain release factor GTP-binding subunit ERF3B	Yes	Yes	Yes	No	No
Q92747	7.00E-145	Actin-related protein 2/3 complex subunit 1A	No	No	No	No	No
P07900	0	Heat shock protein HSP 90-alpha	No	No	No	No	No
O15372	8.00E-63	Eukaryotic translation initiation factor 3 subunit H	No	No	No	--	No
Q14117	0	Dihydropyrimidinase	No	No	No	No	No
P26196	0	Probable ATP-dependent RNA helicase DDX6	Yes	Yes	Yes	No	No
H7C4Y4	0.79	WD repeat-containing protein 49	--	--	--	--	--
P35606	0	Coatomer subunit beta'	Yes	Yes	Yes	No	Yes
P78371	0	T-complex protein 1 subunit beta	Yes	Yes	Yes	Yes	Yes
A5PLL1	1.9	Ankyrin repeat domain-containing protein 34B	--	--	--	--	No
B2RXH2	7.6	Lysine-specific demethylase 4E	--	--	--	--	--
P12236	1.00E-117	ADP/ATP translocase 3	Yes	Yes	Yes	Yes	Yes
Q16851	2.00E-98	UTP--glucose-1-phosphate uridylyltransferase	No	No	No	No	No
P21695	2.00E-120	Glycerol-3-phosphate dehydrogenase [NAD(+)], cytoplasmic	Yes	Yes	Yes	Yes	Yes
P31749	0	RAC-alpha serine/threonine-protein kinase	No	No	No	No	No
P36959	0	GMP reductase 1	Yes	Yes	Yes	Yes	Yes
P54136	0	Arginine--tRNA ligase, cytoplasmic	No	No	Yes	No	No
O95757	0	Heat shock 70 kDa protein 4L	Yes	Yes	No	No	Yes
Q7L2H7	1.00E-50	Eukaryotic translation initiation factor 3 subunit M	No	No	No	--	No
Q13610	1.00E-78	Periodic tryptophan protein 1 homolog	Yes	Yes	Yes	No	No
P55072	0	Transitional endoplasmic reticulum ATPase	Yes	Yes	Yes	No	Yes
O60551	9.00E-170	Glycylpeptide N-tetradecanoyltransferase 2	Yes	Yes	Yes	Yes	Yes
Q92947	0	Glutaryl-CoA dehydrogenase, mitochondrial	--	--	--	--	--
P26639	0	Threonine--tRNA ligase, cytoplasmic	No	No	No	No	No
P55072	0	Transitional endoplasmic reticulum ATPase	No	No	No	No	No

9.16	8.9	9.03	O02286	R11A5.4 Protein R11A5.4, isoform a	R.EHFIAAAFPSAC*GK.T	<b>GTP-binding</b>
8.35	9.71	9.03	G5EFX2	pkn-1 Protein PKN-1, isoform a	K.IADFGLC*K.E	
9.41	8.66	9.035	P91859	F32A7.5 Protein F32A7.5, isoform d	K.DISGEQLQAILC*GK.Q	
7.85	10.22	9.035	Q17474	B0334.3 Protein B0334.3, isoform a	K.VVQIDIC*PEEFHQNVK.T	
10.31	7.77	9.04	Q18496	acs-19 Protein ACS-19, isoform a	K.TNISYNC*LER.N	
0	9.05	9.05	O01541	aars-2 Alanine--tRNA ligase, cytoplasmic	K.HIDC*GLGLER.L	
0	9.05	9.05	O17071	rpt-4 Probable 26S protease regulatory subunit 10B	R.NVC*TEAGMFAIR.A	
9.08	9.04	9.06	Q22352	T08H10.1 Protein T08H10.1	K.C*VESQLK.A	
8.91	9.24	9.075	Q94261	cif-1 COP9/Signalosome and eIF3 complex-shared subunit 1	K.C*EPVVDSFIK.N	
0	9.09	9.09	D3YT36	pyk-2 Pyruvate kinase	K.TGVICTIGPAC*SDVE TLR.K	
9.62	8.58	9.1	Q21265	tag-225 Putative metalloproteinase inhibitor tag-225	R.VEGPNALYTVLC*GQ VLPDDR.S	Disulfide
8.94	9.3	9.12	P27604	ahcy-1 Adenosylhomocysteinase	K.ANIIVTTTGC*K.D	
10.31	7.94	9.125	Q19341	haao-1 3-hydroxyanthranilate 3,4-dioxygenase	K.GTFAC*NAPYEAR.W	
8.73	9.52	9.125	Q9TZS5	cct-7 Protein CCT-7, isoform a	R.YNFFEDC*SK.A	
8.47	9.8	9.135	Q94261	cif-1 COP9/Signalosome and eIF3 complex-shared subunit 1	K.ALVDMC*AEAR.L	
9.94	8.4	9.17	Q20643	F52B5.2 Protein F52B5.2	K.SMYEPGVILGGC*TL R.R	
8.52	9.86	9.19	P49041	rps-5 40S ribosomal protein S5	K.TIAEC*LADELINAAK .G	
0	9.21	9.21	Q9NEN6	rps-6 40S ribosomal protein S6	K.GQSC*YR.E	
6.91	11.54	9.225	O17695	hda-1 Histone deacetylase 1	K.GHGEC*AR.F	
7.77	10.73	9.25	P90992	misc-1 Protein MISC-1	R.GC*TPTVLR.A	
0	9.28	9.28	Q10454	F46H5.3 Probable arginine kinase F46H5.3	K.LQAAPEC*HSLLK.K	
0	9.32	9.32	G8JY43	cct-6 Protein CCT-6, isoform b	R.DLLVEVC*R.T	
9.32	0	9.32	G5ED41	cand-1 Protein CAND-1	K.FVDSLSLC*APDDAA R.V	
8.38	10.32	9.35	P34575	cts-1 Probable citrate synthase, mitochondrial	R.FRGYSIPEC*QK.L	
9.22	9.5	9.36	Q09543	paa-1 Probable serine/threonine-protein phosphatase PP2A	R.QNIIC*NSLLNVAK.E	
9.4	0	9.4	Q20264	acs-11 Protein ACS-11	K.AGTVGPAVQGVGC*R .I	
10.67	8.28	9.475	O44549	acdh-3 Protein ACDH-3	R.ASSTC*SVHFDNVR.V	
9.51	0	9.51	Q9NAI5	Y39G8B.1 Protein Y39G8B.1, isoform a	R.DGDHPHC*PFLEEF.-	
9.51	0	9.51	E5QC18	nhr-49 Protein NHR-49, isoform e	R.VC*LFNNTYMTR.D	
9.53	0	9.53	B3GWB2	C08H9.2 Protein C08H9.2, isoform b	R.NLEAETNC*R.I	
9.58	0	9.58	Q86NC9	pnk-1 Protein PNK-1, isoform a	R.VC*AADALPTTTPAA STALR.Q	
8.53	10.64	9.585	Q21926	irs-1 Isoleucine--tRNA ligase, cytoplasmic	K.NLIC*NGLVLASDGA K.M	
9.59	0	9.59	G5EF05	W07E11.1 Protein W07E11.1	R.VCPAPCEGAC*TLGIG SPAVTIK.S	<b>Iron-Sulfur 1 (4Fe-4S)</b>
9.5	9.73	9.615	P02566	unc-54 Myosin-4	R.LPIYTDSC*AR.M	
9.15	10.08	9.615	Q17761	T25B9.9 6-phosphogluconate dehydrogenase, decarboxylating	R.C*LSALKDER.V	

Q16822	0	Phosphoenolpyruvate carboxykinase [GTP], mitochondrial	Yes	Yes	Yes	--	--
Q16513	0	Serine/threonine-protein kinase N2	Yes	Yes	Yes	Yes	No
P46821	1.00E-11	Microtubule-associated protein 1B	No	No	No	--	--
Q9UJ83	0	2-hydroxyacyl-CoA lyase 1	Yes	Yes	No	No	No
Q9NR19	0	Acetyl-coenzyme A synthetase, cytoplasmic	No	No	No	Yes	Yes
P49588	0	Alanine--tRNA ligase, cytoplasmic	No	No	Yes	No	No
P62333	0	26S protease regulatory subunit 10B	Yes	Yes	Yes	No	Yes
O60218	2.00E-78	Aldo-keto reductase family 1 member B10	No	No	No	No	No
Q7L2H7	1.00E-50	Eukaryotic translation initiation factor 3 subunit M	No	No	No	--	--
P14618	0	Pyruvate kinase PKM	No	No	No	No	No
P16035	9.00E-10	Metalloproteinase inhibitor 2	Yes	Yes	--	--	--
P23526	0	Adenosylhomocysteinase	Yes	Yes	Yes	Yes	No
P46952	2.00E-70	3-hydroxyanthranilate 3,4-dioxygenase	No	No	--	Yes	--
Q99832	0	T-complex protein 1 subunit eta	Yes	Yes	Yes	Yes	Yes
Q7L2H7	1.00E-50	Eukaryotic translation initiation factor 3 subunit M	No	No	No	--	No
Q8IXN4	7.00E-31	MAK protein	No	Yes	Yes	No	No
P46782	3.00E-125	40S ribosomal protein S5	Yes	Yes	Yes	No	Yes
P62753	8.00E-100	40S ribosomal protein S6	Yes	Yes	Yes	Yes	Yes
Q13547	0	Histone deacetylase 1	Yes	Yes	Yes	Yes	Yes
Q02978	8.00E-149	Mitochondrial 2-oxoglutarate/malate carrier protein	Yes	Yes	No	No	Yes
P06732	4.00E-82	Creatine kinase M-type	No	--	No	--	--
P40227	0	T-complex protein 1 subunit zeta	No	No	No	No	No
Q86VP6	0	Cullin-associated NEDD8-dissociated protein 1	No	No	No	--	No
O75390	0	Citrate synthase, mitochondrial	Yes	Yes	Yes	No	Yes
P30153	0	Serine/threonine-protein phosphatase 2A 65 kDa regulatory subunit A alpha isoform	No	No	No	No	No
Q4G176	3.00E-54	Acyl-CoA synthetase family member 3, mitochondrial	No	No	No	No	No
P45954	3.00E-178	Short/branched chain specific acyl-CoA dehydrogenase, mitochondrial	Yes	Yes	Yes	No	Yes
P14550	4.00E-97	Alcohol dehydrogenase [NADP(+)]	No	No	No	--	--
Q14541	5.00E-33	Hepatocyte nuclear factor 4-gamma	No	No	No	--	--
Q00341	6.00E-134	Vigilin	No	No	No	--	--
Q9NVE7	7.00E-88	Pantothenate kinase 4	No	No	--	No	No
P41252	0	Isoleucine--tRNA ligase, cytoplasmic	No	No	No	No	Yes
Q12882	3.00E-14	Dihydropyrimidine dehydrogenase [NADP(+)]	Yes	Yes	--	--	--
P13533	0	Myosin-6	No	No	Yes	No	No
P52209	0	6-phosphogluconate dehydrogenase, decarboxylating	Yes	Yes	Yes	Yes	No

0	9.64	9.64	P47208	cct-4 T-complex protein 1 subunit delta	R.SIHDALC*VIR.C	
9.64	0	9.64	O01541	aars-2 Alanine--tRNA ligase, cytoplasmic	K.VNDESNEFNVSNC*QVR.G	
9.99	9.3	9.645	Q18040	C16A3.10 Probable ornithine aminotransferase, mitochondrial	K.VLPMNTGVEAC*ESAVK.L	
11.94	7.38	9.66	Q9BKS1	elc-1 Protein ELC-1	K.VC*QYFAYK.V	
8.41	11.04	9.725	O45679	cysl-2 Cysteine synthase	K.VEYMNPAC*SVK.D	
9.94	9.53	9.735	G5EDY2	wars-1 Protein WARS-1	R.AIFGFTPEDC*LGK.A	
9.55	10.05	9.8	O44906	W05G11.6 Protein W05G11.6, isoform a	R.IAC*NIGR.D	
9.9	9.82	9.86	Q19905	sqv-4 UDP-glucose 6-dehydrogenase	K.AAESIGC*ILR.E	
0	9.94	9.94	Q19246	dhs-25 Protein DHS-25	K.SLGTPSILVNC*AGITK.D	
8.39	11.55	9.97	Q9XWI6	eif-3.B Eukaryotic translation initiation factor 3 subunit	R.YFVTC*STLGGR.A	
10.24	9.73	9.985	G5EGK8	let-92 Serine/threonine-protein phosphatase	R.NVVTVFSAPNYC*YR.C	

P50991	0	T-complex protein 1 subunit delta	Yes	Yes	Yes	Yes	Yes
P49588	0	Alanine--tRNA ligase, cytoplasmic	No	No	No	No	No
P04181	0	Ornithine aminotransferase, mitochondrial	No	No	No	No	No
Q15369	9.00E-59	Transcription elongation factor B polypeptide 1	Yes	Yes	Yes	No	Yes
P35520	8.00E-62	Cystathionine beta-synthase	No	No	No	No	Yes
P23381	0	Tryptophan--tRNA ligase, cytoplasmic	Yes	Yes	No	Yes	No
Q16822	0	Phosphoenolpyruvate carboxykinase [GTP], mitochondrial	No	No	No	--	--
O60701	0	UDP-glucose 6-dehydrogenase	No	No	No	--	No
Q92506	2.00E-76	Estradiol 17-beta-dehydrogenase 8	Yes	Yes	No	No	No
P55884	1.00E-130	Eukaryotic translation initiation factor 3 subunit B	No	No	No	No	No
P62714	0	Serine/threonine-protein phosphatase 2A catalytic subunit beta isoform	Yes	Yes	Yes	Yes	Yes

**Table 3A-2.** MS results showing the 338 cysteine-containing peptides identified in *daf-2* and *daf-16;daf-2* lysates, in order from average light:heavy ratios of < 1 (decreased cysteine labeling in *daf-2*) to > 1 (increased cysteine labeling in *daf-2*). Human homologues and cysteine conservation across various species were determined as described for Table 3A-1.

Run 1	Run 2	Average	<i>C. elegans</i>			
			Uniprot ID	Description	Sequence	Function
0.19	0.18	0.185	P18948	vit-6 Vitellogenin-6	R.VIC*PIAEVGTK.F	
0.16	0.21	0.185	P18948	vit-6 Vitellogenin-6	K.TEEGLIC*R.V	
0.19	0.2	0.195	P18948	vit-6 Vitellogenin-6	R.EC*NEEQLEQIYR.H	
0.2	0.22	0.21	P18948	vit-6 Vitellogenin-6	R.SYANNESPC*EQTFSS R.V	
0.21	0.22	0.215	P05690	vit-2 Vitellogenin-2	R.VAIVC*SK.V	
0.23	0.21	0.22	P06125	vit-5 Vitellogenin-5	R.APLTTC*YSLVAK.D	
0.23	0.27	0.25	P18948	vit-6 Vitellogenin-6	R.NQFTPC*YSVLAK.D	
0.37	0.34	0.355	O46009	ZK228.3 Protein ZK228.3	K.ARDGVVYSVAC*STH QFV.-	
0.38	0.36	0.37	G4S185	C17H12.13 Protein C17H12.13, isoform b	R.DLVQDSLQC*SSTCVI R.D	
0.4	0.45	0.425	O61217	K02D7.1 Protein K02D7.1	R.ADLGHC*GSGLGPIG DTVQDATILPYSK.I	
0.41	0.48	0.445	O18000	pes-9 Protein PES-9	R.EGC*SIPITLTFQELTG K.S	
0.45	0.48	0.465	Q20222	lbp-3 Fatty acid-binding protein homolog 3	K.MVNNGITC*R.R	Redox-active disulfide
0.51	0.47	0.49	O16294	F32D1.5 Probable GMP reductase	R.SAC*TYTGAK.H	NADP-binding
0.44	0.54	0.49	O61217	K02D7.1 Protein K02D7.1	K.TVGADALGMSTC*H EVTVAR.Q	
0.64	0.39	0.515	Q93934	R07H5.8 Protein R07H5.8	K.GVEASVTC*GSYAAQ EIIKK.H	
0.49	0.56	0.525	P29691	eef-2 Elongation factor 2	R.ETVQSESNQIC*LSK.S	
0.53	0.54	0.535	P42170	rnr-2 Ribonucleoside-diphosphate reductase small chain	R.DFAC*LLYSK.L	
0.53	0.54	0.535	Q8MNV6	C16A3.10 Protein C16A3.10, isoform b	K.GVSDLC*KK.Y	
0.59	0.53	0.56	Q93576	ndk-1 Nucleoside diphosphate kinase	R.NIC*HGSDAVDSANR. E	
0.5	0.65	0.575	O18000	pes-9 Protein PES-9	K.LETIGTIC*ELADLGT QELEGK.T	
0.54	0.62	0.58	Q9TZ33	ucr-2.3 Protein UCR-2.3	R.TTQVQDIEGC*K.R	
0.57	0.6	0.585	Q10657	tpi-1 Triosephosphate isomerase	K.AGVLVAAQNC*YK.V	
0.62	0.57	0.595	Q93576	ndk-1 Nucleoside diphosphate kinase	R.GDFC*IQTGR.N	
0.6	0.59	0.595	G8JYF5	hsp-60 Protein HSP-60, isoform b	R.VTDALC*ATR.A	
0.62	0.59	0.605	G8JYF5	hsp-60 Protein HSP-60, isoform b	K.ANEEAGDGTTC*ATV LAR.A	
0.58	0.64	0.61	P29691	eef-2 Elongation factor 2	K.TC*DPNGPLMMYISK .M	
0.62	0.61	0.615	Q22799	dlc-1 Dynein light chain 1, cytoplasmic	K.NADMSDDMQQDAID C*ATQALEK.Y	

Human			Conserved Cysteine				
Uniprot ID	E-value	Description	Human	Mouse	Fly	Yeast	Mustard
Q8N8U9	8.00E-05	BMP-binding endothelial regulator protein	--	No	--	--	--
Q8N8U9	8.00E-05	BMP-binding endothelial regulator protein	--	--	--	--	--
Q8N8U9	8.00E-05	BMP-binding endothelial regulator protein	--	--	No	--	--
Q8N8U9	8.00E-05	BMP-binding endothelial regulator protein	--	No	Yes	--	--
Q9Y6R7	2.00E-05	IgGfc-binding protein	--	--	No	--	--
Q8N8U9	1.00E-05	BMP-binding endothelial regulator protein	Yes	--	--	--	--
Q8N8U9	8.00E-05	BMP-binding endothelial regulator protein	--	--	--	--	--
Q96M93	0.92	Adenosine deaminase domain-containing protein 1	--	--	--	--	--
E9PD17	0.47	UDP-glucuronosyltransferase 3A1	--	--	--	--	--
P00491	2.00E-79	Purine nucleoside phosphorylase	Yes	Yes	Yes	Yes	--
Q96KP4	0	Cytosolic non-specific dipeptidase	No	No	No	No	--
Q01469	4.00E-08	Fatty acid-binding protein, epidermal	Yes	Yes	--	--	--
P36959	0	GMP reductase 1	Yes	Yes	Yes	Yes	No
P00491	2.00E-79	Purine nucleoside phosphorylase	No	No	No	No	--
P55263	8.00E-120	Adenosine kinase	No	No	Yes	No	No
P13639	0	Elongation factor 2	Yes	Yes	Yes	No	No
P31350	5.00E-169	Ribonucleoside-diphosphate reductase subunit M2	Yes	Yes	No	Yes	Yes
P04181	2.00E-129	Ornithine aminotransferase, mitochondrial	Yes	Yes	Yes	Yes	Yes
P22392	8.00E-75	Nucleoside diphosphate kinase B	No	No	No	Yes	No
Q96KP4	0	Cytosolic non-specific dipeptidase	No	No	No	No	--
P22695	1.00E-34	Cytochrome b-c1 complex subunit 2, mitochondrial	No	No	No	No	No
P60174	2.00E-107	Triosephosphate isomerase	Yes	Yes	No	No	No
P22392	8.00E-75	Nucleoside diphosphate kinase B	Yes	Yes	Yes	No	No
P10809	1.00E-81	60 kDa heat shock protein, mitochondrial	No	No	No	No	No
P10809	1.00E-81	60 kDa heat shock protein, mitochondrial	No	No	No	No	No
P13639	0	Elongation factor 2	Yes	Yes	Yes	Yes	Yes
Q96FJ2	2.00E-60	Dynein light chain 2, cytoplasmic	Yes	Yes	Yes	No	No

0.63	0.61	0.62	Q18040	C16A3.10 Probable ornithine aminotransferase, mitochondrial	K.VLPMNTGVEAC*ESAVK.L	
0.62	0.62	0.62	Q21217	gta-1 Probable 4-aminobutyrate aminotransferase, mitocho	R.SLC*MLSVTR.S	
0.68	0.56	0.62	Q27481	uba-1 Protein UBA-1, isoform a	K.LSETDC*QPR.Q	
0.61	0.64	0.625	Q21824	prdx-3 Probable peroxiredoxin prdx-3	R.HTTC*NDLPVGR.S	
0.6	0.71	0.655	Q10663	gei-7 Bifunctional glyoxylate cycle protein	R.GTGC*VPLYNLMEDAATAEISR.A	
0.67	0.65	0.66	Q9N599	pas-3 Proteasome subunit alpha type-4	R.NSYGEEMPVEQLVQNLK*NEK.Q	
0.66	0.66	0.66	P41932	par-5 14-3-3-like protein 1	K.VEQELNDIC*QDVLK.L	
0.67	0.66	0.665	Q7Z139	hyl-2 Protein HYL-2	R.MAEC*AMR.A	
0.79	0.56	0.675	O44727	cpn-4 Protein CPN-4	K.EDFDC*EASR.D	
0.66	0.7	0.68	O44549	acdh-3 Protein ACDH-3	K.YAIEC*LNAGR.I	
0.64	0.74	0.69	Q9XW92	vha-13 V-type proton ATPase catalytic subunit A	K.YSNSDAIIVGC*GER.G	
0.73	0.66	0.695	Q23621	gdh-1 Glutamate dehydrogenase	K.C*AVVDVPPFGGAK.G	<b>ADP-ribosylcysteine</b>
0.72	0.67	0.695	Q23621	gdh-1 Glutamate dehydrogenase	K.AVGKDC*PVEPNAAF.AAK.I	
0.67	0.74	0.705	O45246	hsp-70 Protein HSP-70	R.ARFEELC*ADLFR.S	
0.75	0.67	0.71	P91856	F26H9.5 Probable phosphoserine aminotransferase	R.SIMNVC*FR.I	
0.73	0.69	0.71	C1P636	uba-1 Protein UBA-1, isoform c	R.ATSC*YER.L	
0.72	0.7	0.71	B2D6P1	rmd-2 Protein RMD-2, isoform c	K.FC*NEIGNR.V	
0.67	0.75	0.71	Q95YF3	cgh-1 ATP-dependent RNA helicase cgh-1	R.NLVC*SDDLTR.G	
0.65	0.78	0.715	O62102	pbs-2 Proteasome subunit beta type	K.LTESIYAC*GAGTAADLDQVTK.M	
0.77	0.7	0.735	Q21193	pfn-3 Profilin-3	K.GLQPEMC*SK.T	
0.69	0.79	0.74	Q95Y04	rps-28 40S ribosomal protein S28	R.TGSQGQC*TQVR.V	
0.73	0.76	0.745	Q19341	haao-1 3-hydroxyanthranilate 3,4-dioxygenase	K.GTFAC*NAPYEAR.W	
0.76	0.75	0.755	O17643	idh-2 Isocitrate dehydrogenase [NADP]	K.C*ATITPDEAR.I	
0.76	0.76	0.76	G5EC98	W06H3.3 Protein W06H3.3	R.AAGLVPDLLIC*R.S	
0.75	0.77	0.76	P05634	msp-10 Major sperm protein 10/36/56/76	K.RLGVDPPC*GVLDPK.E	
0.68	0.84	0.76	Q9XUV0	pbs-5 Proteasome subunit beta type	K.YC*TLYELR.E	
0.78	0.76	0.77	O45865	ant-1.1 Protein ANT-1.1, isoform a	K.GLADC*LIK.I	
0.78	0.76	0.77	Q9U2X0	prmt-1 Protein PRMT-1	R.LYVC*AIEDR.Q	<b>S-nitrosocysteine</b>
0.72	0.83	0.775	P91917	tag-210 Putative GTP-binding protein tag-210	K.SEAQAENFPFC*TIDPNESR.V	
0.67	0.88	0.775	O17680	sams-1 Probable S-adenosylmethionine synthase 1	K.VAC*ETVTK.T	<b>Disulfide</b>
0.76	0.8	0.78	P40614	F01G4.6 Phosphate carrier protein, mitochondrial	R.GC*APMIYK.A	
0.73	0.83	0.78	Q9U1Q4	vrs-2 Valine--tRNA ligase	K.C*IDTGLR.L	
0.78	0.8	0.79	O45495	uev-1 Protein UEV-1	R.IYNLQIQC*GGNYPR.E	
0.76	0.82	0.79	Q22370	ucr-2.2 Protein UCR-2.2	R.NGGLGNSIYAPC*SK.I	
0.82	0.77	0.795	P24886	nd4l NADH-ubiquinone oxidoreductase chain 4L	K.FFGSDNC*IF.-	

P04181	0	Ornithine aminotransferase, mitochondrial	No	No	No	No	No
P80404	8.00E-168	4-aminobutyrate aminotransferase, mitochondrial	No	No	No	No	No
P22314	0	Ubiquitin-like modifier-activating enzyme 1	Yes	Yes	No	No	No
E9PH29	5.00E-94	Thioredoxin-dependent peroxide reductase, mitochondrial	No	No	No	No	No
Q9Y4D2	3.7	Sn1-specific diacylglycerol lipase alpha	--	--	--	Yes	No
P25789	1.00E-115	Proteasome subunit alpha type-4	Yes	Yes	Yes	No	Yes
P63104	3.00E-135	14-3-3 protein zeta/delta	Yes	Yes	Yes	No	Yes
Q96G23	2.00E-39	Ceramide synthase 2	No	No	No	No	No
P51911	5.00E-17	Calponin-1	No	No	No	--	No
P45954	3.00E-178	Short/branched chain specific acyl-CoA dehydrogenase, mitochondrial	No	No	No	No	No
P38606	0	V-type proton ATPase catalytic subunit A	Yes	Yes	Yes	Yes	Yes
P00367	0	Glutamate dehydrogenase 1, mitochondrial	Yes	Yes	Yes	No	No
P00367	0	Glutamate dehydrogenase 1, mitochondrial	No	No	No	No	--
P11142	0	Heat shock cognate 71 kDa protein	No	Yes	Yes	Yes	No
Q9Y617	4.00E-139	Phosphoserine aminotransferase	No	No	No	No	No
P22314	0	Ubiquitin-like modifier-activating enzyme 1	No	No	No	No	No
Q96DB5	6.00E-27	Regulator of microtubule dynamics protein 1	No	No	--	--	--
P26196	0	Probable ATP-dependent RNA helicase DDX6	Yes	Yes	Yes	Yes	Yes
Q99436	2.00E-69	Proteasome subunit beta type-7	Yes	Yes	Yes	No	Yes
P47736	8.30E+00	Rap1 GTPase-activating protein 1	No	Yes	No	No	Yes
P62857	1.00E-30	40S ribosomal protein S28	Yes	Yes	Yes	No	No
P46952	2.00E-70	3-hydroxyanthranilate 3,4-dioxygenase	No	No	--	Yes	--
P48735	0	Isocitrate dehydrogenase [NADP], mitochondrial	Yes	Yes	Yes	Yes	Yes
Q9NRF8	0	CTP synthase 2	Yes	Yes	Yes	Yes	Yes
Q9P0L0	2.00E-06	Vesicle-associated membrane protein-associated protein A	No	No	--	--	--
P28062	4.00E-64	Proteasome subunit beta type-8	Yes	Yes	Yes	Yes	Yes
P12235	1.00E-143	ADP/ATP translocase 1	Yes	Yes	Yes	No	No
Q99873	1.00E-170	Protein arginine N-methyltransferase 1	No	No	No	No	No
Q9NTK5	0	Obg-like ATPase 1	Yes	Yes	Yes	No	Yes
Q00266	0	S-adenosylmethionine synthase isoform type-1	Yes	Yes	Yes	Yes	Yes
Q00325	9.00E-154	Phosphate carrier protein, mitochondrial	No	No	No	No	No
P26640	0	Valine--tRNA ligase	Yes	Yes	Yes	No	No
Q13404	1.00E-64	Ubiquitin-conjugating enzyme E2 variant 1	Yes	Yes	Yes	Yes	Yes
P22695	1.00E-43	Cytochrome b-c1 complex subunit 2, mitochondrial	No	No	No	No	No
C9J9N5	0.47	Amino acid transporter	--	--	--	--	--

0.74	0.85	0.795	Q9NF11	Y105E8B.5 Protein Y105E8B.5	R.SSC*PEPMTVDFIR.V	
0.76	0.84	0.8	O44549	aedh-3 Protein ACDH-3	R.ASSTC*SVHFDNVR.V	
0.74	0.86	0.8	O45418	fkf-6 Protein FKB-6	K.AAAQQIIVC*R.N	
0.85	0.76	0.805	Q21032	idh-1 Isocitrate dehydrogenase [NADP]	K.SDGGFVWAC*K.N	
0.83	0.78	0.805	G5EEK8	sca-1 Calcium ATPase	K.NC*LFSGTNVASGK.A	
0.81	0.82	0.815	Q9N362	Y55F3AM.13 Protein Y55F3AM.13	K.AEQILAGSC*DQSFVTR.E	
0.82	0.82	0.82	Q93573	tct-1 Translationally-controlled tumor protein homolog	K.LVEMNC*YEDASMF K.A	
0.82	0.83	0.825	O16259	sti-1 Protein STI-1	K.AAC*LVAMR.E	
0.76	0.9	0.83	Q9N358	cct-8 T-complex protein 1 subunit theta	K.ACVTTC*PANSFNFNVDNIR.I	
0.83	0.84	0.835	O01504	rpa-2 60S acidic ribosomal protein P2	K.VLEAGGLDC*DMENANSVVDALK.G	
0.84	0.84	0.84	Q10663	gei-7 Bifunctional glyoxylate cycle protein	K.DNIVGLNC*GR.W	
0.84	0.84	0.84	P53013	eft-3 Elongation factor 1-alpha	K.QLIVAC*NK.M	
0.82	0.86	0.84	Q21217	gta-1 Probable 4-aminobutyrate aminotransferase, mitocho	K.AVQTMLC*GTSANENAIK.T	<b>Iron-Sulfur (2Fe-2S)</b>
0.88	0.8	0.84	O01974	eif-3.H Eukaryotic translation initiation factor 3 subunit	R.LEITNC*FPTVR.N	
0.88	0.81	0.845	Q95YA9	cas-1 Adenylyl cyclase-associated protein	K.VAQGC*EIVTSK.S	
0.85	0.84	0.845	P50093	phb-2 Mitochondrial prohibitin complex protein 2	R.VLPSIC*NEVLK.G	
0.84	0.86	0.85	Q95QW0	eif-3.L Eukaryotic translation initiation factor 3 subunit	R.NAFATGC*PK.F	
0.72	0.98	0.85	Q07749	unc-60 Actin-depolymerizing factor 2, isoform c	K.VIFVQYC*PDNAPVR.R	
0.9	0.8	0.85	Q21032	idh-1 Isocitrate dehydrogenase [NADP]	K.DLAIC*VK.G	
0.85	0.86	0.855	O17921	tbb-1 Protein TBB-1	K.NMMAAC*DPR.H	
0.79	0.92	0.855	Q93619	tag-173 Protein TAG-173	R.SGNQFDC*GK.L	
1	0.73	0.865	D3YT81	dld-1 Protein DLD-1, isoform b	R.EANLAAAYC*GK.A	
0.92	0.81	0.865	Q9TY00	M57.2 Protein M57.2	R.LVFC*ETPLVEK.T	
0.85	0.88	0.865	Q95Y85	Y110A7A.6 Protein Y110A7A.6, isoform b	R.VFFVESVC*DDPDIINSNITEVK.I	
0.84	0.9	0.87	Q20627	pam-1 Protein PAM-1, isoform a	R.YAFPC*FDEPIYK.A	
0.89	0.86	0.875	Q9XWW2	mrg-1 Protein MRG-1, isoform a	K.ITNLALIC*TAR.G	
0.85	0.9	0.875	P27604	ahcy-1 Adenosylhomocysteinase	K.ANIIVTTTGC*K.D	
0.88	0.88	0.88	P52011	cyn-3 Peptidyl-prolyl cis-trans isomerase 3	R.ALC*TGENGIGK.S	
0.83	0.94	0.885	P34659	snr-5 Probable small nuclear ribonucleoprotein F	R.C*NNVLYVGGVDGENETSA.-	
0.81	0.96	0.885	P50432	mel-32 Serine hydroxymethyltransferase	R.YYGGNEFIDQMELLC*QK.R	
0.85	0.94	0.895	P53596	C05G5.4 Probable succinyl-CoA ligase [ADP/GDP-forming] sub	R.GC*IGIVSR.S	
0.92	0.88	0.9	Q21746	sgt-1 Protein SGT-1	R.LEQYDLAIQDC*R.T	
0.92	0.89	0.905	O17953	dld-1 Dihydropyridyl dehydrogenase	R.GIDC*TASLNLPK.M	
0.91	0.9	0.905	Q20655	ftt-2 14-3-3-like protein 2	R.DIC*QDVLNLLDK.F	

P00492	5.00E-61	Hypoxanthine-guanine phosphoribosyltransferase	No	No	--	--	No
P45954	3.00E-178	Short/branched chain specific acyl-CoA dehydrogenase, mitochondrial	Yes	Yes	Yes	No	Yes
Q02790	8.00E-112	Peptidyl-prolyl cis-trans isomerase FKBP4	Yes	Yes	Yes	--	--
O75874	0	Isocitrate dehydrogenase [NADP] cytoplasmic	Yes	Yes	Yes	No	Yes
P16615	0	Sarcoplasmic/endoplasmic reticulum calcium ATPase 2	No	No	No	Yes	No
O75037	7.5	Kinesin-like protein KIF21B	--	--	--	--	--
P13693	2.00E-24	Translationally-controlled tumor protein	No	No	No	No	No
F5H0T1	6.00E-125	Stress-induced-phosphoprotein 1	No	No	No	No	No
P50990	0	T-complex protein 1 subunit theta	No	No	No	No	Yes
P05387	2.00E-17	60S acidic ribosomal protein P2	No	No	No	No	No
Q9Y4D2	3.7	Sn1-specific diacylglycerol lipase alpha	--	--	--	Yes	Yes
Q05639	0	Elongation factor 1-alpha 2	No	No	No	No	Yes
P80404	8.00E-168	4-aminobutyrate aminotransferase, mitochondrial	Yes	Yes	Yes	No	No
O15372	8.00E-63	Eukaryotic translation initiation factor 3 subunit H	Yes	Yes	Yes	--	Yes
Q01518	1.00E-98	Adenylyl cyclase-associated protein 1	Yes	Yes	No	No	No
J3KPX7	2.00E-132	Prohibitin-2	No	No	Yes	No	No
Q9Y262	1.00E-144	Eukaryotic translation initiation factor 3 subunit L	Yes	Yes	Yes	--	Yes
E9PQB7	9.00E-08	Cofilin-1	No	No	Yes	No	Yes
O75874	0	Isocitrate dehydrogenase [NADP] cytoplasmic	Yes	Yes	Yes	No	No
P07437	0	Tubulin beta chain	Yes	Yes	Yes	No	No
P21953	4.00E-176	2-oxoisovalerate dehydrogenase subunit beta, mitochondrial	Yes	Yes	Yes	Yes	Yes
P09622	0	Dihydrolipoyl dehydrogenase, mitochondrial	No	No	No	No	--
Q92696	5.00E-68	Geranylgeranyl transferase type-2 subunit alpha	No	--	--	--	--
B0FLL2	7.00E-163	6-phosphofructo-2-kinase/fructose-2, 6-bisphosphatase 2 transcript variant 3	Yes	Yes	Yes	No	Yes
E9PLK3	0	Puromycin-sensitive aminopeptidase	Yes	Yes	Yes	Yes	Yes
B3KTM8	1.00E-26	Mortality factor 4-like protein 1	No	No	No	Yes	No
P23526	0	Adenosylhomocysteinase	Yes	Yes	Yes	Yes	No
P30405	1.00E-77	Peptidyl-prolyl cis-trans isomerase F, mitochondrial	Yes	Yes	Yes	Yes	Yes
P62306	3.00E-34	Small nuclear ribonucleoprotein F	Yes	Yes	Yes	Yes	Yes
P34896	0	Serine hydroxymethyltransferase, cytosolic	Yes	Yes	No	Yes	Yes
P53597	5.00E-132	Succinyl-CoA ligase [ADP/GDP-forming] subunit alpha, mitochondrial	No	No	No	No	No
O43765	5.00E-61	Small glutamine-rich tetratricopeptide repeat-containing protein alpha	Yes	Yes	Yes	No	Yes
P09622	0	Dihydrolipoyl dehydrogenase, mitochondrial	No	No	Yes	No	No
P63104	2.00E-145	14-3-3 protein zeta/delta	Yes	Yes	Yes	No	Yes

0.96	0.86	0.91	G5EGK8	let-92 Serine/threonine-protein phosphatase	R.NVVTVFSAPNYC*YR.C	
0.83	0.99	0.91	Q19749	F23B12.5 Dihydrolipoyllysine-residue acetyltransferase comp	K.ASALAC*QR.V	
0.96	0.87	0.915	P47207	cct-2 T-complex protein 1 subunit beta	K.LGEAC*SVVLR.G	
0.87	0.97	0.92	Q9N4P2	glrx-21 Protein GLRX-21, isoform a	K.TSC*TFCNR.A	<b>S-glutathionyl cysteine, Redox-active disulfide</b>
0.91	0.93	0.92	P50432	mel-32 Serine hydroxymethyltransferase	K.AIIAGVSC*YAR.H	
0.92	0.93	0.925	Q07750	unc-60 Actin-depolymerizing factor 1, isoforms a/b	R.TDNLTDC*R.Y	
0.95	0.91	0.93	P47209	cct-5 T-complex protein 1 subunit epsilon	R.MLSIEQC*PNNK.A	
0.94	0.92	0.93	O18229	Y57G11C.3 Putative 6-phosphogluconolactonase	K.NVAFIIC*GK.Q	
0.91	0.95	0.93	Q9TZS5	cct-7 Protein CCT-7, isoform a	R.QLC*QNAGLDALDV LNK.L	
0.92	0.95	0.935	Q22494	vha-15 Probable V-type proton ATPase subunit H 2	K.LAC*FGTTR.M	
0.9	0.97	0.935	Q20121	acs-4 Protein ACS-4	R.YLEGYC*SPFLDR.I	
0.97	0.91	0.94	H2L023	cas-1 Protein CAS-1, isoform b	K.LVTVVSDIC*.-	
0.92	0.96	0.94	Q20585	rpn-7 26S proteasome non-ATPase regulatory subunit 6	R.LIATGQLQC*R.I	
0.88	1	0.94	O44451	C04C3.3 Pyruvate dehydrogenase E1 component subunit beta.	K.VVC*PYSAEADAK.G	
0.94	0.95	0.945	P52018	cyn-11 Peptidyl-prolyl cis-trans isomerase 11	K.LPIVVVQC*GQL.-	
0.91	0.98	0.945	O17915	ran-1 GTP-binding nuclear protein ran-1	R.VC*ENIPIVLCGNK.V	
0.91	0.98	0.945	O17915	ran-1 GTP-binding nuclear protein ran-1	R.VCENIPIVLC*GNK.V	
0.94	0.96	0.95	Q9N358	cct-8 T-complex protein 1 subunit theta	R.IAVYTC*PFDLTQTET K.G	
0.9	1	0.95	P53596	C05G5.4 Probable succinyl-CoA ligase [ADP/GDP-forming] sub	R.LVGPNC*PGIISADQC K.I	
0.9	1	0.95	P53596	C05G5.4 Probable succinyl-CoA ligase [ADP/GDP-forming] sub	R.LVGPNC*PGIISADQC* K.I	
0.88	1.02	0.95	Q19626	vha-12 Probable V-type proton ATPase subunit B	K.NTIC*EFTGDILR.T	
0.98	0.93	0.955	Q95ZN7	nmt-1 Glycylpeptide N-tetradecanoyltransferase	K.C*ADMKPSQIGLVLQ.	
0.92	0.99	0.955	Q19825	rrt-1 Probable arginine--tRNA ligase, cytoplasmic	R.STIIGDSIC*R.L	
0.95	0.97	0.96	Q9XW92	vha-13 V-type proton ATPase catalytic subunit A	K.LAANNPLLC*GQR.V	
0.75	1.17	0.96	G5EBR1	gdi-1 Protein GDI-1, isoform a	K.C*GDEIVR.G	
0.8	1.14	0.97	Q86S29	cct-7 Protein CCT-7, isoform b	K.C*AATTLSSK.L	
0.94	1.01	0.975	G5EDW8	VF13D12L.3 Protein VF13D12L.3	K.SEADLGQC*FVAIDPE AFAPGFADR.L	
0.94	1.01	0.975	Q27535	ZC434.8 Probable arginine kinase ZC434.8	R.SLQGYPFNPC*LSETN YK.M	
1.02	0.93	0.975	P52015	cyn-7 Peptidyl-prolyl cis-trans isomerase 7	K.SEC*LIADC*GQL.-	
0.91	1.04	0.975	Q20057	F35G12.11 Protein F35G12.11	R.C*QHPEGGEK.V	
0.89	1.06	0.975	Q05036	C30C11.4 Uncharacterized protein C30C11.4	K.VSDC*VLAVPSYFTD VQR.R	
1	0.96	0.98	Q94272	fah-1 Protein FAH-1	R.IQQLSEDC*AVLR.D	
0.96	1.02	0.99	Q10454	F46H5.3 Probable arginine kinase F46H5.3	R.FLQAANAC*R.Y	

P62714	0	Serine/threonine-protein phosphatase 2A catalytic subunit beta isoform	Yes	Yes	Yes	Yes	Yes
H0YDD4	3.00E-169	Acetyltransferase component of pyruvate dehydrogenase complex	Yes	Yes	No	No	No
P78371	0	T-complex protein 1 subunit beta	Yes	Yes	Yes	Yes	Yes
Q9NS18	1.00E-17	Glutaredoxin-2, mitochondrial	Yes	Yes	Yes	Yes	Yes
P34896	0	Serine hydroxymethyltransferase, cytosolic	Yes	Yes	Yes	No	No
Q9Y281	1.00E-09	Cofilin-2	Yes	Yes	Yes	Yes	Yes
P48643	0	T-complex protein 1 subunit epsilon	Yes	Yes	Yes	No	Yes
O95336	3.00E-26	6-phosphogluconolactonase	No	No	No	No	Yes
Q99832	0	T-complex protein 1 subunit eta	Yes	Yes	Yes	Yes	Yes
Q9UI12	9.00E-167	V-type proton ATPase subunit H	No	No	Yes	--	No
O60488	0	Long-chain-fatty-acid--CoA ligase 4	No	No	No	No	No
Q01518	1.00E-108	Adenylyl cyclase-associated protein 1	No	No	--	No	No
Q15008	1.00E-126	26S proteasome non-ATPase regulatory subunit 6	Yes	Yes	No	Yes	Yes
P11177	1.00E-172	Pyruvate dehydrogenase E1 component subunit beta, mitochondrial	No	No	No	No	No
O43447	6.00E-90	Peptidyl-prolyl cis-trans isomerase H	Yes	Yes	Yes	No	Yes
P62826	2.00E-139	GTP-binding nuclear protein Ran	Yes	Yes	Yes	Yes	Yes
P62826	2.00E-139	GTP-binding nuclear protein Ran	Yes	Yes	Yes	Yes	Yes
P50990	0	T-complex protein 1 subunit theta	Yes	Yes	Yes	Yes	No
P53597	5.00E-132	Succinyl-CoA ligase [ADP/GDP-forming] subunit alpha, mitochondrial	Yes	Yes	Yes	Yes	Yes
P53597	5.00E-132	Succinyl-CoA ligase [ADP/GDP-forming] subunit alpha, mitochondrial	Yes	Yes	Yes	No	Yes
P21281	0	V-type proton ATPase subunit B, brain isoform	Yes	Yes	Yes	No	No
O60551	3.00E-170	Glycylpeptide N-tetradecanoyltransferase 2	Yes	Yes	Yes	No	No
P54136	0	Arginine--tRNA ligase, cytoplasmic	No	No	Yes	No	No
P38606	0	V-type proton ATPase catalytic subunit A	No	No	No	--	No
P50395	0	Rab GDP dissociation inhibitor beta	No	No	No	No	No
Q99832	0	T-complex protein 1 subunit eta	Yes	Yes	Yes	Yes	Yes
P00966	2.6	Argininosuccinate synthase	--	--	No	--	--
P12277	1.00E-83	Creatine kinase B-type	No	No	Yes	--	--
P30405	1.00E-78	Peptidyl-prolyl cis-trans isomerase F, mitochondrial	No	No	No	No	No
P84090	3.00E-24	Enhancer of rudimentary homolog	No	No	--	--	--
O95757	0	Heat shock 70 kDa protein 4L	Yes	Yes	Yes	No	Yes
P16930	0	Fumarylacetoacetase	No	No	No	--	No
P06732	4.00E-82	Creatine kinase M-type	No	No	Yes	--	--

0.94	1.04	0.99	Q19842	pcca-1 Propionyl-CoA carboxylase alpha chain, mitochondri	K.MADEAVC*VGEAPT AK.S	
1.15	0.84	0.995	G5EBK3	erm-1 ERM-1B	K.YGDYVPETHVAGC*L TADR.L	
0.99	1	0.995	H2L0B0	nhr-104 Protein NHR-104, isoform a	K.SEGLLC*K.K	
0.99	1	0.995	Q17761	T25B9.9 6-phosphogluconate dehydrogenase, decarboxylating	K.SNGEPC*CDWVGNA GSGHFVK.M	
0.96	1.03	0.995	P34575	cts-1 Probable citrate synthase, mitochondrial	R.FRGSYIPEC*QK.L	
0.94	1.06	1	Q9N5B3	W08E12.7 Protein W08E12.7	K.MGVVEC*EK.Y	
0.97	1.04	1.005	Q9N4J8	cct-3 Protein CCT-3	R.ESGHQVQIGNINAC* K.T	
1.08	0.94	1.01	Q19825	rrt-1 Probable arginine--tRNA ligase, cytoplasmic	R.LALC*DVTR.K	
1.07	0.95	1.01	Q21926	irs-1 Isoleucine--tRNA ligase, cytoplasmic	K.LLDC*PNR.Q	
1.02	1	1.01	Q19626	vha-12 Probable V-type proton ATPase subunit B	R.EDHSDVSNQLYAC*Y AIGK.D	
0.83	1.2	1.015	Q21265	tag-225 Putative metalloproteinase inhibitor tag-225	R.VEGPNALYTVLC*GQ VLPDDR.S	Disulfide
1.01	1.02	1.015	P17331	gpd-4 Glyceraldehyde-3-phosphate dehydrogenase 4	K.YDASNDHVISNASC* TTNCLAPLAK.V	Active site nucleophile
1.01	1.02	1.015	P17331	gpd-4 Glyceraldehyde-3-phosphate dehydrogenase 4	K.YDASNDHVISNASCT TNC*LAPLAK.V	
0.99	1.04	1.015	Q05036	C30C11.4 Uncharacterized protein C30C11.4	R.FIPFIPC*K.V	
0.97	1.06	1.015	Q04908	rpn-3 26S proteasome non-ATPase regulatory subunit 3	K.GVKPVFASPESDC*Y LR.L	
1.03	1.01	1.02	P46554	B0285.4 Probable leucine carboxyl methyltransferase 1	R.TNDDATQC*K.Y	
1	1.04	1.02	O17921	tbb-1 Protein TBB-1	R.EIVHVQAGQC*GNQI GSK.F	
0.98	1.07	1.025	Q9BL27	Y71H2AR.1 Protein Y71H2AR.1	K.LTC*IPTLLEVGNK.A	
0.93	1.12	1.025	P49197	rps-21 40S ribosomal protein S21	R.YAIC*GAIR.R	
0.99	1.07	1.03	Q17763	atp-5 Protein ATP-5	R.IPDPC*NIGLNETPEIE NR.F	
0.96	1.1	1.03	Q20772	F54D5.7 Probable glutaryl-CoA dehydrogenase, mitochondrial	R.AITGLNGFC*.-	
0.93	1.13	1.03	Q19825	rrt-1 Probable arginine--tRNA ligase, cytoplasmic	R.DAVAFGC*VK.Y	
1	1.08	1.04	P46562	alh-9 Putative aldehyde dehydrogenase family 7 member A1	R.STC*TINYSK.E	
0.98	1.1	1.04	O18240	rps-18 Protein RPS-18	R.FAFVC*CR.K	
0.98	1.1	1.04	O18240	rps-18 Protein RPS-18	R.FAFVCC*R.K	
1.07	1.02	1.045	Q20585	rpn-7 26S proteasome non-ATPase regulatory subunit 6	R.C*NEVQEQLTGGGLN GTLIPVR.E	
1.03	1.06	1.045	H2KYJ5	mtch-1 Protein MTCH-1, isoform a	K.YTTC*AQALAVIGK.Q	
1.27	0.83	1.05	Q2HQL4	gln-3 Glutamine synthetase	R.VAEFGVIASFDC*KP IK.G	
1.12	0.98	1.05	Q17335	H24K24.3 Alcohol dehydrogenase class-3	K.FFGATEC*INPK.S	
0.99	1.11	1.05	Q9BL27	Y71H2AR.1 Protein Y71H2AR.1	K.ILTTGESWC*PDCVV AEPVVEVIK.D	Active site nucleophile/Redox-active disulfide
1.18	0.93	1.055	O61790	R12E2.11 Protein R12E2.11	R.MAAQAMC*EK.I	
0.92	1.19	1.055	Q93934	R07H5.8 Protein R07H5.8	K.ANGWETTC*VK.E	
1.06	1.05	1.055	Q2HQL4	gln-3 Glutamine synthetase	R.TVC*LEGAER.K	

P05165	0	Propionyl-CoA carboxylase alpha chain, mitochondrial	Yes	Yes	No	No	No
P15311	0	Ezrin	No	No	No	--	--
B3KY83	2.00E-18	Retinoic acid receptor RXR-alpha	Yes	Yes	Yes	--	--
P52209	0	6-phosphogluconate dehydrogenase, decarboxylating	Yes	Yes	Yes	Yes	Yes
O75390	0	Citrate synthase, mitochondrial	Yes	Yes	Yes	No	Yes
Q9UQ80	1.00E-128	Proliferation-associated protein 2G4	Yes	Yes	Yes	No	Yes
P49368	0	T-complex protein 1 subunit gamma	No	No	No	No	No
P54136	0	Arginine--tRNA ligase, cytoplasmic	Yes	Yes	Yes	No	Yes
P41252	0	Isoleucine--tRNA ligase, cytoplasmic	No	No	No	No	No
P21281	0	V-type proton ATPase subunit B, brain isoform	Yes	Yes	Yes	No	No
P16035	9.00E-10	Metalloproteinase inhibitor 2	Yes	Yes	--	--	--
P04406	0	Glyceraldehyde-3-phosphate dehydrogenase	Yes	Yes	Yes	Yes	Yes
P04406	0	Glyceraldehyde-3-phosphate dehydrogenase	Yes	Yes	Yes	Yes	Yes
O95757	0	Heat shock 70 kDa protein 4L	No	No	No	No	No
O43242	1.00E-118	26S proteasome non-ATPase regulatory subunit 3	No	No	No	Yes	No
Q9UIC8	7.00E-75	Leucine carboxyl methyltransferase 1	Yes	Yes	Yes	Yes	No
P07437	0	Tubulin beta chain	Yes	Yes	Yes	Yes	Yes
Q9BRA2	4.00E-20	Thioredoxin domain-containing protein 17	No	No	No	--	No
P63220	1.00E-35	40S ribosomal protein S21	Yes	Yes	Yes	No	Yes
E7EVL6	0.17	Replication initiator 1	--	--	--	--	--
Q92947	0	Glutaryl-CoA dehydrogenase, mitochondrial	No	No	No	--	No
P54136	0	Arginine--tRNA ligase, cytoplasmic	Yes	Yes	Yes	No	No
P49419	0	Alpha-aminoadipic semialdehyde dehydrogenase	Yes	Yes	No	--	Yes
P62269	2.00E-86	40S ribosomal protein S18	No	No	No	No	No
P62269	2.00E-86	40S ribosomal protein S18	No	No	No	Yes	Yes
Q15008	1.00E-126	26S proteasome non-ATPase regulatory subunit 6	No	No	No	No	No
Q9Y6C9	9.00E-36	Mitochondrial carrier homolog 2	No	No	No	--	--
P15104	5.00E-178	Glutamine synthetase	No	No	No	No	No
P11766	0	Alcohol dehydrogenase class-3	Yes	Yes	No	No	No
Q9BRA2	4.00E-20	Thioredoxin domain-containing protein 17	Yes	Yes	Yes	--	Yes
E9PFD2	8.00E-50	Uridine 5'-monophosphate synthase	No	No	No	No	No
P55263	8.00E-120	Adenosine kinase	No	No	No	Yes	No
P15104	5.00E-178	Glutamine synthetase	No	No	Yes	Yes	No

1.05	1.06	1.055	Q09607	gst-36 Probable glutathione S-transferase gst-36	R.AGTNAVDC*AR.L	
1	1.11	1.055	Q9N456	glrx-10 Protein GLRX-10	K.SYC*PYCHK.A	<b>Redox-active disulfide</b>
1.09	1.03	1.06	Q95X21	Y71H10B.1 Protein Y71H10B.1, isoform b	K.LTNQMDEEYGC*LGS LFR.T	
1.08	1.04	1.06	P52015	cyn-7 Peptidyl-prolyl cis-trans isomerase 7	R.ALC*TGEK.G	
1.04	1.09	1.065	Q27497	gsp-1 Serine/threonine-protein phosphatase PP1-alpha	R.GNHEC*ASINR.I	
1.01	1.12	1.065	Q8ITZ0	fum-1 Protein FUM-1, isoform b	R.C*GLGELSLPENEPGS SIMPVK.V	
1.06	1.08	1.07	Q23621	gdh-1 Glutamate dehydrogenase	R.YSLDVC*EDEVK.A	
1.03	1.11	1.07	Q9XW92	vha-13 V-type proton ATPase catalytic subunit A	K.C*LGSPEE.E	
1.06	1.09	1.075	O45622	erfa-3 Protein ERFA-3, isoform a	K.TDITYVPC*SGLTGAF IK.D	
1.09	1.08	1.085	Q10454	F46H5.3 Probable arginine kinase F46H5.3	R.SLQGYPFNPC*LSEA NYLEMESK.V	
1.04	1.13	1.085	Q9XVF7	rpl-8 60S ribosomal protein L8	K.AQIQIGNIVPVTLP GTTIC*NVENK.S	
1.03	1.16	1.095	O17643	idh-2 Isocitrate dehydrogenase [NADP]	K.SSGGFVWAC*K.N	
1.1	1.09	1.095	Q95Y90	rpl-9 60S ribosomal protein L9	R.TVC*SHIK.N	
1.11	1.1	1.105	Q22038	rho-1 Ras-like GTP-binding protein rhoA	K.LVIVGDGAC*GK.T	GTP-binding
0.74	1.47	1.105	Q95017	ubc-9 SUMO-conjugating enzyme UBC9	K.NADGTLNLFNWEC* AIPGR.K	
1.26	0.96	1.11	Q93379	gsr-1 Protein GSR-1, isoform a	R.LGGTC*VNVGCVPK. K	<b>FAD-binding/Redox-active disulfide</b>
1.09	1.13	1.11	O02286	R11A5.4 Protein R11A5.4, isoform a	R.GIFIC*DGSQHEADEL IDK.L	
1.08	1.15	1.115	Q93572	rpa-0 60S acidic ribosomal protein P0	K.C*LLVGVDNVGSK.Q	
0.96	1.27	1.115	Q18678	srs-2 Probable serine--tRNA ligase, cytoplasmic	K.YAGVSTC*FR.Q	
1.09	1.18	1.135	Q05062	cdc-42 Cell division control protein 42 homolog	K.YVEC*SALTQK.G	
1.37	0.91	1.14	Q17761	T25B9.9 6-phosphogluconate dehydrogenase, decarboxylating	R.VVVC*AAVR.L	
1.18	1.1	1.14	D7SFI3	C02D5.4 Protein C02D5.4	R.FC*PWAQR.A	<b>Active site nucleophile</b>
1.15	1.14	1.145	P04970	gpd-1 Glyceraldehyde-3-phosphate dehydrogenase 1	K.YDASNDHVVSNASC* TTNCLAPLAK.V	Active site nucleophile
1.14	1.16	1.15	Q19297	F10D7.3 Uncharacterized monothiol glutaredoxin F10D7.3	K.TYC*PWSK.R	Iron-Sulfur (2Fe-2S)
1.12	1.18	1.15	P49041	rps-5 40S ribosomal protein S5	K.TIAEC*LADELINAAK .G	
1.15	1.16	1.155	O45903	W09H1.5 Probable trans-2-enoyl-CoA reductase 1, mitochondr	K.LALNC*VGGR.S	
1.15	1.16	1.155	Q9XW16	eif-3.B Eukaryotic translation initiation factor 3 subunit	R.YFVTC*STLGGR.A	
1.23	1.09	1.16	Q9BL60	vps-20 Protein VPS-20	K.ENC*LEKER.Q	
1.16	1.17	1.165	Q8IA58	F22F7.1 Protein F22F7.1, isoform b	R.ILQQYPDQC*SFYMF K.N	
1.13	1.21	1.17	Q93572	rpa-0 60S acidic ribosomal protein P0	K.AGAIAPC*DVK.L	
1.09	1.25	1.17	G5ECU1	skr-1 Protein SKR-1	K.GLLDVTC*K.T	
1.18	1.19	1.185	Q93830	exos-3 Protein EXOS-3	R.LINPSC*K.I	
1.18	1.21	1.195	O17921	tbb-1 Protein TBB-1	K.TAVC*DIPPR.G	
1.12	1.28	1.2	O16294	F32D1.5 Probable GMP reductase	K.VGIGPGSVC*TTR.K	Thioimide intermediate/Potassium binding

O60760	8.00E-31	Hematopoietic prostaglandin D synthase	No	No	No	--	Yes
P35754	2.00E-26	Glutaredoxin-1	Yes	Yes	Yes	Yes	Yes
P49902	1.00E-173	Cytosolic purine 5'-nucleotidase	No	No	No	--	No
P30405	1.00E-78	Peptidyl-prolyl cis-trans isomerase F, mitochondrial	Yes	Yes	Yes	Yes	Yes
P62140	0	Serine/threonine-protein phosphatase PP1-beta catalytic subunit	Yes	Yes	Yes	Yes	Yes
P07954	4.00E-176	Fumarate hydratase, mitochondrial	No	No	Yes	Yes	Yes
P00367	0	Glutamate dehydrogenase 1, mitochondrial	No	No	No	No	No
P38606	0	V-type proton ATPase catalytic subunit A	Yes	Yes	Yes	No	Yes
Q8IYD1	0	Eukaryotic peptide chain release factor GTP-binding subunit ERF3B	Yes	Yes	Yes	No	No
P06732	4.00E-82	Creatine kinase M-type	No	No	Yes	--	--
P62917	7.00E-134	60S ribosomal protein L8	Yes	Yes	Yes	No	Yes
P48735	0	Isocitrate dehydrogenase [NADP], mitochondrial	Yes	Yes	Yes	No	Yes
P32969	3.00E-84	60S ribosomal protein L9	Yes	Yes	Yes	No	No
P61586	8.00E-125	Transforming protein RhoA	Yes	Yes	Yes	Yes	No
P63279	2.00E-93	SUMO-conjugating enzyme UBC9	Yes	Yes	Yes	No	Yes
P00390	1.00E-180	Glutathione reductase, mitochondrial	Yes	Yes	Yes	Yes	Yes
Q16822	0	Phosphoenolpyruvate carboxykinase [GTP], mitochondrial	Yes	Yes	Yes	--	--
P05388	2.00E-133	60S acidic ribosomal protein P0	Yes	Yes	Yes	No	No
P49591	0	Serine--tRNA ligase, cytoplasmic	Yes	Yes	Yes	Yes	Yes
P60953	2.00E-124	Cell division control protein 42 homolog	Yes	Yes	Yes	Yes	Yes
P52209	0	6-phosphogluconate dehydrogenase, decarboxylating	No	No	No	No	Yes
P78417	2.00E-40	Glutathione S-transferase omega-1	Yes	Yes	Yes	--	No
P04406	0	Glyceraldehyde-3-phosphate dehydrogenase	Yes	Yes	Yes	Yes	Yes
P35754	1.00E-12	Glutaredoxin-1	Yes	Yes	Yes	Yes	Yes
P46782	3.00E-125	40S ribosomal protein S5	Yes	Yes	Yes	No	Yes
Q9BV79	5.00E-92	Trans-2-enoyl-CoA reductase, mitochondrial	Yes	Yes	Yes	No	Yes
P55884	1.00E-130	Eukaryotic translation initiation factor 3 subunit B	No	No	No	No	No
Q96FZ7	5.00E-54	Charged multivesicular body protein 6	No	No	No	No	No
Q8NBX0	4.00E-88	Saccharopine dehydrogenase-like oxidoreductase	No	No	No	--	No
P05388	2.00E-133	60S acidic ribosomal protein P0	Yes	Yes	No	No	No
P63208	3.00E-73	S-phase kinase-associated protein 1	Yes	Yes	Yes	Yes	Yes
Q9NQ75	6.00E-50	Exosome complex component RRP40	Yes	Yes	Yes	No	Yes
P07437	0	Tubulin beta chain	Yes	Yes	Yes	Yes	Yes
P36959	0	GMP reductase 1	Yes	Yes	Yes	Yes	Yes

1.19	1.22	1.205	P54216	aldo-1 Fructose-bisphosphate aldolase 1	R.ALQASC*LAK.W	
1.19	1.22	1.205	Q22067	T01C8.5 Probable aspartate aminotransferase, cytoplasmic	R.INIC*GLNTK.N	
1.17	1.24	1.205	Q9XW92	vha-13 V-type proton ATPase catalytic subunit A	K.YDRFC*PFYK.T	
1.17	1.26	1.215	O18650	rps-19 40S ribosomal protein S19	R.GVAPNHFQTSAGNC*LR.K	
1.15	1.28	1.215	Q22494	vha-15 Probable V-type proton ATPase subunit H 2	R.EAALQMVC*K.T	
1.1	1.33	1.215	Q9BKU5	Y37E3.8 Protein Y37E3.8, isoform a	K.SPVIDC*TK.L	
1.09	1.34	1.215	O17695	hda-1 Histone deacetylase 1	K.GHGEC*AR.F	
1.26	1.18	1.22	P52015	cyn-7 Peptidyl-prolyl cis-trans isomerase 7	K.SECLIADC*GQL.-	<b>S-nitrosocysteine</b>
1.21	1.23	1.22	Q17409	tba-1 Alpha-1 tubulin	R.TIQVDWC*PTGFK.V	
1.04	1.4	1.22	Q22067	T01C8.5 Probable aspartate aminotransferase, cytoplasmic	R.SFGVQC*LSGTGALR.A	
1.53	0.94	1.235	Q09533	rpl-10 60S ribosomal protein L10	R.ANVDTFPAC*VHMM SNER.E	
1.22	1.25	1.235	Q03577	drs-1 Aspartate--tRNA ligase, cytoplasmic	R.IQAGIC*NQFR.N	
1.39	1.09	1.24	Q94261	cif-1 COP9/Signalosome and eIF3 complex-shared subunit 1	K.C*EPVVDSFIK.N	
1.13	1.35	1.24	O45679	cysl-2 Cysteine synthase	K.VEYMN PAC*SVK.D	
1.25	1.24	1.245	Q17761	T25B9.9 6-phosphogluconate dehydrogenase, decarboxylating	R.C*LSALKDER.V	
1.06	1.44	1.25	P54811	cdc-48.1 Transitional endoplasmic reticulum ATPase homolog	R.GVLFYGP PG C*GK.T	
1.26	1.25	1.255	P49041	rps-5 40S ribosomal protein S5	K.AAC*PIVER.L	
1.23	1.29	1.26	Q9XUY0	F56G4.6 Protein F56G4.6	R.NC*YGVIR.C	
1.15	1.38	1.265	P54811	cdc-48.1 Transitional endoplasmic reticulum ATPase homolog	K.NTVGFSGADLTEIC*QR.A	
1.14	1.39	1.265	P37165	ubl-1 Ubiquitin-like protein 1-40S ribosomal protein S27	R.C*HDTLVVDTATAAA TSGEK.G	
1.18	1.35	1.265	G8JYG1	nxt-1 Protein NXT-1, isoform b	K.TTQEINKEDEELC*NE SK.K	
1.31	1.23	1.27	Q22352	T08H10.1 Protein T08H10.1	K.C*VESQLK.A	
1.29	1.25	1.27	O44480	rpl-20 60S ribosomal protein L18a	R.DTTVAGAVTQC*YR.D	
1.29	1.27	1.28	Q8WTM6	arx-4 Probable actin-related protein 2/3 complex subunit	R.NC*FASVFEK.Y	
1.23	1.33	1.28	H2KZ06	clec-266 Protein CLEC-266, isoform a	K.FYSIC*ER.N	
1.3	1.27	1.285	O02286	R11A5.4 Protein R11A5.4, isoform a	K.LEAYENNYIC*R.T	
1.26	1.32	1.29	P48152	rps-3 40S ribosomal protein S3	R.AC*YGVLR.F	
1.18	1.42	1.3	G5EE04	hip-1 Protein HIP-1	K.TDLATAC*K.L	
1.34	1.28	1.31	Q22993	pmt-2 Protein PMT-2	R.DC*IQHDPTEK.L	
0.98	1.64	1.31	Q22633	hpd-1 4-hydroxyphenylpyruvate dioxygenase	R.GC*EFLSIPSSYYDNL K.E	
1.34	1.29	1.315	Q94261	cif-1 COP9/Signalosome and eIF3 complex-shared subunit 1	R.LIGELEC*NLETLQDR.F	
1.3	1.36	1.33	Q21215	rack-1 Guanine nucleotide-binding protein subunit beta-2-	K.LWNTLAQC*K.Y	
1.33	1.36	1.345	Q19905	sqv-4 UDP-glucose 6-dehydrogenase	K.AAESIGC*ILR.E	
1.38	1.35	1.365	Q21215	rack-1 Guanine nucleotide-binding protein subunit beta-2-	K.VVNLGNC*R.L	

P04075	3.00E-166	Fructose-bisphosphate aldolase A	No	No	No	--	No
P17174	1.00E-157	Aspartate aminotransferase, cytoplasmic	No	Yes	No	No	No
P38606	0	V-type proton ATPase catalytic subunit A	Yes	Yes	Yes	Yes	Yes
P39019	1.00E-47	40S ribosomal protein S19	No	No	No	No	No
Q9U112	9.00E-167	V-type proton ATPase subunit H	Yes	Yes	Yes	No	No
P46776	8.00E-71	60S ribosomal protein L27a	No	No	No	No	No
Q13547	0	Histone deacetylase 1	Yes	Yes	Yes	Yes	Yes
P30405	1.00E-78	Peptidyl-prolyl cis-trans isomerase F, mitochondrial	Yes	Yes	No	No	Yes
Q9BQE3	0	Tubulin alpha-1C chain	Yes	Yes	Yes	Yes	Yes
P17174	1.00E-157	Aspartate aminotransferase, cytoplasmic	No	No	No	No	Yes
P27635	3.00E-111	60S ribosomal protein L10	Yes	Yes	Yes	Yes	Yes
P14868	0	Aspartate--tRNA ligase, cytoplasmic	Yes	Yes	Yes	Yes	No
Q7L2H7	1.00E-50	Eukaryotic translation initiation factor 3 subunit M	No	No	No	--	--
P35520	8.00E-62	Cystathionine beta-synthase	No	No	No	No	Yes
P52209	0	6-phosphogluconate dehydrogenase, decarboxylating	Yes	Yes	Yes	Yes	No
P55072	0	Transitional endoplasmic reticulum ATPase	Yes	Yes	Yes	No	Yes
P46782	3.00E-125	40S ribosomal protein S5	Yes	Yes	Yes	Yes	Yes
Q9Y282	3.2	Endoplasmic reticulum-Golgi intermediate compartment protein 3	--	--	--	--	--
P55072	0	Transitional endoplasmic reticulum ATPase	Yes	Yes	Yes	No	Yes
P62979	4.00E-43	Ubiquitin-40S ribosomal protein S27a	Yes	Yes	Yes	Yes	Yes
Q9NPJ8	3.00E-18	NTF2-related export protein 2	Yes	Yes	No	--	No
O60218	2.00E-78	Aldo-keto reductase family 1 member B10	No	No	No	No	No
Q02543	1.00E-78	60S ribosomal protein L18a	Yes	Yes	Yes	No	No
O15144	2.00E-156	Actin-related protein 2/3 complex subunit 2	Yes	Yes	Yes	No	No
P07306	8.00E-06	Asialoglycoprotein receptor 1	Yes	Yes	--	--	--
Q16822	0	Phosphoenolpyruvate carboxykinase [GTP], mitochondrial	No	No	No	--	--
P23396	1.00E-127	40S ribosomal protein S3	Yes	Yes	Yes	No	Yes
P50502	5.00E-78	Hsc70-interacting protein	Yes	Yes	Yes	No	No
Q9NZJ6	2.00E-05	Ubiquinone biosynthesis O-methyltransferase, mitochondrial	No	No	No	No	No
P32754	2.00E-173	4-hydroxyphenylpyruvate dioxygenase	No	No	No	--	No
Q7L2H7	1.00E-50	Eukaryotic translation initiation factor 3 subunit M	No	No	No	--	No
P63244	5.00E-168	Guanine nucleotide-binding protein subunit beta-2-like 1	Yes	Yes	Yes	Yes	Yes
O60701	0	UDP-glucose 6-dehydrogenase	No	No	No	--	No
P63244	5.00E-168	Guanine nucleotide-binding protein subunit beta-2-like 1	Yes	Yes	Yes	No	Yes

1.25	1.48	1.365	P49196	rps-12 40S ribosomal protein S12	K.IIGEYCGLC*K.Y	
1.25	1.48	1.365	P49196	rps-12 40S ribosomal protein S12	K.IIGEYC*GLCK.Y	
1.31	1.43	1.37	P46561	atp-2 ATP synthase subunit beta, mitochondrial	R.C*IAMDGTEGLVR.G	
1.3	1.47	1.385	Q8WQA8	rps-20 Protein RPS-20	K.TPC*GEGSK.T	
1.47	1.31	1.39	P62784	his-1 Histone H4	R.DAVTYC*EHAK.R	
1.25	1.54	1.395	Q9N4A5	Y77E11A.1 Protein Y77E11A.1	K.GFDIKDC*LQR.D	
1.59	1.23	1.41	Q23381	mmcm-1 Probable methylmalonyl-CoA mutase, mitochondrial	R.LPAC*ANQILEK.L	
1.31	1.52	1.415	P53013	eft-3 Elongation factor 1-alpha	R.GSVC*SDSK.Q	
1.4	1.45	1.425	P48152	rps-3 40S ribosomal protein S3	R.GLC*AVAQCESLR.Y	
1.4	1.45	1.425	P48152	rps-3 40S ribosomal protein S3	R.GLCAVAQC*ESLR.Y	
0.91	2	1.455	P91998	F53F1.3 Protein F53F1.3	K.IC*NLNLDK.H	
1.58	1.34	1.46	P91500	T27A3.6 Protein T27A3.6	K.AYVLALAGC*TNSGK.S	
1.46	1.46	1.46	O02056	rpl-4 60S ribosomal protein L4	K.LGPVVIYGQDAEC*A.R.A	
1.37	1.55	1.46	Q9N4L8	lpd-5 Protein LPD-5	K.EDAIAFC*EK.N	
1.38	1.55	1.465	Q9BKU5	Y37E3.8 Protein Y37E3.8, isoform a	K.NQHYC*PTVNVER.L	
1.44	1.5	1.47	Q22100	kat-1 Protein KAT-1	K.SGQIGVAAIC*NGGG.GSSGMVIQK.L	Active site (proton acceptor)
1.45	1.52	1.485	O45865	ant-1.1 Protein ANT-1.1, isoform a	K.NTLDC*AK.K	
1.42	1.56	1.49	Q95X44	vha-8 Protein VHA-8	R.LVEQLLPEC*LDGLQ.K.E	
1.51	1.48	1.495	G5EFE6	cpt-2 Protein CPT-2, isoform b	K.EFVPTYESC*STAAFL.K.G	
1.48	1.51	1.495	Q21962	R12C12.1 Protein R12C12.1, isoform a	R.NLVC*TCPPIESYQ.-	
1.48	1.51	1.495	Q21962	R12C12.1 Protein R12C12.1, isoform a	R.NLVCTC*PPIESYQ.-	
1.48	1.51	1.495	O02640	mdh-1 Probable malate dehydrogenase, mitochondrial	K.NVQC*AYVASDAVK.G	
1.33	1.66	1.495	Q18688	daf-21 Heat shock protein 90	K.LGLDIGDDEIEDSAVP.SSC*TAEAK.I	
1.42	1.6	1.51	Q95YF3	cgh-1 ATP-dependent RNA helicase cgh-1	K.GVEFEDFC*LGR.D	
1.39	1.65	1.52	P34455	aco-2 Probable aconitate hydratase, mitochondrial	K.VSLIGSC*TNSSYED.MTR.A	Iron-Sulfur (4Fe-4S)
1.85	1.22	1.535	Q69Z12	K08E3.10 Protein K08E3.10	K.KVEAAC*GR.S	
1.44	1.65	1.545	Q19264	F09E5.3 Putative deoxyribose-phosphate aldolase	R.IGASSLLDDC*LK.G	
1.27	1.84	1.555	Q17489	unc-44 Protein UNC-44, isoform a	K.DGSSPFDNQEEDIPIASC*K.Q	
1.37	1.75	1.56	Q95XQ8	mcm-4 Protein MCM-4	R.IC*VADVQR.S	
1.63	1.5	1.565	G5ECR7	elb-1 Protein ELB-1	K.AQC*PAALGLR.L	
1.57	1.56	1.565	Q21230	K04G2.1 Eukaryotic translation initiation factor 2 subunit	R.LFFLQCTNC*GSR.C	
1.75	1.39	1.57	G5EF01	tbb-6 Protein TBB-6	K.EIINVQVQGC*GNQIG.AK.F	
1.5	1.64	1.57	O02056	rpl-4 60S ribosomal protein L4	R.SGQGAFGNMC*R.G	
1.48	1.66	1.57	Q22054	rps-16 40S ribosomal protein S16	K.KTATAVAHC*K.K	
1.89	1.28	1.585	O01576	npp-11 Protein NPP-11	K.C*ADFLLDQITK.S	
1.54	1.64	1.59	H2KZV8	mlp-1 Protein MLP-1, isoform b	K.GVGFLGAGC*LTTD.SGEK.F	

P25398	2.00E-47	40S ribosomal protein S12	Yes	Yes	Yes	No	Yes
P25398	2.00E-47	40S ribosomal protein S12	No	No	No	No	No
P06576	0	ATP synthase subunit beta, mitochondrial	No	No	No	No	No
P60866	8.00E-56	40S ribosomal protein S20	Yes	Yes	Yes	No	Yes
P62805	4.00E-66	Histone H4	No	No	No	No	No
Q2TB90	1.00E-93	Putative hexokinase HKDC1	Yes	Yes	No	No	No
P22033	0	Methylmalonyl-CoA mutase, mitochondrial	No	No	--	--	--
Q05639	0	Elongation factor 1-alpha 2	Yes	Yes	No	Yes	No
P23396	1.00E-127	40S ribosomal protein S3	Yes	Yes	Yes	No	Yes
P23396	1.00E-127	40S ribosomal protein S3	No	No	No	No	No
Q04828	4.00E-49	Aldo-keto reductase family 1 member C1	No	No	--	No	--
O96007	6.00E-32	Molybdopterin synthase catalytic subunit	No	No	No	Yes	No
P36578	1.00E-133	60S ribosomal protein L4	No	No	No	No	No
O43181	4.00E-44	NADH dehydrogenase [ubiquinone] iron-sulfur protein 4, mitochondrial	No	No	Yes	--	No
P46776	8.00E-71	60S ribosomal protein L27a	Yes	Yes	No	No	Yes
P24752	2.00E-155	Acetyl-CoA acetyltransferase, mitochondrial	Yes	Yes	Yes	Yes	Yes
P12235	1.00E-143	ADP/ATP translocase 1	Yes	Yes	Yes	Yes	Yes
P36543	1.00E-87	V-type proton ATPase subunit E 1	No	No	No	No	No
P23786	4.00E-128	Carnitine O-palmitoyltransferase 2, mitochondrial	Yes	Yes	Yes	No	--
P23378	0	Glycine dehydrogenase (decarboxylating), mitochondrial	Yes	Yes	Yes	Yes	Yes
P23378	0	Glycine dehydrogenase (decarboxylating), mitochondrial	Yes	Yes	Yes	Yes	No
P40926	7.00E-131	Malate dehydrogenase, mitochondrial	Yes	Yes	Yes	No	Yes
P07900	0	Heat shock protein HSP 90-alpha	No	No	No	No	No
P26196	0	Probable ATP-dependent RNA helicase DDX6	Yes	Yes	Yes	No	No
Q99798	0	Aconitate hydratase, mitochondrial	Yes	Yes	Yes	Yes	Yes
P14649	2.00E-17	Myosin light chain 6B	No	No	No	No	No
Q9Y315	4.00E-87	Deoxyribose-phosphate aldolase	No	No	--	--	--
Q8N8A2	0	Serine/threonine-protein phosphatase 6 regulatory ankyrin repeat subunit B	No	No	--	--	--
P33991	0	DNA replication licensing factor MCM4	No	No	No	No	No
Q15370	5.00E-19	Transcription elongation factor B polypeptide 2	No	No	No	--	--
P20042	6.00E-75	Eukaryotic translation initiation factor 2 subunit 2	Yes	Yes	Yes	Yes	Yes
P68371	1.00E-175	Tubulin beta-4B chain	Yes	Yes	Yes	Yes	Yes
P36578	1.00E-133	60S ribosomal protein L4	Yes	Yes	Yes	Yes	Yes
P62249	2.00E-76	40S ribosomal protein S16	Yes	Yes	Yes	No	Yes
P98088	1.70E-47	Mucin-5AC	No	No	No	--	--
P50461	9.00E-29	Cysteine and glycine-rich protein 3	Yes	Yes	No	--	--

1.61	1.58	1.595	Q9GYJ9	snx-1 Protein SNX-1	K.ALSMLAAC*EESTSL SR.A	
1.52	1.69	1.605	P53588	F47B10.1 Probable succinyl-CoA ligase [ADP-forming] subunit	R.C*DVIAQGHQAAR.E	
1.63	1.59	1.61	Q22053	fib-1 rRNA 2-O-methyltransferase fibrillarlin	K.ANC*IDSTAEPEAVFA GEVNK.L	
1.56	1.66	1.61	A3QMC5	rpl-34 Protein RPL-34	R.AYGGC*LSPNAVK.E	
1.46	1.77	1.615	Q8WQA8	rps-20 Protein RPS-20	K.VC*AQLIDGAK.N	
1.58	1.66	1.62	O17234	gsto-3 Protein GSTO-3, isoform a	R.FC*PYAQR.V	<b>Active site nucleophile</b>
1.54	1.72	1.63	Q09533	rpl-10 60S ribosomal protein L10	K.MLSC*AGADR.L	
1.65	1.64	1.645	Q27371	mup-2 Troponin T	R.NFLAAVC*R.V	
1.68	1.67	1.675	Q9N5K2	rpb-5 DNA-directed RNA polymerases I, II, and III subunit	R.IQQC*DPVAR.Y	
1.57	1.81	1.69	P48150	rps-14 40S ribosomal protein S14	R.IEDVTPIPSDC*TR.R	
1.59	1.8	1.695	Q9TXP0	rps-27 40S ribosomal protein S27	K.LTEGC*SFR.K	
1.71	1.71	1.71	P02566	unc-54 Myosin-4	K.C*NLTLDQK.G	
1.67	1.76	1.715	Q96618	pbs-1 Proteasome subunit beta type	K.ITPITDNMVVC*R.S	
1.54	1.9	1.72	P50432	mel-32 Serine hydroxymethyltransferase	K.AVMDALGSAMC*NK. Y	
1.67	1.8	1.735	P46769	rps-0 40S ribosomal protein SA	K.LIDIGVPC*NNK.G	
1.74	1.77	1.755	P53588	F47B10.1 Probable succinyl-CoA ligase [ADP-forming] subunit	R.ILPC*DNLDEAAK.M	
1.77	1.75	1.76	O01974	eif-3.H Eukaryotic translation initiation factor 3 subunit	K.SC*SSDKYSTR.H	
1.74	1.79	1.765	P02566	unc-54 Myosin-4	R.LPIYTDSC*AR.M	
1.76	1.82	1.79	P48158	rpl-23 60S ribosomal protein L23	R.ISLGLPVGAVMNC*A DNTGAK.N	
1.64	1.96	1.8	Q27389	rpl-16 60S ribosomal protein L13a	R.C*NINPAR.G	
1.59	2.01	1.8	O17586	pas-1 Proteasome subunit alpha type-6	K.NGYDMPC*ELLAK.K	
1.75	1.87	1.81	Q22100	kat-1 Protein KAT-1	K.DGLTDAYDKVHMGN C*GEK.T	
1.66	1.96	1.81	P46769	rps-0 40S ribosomal protein SA	R.FSPGC*LTNQIQK.T	
1.74	1.89	1.815	O02141	C46G7.2 Protein C46G7.2	K.SDSVSTLAPSLALPQ YC*R.E	
1.59	2.08	1.835	H2KZV8	mlp-1 Protein MLP-1, isoform b	K.LLDSCTVAPHEAELY C*K.Q	
1.79	1.9	1.845	Q21307	mek-1 Protein MEK-1, isoform a	K.LC*DFGIAGR.L	
1.94	1.76	1.85	Q21284	K07E3.4 Protein K07E3.4, isoform a	K.LPIC*MAK.T	
1.87	1.88	1.875	Q22101	T02G5.7 Protein T02G5.7	K.GPMGLC*AEK.T	
1.98	1.79	1.885	P30627	glb-1 Globin-like protein	R.QEISDLC*VK.S	
1.95	1.82	1.885	O76449	ZK1055.7 Protein ZK1055.7	K.EDWTSAPLVLSTAQP C*LAGR.I	
1.92	1.94	1.93	P02566	unc-54 Myosin-4	K.ASNMYGIGC*EEFLK. A	
2.12	1.75	1.935	Q22392	dhs-19 Protein DHS-19	K.TGCVGLVDYC*ASK. H	
2.11	1.82	1.965	O45812	T23G11.7 Protein T23G11.7, isoform b	K.STQIFTC*LR.D	
2.4	1.56	1.98	P37806	unc-87 Protein unc-87	R.FASQAGMIGFGTC*R. N	
1.82	2.15	1.985	Q9UAQ6	rab-1 Protein RAB-1	R.YAC*ENVNK.L	
1.88	2.12	2	P49196	rps-12 40S ribosomal protein S12	K.GLHETC*K.A	

O60749	4.00E-95	Sorting nexin-2	No	No	Yes	No	Yes
Q9P2R7	0	Succinyl-CoA ligase [ADP-forming] subunit beta, mitochondrial	Yes	Yes	Yes	Yes	Yes
P22087	6.00E-133	rRNA 2'-O-methyltransferase fibrillar	Yes	Yes	Yes	--	Yes
P49207	2.00E-29	60S ribosomal protein L34	No	No	No	No	No
P60866	8.00E-56	40S ribosomal protein S20	Yes	Yes	Yes	No	Yes
P78417	1.00E-38	Glutathione S-transferase omega-1	Yes	Yes	Yes	No	No
P27635	3.00E-111	60S ribosomal protein L10	Yes	Yes	Yes	Yes	Yes
P45379	1.60E-20	Troponin T, cardiac muscle	No	No	No	--	--
P19388	2.00E-122	DNA-directed RNA polymerases I, II, and III subunit RPABC1	No	No	No	No	No
P62263	9.00E-84	40S ribosomal protein S14	No	No	No	No	No
P42677	8.00E-38	40S ribosomal protein S27	Yes	Yes	Yes	No	Yes
P13533	0	Myosin-6	No	No	Yes	No	No
P28072	2.00E-66	Proteasome subunit beta type-6	Yes	Yes	Yes	Yes	Yes
P34896	0	Serine hydroxymethyltransferase, cytosolic	No	No	No	No	No
P08865	6.00E-107	40S ribosomal protein SA	Yes	Yes	Yes	Yes	No
Q9P2R7	0	Succinyl-CoA ligase [ADP-forming] subunit beta, mitochondrial	Yes	Yes	No	No	No
O15372	8.00E-63	Eukaryotic translation initiation factor 3 subunit H	No	No	No	--	No
P13533	0	Myosin-6	No	No	Yes	No	No
P62829	4.00E-85	60S ribosomal protein L23	Yes	Yes	Yes	Yes	Yes
P40429	3.00E-73	60S ribosomal protein L13a	No	No	Yes	No	No
P60900	2.00E-102	Proteasome subunit alpha type-6	No	No	No	Yes	No
P24752	2.00E-155	Acetyl-CoA acetyltransferase, mitochondrial	Yes	Yes	Yes	No	Yes
P08865	6.00E-107	40S ribosomal protein SA	No	No	No	No	No
Q9UM73	0.7	ALK tyrosine kinase receptor	--	--	--	--	--
P50461	9.00E-29	Cysteine and glycine-rich protein 3	Yes	Yes	Yes	--	Yes
O14733	1.00E-111	Dual specificity mitogen-activated protein kinase kinase 7	Yes	Yes	Yes	Yes	No
P11586	0	C-1-tetrahydrofolate synthase, cytoplasmic	Yes	Yes	Yes	Yes	Yes
P24752	1.00E-127	Acetyl-CoA acetyltransferase, mitochondrial	Yes	Yes	Yes	No	Yes
Q9ULR3	0.39	Protein phosphatase 1H	--	--	--	--	--
Q9Y6X9	4.8	MORC family CW-type zinc finger protein 2	No	No	--	--	--
P13533	0	Myosin-6	No	No	No	No	No
Q8N3Y7	1.00E-98	Epidermal retinol dehydrogenase 2	Yes	Yes	No	No	No
Q9NP79	2.00E-51	Vacuolar protein sorting-associated protein VTA1 homolog	Yes	Yes	Yes	--	No
K7ER02	1.00E-17	Calponin-1	No	No	--	--	--
P62820	1.00E-120	Ras-related protein Rab-1A	No	No	Yes	No	No
P25398	2.00E-47	40S ribosomal protein S12	No	No	Yes	No	No

1.86	2.26	2.06	O45924	Y39E4A.3 Protein Y39E4A.3, isoform a	R.GYTMENFMNQC*YGNADDLGK.G	
1.97	2.24	2.105	Q09444	ubh-4 Probable ubiquitin carboxyl-terminal hydrolase ubh	R.GHC*LSNSEIR.T	
2.15	2.1	2.125	Q09596	gst-5 Probable glutathione S-transferase 5	K.ETC*AAPFGQLPFLEVDGK.K	
2.04	2.27	2.155	G5ECV9	alh-3 Protein ALH-3	K.GENC*IAAGR.V	Active site
1.84	2.51	2.175	Q9N3C9	rpb-7 Protein RPB-7	K.LFNEVEGTC*TGK.Y	
1.35	3	2.175	P34574	chc-1 Probable clathrin heavy chain 1	R.AAIGQLC*EK.A	
2.22	2.14	2.18	Q69Z13	K08E3.5 Protein K08E3.5, isoform f	K.LNGGLGTSMGC*K.G	
2.08	2.29	2.185	O01692	rps-17 40S ribosomal protein S17	R.VC*DEVAIIGSK.P	
2.17	2.21	2.19	Q19246	dhs-25 Protein DHS-25	K.TPMTEAMPPTVLAEIC*K.G	
2.2	2.32	2.26	A7LPE5	gpdh-2 Protein GPDH-2, isoform c	K.NVVAC*AAGFTDGLGYGDNTK.A	
2.14	2.56	2.35	Q17334	sodh-1 Alcohol dehydrogenase 1	K.LMNFNC*LNCFCK.K	Zinc-binding
2.14	2.56	2.35	Q17334	sodh-1 Alcohol dehydrogenase 1	K.LMNFNCLNC*EFCK.K	Zinc-binding
2.14	2.56	2.35	Q17334	sodh-1 Alcohol dehydrogenase 1	K.LMNFNCLNCFCK.K	Zinc-binding
2.33	2.43	2.38	Q18212	hel-1 Spliceosome RNA helicase DDX39B homolog	K.YFVLDEC*DK.M	
2.32	2.45	2.385	O44906	W05G11.6 Protein W05G11.6, isoform a	K.AELMNPAGIYIC*DG SQK.E	
2.25	2.56	2.405	O44906	W05G11.6 Protein W05G11.6, isoform a	K.TNAMAMESC*R.A	
2.27	2.55	2.41	Q18496	acs-19 Protein ACS-19, isoform a	K.TNISYNC*LER.N	
2.27	2.63	2.45	P90889	F55H12.4 Protein F55H12.4	R.GSTGHC*YK.K	
2.7	2.21	2.455	G5EF87	swn-1 Protein SWSN-1	K.GVQAAAASC*LAAAVK.A	
2.3	3.04	2.67	Q23621	gdh-1 Glutamate dehydrogenase	K.NFDPFTELMYEKC*DI FVPAACEK.S	
2.3	3.04	2.67	Q23621	gdh-1 Glutamate dehydrogenase	K.CDIFVPAAC*EK.S	
2.67	2.75	2.71	G5EES6	ufd-3 Protein UFD-3, isoform b	K.ALAVTQGGC*LISGGRDET VK.F	
2.6	2.94	2.77	G5EG13	dhs-12 Protein DHS-12	R.AAIVNIGSDC*ASQALNLR.G	
2.55	3	2.775	O17759	tk1-1 Protein TKT-1	R.ISSIEMTC*ASK.S	
2.69	2.88	2.785	Q10457	B0286.3 Probable multifunctional protein ADE2	R.MPNGIGC*TTVLDPSEAAALAAK.I	
2.82	2.79	2.805	P91859	F32A7.5 Protein F32A7.5, isoform d	K.DISGEQLQAILC*GK.Q	
2.36	3.32	2.84	Q19655	F20D6.11 Protein F20D6.11	K.FSGC*NQGSTK.E	
2.75	3.06	2.905	P27639	inf-1 Eukaryotic initiation factor 4A	K.RAIVPC*TTGK.D	
2.59	3.31	2.95	Q27464	gspd-1 Glucose-6-phosphate 1-dehydrogenase	K.SSC*ELSTHLAK.L	
2.67	3.29	2.98	Q23624	ZK829.7 Protein ZK829.7	R.AILEVC*DPSSALDADQSGGVPIPAATSE.-	
4.81	1.41	3.11	Q93874	rab-14 Protein RAB-14	K.AFAEENGLTFLEC*SAK.T	
3.25	3	3.125	Q23069	moc-2 Protein MOC-2	R.VCVITVSDTC*SAGTR.T	
3.4	3.66	3.53	O44906	W05G11.6 Protein W05G11.6, isoform a	K.FIAAAFPSAC*GK.T	GTP-binding
4.22	4.49	4.355	Q17334	sodh-1 Alcohol dehydrogenase 1	K.DTNLAAAAPILC*AGVTVYK.A	Zinc-binding (catalytic)

P12694	0	2-oxoisovalerate dehydrogenase subunit alpha, mitochondrial	Yes	Yes	Yes	No	Yes
Q9Y5K5	1.00E-97	Ubiquitin carboxyl-terminal hydrolase isozyme L5	No	No	No	--	No
O60760	2.00E-35	Hematopoietic prostaglandin D synthase	No	No	No	--	--
Q3SY69	0	Mitochondrial 10-formyltetrahydrofolate dehydrogenase	Yes	Yes	Yes	Yes	Yes
P62487	2.00E-98	DNA-directed RNA polymerase II subunit RPB7	Yes	Yes	Yes	Yes	Yes
Q00610	0	Clathrin heavy chain 1	Yes	Yes	Yes	No	Yes
Q16851	0	UTP--glucose-1-phosphate uridylyltransferase	Yes	Yes	Yes	Yes	Yes
P08708	1.00E-55	40S ribosomal protein S17	Yes	Yes	Yes	Yes	No
Q92506	2.00E-76	Estradiol 17-beta-dehydrogenase 8	No	No	No	No	No
P21695	2.00E-120	Glycerol-3-phosphate dehydrogenase [NAD(+)], cytoplasmic	No	No	Yes	No	No
P08319	7.00E-20	Alcohol dehydrogenase 4	Yes	Yes	Yes	Yes	Yes
P08319	7.00E-20	Alcohol dehydrogenase 4	Yes	Yes	Yes	Yes	Yes
P08319	7.00E-20	Alcohol dehydrogenase 4	Yes	Yes	Yes	Yes	Yes
Q13838	0	Spliceosome RNA helicase DDX39B	Yes	Yes	Yes	Yes	Yes
Q16822	0	Phosphoenolpyruvate carboxykinase [GTP], mitochondrial	Yes	Yes	Yes	--	--
Q16822	0	Phosphoenolpyruvate carboxykinase [GTP], mitochondrial	No	No	No	--	--
Q9NR19	0	Acetyl-coenzyme A synthetase, cytoplasmic	No	No	No	Yes	Yes
B2RXH2	7.6	Lysine-specific demethylase 4E	--	--	--	--	--
Q8TAQ2	4.00E-133	SWI/SNF complex subunit SMARCC2	No	No	--	No	No
P00367	0	Glutamate dehydrogenase 1, mitochondrial	Yes	Yes	Yes	No	Yes
P00367	0	Glutamate dehydrogenase 1, mitochondrial	No	No	No	No	No
Q9Y263	5.00E-75	Phospholipase A-2-activating protein	No	No	No	No	No
Q8NEX9	8.00E-12	Short-chain dehydrogenase/reductase family 9C member 7	No	No	No	No	No
P29401	0	Transketolase	No	Yes	No	No	No
P22234	9.00E-148	Multifunctional protein ADE2	Yes	Yes	Yes	No	--
P46821	1.00E-11	Microtubule-associated protein 1B	No	No	No	--	--
Q96NN9	5.00E-99	Apoptosis-inducing factor 3	No	No	No	--	No
Q14240	0	Eukaryotic initiation factor 4A-II	Yes	Yes	Yes	No	No
P11413	0	Glucose-6-phosphate 1-dehydrogenase	No	No	No	No	No
Q00796	1.00E-11	Sorbitol dehydrogenase	Yes	--	No	--	--
P61106	5.00E-130	Ras-related protein Rab-14	No	No	No	No	No
Q9NQX3	6.00E-37	Gephyrin	Yes	Yes	Yes	--	No
Q16822	0	Phosphoenolpyruvate carboxykinase [GTP], mitochondrial	Yes	Yes	Yes	--	--
P08319	7.00E-20	Alcohol dehydrogenase 4	Yes	Yes	Yes	Yes	Yes

4.04	5.14	4.59	Q93545	F20G2.2 Protein F20G2.2	K.SC*SIDLAK.Y	
12.61	15.62	14.115	O16228	djr-1.2 Protein DJR-1.2	K.LAEC*PVIGELK.T	

O14756	2.00E-16	17-beta-hydroxysteroid dehydrogenase type 6	No	No	No	No	No
Q99497	5.00E-42	Protein deglycase DJ-1	No	No	No	--	Yes

**Table 4A-1.** MS results showing the 87 *C. elegans* serine hydrolase proteins (based on homology to human serine hydrolases if unannotated) labeled by FP-biotin in 4 day old *daf-2* and *daf-16;daf-2* mutants. Proteins are listed by fold change from most decreased to most increased in *daf-2* mutants. Human homologues and conservation of the active site serine in *C. elegans* are indicated.

Protein	DAF16		DAF2		Fold Change	Consv. Act. Site	Human Homologue
	1	2	1	2			
Beta-lactamase domain-containing protein 2	0	6	0	0	0.000	yes	Serine beta-lactamase-like protein
Putative serine protease K12H4.7	2	8	0	0	0.000	yes	Thymus-specific serine protease
Protein F09C8.1	159	119	28	22	0.180	yes	Phospholipase B1
Protein LIPS-15	25	43	17	4	0.309	no	Lysosomal thioesterase PPT2
Protein FAAH-1, isoform a	131	123	66	23	0.350	yes	Fatty-acid amide hydrolase 1
Protein F56C11.6, isoform a	4	6	2	0	0.400	yes	Cholinesterase
Uncharacterized NTE family protein ZK370.4	33	28	21	6	0.443	yes	Patatin-like phospholipase domain-containing protein 7
Protein FAAH-3	42	55	28	19	0.485	yes	Fatty-acid amide hydrolase
Uncharacterized serine carboxypeptidase K10B2.2	8	50	21	8	0.500	yes	Lysosomal protective protein (Cathepsin A)
Protein Y16B4A.2	176	195	114	72	0.501	yes	Lysosomal protective protein (Cathepsin A)
Protein FAAH-2	62	95	44	35	0.503	yes	Fatty-acid amide hydrolase
Protein PCP-2	5	12	6	3	0.529	yes	Thymus-specific serine protease
Protein F16F9.4	3	29	11	6	0.531	yes	Neutral cholesterol ester hydrolase 1
Protein TRY-1	0	13	7	0	0.538	yes	Serine protease 33, EOS
Protein R07B7.8	34	62	31	25	0.583	yes	Phospholipase B1
Protein TSN-1	6	14	8	4	0.600	no	Staphylococcal nuclease domain-containing protein 1
Protein K11G9.1	82	78	54	55	0.681	yes	Cholinesterase
Protein K10C2.1	329	258	176	268	0.756	no	Lysosomal protective protein
Protein D2024.2	76	92	73	60	0.792	yes	Probable arylformamidase
Protein LIPS-5, isoform a	5	5	4	0	0.800	yes	Lysosomal acid lipase/cholesteryl ester hydrolase
Protein FAAH-4, isoform b	202	0	126	202	0.812	yes	Fatty-acid amide hydrolase
Protein FIL-1	4	13	10	4	0.824	no	Fasting Induced Lipase
Protein FAAH-4, isoform a	202	167	126	202	0.889	yes	Fatty-acid amide hydrolase
Dipeptidyl peptidase family member 1	8	16	11	0	0.917	yes	Dipeptidyl peptidase 4
Dipeptidyl peptidase family member 2	127	141	115	142	0.959	yes	Seprase
Protein LACT-4	142	68	106	97	0.967	yes	Serine beta-lactamase-like protein
Protein DPF-5	106	121	126	95	0.974	yes	Acylamino-acid-releasing enzyme
Protein PCP-3	0	0	0	0	0.000	yes	Thymus-specific serine protease

Protein Y37H2A.13	0	0	0	0	0.000	no	Dipeptidyl peptidase
Protein T08B1.4, isoform b	21	22	26	18	1.023	no	triacylglycerol lipase
Uncharacterized serine carboxypeptidase F13D12.6	178	215	136	268	1.028	yes	Lysosomal protective protein
Bifunctional glyoxylate cycle protein	7	12	15	5	1.053	no	Sn1-specific diacylglycerol lipase alpha
Protein Y71H2AM.13	84	95	111	92	1.134	yes	Liver carboxylesterase 1
Protein W02B12.1	30	36	37	41	1.182	no	Phospholipase A2
Protein PES-9	3	7	6	0	1.200	no	Cytosolic non-specific dipeptidase
Uncharacterized serine carboxypeptidase F41C3.5	906	801	697	1533	1.306	yes	Lysosomal protective protein
Protein R05D7.4	106	106	154	123	1.307	yes	Abhydrolase domain-containing protein 11
Protein DPF-3, isoform a	210	209	291	264	1.325	yes	Dipeptidyl peptidase
Protein DPF-3, isoform b	210	209	291	264	1.325	yes	Dipeptidyl peptidase
Acetylcholinesterase	0	3	6	2	1.333	yes	Cholinesterase
Protein ACE-3	0	3	6	2	1.333	yes	Cholinesterase
Protein B0238.1	340	299	329	526	1.338	yes	Carboxylesterase 5A
Protein ATH-1	143	284	233	357	1.382	yes	Acyl-protein thioesterase 1
Protein F47A4.5	6	4	7	0	1.400	yes	calcium-independent phospholipase A2
Protein GYG-1, isoform b	0	6	10	7	1.417	no	GYG1 protein
Protein LACT-1	72	136	160	143	1.457	no	Beta-lactamase
Esterase CM06B1	49	44	85	67	1.634	yes	Cholinesterase
Protein F55F3.2, isoform b	14	36	46	39	1.700	no	Brain carboxylesterase
Protein F55F3.2, isoform a	14	36	46	39	1.700	no	Brain carboxylesterase
Protein K01A2.5	60	60	105	114	1.825	yes	Valacyclovir hydrolase
Protein Y45F10A.3	33	61	79	105	1.957	yes	Arylformamidase
Protein Y65B4BR.1	0	0	2	0	2.000	no	Phospholipase A2
Protein LACT-3	0	6	13	0	2.167	yes	Serine beta-lactamase-like protein LACTB,
Protein F15A8.6	4	4	9	0	2.250	yes	Cholinesterase
Prolyl carboxy peptidase like protein 5	38	23	47	98	2.377	yes	Lysosomal Pro-X carboxypeptidase
Protein Y48G10A.1	299	198	396	798	2.402	yes	S-formylglutathione hydrolase
Putative serine protease pcp-1	0	3	10	5	2.500	yes	Lysosomal Pro-X carboxypeptidase
Protein Y49E10.16, isoform a	23	17	53	49	2.550	yes	Monoglyceride lipase
Protein Y43F8A.3, isoform b	4	10	0	18	2.571	yes	Neutral cholesterol ester hydrolase 1
Gut esterase 1	297	710	1227	1511	2.719	yes	Brain carboxylesterase
Protein M05B5.4	31	38	96	93	2.739	yes	phospholipase A2
Protein T08B2.7, isoform b	4	8	22	11	2.750		
Protein T08B2.7, isoform a	4	8	22	11	2.750		
Protein Y73B6BL.4	0	0	4	2	3.000	yes	Calcium-independent phospholipase A2-gamma
Protein C45B2.6	0	0	3	0	3.000	yes	calcium-independent phospholipase A2
Dipeptidyl peptidase family member 6	0	0	3	3	3.000	yes	Acylamino-acid-releasing enzyme

Protein D1054.1	0	4	20	7	3.375	yes	Patatin-like phospholipase domain-containing protein 4
Protein Y40D12A.2	2	7	16	0	3.556	yes	Lysosomal protective protein (Cathepsin A)
Protein LIPS-17	5	30	84	50	3.829		Lipase Class 2
Protein TKT-1	2	8	34	12	4.600	?	Transketolase
Protein F13H8.11	3	9	34	22	4.667	yes	Phospholipase B1
Protein K07C11.4	12	19	91	59	4.839	yes	Cocaine esterase
Protein DPF-4	2	5	26	8	4.857	yes	Acylamino-acid-releasing enzyme
Probable protein phosphatase methylesterase 1	11	12	39	73	4.870	yes	Protein phosphatase methylesterase 1
Protein C40H1.9	0	0	2	8	5.000	yes	Monoglyceride lipase
Protein Y43F8A.3, isoform a	4	10	56	18	5.286	yes	Neutral cholesterol ester hydrolase 1
Putative subtilase-type proteinase F21H12.6	8	11	78	34	5.895	yes	Tripeptidyl-peptidase 2
Protein W07A8.2, isoform a	0	0	16	9	12.500	yes	calcium-independent phospholipase A2
Protein W07A8.2, isoform c	0	0	16	9	12.500	yes	calcium-independent phospholipase A3
Protein W07A8.2, isoform b	0	0	16	9	12.500	yes	calcium-independent phospholipase A4
Protein IPLA-1, isoform c	0	0	22	4	13.000	yes	Phospholipase DDHD1
Protein IPLA-1, isoform b	0	0	22	4	13.000	yes	Phospholipase DDHD1
Protein IPLA-1, isoform a	0	0	22	4	13.000	yes	Phospholipase DDHD1
Protein IPLA-1, isoform d	0	0	22	4	13.000	yes	Phospholipase DDHD1
Intracellular phospholipase A1	0	0	22	4	13.000	yes	Phospholipase DDHD1
Protein C23H4.2	0	0	13	13	13.000	yes	Cocaine esterase (Carboxylesterase)
Protein C17H12.4	0	0	23	4	13.500	yes	Liver carboxylesterase 1

**Table 6A-1.** MS results showing the 363 biotin-PG-labeled proteins in human healthy and RA sera. Highlighted in green are the 150 proteins that have at least 5 spectral counts in at least 1 run and a greater than 2-fold average spectral count than the control sample. Highlighted in orange are the 5 keratin proteins with possible RA significance as they are increased more than 2-fold in RA samples versus healthy samples and not identified in the controls. Highlighted in red are the other keratin proteins that were removed from analysis due to the significantly high number of spectral counts in the control samples.

biotin-PG	Healthy				RA1				RA2				
	+	+	-	-	+	+	-	-	+	+	+	-	-
Protein	1	2	1	2	1	2	1	2	1	2	3	1	2
HBB Hemoglobin subunit beta	9	9	2	0	16	23	2	0	4	7	5	2	0
IGKC Ig kappa chain C region	244	122	5	6	306	206	17	0	163	288	179	8	4
IGHM Ig mu chain C region	153	103	3	13	82	61	10	0	81	172	111	0	3
ALB Serum albumin	1172	532	10	15	911	963	28	15	603	840	1239	0	22
IGHG1 Ig gamma-1 chain C region	974	378	17	35	522	521	28	46	445	970	726	6	16
HP Haptoglobin	172	71	2	4	184	187	9	0	107	207	125	0	2
IGHG3 Ig gamma-3 chain C region	716	246	18	22	385	358	16	0	276	728	534	0	7
APOA1 Apolipoprotein A-I	419	287	0	6	256	257	22	4	241	242	297	0	3
C4B Complement C4-B	311	150	8	5	146	152	5	6	116	234	202	2	0
IGHG4 Ig gamma-4 chain C region	708	222	12	23	415	423	17	31	331	603	504	0	5
IGHG2 Ig gamma-2 chain C region	635	207	0	0	420	429	16	13	312	507	415	0	4
C3 Complement C3	849	442	9	11	403	454	17	7	501	895	417	4	4
IGLL5 Immunoglobulin lambda-like polypeptide 5	186	85	3	0	56	30	6	0	154	170	79	0	0
APOA2 Apolipoprotein A-II	48	32	3	0	42	35	5	0	27	49	28	0	0
IGLC2 Ig lambda-2 chain C regions	219	111	3	4	63	30	6	0	183	201	122	0	0
Ig kappa chain V-III region HAH	38	15	0	0	69	20	4	0	22	37	44	0	0
Ig heavy chain V-III region VH26	46	19	0	0	35	24	2	0	17	29	23	0	0
C4BPA C4b-binding protein alpha chain	61	71	0	0	34	26	2	0	29	71	29	0	0
IGHA1 Ig alpha-1 chain C region	257	155	2	3	137	36	5	0	186	217	170	0	0
SERPINA1 Alpha-1-antitrypsin	107	68	0	2	43	30	2	0	20	29	31	0	0
SERPING1 Plasma protease C1 inhibitor	95	30	0	0	55	22	2	0	16	47	38	0	0
HPR Haptoglobin-related protein	49	30	0	0	92	61	3	0	46	54	43	0	0
APOB Apolipoprotein B-100	129	127	0	4	120	64	2	3	85	208	102	0	0

CFH Complement factor H	289	158	2	0	181	100	2	0	104	226	206	0	0
HPX Hemopexin	597	322	0	0	263	417	6	2	295	547	433	0	0
KRT75 Keratin, type II cytoskeletal 75	0	61	0	21	0	0	0	0	0	48	0	0	0
PLG Plasminogen	114	74	0	2	66	37	0	0	33	69	69	0	0
IGHA2 Ig alpha-2 chain C region	192	113	0	3	123	0	0	0	0	155	140	0	0
A2M Alpha-2-macroglobulin	266	163	2	0	75	38	0	0	68	139	71	0	0
CP Ceruloplasmin	375	183	0	2	365	248	0	0	137	328	244	0	0
IGKV4-1 Ig kappa chain V-IV region	19	19	0	0	16	23	0	0	17	29	13	0	0
C9 Complement component C9	37	25	0	0	36	21	0	0	17	36	31	0	0
KLKB1 Plasma kallikrein	15	14	0	0	17	6	0	0	10	17	13	0	0
ITIH2 Inter-alpha-trypsin inhibitor heavy chain H2	63	62	0	0	69	22	0	0	45	61	71	0	0
C8B Complement component C8 beta chain	8	13	0	0	17	11	0	0	8	11	8	0	0
KNG1 Kininogen-1	50	34	0	0	47	24	0	0	23	29	47	0	0
TF Serotransferrin	324	202	0	0	170	162	0	0	111	244	189	0	0
CFI Complement factor I	14	6	0	0	11	6	0	0	8	10	14	0	0
APOH Beta-2-glycoprotein 1	68	50	0	0	36	41	0	0	21	40	60	0	0
ITIH1 Inter-alpha-trypsin inhibitor heavy chain H1	55	31	0	0	33	35	0	0	22	59	31	0	0
TTR Transthyretin	26	27	0	0	13	18	0	0	9	27	19	0	0
C5 Complement C5	47	45	0	0	85	35	0	0	38	66	36	0	0
ITIH4 Inter-alpha-trypsin inhibitor heavy chain H4	56	40	0	0	69	19	0	0	32	38	49	0	0
C1R Complement C1r subcomponent	25	15	0	0	32	14	0	0	10	21	18	0	0
AGT Angiotensinogen	8	11	0	0	15	5	0	0	10	11	5	0	0
F2 Prothrombin	56	24	0	0	31	25	0	0	18	42	34	0	0
RBP4 Retinol-binding protein 4	14	13	0	0	10	9	0	0	15	6	4	0	0
C1S Complement C1s subcomponent	21	11	0	0	25	9	0	0	15	31	22	0	0
CFB cDNA FLJ55673, highly similar to Complement factor B (EC 3.4.21.47)	125	95	0	0	51	46	0	0	40	104	104	0	0
C1QB Complement C1q subcomponent subunit B	6	3	0	0	4	4	0	0	6	8	10	0	0
C8G Complement component C8 gamma chain	10	6	0	0	7	2	0	0	7	11	12	0	0
PON1 Serum paraoxonase/arylesterase 1	9	6	0	0	22	8	0	0	13	16	17	0	0
GC Vitamin D-binding protein	64	37	0	0	31	34	0	0	24	19	22	0	0
LGALS3BP Galectin-3-binding protein	5	3	0	0	4	3	0	0	2	5	8	0	0
APCS Serum amyloid P-component	9	5	0	0	9	3	0	0	4	12	6	0	0
CLU Clusterin	16	15	0	0	25	9	0	0	8	7	21	0	0
AMBP Protein AMBP	28	16	0	0	16	6	0	0	11	11	23	0	0

C6 Complement component C6	4	9	0	0	11	7	0	0	3	12	5	0	0
A1BG Alpha-1B-glycoprotein	19	9	0	0	13	6	0	0	4	17	16	0	0
SERPINF1 Pigment epithelium derived factor	17	16	0	0	12	2	0	0	11	14	6	0	0
PROS1 Vitamin K-dependent protein S	10	19	0	0	12	7	0	0	5	18	22	0	0
HBA2 Hemoglobin subunit alpha	14	7	0	0	16	16	0	0	2	11	8	0	0
APOC3 Apolipoprotein C-III	0	5	0	0	6	5	0	0	7	8	5	0	0
SERPINC1 Antithrombin-III	163	73	0	0	84	52	0	0	49	92	52	0	0
AHSG Alpha-2-HS-glycoprotein	44	43	0	0	39	5	0	0	17	28	27	0	0
PGLYRP2 N-acetylmuramoyl-L-alanine amidase	14	7	0	0	7	6	0	0	4	12	4	0	0
APOE Apolipoprotein E	13	11	0	0	23	3	0	0	7	12	17	0	0
APOA4 Apolipoprotein A-IV	50	29	0	0	32	18	0	0	12	31	65	0	0
IGFALS Insulin-like growth factor-binding protein complex acid labile subunit	15	11	0	0	15	2	0	0	4	10	7	0	0
C7 Complement component C7	15	11	0	0	20	9	0	0	13	24	40	0	0
FCN3 Ficolin-3	10	7	0	0	13	0	0	0	8	14	5	0	0
SERPINA3 Alpha-1-antichymotrypsin	30	23	0	0	75	34	0	0	26	13	31	0	0
F13B Coagulation factor XIII B chain	0	11	0	0	16	8	0	0	5	15	15	0	0
VTN Vitronectin	32	10	0	0	10	12	0	0	4	17	15	0	0
GPLD1 Phosphatidylinositol-glycan-specific phospholipase D	4	3	0	0	9	8	0	0	4	17	11	0	0
SERPINA4 Kallistatin	3	5	0	0	11	7	0	0	2	3	4	0	0
APOL1 Apolipoprotein L1	0	6	0	0	5	2	0	0	4	2	4	0	0
GSN Gelsolin	30	9	0	0	20	0	0	0	13	14	22	0	0
APOC2 Apolipoprotein C-II	0	4	0	0	9	5	0	0	5	3	10	0	0
FN1 Fibronectin	36	29	0	0	61	49	0	0	77	184	97	0	0
SERPIND1 Heparin cofactor 2	4	8	0	0	15	2	0	0	3	21	8	0	0
CD5L CD5 antigen-like	8	4	0	0	5	0	0	0	0	9	4	0	0
Ig kappa chain V-III region VG	16	0	0	0	39	9	0	0	12	14	9	0	0
F12 Coagulation factor XII	25	11	0	0	22	0	0	0	0	44	23	0	0
C8A Complement component C8 alpha chain	7	0	0	0	9	0	0	0	2	6	4	0	0
CFHR1 Complement factor H-related protein 1	0	13	0	0	6	9	0	0	0	26	14	0	0
SAA4 Serum amyloid A-4 protein	4	0	0	0	10	16	0	0	4	0	8	0	0
IGKV1-5 Ig kappa chain V-I region HK102	10	0	0	0	9	0	0	0	3	18	6	0	0
SERPINF2 Alpha-2-antiplasmin	4	5	0	0	7	0	0	0	0	4	0	0	0
PZP Pregnancy zone protein	0	22	0	0	13	0	0	0	11	16	0	0	0
MYH9 Myosin-9	8	9	0	0	16	0	0	0	0	10	0	0	0

CPN2 Carboxypeptidase N subunit 2	0	3	0	0	5	0	0	0	0	2	4	0	0
LUM Lumican	3	4	0	0	6	0	0	0	0	2	0	0	0
APOD Apolipoprotein D	3	0	0	0	12	0	0	0	0	9	9	0	0
Uncharacterized protein	19	3	0	0	15	0	0	0	0	0	14	0	0
SERPINA10 Protein Z-dependent protease inhibitor	0	4	0	0	0	0	0	0	5	4	0	0	0
Ig heavy chain V-I region V35	9	2	0	0	0	0	0	0	2	10	0	0	0
MACF1 Microtubule-actin cross-linking factor 1, isoforms 1/2/3/5	4	0	0	0	0	0	0	0	2	5	0	0	0
QSOX1 Sulfhydryl oxidase 1	0	2	0	0	5	0	0	0	0	0	2	0	0
C2 Complement C2	0	0	0	0	9	0	0	0	0	10	0	0	0
CFB Complement factor B	0	0	0	0	0	46	0	0	40	0	0	0	0
SAA2 Serum amyloid A-2 protein	0	0	0	0	9	14	0	0	0	0	0	0	0
Ig kappa chain V-III region NG9	0	0	0	0	18	0	0	0	0	0	10	0	0
TTN Titin	5	4	0	0	0	2	0	0	4	2	3	0	0
ORM2 Alpha-1-acid glycoprotein 2	6	7	0	0	3	0	0	0	3	0	0	0	0
ECM1 Extracellular matrix protein 1	2	0	0	0	3	7	0	0	0	3	0	0	0
APOC1 Apolipoprotein C-I	0	4	0	0	5	0	0	0	0	0	0	0	0
ORM1 Alpha-1-acid glycoprotein 1	7	0	0	0	3	0	0	0	0	0	0	0	0
KRT82 Keratin, type II cuticular Hb2	0	8	0	0	0	0	0	0	24	0	0	0	0
KRT83 Keratin, type II cuticular Hb3	0	14	0	0	0	0	0	0	44	0	0	0	0
KRT81 Keratin, type II cuticular Hb1	0	14	0	0	0	0	0	0	45	0	0	0	0
KRT79 Keratin, type II cytoskeletal 79	0	61	0	0	0	0	0	0	0	0	0	0	0
Ig kappa chain V-III region CLL	0	0	0	0	22	0	0	0	0	0	0	0	0
KRT33B Keratin, type I cuticular Ha3-II	0	0	0	0	8	0	0	0	0	0	0	0	0
KRT33A Keratin, type I cuticular Ha3-I	0	0	0	0	6	0	0	0	0	0	0	0	0
PKP1 Plakophilin-1	0	0	0	0	0	13	0	0	0	0	0	0	0
ENO1 Alpha-enolase	0	0	0	0	0	8	0	0	0	0	0	0	0
SBSN Suprabasin	0	0	0	0	0	5	0	0	0	0	0	0	0
CAT Catalase	0	0	0	0	0	8	0	0	0	0	0	0	0
NCCRP1 Non-specific cytotoxic cell receptor protein 1 homolog	0	0	0	0	0	5	0	0	0	0	0	0	0
Ig heavy chain V-II region ARH-77	0	0	0	0	0	0	0	0	0	5	0	0	0
RPL4 60S ribosomal protein L4	0	0	0	0	0	0	0	0	0	5	0	0	0
PRSS1 Trypsin-1	0	0	0	0	0	0	0	0	0	0	6	0	0
PRSS2 Trypsin-2	0	0	0	0	0	0	0	0	0	0	6	0	0

ARG1 Arginase-1	0	0	0	0	0	23	0	0	0	0	0	0	0
HBD Hemoglobin subunit delta	6	0	0	0	16	0	2	0	0	0	0	2	0
KPRP Keratinocyte proline-rich protein	0	3	3	0	0	58	4	3	0	2	0	0	0
SERPINB12 Serpin B12	0	0	3	0	0	18	0	0	0	2	0	0	0
HRNR Hornerin	0	0	8	0	0	130	0	0	0	7	0	0	0
FLG2 Filaggrin-2	0	4	5	0	0	16	0	0	0	0	0	0	0
HABP2 Hyaluronan-binding protein 2	3	6	0	0	2	0	0	0	0	0	3	0	0
PRSS3 Trypsin-3	0	3	0	0	0	0	0	0	0	5	0	0	0
IGJ Immunoglobulin J chain	0	0	0	0	4	0	0	0	0	10	0	0	0
CLEC3B Tetranectin	0	0	0	0	2	0	0	0	0	0	5	0	0
SAA1 Serum amyloid A-1 protein	0	0	0	0	8	0	0	0	0	0	3	0	0
DSC1 Desmocollin-1	0	0	0	0	0	6	0	0	0	0	0	0	0
CFHR3 Complement factor H-related protein 3	0	0	0	0	9	0	0	0	0	0	0	0	0
HRG Histidine-rich glycoprotein	29	14	7	8	21	7	8	8	12	11	24	2	5
ACTB Actin, cytoplasmic 1	0	0	0	2	0	11	4	5	0	0	0	0	0
JUP Junction plakoglobin	2	8	3	6	0	115	5	18	0	6	0	0	0
DSG1 Desmoglein-1	0	0	6	0	0	33	2	4	0	3	0	0	0
DSP Desmoplakin	0	8	14	7	0	106	5	13	2	9	2	0	0
TGM3 Protein-glutamine gamma-glutamyltransferase E	0	0	2	0	0	17	0	0	0	0	0	0	0
BLMH Bleomycin hydrolase	0	0	2	0	0	7	0	0	0	0	0	0	0
SERPINB3 Serpin B3	0	0	2	0	0	5	0	0	0	0	0	0	0
KRT86 Keratin, type II cuticular Hb6	0	14	0	0	22	0	0	0	45	0	0	0	0
KRT85 Keratin, type II cuticular Hb5	0	14	0	0	17	0	0	0	45	0	0	0	0
KRT71 Keratin, type II cytoskeletal 71	0	13	0	0	0	34	0	0	0	0	0	0	0
KRT17 Keratin, type I cytoskeletal 17	0	6	0	0	0	73	0	0	0	6	0	0	0
KRT13 Keratin, type I cytoskeletal 13	0	0	0	0	2	28	0	0	0	0	0	0	0
KRT27 Keratin, type I cytoskeletal 27	0	2	0	0	0	0	0	0	0	0	0	0	0
KRT28 Keratin, type I cytoskeletal 28	0	0	0	0	0	3	0	0	0	0	0	0	0
KRT10 Keratin, type I cytoskeletal 10	82	180	257	194	77	730	241	232	79	154	50	72	15
KRT9 Keratin, type I cytoskeletal 9	25	80	191	120	21	1080	104	327	30	119	43	37	13
KRT1 Keratin, type II cytoskeletal 1	105	195	322	252	87	767	237	408	91	230	151	79	28
KRT16 Keratin, type I cytoskeletal 16	0	24	17	41	9	80	23	21	0	14	4	0	3
KRT14 Keratin, type I cytoskeletal 14	4	19	28	55	0	130	32	34	2	21	9	4	3
KRT2 Keratin, type II cytoskeletal 2 epidermal	68	156	204	96	43	583	231	135	35	156	45	31	14

KRT5 Keratin, type II cytoskeletal 5	26	86	85	33	18	259	85	53	16	63	28	10	0
KRT18 Keratin, type I cytoskeletal 18	0	0	3	19	0	0	3	0	0	0	0	0	0
KRT36 Keratin, type I cuticular Ha6	0	0	0	19	0	0	3	0	0	0	0	0	0
KRT84 Keratin, type II cuticular Hb4	0	17	0	0	0	0	33	0	20	19	0	0	0
KRT4 Keratin, type II cytoskeletal 4	0	0	0	0	0	0	0	3	0	0	0	0	0
KRT3 Keratin, type II cytoskeletal 3	0	43	55	0	10	0	76	0	0	45	0	0	0
KRT8 Keratin, type II cytoskeletal 8	0	13	0	0	4	0	0	29	0	17	0	0	0
KRT78 Keratin, type II cytoskeletal 78	0	0	16	3	0	38	24	0	0	0	0	0	0
KRT77 Keratin, type II cytoskeletal 1b	15	14	34	18	0	56	27	0	0	0	0	0	0
KRT80 Keratin, type II cytoskeletal 80	0	0	2	0	0	2	0	0	0	0	0	0	0
KRT6A Keratin, type II cytoskeletal 6A	0	107	75	32	17	169	81	58	16	95	27	10	0
KRT31 Keratin, type I cuticular Ha1	0	0	0	19	8	0	0	0	22	0	0	0	0
C4BPB C4b-binding protein beta chain	3	4	0	0	3	0	0	0	0	4	3	0	0
CPB2 Carboxypeptidase B2	3	0	0	0	3	0	0	0	0	4	4	0	0
HBE1 Hemoglobin subunit epsilon	3	0	0	0	2	0	0	0	0	2	2	0	0
SERPINA5 Plasma serine protease inhibitor	0	3	0	0	2	0	0	0	0	3	2	0	0
F5 Coagulation factor V	3	4	0	0	0	0	0	0	0	3	2	0	0
PROC Vitamin K-dependent protein C	0	3	0	0	4	0	0	0	0	4	2	0	0
SHBG Sex hormone-binding globulin	0	4	0	0	2	0	0	0	0	2	2	0	0
MASP1 Mannan-binding lectin serine protease 1	0	2	0	0	2	0	0	0	0	0	2	0	0
Ig kappa chain V-I region Walker	0	2	0	0	3	0	0	0	0	3	0	0	0
TTN Titin	3	2	0	0	2	0	0	0	0	0	0	0	0
CTLA4 Cytotoxic T-lymphocyte protein 4	0	0	0	0	2	0	0	0	0	2	4	0	0
C1QC Complement C1q subcomponent subunit C	0	3	0	0	0	0	0	0	0	0	3	0	0
CRP C-reactive protein	0	0	0	0	3	3	0	0	0	0	0	0	0
LCAT Phosphatidylcholine-sterol acyltransferase	2	0	0	0	0	0	0	0	2	0	0	0	0
INO80 DNA helicase INO80	0	2	0	0	0	2	0	0	0	0	0	0	0
CHD5 Chromodomain-helicase DNA-binding protein 5	0	0	0	0	0	2	0	0	2	0	0	0	0
DOCK10 Dedicator of cytokinesis protein 10	2	0	0	0	0	0	0	0	0	2	0	0	0
C1QA Complement C1q subcomponent subunit A	0	2	0	0	0	0	0	0	0	2	0	0	0
AFM Afamin	0	2	0	0	3	0	0	0	0	0	0	0	0

F9 Coagulation factor IX	0	0	0	0	0	0	0	0	0	2	3	0	0	0
CD14 Monocyte differentiation antigen CD14	2	0	0	0	0	0	0	0	0	0	3	0	0	0
PRG4 Proteoglycan 4	0	2	0	0	0	0	0	0	0	0	3	0	0	0
FETUB Fetuin-B	0	3	0	0	0	0	0	0	0	0	0	2	0	0
ITIH3 Inter-alpha-trypsin inhibitor heavy chain H3	2	0	0	0	4	0	0	0	0	0	0	0	0	0
HIST1H1E Histone H1.4	2	0	0	0	0	0	0	0	0	0	0	0	0	0
HIST1H1B Histone H1.5	2	0	0	0	0	0	0	0	0	0	0	0	0	0
C3orf19 Uncharacterized protein C3orf19	2	0	0	0	0	0	0	0	0	0	0	0	0	0
ALPPL2 Alkaline phosphatase, placental-like	2	0	0	0	0	0	0	0	0	0	0	0	0	0
SCIN Adseverin	2	0	0	0	0	0	0	0	0	0	0	0	0	0
RHPN2 Rhopilin-2	2	0	0	0	0	0	0	0	0	0	0	0	0	0
C18orf34 Uncharacterized protein C18orf34	2	0	0	0	0	0	0	0	0	0	0	0	0	0
EMILIN1 EMILIN-1	2	0	0	0	0	0	0	0	0	0	0	0	0	0
TCOF1 Treacle protein	2	0	0	0	0	0	0	0	0	0	0	0	0	0
SLTM SAFB-like transcription modulator	2	0	0	0	0	0	0	0	0	0	0	0	0	0
KIAA0319 Dyslexia-associated protein KIAA0319	2	0	0	0	0	0	0	0	0	0	0	0	0	0
DNMBP Dynamin-binding protein	2	0	0	0	0	0	0	0	0	0	0	0	0	0
TIAM1 T-lymphoma invasion and metastasis-inducing protein 1	2	0	0	0	0	0	0	0	0	0	0	0	0	0
MYOM2 Myomesin-2	2	0	0	0	0	0	0	0	0	0	0	0	0	0
C18orf34 Uncharacterized protein C18orf34	2	0	0	0	0	0	0	0	0	0	0	0	0	0
CHD9 Chromodomain-helicase DNA-binding protein 9	2	0	0	0	0	0	0	0	0	0	0	0	0	0
RBBP6 E3 ubiquitin-protein ligase RBBP6	2	0	0	0	0	0	0	0	0	0	0	0	0	0
BRWD1 Bromodomain and WD repeat-containing protein 1	2	0	0	0	0	0	0	0	0	0	0	0	0	0
MED12L Mediator of RNA polymerase II transcription subunit 12-like protein	2	0	0	0	0	0	0	0	0	0	0	0	0	0
MEGF8 Multiple epidermal growth factor-like domains protein 8	2	0	0	0	0	0	0	0	0	0	0	0	0	0
ARFGEF3 Brefeldin A-inhibited guanine nucleotide-exchange protein 3	2	0	0	0	0	0	0	0	0	0	0	0	0	0
AHNAK Neuroblast differentiation-associated protein AHNAK	2	0	0	0	0	0	0	0	0	0	0	0	0	0
HECTD4 Probable E3 ubiquitin-protein ligase HECTD4	2	0	0	0	0	0	0	0	0	0	0	0	0	0
NEB Nebulin	2	0	0	0	0	0	0	0	0	0	0	0	0	0

OBSCN Obscurin	2	0	0	0	0	0	0	0	0	0	0	0	0
FSIP2 Fibrous sheath-interacting protein 2	2	0	0	0	0	0	0	0	0	0	0	0	0
S100A7A Protein S100-A7A	0	2	0	0	0	0	0	0	0	0	0	0	0
KIAA0391 Mitochondrial ribonuclease P protein 3	0	2	0	0	0	0	0	0	0	0	0	0	0
ARL6IP4 ADP-ribosylation factor-like protein 6-interacting protein 4	0	2	0	0	0	0	0	0	0	0	0	0	0
CSNK2A1 Casein kinase II subunit alpha	0	2	0	0	0	0	0	0	0	0	0	0	0
UBN1 Ubinuclein-1	0	2	0	0	0	0	0	0	0	0	0	0	0
COL7A1 Collagen alpha-1(VII) chain	0	2	0	0	0	0	0	0	0	0	0	0	0
REV3L DNA polymerase zeta catalytic subunit	0	2	0	0	0	0	0	0	0	0	0	0	0
SACS Sacsin	0	2	0	0	0	0	0	0	0	0	0	0	0
PLEC Plectin	0	2	0	0	0	0	0	0	0	0	0	0	0
APOM Apolipoprotein M	0	0	0	0	4	0	0	0	0	0	0	0	0
MLL Histone-lysine N-methyltransferase MLL	0	0	0	0	4	0	0	0	0	0	0	0	0
LPA Apolipoprotein(a)	0	0	0	0	4	0	0	0	0	0	0	0	0
LBP Lipopolysaccharide-binding protein	0	0	0	0	3	0	0	0	0	0	0	0	0
FBLN1 Fibulin-1	0	0	0	0	3	0	0	0	0	0	0	0	0
PCCA Propionyl-CoA carboxylase alpha chain, mitochondrial	0	0	0	0	3	0	0	0	0	0	0	0	0
AHNAK Neuroblast differentiation-associated protein AHNAK	0	0	0	0	3	0	0	0	0	0	0	0	0
PPBP Platelet basic protein	0	0	0	0	2	0	0	0	0	0	0	0	0
GTF2E1 General transcription factor IIE subunit 1	0	0	0	0	2	0	0	0	0	0	0	0	0
PINK1 Serine/threonine-protein kinase PINK1, mitochondrial	0	0	0	0	2	0	0	0	0	0	0	0	0
BCDIN3D Probable methyltransferase BCDIN3D	0	0	0	0	2	0	0	0	0	0	0	0	0
NUFIP2 Nuclear fragile X mental retardation-interacting protein 2	0	0	0	0	2	0	0	0	0	0	0	0	0
ARHGEF11 Rho guanine nucleotide exchange factor 11	0	0	0	0	2	0	0	0	0	0	0	0	0
GLDC Glycine dehydrogenase	0	0	0	0	2	0	0	0	0	0	0	0	0
ASTN2 Astrotactin-2	0	0	0	0	2	0	0	0	0	0	0	0	0
TPR Nucleoprotein TPR	0	0	0	0	2	0	0	0	0	0	0	0	0
SPTBN2 Spectrin beta chain, non-erythrocytic 2	0	0	0	0	2	0	0	0	0	0	0	0	0
KAT6A Histone acetyltransferase KAT6A	0	0	0	0	2	0	0	0	0	0	0	0	0
DUSP26 Dual specificity protein phosphatase 26	0	0	0	0	0	2	0	0	0	0	0	0	0

GGCT Gamma-glutamylcyclotransferase	0	0	0	0	0	4	0	0	0	0	0	0	0
ANXA2 Annexin A2	0	0	0	0	0	4	0	0	0	0	0	0	0
ATP6V1E2 V-type proton ATPase subunit E 2	0	0	0	0	0	2	0	0	0	0	0	0	0
CPA4 Carboxypeptidase A4	0	0	0	0	0	2	0	0	0	0	0	0	0
KIAA1257 Uncharacterized protein KIAA1257	0	0	0	0	0	2	0	0	0	0	0	0	0
PRDX2 Peroxiredoxin-2	0	0	0	0	0	4	0	0	0	0	0	0	0
AGK Acylglycerol kinase, mitochondrial	0	0	0	0	0	2	0	0	0	0	0	0	0
DDX21 Nucleolar RNA helicase 2	0	0	0	0	0	2	0	0	0	0	0	0	0
FAM116B Protein FAM116B	0	0	0	0	0	2	0	0	0	0	0	0	0
CKAP2 Cytoskeleton-associated protein 2	0	0	0	0	0	2	0	0	0	0	0	0	0
POF1B Protein POF1B	0	0	0	0	0	4	0	0	0	0	0	0	0
PLCB3 1-phosphatidylinositol 4,5-bisphosphate phosphodiesterase beta-3	0	0	0	0	0	2	0	0	0	0	0	0	0
TOP2A DNA topoisomerase 2-alpha	0	0	0	0	0	2	0	0	0	0	0	0	0
MATR3 Matrin-3	0	0	0	0	0	2	0	0	0	0	0	0	0
COL4A2 Collagen alpha-2(IV) chain	0	0	0	0	0	2	0	0	0	0	0	0	0
HDAC6 Histone deacetylase 6	0	0	0	0	0	2	0	0	0	0	0	0	0
FAM47C Putative protein FAM47C	0	0	0	0	0	2	0	0	0	0	0	0	0
SCN11A Sodium channel protein type 11 subunit alpha	0	0	0	0	0	2	0	0	0	0	0	0	0
CEP290 Centrosomal protein of 290 kDa	0	0	0	0	0	2	0	0	0	0	0	0	0
DNAH2 Dynein heavy chain 2, axonemal	0	0	0	0	0	2	0	0	0	0	0	0	0
AGRN Agrin	0	0	0	0	0	2	0	0	0	0	0	0	0
BOD1L1 Biorientation of chromosomes in cell division protein 1-like 1	0	0	0	0	0	2	0	0	0	0	0	0	0
FLG Filaggrin	0	0	0	0	0	2	0	0	0	0	0	0	0
SEPP1 Selenoprotein P	0	0	0	0	0	0	0	0	2	0	0	0	0
ARL6IP4 ADP-ribosylation factor-like protein 6-interacting protein 4	0	0	0	0	0	0	0	0	2	0	0	0	0
ZNF609 Zinc finger protein 609	0	0	0	0	0	0	0	0	2	0	0	0	0
KDM2A Lysine-specific demethylase 2A	0	0	0	0	0	0	0	0	4	0	0	0	0
CEP135 Centrosomal protein of 135 kDa	0	0	0	0	0	0	0	0	2	0	0	0	0
CACNA1A Voltage-dependent P/Q-type calcium channel subunit alpha-1A	0	0	0	0	0	0	0	0	2	0	0	0	0

UGGT1 UDP-glucose:glycoprotein glucosyltransferase 1	0	0	0	0	0	0	0	0	0	2	0	0	0	0
CENPF Centromere protein F	0	0	0	0	0	0	0	0	0	2	0	0	0	0
MGA MAX gene-associated protein	0	0	0	0	0	0	0	0	0	2	0	0	0	0
Ig kappa chain V-I region HK101	0	0	0	0	0	0	0	0	0	0	4	0	0	0
GPX3 Glutathione peroxidase 3	0	0	0	0	0	0	0	0	0	0	2	0	0	0
PLA2G7 Platelet-activating factor acetylhydrolase	0	0	0	0	0	0	0	0	0	0	2	0	0	0
PIGR Polymeric immunoglobulin receptor	0	0	0	0	0	0	0	0	0	0	2	0	0	0
SRFBP1 Serum response factor binding protein 1	0	0	0	0	0	0	0	0	0	0	2	0	0	0
VASH1 Vasohibin-1	0	0	0	0	0	0	0	0	0	0	2	0	0	0
MAP7D2 MAP7 domain-containing protein 2	0	0	0	0	0	0	0	0	0	0	2	0	0	0
FAM98A Protein FAM98A	0	0	0	0	0	0	0	0	0	0	2	0	0	0
INA Alpha-internexin	0	0	0	0	0	0	0	0	0	0	2	0	0	0
ATPIA1 Sodium/potassium-transporting ATPase subunit alpha-1	0	0	0	0	0	0	0	0	0	0	2	0	0	0
FER Tyrosine-protein kinase Fer	0	0	0	0	0	0	0	0	0	0	2	0	0	0
FANCI Fanconi anemia group I protein	0	0	0	0	0	0	0	0	0	0	4	0	0	0
RBM15 Putative RNA-binding protein 15	0	0	0	0	0	0	0	0	0	0	2	0	0	0
COL24A1 Collagen alpha-1(XXIV) chain	0	0	0	0	0	0	0	0	0	0	2	0	0	0
MYOIF Unconventional myosin-If	0	0	0	0	0	0	0	0	0	0	2	0	0	0
EPHA8 Ephrin type-A receptor 8	0	0	0	0	0	0	0	0	0	0	2	0	0	0
RIMS1 Regulating synaptic membrane exocytosis protein 1	0	0	0	0	0	0	0	0	0	0	2	0	0	0
TIAM1 T-lymphoma invasion and metastasis-inducing protein 1	0	0	0	0	0	0	0	0	0	0	2	0	0	0
CCDC108 Coiled-coil domain-containing protein 108	0	0	0	0	0	0	0	0	0	0	2	0	0	0
PCNXL3 Pecanex-like protein 3	0	0	0	0	0	0	0	0	0	0	2	0	0	0
KIAA2026 Uncharacterized protein KIAA2026	0	0	0	0	0	0	0	0	0	0	2	0	0	0
ITPR1 Inositol 1,4,5-trisphosphate receptor type 1	0	0	0	0	0	0	0	0	0	0	2	0	0	0
PDZD2 PDZ domain-containing protein 2	0	0	0	0	0	0	0	0	0	0	2	0	0	0
MYO5A Unconventional myosin-Va	0	0	0	0	0	0	0	0	0	0	2	0	0	0
KIAA1109 Uncharacterized protein KIAA1109	0	0	0	0	0	0	0	0	0	0	2	0	0	0

ARID5B AT-rich interactive domain-containing protein 5B	0	0	0	0	0	0	0	0	0	0	0	2	0	0
STIM1 Stromal interaction molecule 1	0	0	0	0	0	0	0	0	0	0	0	2	0	0
USP8 Ubiquitin carboxyl-terminal hydrolase 8	0	0	0	0	0	0	0	0	0	0	0	2	0	0
PDE1C Calcium/calmodulin-dependent 3',5'-cyclic nucleotide phosphodiesterase 1C	0	0	0	0	0	0	0	0	0	0	0	2	0	0
FAM21C WASH complex subunit FAM21C	0	0	0	0	0	0	0	0	0	0	0	2	0	0
EXTL3 Exostosin-like 3	0	0	0	0	0	0	0	0	0	0	0	2	0	0
MTR Methionine synthase	0	0	0	0	0	0	0	0	0	0	0	2	0	0
SUV420H1 Histone-lysine N-methyltransferase SUV420H1	0	0	0	0	0	0	0	0	0	0	0	2	0	0
MYH11 Myosin-11	0	0	0	0	0	0	0	0	0	0	0	2	0	0
BSN Protein bassoon	0	0	0	0	0	0	0	0	0	0	0	2	0	0
ABCC2 Canalicular multispecific organic anion transporter 1	0	0	0	0	0	0	0	0	0	0	0	2	0	0
ZZEF1 Zinc finger ZZ-type and EF-hand domain-containing protein 1	0	0	0	0	0	0	0	0	0	0	0	2	0	0
SPINK5 Serine protease inhibitor Kazal-type 5	0	0	0	0	0	0	0	0	3	0	0	0	0	0
MST1 Hepatocyte growth factor-like protein	0	0	0	0	0	0	0	0	0	3	0	0	0	0
THBS1 Thrombospondin-1	0	0	0	0	0	0	0	0	0	3	0	0	0	0
ALMS1 Alstrom syndrome protein 1	0	0	0	0	0	0	0	0	0	3	0	0	0	0
CFHR2 Complement factor H-related protein 2	0	0	0	0	0	0	0	0	0	0	3	0	0	0
LYL1 Protein lyl-1	0	0	0	0	0	0	0	0	0	0	3	0	0	0
ZNF469 Zinc finger protein 469	0	0	0	0	0	0	0	0	0	0	3	0	0	0
PRDX1 Peroxiredoxin-1	0	0	0	0	0	3	0	0	0	0	0	0	0	0
CASP14 Caspase-14	0	0	0	0	0	3	0	0	0	0	0	0	0	0
PKM Pyruvate kinase isozymes M1/M2	0	0	0	0	0	3	0	0	0	0	0	0	0	0
CTSD Cathepsin D	0	0	0	0	0	3	0	0	0	0	0	0	0	0
Uncharacterized protein	0	0	0	0	0	3	0	0	0	0	0	0	0	0
TGM1 Protein-glutamine gamma-glutamyltransferase K	0	0	0	0	0	3	0	0	0	0	0	0	0	0
DDX42 ATP-dependent RNA helicase DDX42	3	0	0	0	0	0	0	0	0	0	0	0	0	0
BCL9 B-cell CLL/lymphoma 9 protein	3	0	0	0	0	0	0	0	0	0	0	0	0	0
RAB3IL1 Guanine nucleotide exchange factor for Rab-3A	3	0	0	0	0	0	0	0	0	0	0	0	0	0
S100A8 Protein S100-A8	0	3	0	0	0	0	0	0	0	0	0	0	0	0
F11 Coagulation factor XI	0	3	0	0	0	0	0	0	0	0	0	0	0	0
TLL1 Tolloid-like protein 1	0	3	0	0	0	0	0	0	0	0	0	0	0	0
DCD Dermcidin	0	0	12	9	0	0	20	11	0	0	0	0	0	0

LYZ Lysozyme C	0	0	0	0	0	0	2	0	0	2	0	0	0
ACE Angiotensin-converting enzyme	0	0	0	0	0	0	0	82	0	40	31	0	0
ACTA2 Actin, aortic smooth muscle	0	0	0	0	0	0	2	0	0	0	0	0	0
ACTA1 Actin, alpha skeletal muscle	0	0	0	0	0	0	2	0	0	0	0	0	0
UBC Polyubiquitin-C	0	0	0	0	0	0	4	0	0	0	0	0	0
UBBP4 Protein UBBP4	0	0	0	0	0	0	4	0	0	0	0	0	0
UBA52 Ubiquitin-60S ribosomal protein L40	0	0	0	0	0	0	4	0	0	0	0	0	0
RPS27A Ubiquitin-40S ribosomal protein S27a	0	0	0	0	0	0	4	0	0	0	0	0	0
LUZP1 Leucine zipper protein 1	0	0	0	0	0	0	2	0	0	0	0	0	0
S100A9 Protein S100-A9	0	0	0	0	0	0	7	0	0	0	0	0	0
DNAH14 Dynein heavy chain 14, axonemal	0	0	0	0	2	0	0	2	0	0	0	0	0
AZGP1 Zinc-alpha-2-glycoprotein	0	0	3	0	4	0	2	0	0	0	0	0	0
GAPDH Glyceraldehyde-3-phosphate dehydrogenase	0	0	5	0	0	13	3	0	0	0	0	0	0
H2AFZ Histone H2A.Z	0	0	0	2	0	0	0	0	0	0	0	0	0
H2AFJ Histone H2A.J	0	0	0	2	0	0	0	0	0	0	0	0	0
HIST1H2AA Histone H2A type 1-A	0	0	0	2	0	0	0	0	0	0	0	0	0
HIST3H2A Histone H2A type 3	0	0	0	2	0	0	0	0	0	0	0	0	0
H2AFV Histone H2A.V	0	0	0	2	0	0	0	0	0	0	0	0	0
HIST2H2AC Histone H2A type 2-C	0	0	0	2	0	0	0	0	0	0	0	0	0
H2AFX Histone H2A.x	0	0	0	2	0	0	0	0	0	0	0	0	0
HIST1H2AM Histone H2A type 1	0	0	0	2	0	0	0	0	0	0	0	0	0
SERPINB4 Serpin B4	0	0	2	0	0	0	0	0	0	0	0	0	0
PARP10 Poly	0	0	2	0	0	0	0	0	0	0	0	0	0
PIP Prolactin-inducible protein	0	0	2	2	0	0	0	0	0	0	0	0	0
HIST4H4 Histone H4	0	0	0	4	0	0	0	0	0	0	0	0	0
S100A7 Protein S100-A7	0	2	2	0	0	0	0	0	0	0	0	0	0